ISSN: 2067-3809

Universitatea Politehnica Timișoara

ACTA TECHNICA CORVINIENSIS – Bulletin of Engineering

Fascicule 4

[October–December]

Tome XVI [2023]

Editura POLITEHNICA

ACTA TECHNICA CORVINIENSIS

Bulletin of Engineering

Edited by:

UNIVERSITY POLITEHNICA TIMISOARA

Universitatea Politehnica Timişoara

Editor / Technical preparation / Cover design:

Assoc. Prof. Eng. KISS Imre, PhD.
UNIVERSITY POLITEHNICA TIMISOARA,
FACULTY OF ENGINEERING HUNEDOARA

Commenced publication year:
2008

ACTA TECHNICA CORVINIENSIS

Bulletin of Engineering

ASSOCIATE EDITORS and REGIONAL COLLABORATORS

The Editor and editorial board members do not receive any remuneration. These positions are voluntary. The members of the Editorial Board may serve as scientific reviewers.

We are very pleased to inform that our journal **ACTA TECHNICA CORVINIENSIS – Bulletin of Engineering** is going to complete its ten years of publication successfully. In a very short period it has acquired global presence and scholars from all over the world have taken it with great enthusiasm. We are extremely grateful and heartily acknowledge the kind of support and encouragement from you.

ACTA TECHNICA CORVINIENSIS – Bulletin of Engineering seeking qualified researchers as members of the editorial team. Like our other journals, **ACTA TECHNICA CORVINIENSIS – Bulletin of Engineering** will serve as a great resource for researchers and students across the globe. We ask you to support this initiative by joining our editorial team. If you are interested in serving as a member of the editorial team, kindly send us your resume to redactie@fih.upt.ro.

ISSN: 2067-3809

INTERNATIONAL SCIENTIFIC COMMITTEE MEMBERS and SCIENTIFIC REVIEWERS

MANAGER & CHAIRMAN

ROMANIA 

Imre KISS, University Politehnica TIMISOARA, Faculty of Engineering HUNEDOARA

INTERNATIONAL SCIENTIFIC COMMITTEE MEMBERS & SCIENTIFIC REVIEWERS from:

ROMANIA 

Viorel–Aurel ȘERBAN, University Politehnica TIMIŞOARA – TIMIŞOARA
Teodor HEPUȚ, University Politehnica TIMIŞOARA – HUNEDOARA
Ilare BORDEAȘU, University Politehnica TIMIŞOARA – TIMIŞOARA
Liviu MARȘAVIA, University Politehnica TIMIŞOARA – TIMIŞOARA
Ioan VIDA–SIMITI, Technical University of CLUJ–NAPOCA – CLUJ–NAPOCA
Sorin VLASE, "Transilvania" University of BRAŞOV – BRAŞOV
Horatiu TEODORESCU DRĂGHICESCU, "Transilvania" University of BRAŞOV – BRAŞOV
Maria Luminița SCUTARU, "Transilvania" University of BRASOV – BRASOV
Carmen ALIC, University Politehnica TIMIŞOARA – HUNEDOARA
Sorin DEACONU, University Politehnica TIMIŞOARA – HUNEDOARA
Liviu MIHON, University Politehnica TIMIŞOARA – TIMIŞOARA
Valeriu RUCAI, University Politehnica BUCUREŞTI – BUCUREŞTI

SLOVAKIA 

Ervin LUMNITZER, Technical University of KOŠICE – KOŠICE
Miroslav BADIDA, Technical University of KOŠICE – KOŠICE
Karol VELIŠEK, Slovak University of Technology BRATISLAVA – TRNAVA
Imrich KISS, Institute of Economic & Environmental Security – KOŠICE
Vladimir MODRAK, Technical University of KOSICE – PRESOV

CROATIA 

Drazan KOZAK, Josip Juraj Strossmayer University of OSIJEK – SLAVONKI BROD
Predrag COSIC, University of ZAGREB – ZAGREB
Milan KLJAJIN, Josip Juraj Strossmayer University of OSIJEK – SLAVONKI BROD
Antun STOIĆ, Josip Juraj Strossmayer University of OSIJEK – SLAVONKI BROD
Ivo ALFIREVIĆ, University of ZAGREB – ZAGREB

HUNGARY 

Imre DEKÁNY, University of SZEGED – SZEGED
Cecilia HODÚR, University of SZEGED – SZEGED
Béla ILLÉS, University of MISKOLC – MISKOLC
Imre RUDAS, Óbuda University of BUDAPEST – BUDAPEST
István BIRÓ, University of SZEGED – SZEGED
Tamás KISS, University of SZEGED – SZEGED
Imre TIMÁR, University of Pannonia – VESZPRÉM
Károly JÁRMAI, University of MISKOLC – MISKOLC
Ádám DÖBRÖCZÖNI, University of MISKOLC – MISKOLC
György SZEIDL, University of MISKOLC – MISKOLC
Miklós TISZA, University of MISKOLC – MISKOLC
József GÁL, University of SZEGED – SZEGED
Ferenc FARKAS, University of SZEGED – SZEGED
Géza HUSI, University of DEBRECEN – DEBRECEN

SERBIA 

Sinisa KUZMANOVIC, University of NOVI SAD – NOVI SAD
Mirjana VOJINOVIĆ MILORADOV, University of NOVI SAD – NOVI SAD
Miroslav PLANČAK, University of NOVI SAD – NOVI SAD

MACEDONIA 

Valentina GECEVSKA, University "St. Cyril and Methodius" SKOPJE – SKOPJE
Zoran PANDILOV, University "St. Cyril and Methodius" SKOPJE – SKOPJE

The SCIENTIFIC COMMITTEE MEMBERS AND REVIEWERS do not receive any remuneration. These positions are voluntary.

We are extremely grateful and heartily acknowledge the kind of support and encouragement from all contributors and all collaborators!

ACTA TECHNICA CORVINIENSIS – Bulletin of Engineering is dedicated to publishing material of the highest engineering interest, and to this end we have assembled a distinguished Editorial Board and Scientific Committee of academics, professors and researchers.

ACTA TECHNICA CORVINIENSIS – Bulletin of Engineering publishes invited review papers covering the full spectrum of engineering. The reviews, both experimental and theoretical, provide general background information as well as a critical assessment on topics in a state of flux. We are primarily interested in those contributions which bring new insights, and papers will be selected on the basis of the importance of the new knowledge they provide.

ACTA TECHNICA CORVINIENSIS – Bulletin of Engineering encourages the submission of comments on papers published particularly in our journal. The journal publishes articles focused on topics of current interest within the scope of the journal and coordinated by invited guest editors. Interested authors are invited to contact one of the Editors for further details.

ACTA TECHNICA CORVINIENSIS – Bulletin of Engineering accept for publication unpublished manuscripts on the understanding that the same manuscript is not under simultaneous consideration of other journals. Publication of a part of the data as the abstract of conference proceedings is exempted.

Manuscripts submitted (original articles, technical notes, brief communications and case studies) will be subject to peer review by the members of the Editorial Board or by qualified outside reviewers. Only papers of high scientific quality will be accepted for publication. Manuscripts are accepted for review only when they report unpublished work that is not being considered for publication elsewhere.

The evaluated paper may be recommended for:

- **Acceptance without any changes** – in that case the authors will be asked to send the paper electronically in the required .doc format according to authors' instructions;
- **Acceptance with minor changes** – if the authors follow the conditions imposed by referees the paper will be sent in the required .doc format;
- **Acceptance with major changes** – if the authors follow completely the conditions imposed by referees the paper will be sent in the required .doc format;
- **Rejection** – in that case the reasons for rejection will be transmitted to authors along with some suggestions for future improvements (if that will be considered necessary).

The manuscript accepted for publication will be published in the next issue of **ACTA TECHNICA CORVINIENSIS – Bulletin of Engineering** after the acceptance date.

All the authors and the corresponding author in particular take the responsibility to ensure that the text of the article does not contain portions copied from any other published material which amounts to plagiarism. We also request the authors to familiarize themselves with the good publication ethics principles before finalizing their manuscripts.

ISSN: 2067–3809

Fascicule 4
[October – December]
tome XVI
[2023]

ACTA Technica CORVINIENSIS
BULLETIN OF ENGINEERING

ISSN: 2067-3809

TABLE of CONTENTS

ACTA TECHNICA CORVINIENSIS – Bulletin of Engineering

Tome XVI [2023]

Fascicule 4 [October – December]

The ACTA TECHNICA CORVINIENSIS – Bulletin of Engineering, Tome XVI [2023], Fascicule 4 [October – December] includes original papers submitted to the Editorial Board, directly by authors or by the regional collaborators of the Journal.
Also, the ACTA TECHNICA CORVINIENSIS – Bulletin of Engineering, Tome XVI [2023], Fascicule 4 [October – December], includes scientific papers presented in the sections of:

- DEMI 2023 – 16th International Conference on Accomplishments in Mechanical and Industrial Engineering, organized by Faculty of Mechanical Engineering, University of Banja Luka (BOSNIA & HERZEGOVINA), co–organized with the Faculty of Mechanical Engineering University of Niš (SERBIA), Faculty of Mechanical Engineering University of Podgorica (MONTENEGRO), Faculty of Engineering Hunedoara, University Politehnica Timișoara (ROMANIA) and Reykjavik University (ICELAND), in Banja Luka (BOSNIA & HERZEGOVINA), in 01–02 June, 2023. The current identification numbers of the selected papers are the #1–6, according to the present contents list.
- ISB–INMA TEH' 2022 – International Symposium (Agricultural and Mechanical Engineering), organized by Politehnica University of Bucharest – Faculty of Biotechnical Systems Engineering (ISB), National Institute of Research–Development for Machines and Installations Designed to Agriculture and Food Industry (INMA Bucharest), Romanian Agricultural Mechanical Engineers Society (SIMAR), National Research & Development Institute for Food Bioresources (IBA Bucharest), National Institute for Research and Development in Environmental Protection (INCDPM), Research–Development Institute for Plant Protection (ICDPP), Research and Development Institute for Processing and Marketing of the Horticultural Products (HORTING), Hydraulics and Pneumatics Research Institute (INOE 2000 IHP) and "Food for Life Technological Platform", in Bucharest, ROMANIA, between 06–07 October, 2022. The current identification numbers of the selected paper is the #19, according to the present contents list.

ACTA TECHNICA CORVINIENSIS – Bulletin of Engineering is a good opportunity for the researchers to exchange information and to present the results of their research activity. Scientists and engineers with an interest in the respective interfaces of engineering fields, technology and materials, information processes, research in various industrial applications are the target and audience of ACTA TECHNICA CORVINIENSIS – Bulletin of Engineering. It publishes articles of interest to researchers and engineers and to other scientists involved with materials phenomena and computational modeling.
The journal's coverage will reflect the increasingly interdisciplinary nature of engineering, recognizing wide–ranging contributions to the development of methods, tools and evaluation strategies relevant to the field. Numerical modeling or simulation, as well as theoretical and experimental approaches to engineering will form the core of ACTA TECHNICA CORVINIENSIS – Bulletin of Engineering's content, however approaches from a range of environmental science and economics are strongly encouraged.
Publishing in ACTA TECHNICA CORVINIENSIS – Bulletin of Engineering is free of charge. There are no author fees. All services including peer review, copy editing, typesetting, production of web pages and reproduction of color images are included. The journal is free of charge to access, read and download. All costs associated with publishing and hosting this journal are funded by ACTA TECHNICA CORVINIENSIS – Bulletin of Engineering as part of its investment in global research and development.

ISSN: 2067–3809

Fascicule 4
[October – December]
tome XVI
[2023]

ACTA Technica CORVINIENSIS
BULLETIN OF ENGINEERING

ISSN: 2067-3809

ACTA TECHNICA CORVINIENSIS – BULLETIN OF ENGINEERING
TOME XVI [2023] | FASCICULE 4 [OCTOBER – DECEMBER]

[1.]Ognjen BOBIČIĆ, [1.]Milanko DAMJANOVIĆ ,[2.]David C. FINGER ,
[1.]Radoje VUJADINOVIĆ, [1.]Boško MATOVIĆ

IMPACT OF NON–EXHAUST PARTICLE EMISSIONS FROM MOTOR VEHICLES ON HUMAN HEALTH

[1.] Faculty of Mechanical Engineering, University of Montenegro, Podgorica, MONTENEGRO
[2.] Department of Engineering, Reykjavik University, Reykjavik, ICELAND

Abstract: According to the World Health Organization (WHO), PM2.5 and PM10 are a leading cause of air pollution and have been identified as having detrimental effects on human health even at low concentrations. By reducing exposure to these particles, countries can significantly decrease the incidence of both short– and long–term illnesses, as well as the overall burden of disease. This paper discusses the impact of the size and concentration of particles from braking systems, tires, and road on the respiratory, cardiovascular, and nervous systems of humans. The paper also presents methods for detecting and measuring non–exhaust emissions from motor vehicles, as well as United Nations Economic Commission for Europe (UNECE) regulations for defining standardised laboratory procedures for testing particle emissions resulting from the wear of brakes in light vehicles with a maximum permissible weight of up to 3500 kg. Based on the reviewed literature, possible mitigation measures to reduce fine particulate emissions are presented. In particular, an adaptation of an adequate braking process can significantly mitigate emissions and subsequently reduce harmful effects on human health and the environment.

Keywords: non–exhaust emissions, particulate matter (PM), human health

INTRODUCTION

Despite all the conducted research, some factors that contribute to the production of non–exhaust emissions have been partially neglected, and their contribution to the overall level of pollutants generated by traffic is decreasing to a much lesser extent compared to exhaust emissions.

Studies have found that the brake system, tire wear, and road surface are the most significant sources of non–exhaust particles (particulate matters), and they can have a substantial impact on human health [1–3]. These PMs are small enough to penetrate deep into the lungs, where they can cause inflammation [4] and damage to lung tissue. This can lead to a variety of respiratory problems, such as asthma and chronic obstructive pulmonary disease [5]. Moreover, exposure to PM from motor vehicle emissions has also been linked to an increased risk of cardiovascular disease [6,7], and some neurodegenerative phenomena and cognitive disorders [8,9]. Therefore, it is essential to take measures to reduce the emission of particulate matter from motor vehicles and limit our exposure to these harmful pollutants.

This paper provides an overview of previous studies examining non–exhaust emissions and their impact on human health, as well as a review of methods for measuring non–exhaust emissions generated by the brake system (brake discs and pads). A brief overview of the brake testing requirements prescribed by The United Nations Global Technical Regulation (UN GTR) will also be provided.

THE IMPACT OF NON–EXHAUST EMISSIONS ON HUMAN HEALTH

The proliferation of road traffic has resulted in significant repercussions, not limited to direct transportation safety concerns, but also with regards to the visible impact of vehicle emissions on the environment and human health, which has been the focus of research over the past two decades in urban areas worldwide [10], due to the increasing presence of motor vehicles and their emissions as a noteworthy source of particulate matter (PM) in the atmosphere, which can severely affect the respiratory system of humans.

According to the European Environment Agency's reports in 2014 and 2016, between 64% and 92% of the EU urban population is exposed to high concentrations of PM10 and PM2.5 particles [11][12], and air pollution is considered the largest environmental risk factor responsible for premature deaths worldwide. The World Health Organization's studies have shown that Europeans' life expectancy can be reduced by an average of about 8.6 months [13][14], or even up to 22 months in the most polluted cities, due to exposure to these particles [14].

Animal studies have demonstrated that exposure to highly polluted ambient air affects lung function and leads to premature death, and the same has been observed in humans, with air pollution contributing to as many as 4.2 million premature deaths globally in 2016 [15][16].

A study conducted in Taipei, Taiwan, investigated the exposure of PM2.5 on human health, specifically on the cardiovascular system [17][18]. The study concluded that

commuters [18] and cyclists [17] are more exposed to PM on routes with heavy traffic compared to those with less traffic. Moreover, the study revealed that pedestrians [17] walking on sidewalks were more exposed to PM than people travelling in cars for the same purpose.

Particle size plays an important role in determining the impact of particles on human health, depending on how deep they can travel into respiratory structures. The authors from the University of Trento, Italy, have presented a classification overview of particles found in urban environments [19] based on their size and mass characteristics. The particles were divided into three groups: coarse, fine, and ultrafine particles, each with their unique characteristics.

Coarse particles (aerodynamic diameter of 2–20μm) [19] are characterised by a larger size and lower numerical representation, but they are considered primary emissions. Fine particles (aerodynamic diameter of 0.1–2μm) [19] are more prevalent and have a smaller mass and volumetric range, while ultrafine particles (aerodynamic diameter of 0.01–0.1μm) [19] have an even smaller mass and volumetric range and higher numerical representation. Ultrafine particles can be further divided into two groups based on their aerodynamic diameter, smaller than 0.01μm (nanoparticles) and those with an aerodynamic diameter between 0.01 and 1μm (Aitken mode). Hence, small particles, with a size of 2.5 μm or less, can penetrate the finest respiratory pathways, while particles of 1 μm can reach the terminal alveolar structures where oxygen and carbon dioxide exchange occur. Nanoparticles of 0.1 μm can directly penetrate into the bloodstream [20][21].

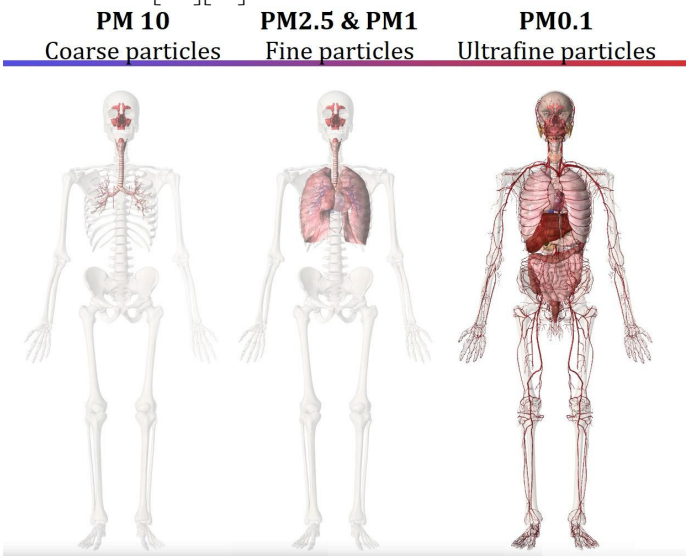

Figure 1. Representation of particles penetration into the human body depending on the size of their aerodynamic diameter. (Modified from [22])

Given the evident impact of particles on human health, viewed from various aspects, it represents an additional threat for chronically ill individuals and those susceptible to rapid changes in health status. In a study conducted by Gonet and Maher (2019) [23], which examines the impact of particles generated by car operation, it was noted that the concentration and size of particles can be strongly linked not only to respiratory and cardiovascular damage but also to neurodevelopment and cognitive functions. As such, the following sections present research on the impact of particles generated by road vehicles on the respiratory, cardiovascular, and nervous systems in humans.

Impact on the respiratory system

The investigation of ambient air pollutants has led to the suspicion that exposure to particles (PM), especially those in the fine (<2.5 mm aerodynamic diameter) and ultrafine range (<0.1 mm;), is considered a key risk factor for many harmful health effects [16][21]. Based on this assumption, it has been concluded that the particular effect of the presence of particles in ambient air is reflected in acute or chronic respiratory problems, which are caused by direct damage to the respiratory organs when inhaling air pollutants. Chronic exposure is associated with cough, sputum production, and reduced lung function [24]. In addition to symptoms, exposure studies in healthy individuals have documented numerous deep inflammatory changes in the respiratory tract, particularly before changes in lung function can be detected [16].

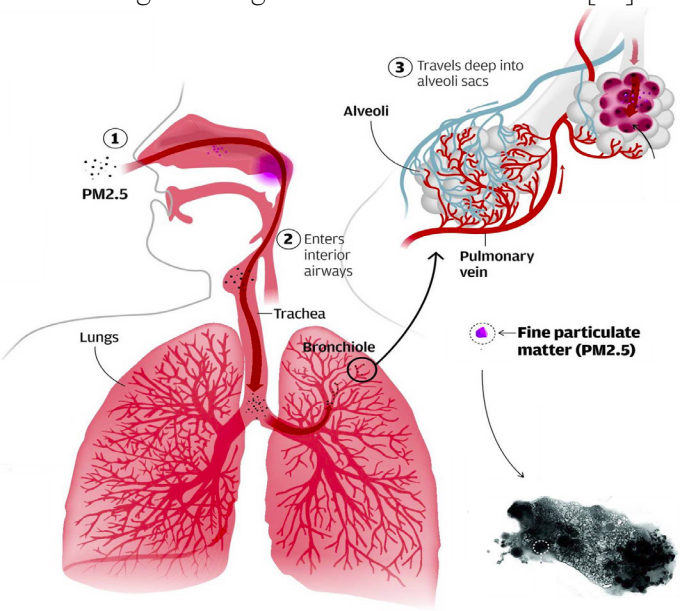

Figure 2. PM particle (specifically PM2.5) and how it can be synthesised into the bloodstream through the respiratory system. (Modified from [21])

A brief review of the literature by Italian researcher Luigi Vimercati (2011) highlighted that emissions from traffic processes, i.e. braking and tire wear, can play a key role in causing allergic conditions [5]. It was also noted that several pollutants (NO2, O3, and PM) are associated with worsening asthma and can significantly contribute to its pathogenesis. Therefore, based on the collected data, it can be concluded that in most industrialised countries, people living in urban areas tend to be more affected by allergic respiratory diseases than those in rural areas [5].

On another note, one experimental indirect study was conducted to investigate the effect of air pollution on changes in Sprague–Dawley rat lung tissue under whole–body exposure to PM1 (particles <1 mm in aerodynamic diameter) pollutants at the National Laboratory Animal Center (Taipei, Taiwan) [16]. It was found that the presence of PM1 particles enhances oxidative stress and inflammatory reactions under subchronic exposure to PM1, resulting from car work, while suppressing glucose metabolism and actin cytoskeleton signalling. These factors can lead to impaired lung function after chronic exposure to PM1 associated with traffic [16].

The study made a significant contribution to the investigation of several potential molecular characteristics associated with early lung damage in response to air pollution associated with traffic processes. These results would further contribute significantly to the screening process of individuals who are more significantly exposed to polluted ambient air, primarily supplied with particles resulting from car work and traffic processes.

Impact on the cardiovascular system

A study by a group of authors from the University of South China [17] examined the impact of PM2.5 particles on human health and provided an overview of previous conclusions on this topic. Long–term exposure to PM2.5 may not only affect the respiratory system but also cause significant structural changes in the heart muscle, such as myocardial hypertrophy (with increased hypertrophic markers) and harmful ventricular remodelling (changes in the size, shape, structure, and function of the heart muscle) [17, 25, 26].

Previous studies have also discussed how PM2.5 can disrupt a significant number of functions in the cardiac autonomic nervous system (ANS) and lead to reduced heart rate variability, which is considered an independent risk factor for cardiovascular morbidity and mortality [6,7,25]. The study also discussed changes in the endocrine system and the function of the hypothalamus and its hormone secretion, conditioned by changes in the heart muscle, but this association has not been sufficiently investigated.

To the extent of the relevance of the examined data, a connection was found between the increased concentration of PM2.5 particles and a range of pathophysiological responses that increase blood pressure and lead to the development of hypertension [17,25,27].

A study conducted in Taiwan examined the effects of PM2.5 exposure on the cardiovascular system of healthy travellers using different modes of transportation. The study involved 120 participants who were classified according to their transportation type, including electric subway trains, gasoline–powered buses, cars, scooters, and pedestrians with and without face masks. Measurements of various parameters were taken during six iterations. Results showed that exposure to PM2.5 is linked to increased systolic blood pressure and heart rate during walking and riding a gasoline–powered scooter. PM2.5 concentration was highest during scooter use and lowest during electric subway train use. The study did not find a significant correlation between PM2.5 and the systolic and diastolic blood pressure or heart rate while walking with a face mask. Overall, the study concluded that PM2.5 has a visible effect on the cardiovascular system. [17]

Impact on the nervous system

Previously, we described the relation of particles with changes in the respiratory and cardiovascular systems, while on the other hand, researchers have also investigated the impact of particles on other organs and systems within the human body. The effects of non–exhaust emissions of nanoparticles produced by vehicular processes have also been examined and linked to neurodevelopment and cognitive impairments.

Researchers von Mikecz, A. and Schikowski, T. (2020) from the Leibniz Research Institute for Environmental Medicine studied the effects of nanoparticles in the air on the nervous system through the aggregation of amyloid proteins, neurodegeneration, and neurodegenerative diseases such as Alzheimer's and Parkinson's disease [28]. Also, a study by a group of researchers from the US, Brazil, Germany, and the UK on various forms of cardiovascular and cerebrovascular diseases indicates their harmful effects on the brain and cognitive processes through vascular and inflammatory mechanisms [28, 29].

Besides age, the environment in which a person lives can also play a role in the development of Alzheimer's and Parkinson's disease. Exposure to certain pollutants in the environment may contribute to an increased risk of developing these diseases. This hypothesis has been confirmed by several studies, which have emphasised that Alzheimer's disease positively correlates with the level of air pollution in urban environments, most significantly with PM [28,30].

Schikowski, T. and Altuğ H.'s (2020) study on the role of air pollution in cognitive decline and impairment [31] confirmed the association between these two components. The collected data is quite heterogeneous, and additional analyses and research are needed to give more importance to this association and explore its relevance in detail [28].

What is also important to emphasise is that the accumulation of amyloid protein within the cells of the central nervous system is a common feature of neuropathology in Alzheimer's and Parkinson's disease and is closely associated with the appearance of amyloid–beta peptides, tau proteins, and alpha–synuclein [28]. In support of this, the study by Gonet and Maher (2019) [23]

on urban air and its contribution to the development of dementia and Alzheimer's disease showed typical features of the pathogenesis of Alzheimer's disease, namely aberrant deposition of amyloid–beta peptides and tau proteins in post–mortem brain samples of clinically healthy people and dogs exposed to lifelong air pollution by living in the researched urban areas of Mexico City or Manchester (UK) [30].

Research has shown that nanoparticles generated from traffic processes, specifically from the wear and tear of brakes and tires in automobiles, have the ability to induce amyloid formation in nano–silicon dioxide. Furthermore, a significant amount of these nanoparticles has been detected in postmortem brains of animals and humans with chronic exposure to air pollution in highly urbanised environments. Epidemiological data has also indicated that living near traffic routes is a risk factor for the development of neurodegenerative diseases, such as Alzheimer's disease [8, 23].

Additionally, a study conducted in China [32] to investigate the effects of air pollution on unborn children (during prenatal development) and the development of ADHD in early childhood yielded significant results. It is particularly noteworthy that with an increase in the presence of PM10, PM2.5, and NO2 during the period considered most sensitive to the development of degenerative behaviours (end of pregnancy and first four months of life), the possibility of hyperactivity in children increases significantly, with a statistically significant association. This conclusion supports the idea that exposure to particles during pregnancy can lead to the development of hyperactive behavior (or ADHD) in early childhood [32].

METHODS FOR DETECTING AND MEASURING NON–EXHAUST EMISSIONS FROM BRAKES

It is crucial to bear in mind that particle emissions related to traffic have been proven to have negative health effects. However, despite the scientific community's increasing interest in studying brake emissions, the vast majority of research findings are inconsistent and vary widely. This introduces a significant degree of uncertainty when attempting to assess the contribution of brake wear emissions to ambient PM levels, as brake wear emission factors are dependent on various parameters such as the type of friction material, brake assembly, and driving conditions [33].

One of the primary reasons for the lack of consistency in measuring particulate matter size and number emission factors, so far, is the absence of standardised methodologies for sampling and measuring brake wear particle emissions [34]. As such, researchers have employed different sampling and measurement techniques and devices, leading to variations in reported results. So, brake wear particles can be detected and measured under controlled laboratory conditions or in uncontrolled real–world settings on the road.

In the context of laboratory methods and devices, the most frequently used ones are pin–on–disc tribometers and inertial brake dynamometers [34]. On the other hand, measurements taken on the road [34] are conducted in uncontrolled, real–world conditions, and the methodology used differs significantly from laboratory methods.

Testing with a brake dynamometer

A brake dynamometer is a testing device or method that is used to simulate the conditions of a vehicle braking system in a laboratory environment. It works by applying a load to the brake system under test and measuring the force generated by the brake during operation. This allows for precise control and evaluation of the brake system's performance under different conditions, such as varying speeds and loads.

To use a brake dynamometer for testing brakes and generating brake PMs, the brake system to be tested is installed onto the dynamometer and connected to its load cell or torque transducer. The brake is then applied under various conditions, such as different speeds and loads, and its performance is evaluated. This evaluation can include measuring the stopping distance, fade resistance, and other characteristics of the brake system.

During testing, brake PMs are generated due to the friction generated between the brake pads and the rotor. These PMs can be collected using appropriate collection methods, such as filters or electrostatic precipitation, and then analysed using techniques such as microscopy or spectroscopy to determine their size, shape, composition, and other properties. [35–38].

Testing with a pin–on–disc tribometer

One method/device for measuring the wear and friction characteristics of brake pads or other brake components, under different conditions, is through testing with a pin–on–disc tribometer. The device consists of a rotating disc and a stationary pin that is pressed against the disc. The frictional force between the pin and disc is measured using a load cell or torque sensor, while the wear of the materials is measured using a profilometer or other measuring devices.

To use a pin–on–disc tribometer, the disc and pin are installed onto the device and brought into contact with each other. The load is then applied to the system, and the disc is rotated at a specified speed. The pin is pressed against the disc with a specified force, and the frictional force between the two materials is measured using the load cell or torque sensor. The test can be run for a specified duration or until a specified amount of wear has occurred.

These wear debris particles can be in the form of particulate matter (PM), which may contain harmful substances such as metals or other toxins.

To measure the PMs generated during testing, appropriate collection methods can be employed, such as using filters or electrostatic precipitation. These methods allow for the collection of wear debris particles in a controlled manner, which can then be analysed using techniques such as microscopy or spectroscopy. These analyses can provide valuable information on the size, shape, composition, and other properties of the wear debris particles [35][37].

On–road testing and measurement

In order to measure emissions under real conditions, it is necessary to conduct on–road testing. This method involves driving a vehicle on a designated test route that is designed to represent typical driving conditions. The route includes various driving conditions, including city, suburban, and highway driving, as well as different braking regimes and speeds. During testing, various instruments are used to measure the emissions produced by the vehicle, including sensors and specialised instruments for measuring particulate matter (PM) [39].

On–road testing is also a method used to evaluate brake performance under real driving conditions. It is important to note that on–road testing has some limitations due to the difficulty in controlling all the variables that can affect brake performance, such as road surface, weather conditions, and traffic flows. On–road testing is usually used in combination with other testing methods, as well as with different measuring instruments [35][40].

REGULATION AND PROPOSED STANDARDISED MEASUREMENT PROCESSES

Since the 1990s, regulations have limited PM emissions from vehicles by collecting PM from exhaust gases and measuring their concentration. The PN method was introduced in Europe in 2011 to improve testing methodology. While stricter regulations on exhaust emissions have reduced particle emissions, non–exhaust PM, from the wear of brakes and tires, has become a new concern. It accounts for nearly half of all PM generated from road transport processes [41]. Despite efforts to develop electrification strategies for road transport, even a fully electric vehicles still emit non–exhaust particles in significant quantities [42].

The above–mentioned scenario has required the development of a set of regulations and legal acts that will address this issue over the past decade. In this regard, the United Nations Economic Commission for Europe (UNECE) has developed a proposal for a new United Nations Global Technical Regulation (UN GTR) [43] based on the Worldwide Harmonized Light Vehicle Test Procedures (WLTP), which represents a regulation for defining harmonised laboratory procedures for testing particle emissions resulting from brake wear in light vehicles, with a maximum allowed mass of up to 3500 kg. The aim of the UN GTR is to improve understanding of different brake systems, reduce inconsistencies, and emissions through a harmonised approach to measuring brake particle emissions.

The regulation resulted from the Non–Road Transport PMP Informal Working Group, which was hired by UNECE VP.29 to study non–exhaust particles from road transport, focusing on brakes and tires as the most relevant sources. The group developed new testing cycles to simulate real–world conditions and established guidelines for reporting brake wear particles. UN GTR provides a globally harmonised methodology for measuring brake wear particles in light–duty vehicles in laboratory conditions, but it doesn't cover other vehicle categories (such as off–road vehicles, special purpose vehicles, etc.).

Test execution

Testing brake emissions consists of three segments, each requiring one or more cycles (trips) under certain conditions. The test itself is performed during the deceleration or stopping process, as this is the way to activate the brake system and, thus the precondition for the formation of particles. The mentioned three segments are:

- Brake cooling adjustment [43] – is process used to standardise and uniform the conditions for testing brakes in different locations and under different real conditions involves adjusting the level of airflow and its velocity, taking into account the design and size of the brake housing and the arrangement and geometry of the air duct system. This process is essential to ensure consistent and comparable results under all testing conditions. This section uses Trip #10 of the WLTP Brake cycle.
- Brake bedding [43] – is necessary to pre–test the brake pair under appropriate conditions and stabilise its response before measuring emissions. This procedure should be carried out either with the same brake pairs used during the brake cooling adjustment segment or with completely new brakes, evaluated after cooling adjustment. This procedure must be carried out for all brake pairs on the front and rear. This section uses five repetitions of the WLTP–Brake cycle.
- Brake emissions measurement [43] – defines the conditions for measuring particle emissions (PM) during brake testing, which the measuring system must meet. The sampling system determines the amount of PM produced by the brakes during the test itself. PM emissions and testing parameters should be presented as particle mass per distance travelled, for the brake pair being tested. It is necessary to assess emissions for both PM_{10} and $PM_{2.5}$ during testing, using separate sampling systems for each threshold (2.5 μm

and 10 µm). This section includes one performance of the WLTP–Brake cycle.

Each of the parameters, requirements of the system, procedures, and trips that further define the aforementioned segments are described in detail in the regulation itself and the WLTP procedure on which the regulation is based.

Minimum requirements for test equipment and automation

It is important to note the minimum testing system requirements (dynamometer and automation) prescribed by the regulation. The diagram illustrating the principle of the brake dynamometer testing system, as shown below, indicates the interactions with the essential subsystems needed to conduct brake emission tests according to UN GTR.

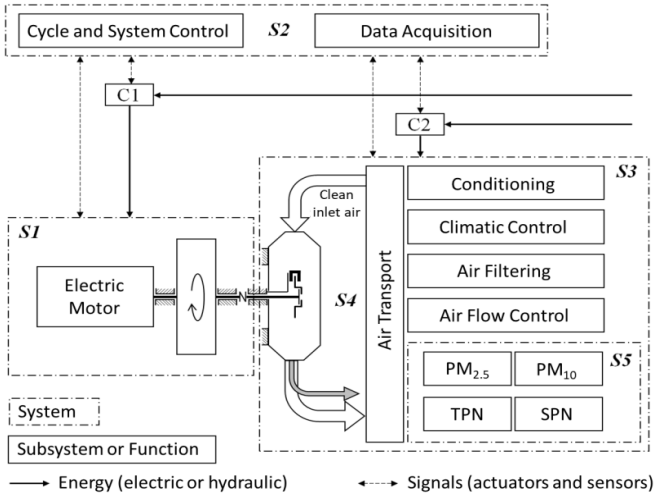

Figure 3. Layout of the test system with the brake dynamometer, where S1: Brake dynamometer, S2: Automation, control, and data acquisition system, S3: Climatic conditioning unit, S4: Brake enclosure and sampling plane, S5: Emissions measurement system. C1 and C2: Testing facility energy controls and monitoring system. The grey arrow represents the aerosol sample from the brake under testing [43].

The brake dynamometer must comprise the following components at a minimum [43]:

- An electric motor that can vary the rotational speed or maintain it at a constant rate. This motor is also responsible for adjusting the test inertia to simulate actual driving conditions and non–friction braking.
- A servo controller, either hydraulic or electric, that activates the brake being tested.
- A mechanical assembly that facilitates the mounting of the brake being tested, permits the disc or drum to rotate freely, and absorbs the reaction forces produced by braking.
- A robust framework that houses all the mandatory subsystems. The framework must have the capacity to withstand the forces and torque generated by the brake under testing.
- Sensors and devices that gather data and supervise the operation of the testing system.

The automation system performs crucial functions for the brake emissions test. It should accelerate and maintain constant speed during acceleration and cruise events, respectively, while reducing the kinetic energy of rotating masses by modulating the frictional torque during deceleration events. Besides, the system should provide an interface to the operator, stores test data, and manages communication with other testing facility systems.

During deceleration events, the automation system uses active torque control to increase or decrease the total effective test inertia. The electric motor can absorb some kinetic energy equivalent to the road loads and non–friction braking from the vehicle's powertrain.

Also, the test system software must have the following functions: automatically execute the driving cycle and closed–loop processes (primarily for brake controls, cooling air handling, and emissions measurements); continuously record data from all relevant sensors to produce specified outputs; and monitor signals, messages, alarms, and emergency stops from the operator and [43].

CONCLUSIONS

Non–exhaust emissions from motor vehicles, such as those generated by the brake system, tire wear, and road surface, contribute significantly to the overall level of pollutants generated by traffic, and have been found to have a substantial impact on human health. Exposure to PM from motor vehicle emissions has been linked to respiratory problems, cardiovascular disease, neurodegenerative phenomena, and cognitive disorders.

It is clear that the impact of PMs on human health represents an additional threat for chronically ill individuals and those susceptible to rapid changes in health status. The study provides a detailed overview of previous research that examined non–exhaust emissions and their impact on human health, as well as a review of methods for measuring non–exhaust emissions generated by the brake system.

The research concludes that while the scientific community's interest in studying brake emissions is increasing, the vast majority of research findings are inconsistent and vary widely, introducing a significant degree of uncertainty when attempting to assess the contribution of brake emissions to overall particulate matter emissions.

However, with the release of the proposal for a new United Nations Global Technical Regulation (UN GTR) it will now be easier to obtain more reliable data through standardised methods for brake lab testing. This is a significant development as it will lead to more accurate information on the contribution of brake emissions to overall PM emissions and will help policymakers take more effective measures to limit exposure to these harmful

pollutants. Precise measurements can inform the development of new regulations on the amount of particles that brakes can produce, conditional on the use of suitable materials and technologies in the production process. In addition, standardised data on the level of PM can significantly influence the recommendation and development of EURO7 norms [44], which will entail restrictions in the domain of non–exhaust emissions in general.

On another note, by adopting and implementing an effective braking process that is tailored to specific conditions, harmful emissions could significantly be reduce, thus improving human health and the environment, which may require additional research.

It is important to continue to monitor research and develop new methodologies to improve our understanding of the impact of non–exhaust emissions on human health, and to implement measures to reduce these emissions in the future.

Note: This paper was presented at DEMI 2023 – 16th International Conference on Accomplishments in Mechanical and Industrial Engineering, organized by Faculty of Mechanical Engineering, University of Banja Luka (BOSNIA & HERZEGOVINA), co–organized with the Faculty of Mechanical Engineering University of Niš (SERBIA), Faculty of Mechanical Engineering University of Podgorica (MONTENEGRO), Faculty of Engineering Hunedoara, University Politehnica Timișoara (ROMANIA) and Reykjavik University (ICELAND), in Banja Luka (BOSNIA & HERZEGOVINA), in 01–02 June, 2023.

References

[1] Zhu, C., Maharajan, K., Liu, K., & Zhang, Y. (2021). Role of atmospheric particulate matter exposure in COVID–19 and other health risks in human: A review. Environmental Research, 198, 111281

[2] Liu, Y., Chen, H., Gao, J., Li, Y., Dave, K., Chen, J., ... & Perricone, G. (2021). Comparative analysis of non–exhaust airborne particles from electric and internal combustion engine vehicles. Journal of Hazardous Materials, 420, 126626

[3] Stafoggia, M., & Faustini, A. (2018). Impact on public health—epidemiological studies: a review of epidemiological studies on non–exhaust particles: identification of gaps and future needs. Non–exhaust emissions, 67–88. Department of Epidemiology, Lazio Region Health Service/ASL Roma 1, Rome, Italy

[4] Grunig, G., Marsh, L. M., Esmaeil, N., Jackson, K., Gordon, T., Reibman, J., ... & Park, S. H. (2014). Perspective: ambient air pollution: inflammatory response and effects on the lung's vasculature. Pulmonary circulation, 4(1), 25–35

[5] Vimercati, L. (2011). Traffic related air pollution and respiratory morbidity. Lung India: official organ of Indian Chest Society, 28(4), 238

[6] Bourdrel, T., Bind, M. A., Béjot, Y., Morel, O., & Argacha, J. F. (2017). Cardiovascular effects of air pollution. Archives of cardiovascular diseases, 110(11), 634–642

[7] Polichetti, G., Cocco, S., Spinali, A., Trimarco, V., & Nunziata, A. (2009). Effects of particulate matter (PM(10), PM(2.5) and PM(1)) on the cardiovascular system. Toxicology, 261(1–2), 1–8

[8] Cristaldi, A., Fiore, M., Oliveri Conti, G., Pulvirenti, E., Favara, C., Grasso, A., Copat, C., & Ferrante, M. (2022). Possible association between $PM_{2.5}$ and neurodegenerative diseases: A systematic review. Environmental research, 208, 112581

[9] Costa, L. G., Cole, T. B., Dao, K., Chang, Y. C., Coburn, J., & Garrick, J. M. (2020). Effects of air pollution on the nervous system and its possible role in neurodevelopmental and neurodegenerative disorders. Pharmacology & therapeutics, 210, 107523

[10] Pant, P., & Harrison, R. M. (2013). Estimation of the contribution of road traffic emissions to particulate matter concentrations from field measurements: A review. Atmospheric environment, 77, 78–97

[11] Guerreiro, C., Leeuw, F., Foltescu, V., et al. (2015). Air quality in Europe – 2014 report. European Environment Agency, Publications Office Technical Report No 5/2014

[12] Horálek, J., Guerreiro, C., Viana, M., et al. (2016). Air quality in Europe – 2016 report. European Environment Agency, Publications Office, Technical Report No 28/2016

[13] Moshammer, H., Forsberg, B., Künzli, N., & Medina, S. (2009). Improving Knowledge and Communication for Decision Making on Air Pollution and Health in Europe (Aphekom). Epidemiology, 20(6), S232–S233

[14] Adamiec, E. (2017). Chemical fractionation and mobility of traffic–related elements in road environments. Environmental Geochemistry and Health, 39(6), 1457–1468

[15] GBoDC, N. (2017). Global Burden of Disease Study 2016 (GBD 2016) disability weights. Seattle, Washington:(IHME) IfHMaE.

[16] Jheng, Y. T., Putri, D. U., Chuang, H. C., Lee, K. Y., Chou, H. C., Wang, S. Y., & Han, C. L. (2021). Prolonged exposure to traffic–related particulate matter and gaseous pollutants implicate distinct molecular mechanisms of lung injury in rats. Particle and fibre toxicology, 18(1), 1–16

[17] Chuang, K. J., Lin, L. Y., Ho, K. F., & Su, C. T. (2020). Traffic–related PM2. 5 exposure and its cardiovascular effects among healthy commuters in Taipei, Taiwan. Atmospheric Environment: X, 7, 100084

[18] Kaur, S., Nieuwenhuijsen, M. J., & Colvile, R. N. (2007). Fine particulate matter and carbon monoxide exposure concentrations in urban street transport microenvironments. Atmospheric Environment, 41(23), 4781–4810

[19] Straffelini, G., & Gialanella, S. (2021). Airborne particulate matter from brake systems: An assessment of the relevant tribological formation mechanisms. Wear, 478, 203883

[20] Yang, L., Li, C., and Tang, X. (2020). The impact of PM2. 5 on the host defense of respiratory system. Frontiers in cell and developmental biology, 8, 91

[21] Abating Potentially Dangerous Particles 2.5 µm and Smaller. From: https://www.semiconductor–digest.com/abating–potentially–dangerous–particles–2–5m–and–smaller/, accessed on: December 21st , 2022.

[22] Penetration of Particles into the Human Body. From:https://seetheair.org/2021/03/01/penetration–of–particles–into–the–human–body/. accessed on: February 11th, 2023.

[23] Gonet, T., & Maher, B. A. (2019). Airborne, vehicle–derived Fe–bearing nanoparticles in the urban environment: a review. Environmental Science & Technology, 53(17), 9970–9991

[24] Sydbom, A., Blomberg, A., Parnia, S., Stenfors, N., Sandström, T., & Dahlen, S. E. (2001). Health effects of diesel exhaust emissions. European Respiratory Journal, 17(4), 733–746

[25] Wang, G., Jiang, R., Zhao, Z., & Song, W. (2013). Effects of ozone and fine particulate matter (PM2. 5) on rat system inflammation and cardiac function. Toxicology letters, 217(1), 23–33

[26] Wold, L. E., Ying, Z., Hutchinson, K. R., Velten, M., Gorr, M. W., Velten, C., ... & Rajagopalan, S. (2012). Cardiovascular remodeling in response to long–term exposure to fine particulate matter air pollution. Circulation: Heart Failure, 5(4), 452–461

[27] Ying, Z., Xu, X., Bai, Y., Zhong, J., Chen, M., Liang, Y., ... & Rajagopalan, S. (2014). Long–term exposure to concentrated ambient PM2. 5 increases mouse blood pressure through abnormal activation of the sympathetic nervous system: a role for hypothalamic inflammation. Environmental health perspectives, 122(1), 79–86

[28] von Mikecz, A., & Schikowski, T. (2020). Effects of airborne nanoparticles on the nervous system: Amyloid protein aggregation, neurodegeneration and neurodegenerative diseases. Nanomaterials, 10(7), 1349

[29] Thal, D. R., Grinberg, L. T., & Attems, J. (2012). Vascular dementia: different forms of vessel disorders contribute to the development of dementia in the elderly brain. Experimental gerontology, 47(11), 816–824
[30] Calderón–Garcidueñas, L., Reynoso–Robles, R., & González–Maciel, A. (2019). Combustion and friction–derived nanoparticles and industrial–sourced nanoparticles: The culprit of Alzheimer and Parkinson's diseases. Environmental research, 176, 108574
[31] Schikowski, T., & Altug, H. (2020). The role of air pollution in cognitive impairment and decline. Neurochemistry International, 104708
[32] Liu, B., Fang, X., Strodl, E., He, G., Ruan, Z., Wang, X., ... & Chen, W. (2022). Fetal Exposure to Air Pollution in Late Pregnancy Significantly Increases ADHD–Risk Behavior in Early Childhood. International Journal of Environmental Research and Public Health, 19(17), 10482
[33] Huber, M. P., Fischer, P., Mamakos, A., Steiner, G., & Klug, A. (2022). Measuring Brake Wear Particles with a Real–Driving Emissions Sampling System on a Brake Dynamometer (No. 2022–01–1180). SAE Technical Paper
[34] Mathissen, M., Grochowicz, J., Schmidt, C., Vogt, R., zum Hagen, F. H. F., Grabiec, T., ... & Grigoratos, T. (2018). A novel real–world braking cycle for studying brake wear particle emissions. Wear, 414, 219–226
[35] Vasiljević, J. Glišović, N. Stojanović i I. Grujić (2021). An overview of non–exhaust brake emission measuring methods. 15th International Conference on Accomplishments in Mechanical and Industrial Engineering – DEMI. Banja Luka.
[36] Park, J., Joo, B., Seo, H., Song, W., Lee, J. J., Lee, W. K., & Jang, H. (2021). Analysis of wear induced particle emissions from brake pads during the worldwide harmonized light vehicles test procedure (WLTP). Wear, 466, 203539
[37] Wahlström, J., Leonardi, M., Tu, M., Lyu, Y., Perricone, G., Gialanella, S., & Olofsson, U. (2020). A study of the effect of brake pad scorching on tribology and airborne particle emissions. Atmosphere, 11(5), 488
[38] Hagino, H., Oyama, M., & Sasaki, S. (2015). Airborne brake wear particle emission due to braking and accelerating. Wear, 334, 44–48
[39] zum Hagen, F. H. F., Mathissen, M., Grabiec, T., Hennicke, T., Rettig, M., Grochowicz, J., ... and Benter, T. (2019). On–road vehicle measurements of brake wear particle emissions. Atmospheric Environment, 217, 116943
[40] Oroumiyeh, F., & Zhu, Y. (2021). Brake and tire particles measured from on–road vehicles: Effects of vehicle mass and braking intensity. Atmospheric Environment: X, 12, 100121
[41] Grigoratos, T., Mamakos, A., Arndt, M., Lugovyy, D., Anderson, R., Hafenmayer, C., ... & Giechaskiel, B. (2023). Characterization of Particle Number Setups for Measuring Brake Particle Emissions and Comparison with Exhaust Setups. Atmosphere, 14(1), 103
[42] Woo, S. H., Jang, H., Lee, S. B., & Lee, S. (2022). Comparison of total PM emissions emitted from electric and internal combustion engine vehicles: An experimental analysis. Science of The Total Environment, 842, 156961
[43] UN GTR (ECE/TRANS/WP.29/AC.3/59). (2023). Proposal for a new UN GTR on Laboratory Measurement of Brake Emissions for Light–Duty Vehicles. UNECE (United Nations Economic Comission for Europe), Informal Working Group on Particulate Measurement Programme, Eighty–seventh session, Geneve.
[44] 2022/0365 (COD). (2022). Proposal for a Regulation of the European Parliament and of the Council on Type–Approval of Motor Vehicles and Engines and of Systems, Components and Separate Technical Units Intended for Such Vehicles, with Respect to Their Emissions and Battery Durability (Euro 7) and Repealing Regulations (EC) No 715/2007 and (EC) No 595/2009. European Commission. Brussels.

ISSN: 2067-3809

ACTA TECHNICA CORVINIENSIS – BULLETIN OF ENGINEERING
TOME XVI [2023] | FASCICULE 4 [OCTOBER – DECEMBER]

[1.]Dragan RODIĆ, [1.]Marin GOSTIMIROVIC, [1.]Milenko SEKULIC,
[1.]Borislav SAVKOVIC, [1.]Andjelko ALEKSIC

OPTIMIZATION SURFACE ROUGHNESS IN POWDER MIXED ELECTRICAL DISCHARGE MACHINING OF TITANIUM ALLOY

[1.] Department of Production Engineering, Faculty of Technical Sciences, University of Novi Sad, 21000 Novi Sad, SERBIA

Abstract: To further improve the efficiency of electrical discharge machining of advanced materials, the possible technological improvement of the process is achieved by adding graphite powder to the dielectric. In this study, the Taguchi approach was applied to determine the effects of input parameters such as discharge current, pulse duration, duty cycle, and graphite powder concentration on surface roughness in machining titanium alloys. L9 orthogonal array, signal–to–noise ratio (S/N), and ANOVA were used to design and analyze the experiment. Discharge current was determined to be the factor that had the strongest influence on surface roughness. Based on ANOVA, pulse duration was the second influential parameter, followed by graphite powder and duty cycle. In addition, an optimum condition was found to improve surface roughness. A discharge current of 1.5 A, a pulse duration of 32 µs, a duty cycle of 30% and a powder concentration of 12 g/l resulted in minimum surface roughness.
Keywords: Taguchi, surface quality, graphite powder, ANOVA, PMEDM

INTRODUCTION

Due to the combination of excellent mechanical properties and outstanding biocompatibility, titanium alloys are often used as a material for the manufacture of complex components. This is precisely why titanium alloys are difficult to process using classical methods, especially from the point of view of tool wear. When it comes to the production of complex parts, it is necessary to analyze the use of electrical discharge machining. In EDM, no mechanical stresses are introduced into the workpiece during machining because there is no direct contact between the electrode and the workpiece.

However, when machining titanium alloys with aluminium impurities, the EDM process becomes unstable and inefficient. In order to establish process stability and improve EDM performance, various researchers have proposed adding powder to the dielectric. In this way, one of the innovative processes called powder–mixed electrical discharge machining (PMEDM) was created.

Electrically conductive powder added to the dielectric reduces the insulating properties and causes an increase in the gap distance between the tool and the workpiece. This increase means a more efficient circulation of the dielectric, i.e. a washout of the working space between the tool and the workpiece. In this way, EDM becomes more stable, which improves the machining performances such as higher machining productivity and lower surface roughness, and also leads to a lower wear rate of the tools. The powder particles change the properties of the discharge channel, which equalises the distribution of sparks among the powder particles and thus reduces the current density [1]. Due to this uniform distribution of the discharges, there is uniform erosion, i.e. flat craters on the workpiece, which leads to a reduction in surface roughness and thus to an increase in machining accuracy.

Various types of electrically conductive powder can be mixed with liquid dielectric, including: aluminum, graphite, silicon, copper, silicon carbide and others. For example, Wong used powders of different electrical conductivity, such as graphite, silicon, aluminum, crushed glass, silicon carbide, and molybdenum sulfate, and studied their influence on the roughness of the treated surface [2]. He concluded that the powders: graphite (grain size 40 µm) and silicon (grain size 45 µm) gave the best results of surface roughness. A significant reduction in the surface roughness was obtained, i.e. Ra = 0.62 µm with silicon powder, while Ra = 0.75 µm was obtained with graphite powder, i.e. a surface with high gloss (mirror effect), which is the opposite of classical EDM, where mostly dull surfaces are obtained. What types of powders can be used with liquid dielectric, what particle size, at what concentration, and what effect they have on the performance of the PMEDM process have been studied by a small number of researchers.

Therefore, the introduction of an additional parameter, for example, the concentration of powder in the dielectric in PMEDM, is a challenge for many researchers. The analysis of the change of the surface roughness depending on the input parameters in PMEDM with chromium powder was processed in the work [3]. The

obtained results show that the discharge current and the concentration of the powder in the dielectric have the greatest influence on the surface roughness in machining carbon steel. By applying the response surface method, a model was created that allows the determination of optimal machining regimes, where the objective function was the minimum surface roughness. Interesting results of the research work on single–objective optimization of the PMEDM procedure are presented in the paper [4]. The aim of the research was to determine the optimal input parameters in PMEDM. Three types of tool steels were machined using three types of tools, first in a dielectric with aluminum mixture and then in a dielectric with graphite powder. In order to optimize the process, Taguchi method was applied according to the experimental plan L27. Based on the Taguchi method, different optimal machining input parameters were determined for the different steels, representing the complexity of the PMEDM system.

Determining the optimal processing parameters for PMEDM remains a topical problem, as evidenced by the numerous research papers on the subject. There is still no concrete answer to the question of which powder concentration gives the best processing performance. Therefore, the main objective of this research is to determine the optimal machining parameters using the Taguchi approach. A single–objective optimization was performed by adjusting input parameters such as discharge current, pulse duration, duty cycle, and graphite powder concentration to achieve minimum surface roughness when machining titanium alloys.

MATERIAL AND METHODS

In the present study, a titanium alloy ($TiAl_4V_6$) was chosen as the workpiece material. The experiments are carried out on an Agie Charmie SP1–U die–sinking EDM machine. A commercial graphite electrode TTK50 with a cross section of 10x10 mm was used as the tool. The pure graphite powder with a particle size of 19 μm (Asbury PM19) was chosen as an additive for the dielectric fluid. In addition, the surfactant Tween 20 $C_{58}H_{114}O_{26}$ is added. The role of the surfactant is to ensure a homogeneous mixture of powder and dielectric during PMEDM. In order to conduct the experiments, a tank with supporting elements for PMEDM was designed, figure 1.

Finally, four input parameters were selected for this study from the preliminary experiments and the available literature on PMEDM [5, 6]. The input parameters were discharge current (Ie), pulse duration (ti), duty cycle (τ), and graphite powder concentration (GR). The conditions for processing titanium alloy are shown in table 1.

The Taguchi plan is a method that allows reducing the number of experimental points by orthogonal arrangements and minimizing the effects outside the influential parameters. It was applied in this study with the aim of more accurately optimizing and analyzing the influence of the input parameters on the tool wear rate. The processing parameters and their values are listed in Table 2. An experimental design according to the Taguchi orthogonal array L9 (34) was established.

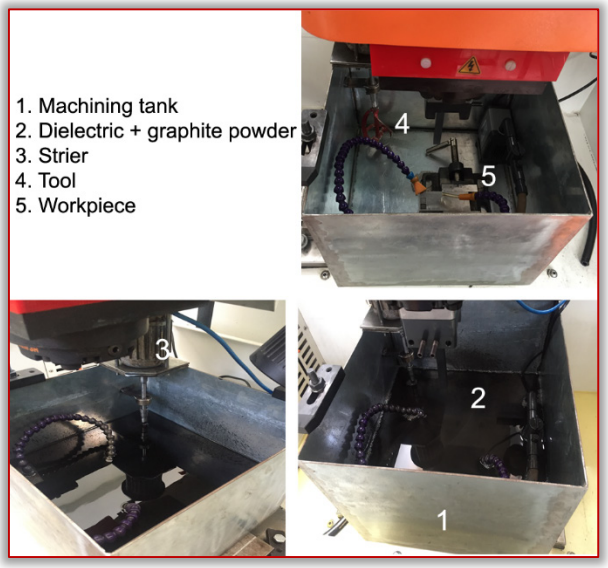

Figure 1. Setup of PMEDM.

Table 1. Machining conditions

Parameters of EDM	Label	Value	Units
Discharge current	I_e	1.5 ÷ 7.5	A
Pulse on time	t_i	24 ÷ 240	μs
Pulse off time	t_o	24 ÷ 240	μs
Open circuit voltage	U_0	100	V
Polarity	Pol	(–)	/
Duty factor	τ	30 ÷ 70	%

Table 2. Taguchi orthogonal array L9 (3^4) at PMEDM $TiAl_6V_4$

No.	Factor				Surface roughness	
	I_e (A)	t_i (μs)	τ (%)	GR g/l	Ra (μm)	S/N
1.	1.5	32	30	0	1.78	–5.01
2.	1.5	75	50	6	2.01	–6.06
3.	1.5	180	70	12	2.61	–8.33
4.	3.2	32	50	12	3.47	–10.81
5.	3.2	75	70	0	4.11	–12.27
6.	3.2	180	30	6	4.47	–13.01
7.	6.0	32	70	6	8.12	–18.19
8.	6.0	75	30	12	7.16	–17.09
9.	6.0	180	50	0	9.84	–19.86

RESULTS AND DISCUSSION

For single objective parameter optimization, the Taguchi method was used, where the output Ra was optimized based on the Taguchi orthogonal array L9 (3^4) for PMEDM titanium alloy. This method does not require the creation of a mathematical model and is an alternative approach to identifying optimal input parameters. The MiniTab 17 software tool was used for statistical data processing. Based on the measured Ra values, the S/N ratio was

calculated for all 9 experiments. The values of the S/N ratio for Ra are calculated based on the Taguchi quality feature "Smaller is better", Table 2.

Table 3 shows the S/N ratios with each factor and the corresponding level for surface roughness. The factors with the largest difference in mean values (max–min) have the greatest influence on the output size. The table shows that discharge current has the greatest influence on Ra, followed by pulse duration, duty cycle and graphite powder concentration.

Table 3. Response table of S/N ratio for surface roughness

Factors	Levels			min–max	Rang
	1	2	3		
(A) Ie	–6.46	–12.03	–18.38	11.91	1
(B) ti	–11.33	–11.81	–13.73	2.39	2
(C) τ	–11.71	–12.24	–12.93	1.22	3
(D) GR	–12.38	–12.42	–12.07	0.34	4

The influence of individual input parameters on the output power of the processing process can be illustrated with the help of a reaction diagram showing the change of the S/N ratio at the moment of changing the level of the control parameter from 1 to 3. Accordingly, the influence of individual parameters on the output characteristics of the processing process is graphically expressed by an angle of the slope of the line connecting different levels of the parameters.

Looking at the slope of the lines, we can see that the steepest line applies to factor A, then B, then C, and finally D. This order corresponds to the calculated rank (Table 7–2). According to Figure 2, the highest S/N ratio indicates the optimal level of each factor. Therefore, based on the "smaller is better" criterion, the optimum combination of the PMEDM titanium alloy input parameters as a function of surface roughness is A=1, B=1, C=1 and D=3.

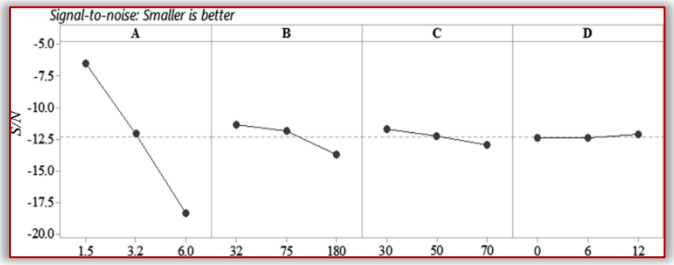

Figure 2. Graphic representation of the S/N ratio for Ra

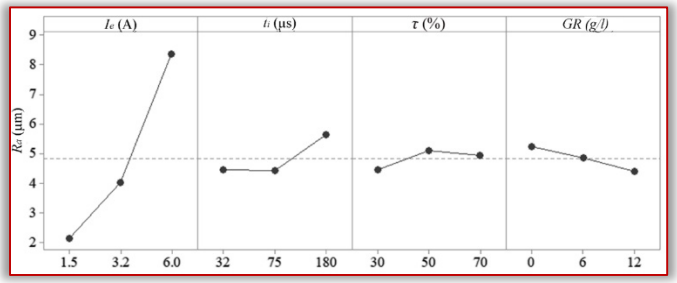

Figure 3. Response ANOVA graph for the Ra

The prediction of the output power value (Ra = 1.72 µm) and the calculation of the corresponding S/N ratio (S/N = –19.42) based on the optimal combination of input parameters can be found in Table 4.

Based on the ANOVA analysis performed using the F–test, the influence, i.e., the percentage involvement of each factor in PMEDM titanium alloy on surface roughness can be seen. Factors with an F–value of less than 1 were excluded from the analysis, which was the case for the impulse action coefficient (factor C) and the concentration of graphite powder (factor D). After excluding insignificant factors, the analysis ANOVA for the remaining members is shown in the reduced Table 5, where the percentage participation for factors A and B is given. Discharge current has the greatest influence on the mean arithmetic roughness of the treated surface, with a percentage of 93.08%. The percentage of 4.35% is taken by the pulse length for the set processing conditions. The presented ANOVA analysis confirms the results obtained with the Taguchi method.

Table 4. Optimal setting of input parameters with confirmation experiment

Input	Level	Value	Ra	Confirmation experiment
I_e (A)	1	1.5	S/N = –4.71	Ra=1.62 µm
t_i (µs)	1	32		
τ (%)	1	30	Ra = 1.72 µm	
GR (g/l)	3	12		

The average error between the EDM output values obtained by prediction based on Taguchi analysis and the values obtained after the verification experiments (with optimal input parameter values) was only 5.8%. Therefore, the single–objective optimization of the input parameters of the PMEDM can be considered successful. This analysis confirmed the order of influence of input parameters during processing compared to published research on PMEDM titanium alloys.

Table 5. Reduced ANOVA table for Ra

Source	DF	Sum sq	Mean sq	F–value	Percent %
A – I_e	2	61.465	30.7325	72.55	93.08
B – t_i	2	2.873	1.4367	3.39	4.35
D – GR	4	1.694	0.4236		2.57
Error	8	66.033			
Total	2	61.465	30.7325	72.55	93.08

In addition to discharge current, which had the greatest influence on Ra as expected, pulse duration, duty cycle, and graphite powder concentration had less influence than expected. This can be explained by the results of the preliminary tests. The explanation for excluding duty cycle from the analysis of ANOVA is justified by the fact that this parameter does not have a significant effect on surface roughness at relatively short pulse durations, up to 180 µs in this study. A significant effect of the pulse action

coefficient is expected for values of pulse length greater than 200 μs, since a higher discharge energy occurs. A higher discharge energy has a detrimental effect on the surface roughness of titanium alloy if the pause duration is too short (calculated in τ > 90%), which has been confirmed in research [7].

CONCLUSION

The aim of this study is to optimize Ra using the Taguchi approach and to determine the influence of the main input factors. Based on the experimental and statistical results, the discharge current (Ie), pulse duration (ti), duty cycle (τ) and graphite powder concentration (GR) were the main factors that affected the Ra. According to the Taguchi method, the discharge current has the greatest influence on Ra, followed by the pulse duration, duty cycle, and graphite powder concentration. This statement was confirmed by the ANOVA analysis using the F–test. The influence, i.e. percentage participation of each factor in PMEDM titanium alloy on surface roughness for discharge current is 93.08%. The percentage of 4.35% is taken by the pulse duration for the specified machining conditions. Based on the "smaller is better" criterion, the optimal combination of PMEDM input parameters for the titanium alloy as a function of surface roughness is A=1, B=1, C=1, and D=3. The prediction of the output power gave a value of Ra = 1.72 μm, while the confirming experiment gave a value of 1.66 μm. Therefore, the single–objective optimization of the input parameters of the PMEDM can be considered successful. Although the analysis of ANOVA showed that graphite powder has no influence, the minimum Ra value is achieved with a concentration of 12 g/l. Future research should focus on wider intervals of input factors as well as on different powder types.

Acknowledgement

This paper has been supported by the Provincial Secretariat for Higher Education and Scientific Research through the project no. 142–451–1772/2022–01/01: "Research on the innovative process of electrical discharge machining of titanium alloy".

Note: This paper was presented at DEMI 2023 – 16th International Conference on Accomplishments in Mechanical and Industrial Engineering, organized by Faculty of Mechanical Engineering, University of Banja Luka (BOSNIA & HERZEGOVINA), co–organized with the Faculty of Mechanical Engineering University of Niš (SERBIA), Faculty of Mechanical Engineering University of Podgorica (MONTENEGRO), Faculty of Engineering Hunedoara, University Politehnica Timișoara (ROMANIA) and Reykjavik University (ICELAND), in Banja Luka (BOSNIA & HERZEGOVINA), in 01–02 June, 2023

References

[1] Ramana, P., Kharub M., Singh J.,Singh J. (2021). On material removal and tool wear rate in powder contained electric discharge machining of die steels. Materials Today: Proceedings, Vol. 38, pp. 2411–2416.

[2] Wong, Y.S., Lim L.C., Rahuman I.,Tee W.M. (1998). Near–mirror–finish phenomenon in EDM using powder–mixed dielectric. Journal of Materials Processing Technology, Vol. 79, pp. 30–40.

[3] Ojha, K., Garg R.K.,Singh K.K. (2013). Effect of chromium powder suspended dielectric on surface roughness in PMEDM process. Tribology – Materials, Surfaces & Interfaces, Vol. 5, pp. 165–171.

[4] Bhattacharya, A., Batish A., Singh G.,Singla V.K. (2011). Optimal parameter settings for rough and finish machining of die steels in powder–mixed EDM. The International Journal of Advanced Manufacturing Technology, Vol. 61, pp. 537–548.

[5] Hasçalık, A.,Çaydaş U. (2007). Electrical discharge machining of titanium alloy (Ti–6Al–4V). Applied surface science, Vol. 253, pp. 9007–9016.

[6] Huu–Phan, N., Tien–Long B., Quang–Dung L., Duc–Toan N.,Muthuramalingam T. (2019). Multi–criteria decision making using preferential selection index in titanium based die–sinking PMEDM. Journal of the Korean Society for Precision Engineering, Vol. 36, pp. 793–802.

[7] Kumar, M., Datta S.,Kumar R. (2018). Electro–discharge Machining Performance of Ti–6Al–4V Alloy: Studies on Parametric Effect and Phenomenon of Electrode Wear. Arabian Journal for Science and Engineering, pp. 1–16.

ISSN: 2067-3809

[1.] Bethany BRONKEMA, [1.] Gudrún SÆVARSDÓTTIR, [1.] David C. FINGER

LIFE–CYCLE COMPARISON OF THE HALL–HEROULT PROCESS, INERT ELECTRODES, AND ENERGY SUPPLY IN ALUMINUM PRODUCTION

[1.] School of Engineering, Reykjavik University, Menntavegur 1, 102 Reykjavik, ICELAND

Abstract: Aluminum (Al) production consumes 14 kWh of electricity per kg Al and produces 1.1 billion tonnes of carbon emissions ($CO_{2,eq}$) annually. The Hall–Heroult process is currently the only industrial process for Al production, producing two tonnes of $CO_{2,eq}$ per tonne Al by carbon anode electrolysis. Electrodes that do not participate in the electrolysis of alumina can reduce the impact of Al production. Transitioning to inert anodes implies redesign of electrolysis cells to optimize energy requirements. We performed a life–cycle analysis to compare the ecological footprint of Hall–Heroult and inert production using GaBi software and the ecoinvent database, complemented with primary data. Results were calculated for two Hall–Heroult and fifteen inert scenarios, varying power between 13.5 kWh and 17 kWh for six different energy mixes: Icelandic hydropower, global mix, natural gas, coal, nuclear, and geothermal. A final "best–case" scenario uses hydropower data as the power source for alumina refinement (shown in electrolysis) .The results reveal that the energy mix dominates the impact on the ecological footprint in the earlier refinement and electrolysis stages. However, using inert electrodes in smelters powered with renewable electricity can lower the carbon footprint of aluminum production by over 80%.

Keywords: aluminum production, inert anodes, LCA

INTRODUCTION

Aluminum production alone currently accounts for around 2% of global carbon dioxide emissions. To produce aluminum, bauxite ore is mined and refined to alumina, then processed by electrolysis requiring between 12 and 17 kWh per kg Al [8]. Conventionally, electrolysis requires anodes made of carbon, a feedstock of alumina (aluminum oxide), and electrical energy applied as a DC current in the Hall–Heroult process. The electrolysis produces pure liquid aluminum and carbon dioxide. Carbon monoxide is coevolved, as are smaller amounts of fluorocarbons and sulfur compounds due to impurities in the anodes.

$$1/2Al_2O_{3(solution)}+3/4C_{(s)}=Al_{(l)}+3/4CO_{2(g)}$$

and

$$1/2Al_2O_{3(solution)}+3/2C_{(s)}=Al_{(l)}+3/2CO_{(g)}$$

Carbon emissions also occur during the manufacturing of the carbon anodes [6].

Inert metal anodes (IMA), in place of carbon, can eliminate the carbon emissions from alumina electrolysis and limit those produced in anode production, substantially reducing the carbon footprint of the entire smelting process [8]. IMA evolve oxygen rather than carbon dioxide and other hydrocarbons.

$$1/2Al_2O_{3(solution)}=Al_{(l)}+3/4O_{2(g)}$$

Attempts to develop industry–level inert anodes with similar performance to the Hall–Heroult process started in the early 20th century. Anode research mainly focused on three classes of materials: ceramic, metal, and cermet [7]. In the 1990s The Aluminum Company of America – later, Alcoa – patented the process and apparatus for low temperature aluminum electrolysis, recommending the use of inert anodes composed of 17%wt Cu and 83%wt other oxides, namely NiO and Fe_2O_3. More recently, Padamata et al. confirmed the efficiency of Cu–Ni–Fe anodes in a 2018 review of industry progress. Cu–Ni–Fe anodes form protective oxide layers during electrolysis, slowing down the corrosive effects of the electrolyte [7]. Gunnarsson et al. (2019) revealed the production of Al with 99.22% purity using 20%wt Cu, 42%wt Ni, 38%wt Fe anode and TiB_2 cathode with a 21mm distance between vertical electrodes. This experiment produces low current efficiencies of 71–73%, but low rates of aluminum contamination by electrode material [2].

Directly substituting IMA into existing electrolytic cells would however increase the energy requirement for smelting plants by up to 25% as the reaction products are higher energy molecules [8]. Producing oxygen at the anode instead of carbon dioxide drives up the operating voltage by about one volt, corresponding to over a 3 kWh/kg Al electrical power increase [9]. According to Haupin and Kvande (2000), it is thermodynamically possible to operate inert anode cells at 13.2 kWh/kg Al by reducing the anode–cathode distance and thereby reducing the voltage drop across the electrolyte. Maintaining the power requirement at 13.5 kWh would require the electrolytic cells to be retrofitted [8]. In 1994, Moltech published U.S. Pat. No. 5,362,366 detailing an anode–cathode arrangement for non–consumable anodes and cathodes that maintains the efficiency of

conventional electrolysis. These arrangements primarily allow the new electrodes to be positioned vertically in existing cells, with groups of inert anodes filling the place conventionally filled by a single carbon anode [10].

La Camera et al. (1995) also rely on vertical arrangements to obtain low–temperature electrolysis results in their 1995 patent. Brown (2001) shows that considerable energy savings of up to 30% can be obtained by using vertical electrode cells (VEC) over conventional arrangements while also limiting operating costs due to the reduced rate of anode replacement. However, he also outlines substantial engineering challenges related to the implementation of VEC, namely electrode manufacturing and alumina–feeder technology [1].

In total, alumina electrolysis requires an anode, cathode, electrolyte, container, method of delivering electricity, alumina feeder, and product extraction system. Out of these elements, it is reasonable to assume that the container, method of delivering electricity, alumina feeder, and product extraction system could remain constant in a retrofit. In addition to the environmental aims of IMA, they also represent a potential for financial and occupational improvement [5]. As IMA theoretically do not participate in the electrolysis reaction, their slow rate of decomposition eliminates many costs associated with frequent replacement of carbon anodes. Anode changing also creates the highest exposure of aluminum workers to particulate matter and toxic gases from the process, so IMA have the potential to improve working conditions in smelters as well [5].

Around 70% of the global carbon dioxide emissions from aluminum smelting currently come from the high electrical energy requirements of the process. The Life Cycle Inventory (LCI) data published by the International Aluminium Institute (IAI) reveals that the geographic location of aluminum smelters and the corresponding energy mix had a significant environmental effect [12]. In a comparative LCA of smelting technologies including pre–baked and inert anodes, Kovács and Kiss (2015) also emphasize the importance of energy mix. However, their LCA does not include emission values related to the retrofit of the smelters required to minimize energy consumption. There is a need to understand how the IMA electrolysis process partnered with the costs of a retrofit compare to the Hall–Heroult process with various energy inputs.

This study aims to focus on the advantages of IMA compared to the Hall–Heroult process and to calculate a full LCA for different energy sources and requirements. In this study, we calculated the LCA for fifteen scenarios, addressing an energy requirement of 13.5 kWh/kg Al, 17 kWh/kg Al (corresponding to roughly a 25% increase), and six different energy mixes.

METHODS

To compare the LCA of inert anodes, carbon anodes, and different energy mixes we developed fifteen realistic scenarios (Table 1). For comparative purposes, a GaBi flow was constructed for the Hall–Heroult process to ensure consistent inputs with the modeled IMA process, such as electricity inputs and material flow datasets. The results from this flow are included as Scenarios I and II.

Table 1. Hall–Heroult and IMA scenarios

Scen no.	Process	Power Requirement*	Energy Source
I	HH	14.1**	Hydro
II	HH	14.1**	Global
III	Inert	13.5	Hydro
IV	Inert	17	Hydro
V	Inert	13.5	Global
VI	Inert	17	Global
VII	Inert	13.5	Natural Gas
VIII	Inert	17	Natural Gas
IX	Inert	13.5	Coal
X	Inert	17	Coal
XI	Inert	13.5	Nuclear
XII	Inert	17	Nuclear
XIII	Inert	13.5	Geothermal
XIV	Inert	17	Geothermal
XV	Inert	13.5	Hydro***

* kWh per kg Al; ** European average; *** including adjusting the electricity input for the alumina refinement stage

The full LCA was established by the ISO 14044 standards to define a goal and scope of the study. GaBi software by Sphera (Sphera Solutions Inc., 2021) was used to model the LCA process chain, calculate the impact categories, and perform a sensitivity analysis.

Goal

The goal of this LCA was to fully characterize the effect of a transition to inert electrodes on the aluminum production process. Values obtained from the modeling of inert electrodes were compared to those in the literature relating to carbon anodes in the Hall–Heroult process.

Scope Definition

Five main unit processes were considered in the model: the electrolytic smelter retrofit process, inert anode manufacturing, inert cathode manufacturing, electrolysis, and inert electrode recycling. These processes occur within the aluminum production chain between the refinement of alumina and the casting of ingots.

This LCA represents a gate–to–gate model within the aluminum production process, although it contains a cradle–to–grave model of the inert electrodes themselves.

The functional unit for this LCA was defined as 1 tonne Al. This is consistent with other aluminum–related LCAs, such as the one performed by the International Aluminium Industry (*Life Cycle Inventory (LCI) Data and Environmental Metrics*, 2017). In the individual unit processes 1 kilogram Al was used, which was then scaled up in the larger LCA. Electricity inputs to the system were implemented at the highest level of the LCA for ease of comparison. Adjustments to the electricity inputs were critical in comparing Icelandic energy mixes to global energy mixes in the different scenarios considered for the results of this LCA.

Impact Categories

GaBi Software and ecoinvent environmental quantities were used to assess the environmental impact of the constructed flow. Of the significant number of options available in the software, six impact categories were evaluated:

i) global warming potential over 100 years (GWP100),
ii) primary energy demand (PED),
iii) human toxicity potential (HTP),
iv) acidification potential (AP),
v) terrestric ecotoxicity potential (TETP), and
vi) freshwater use.

Sensitivity Analysis

Three main parameters were chosen as the subjects of a sensitivity analysis: the energy source, the method of alumina refinement, and the amount of anode and cathode required per kg of Al. The GWP100 was chosen as the main indicator of environmental impact.

RESULTS

The results of the LCA from the fifteen scenarios described by Table 1 were evaluated regarding the six impact categories: GWP100, PED, HTP, AP, TETP, and freshwater use.

Global Warming Potential

The GWP100 was calculated and is displayed in Figure 1. The scenario with the highest GWP100 is Scenario X (inert, 17kWh, coal) at 21,881 kg $CO_{2,\ eq}$ per tonne Al while the scenario with the lowest is Scenario XV (inert, 13.5kWh, hydro) at 820 kg $CO_{2,\ eq}$ per tonne Al.

Primary Energy Demand

The PED was calculated for all scenarios. These results are shown in Figure 2. Scenario X (inert, 17, coal) has the highest PED at 319,584 MJ per tonne Al and Scenario III has the lowest PED at 80,052 MJ per tonne Al.

Human Toxicity Potential

In Figure 3, the HTP for the Hall–Heroult and IMA scenarios is displayed. The highest HTP is 17,505 kg DCB_{eq} per tonne Al for Scenario II (HH, 14.1kWh, global) and the lowest HTP is 2,992 kg DCB_{eq} per tonne Al for Scenario XV (inert, 13.5kWh, hydro).

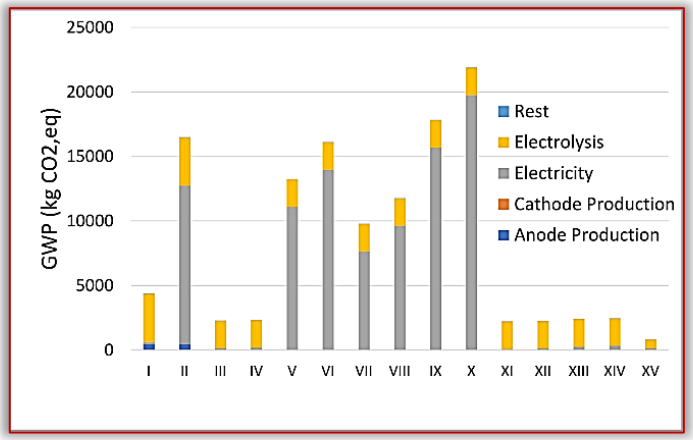

Figure 1. GWP100 for the fifteen scenarios

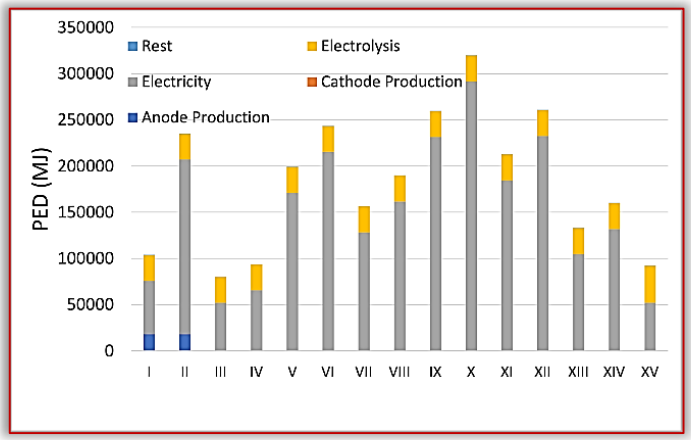

Figure 2. PED for the fifteen scenarios

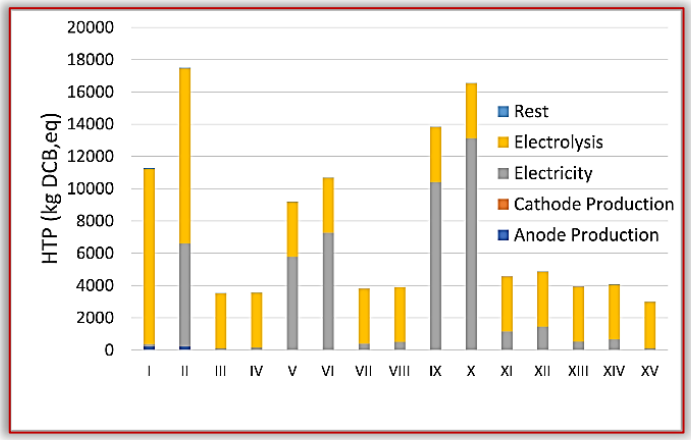

Figure 3. HTP for the fifteen scenarios

Acidification Potential

In Figure 4, the AP for the Hall–Heroult and IMA scenarios is displayed. The scenario with the highest AP is Scenario X (inert, 17kWh, coal) at 150 kg $SO_{2,\ eq}$ per tonne Al while the scenario with the lowest is Scenario XV (inert, 13.5kWh, hydro) at 15 kg $SO_{2,\ eq}$ per tonne Al.

Terrestric Toxicity Potential

In Figure 5, the TETP for the Hall–Heroult and IMA scenarios is displayed. Scenario X (inert, 17, coal) has the highest TETP at 70 kg DCB_{eq} per tonne Al and Scenario XV has the lowest TETP at 27 kg DCB_{eq} per tonne Al.

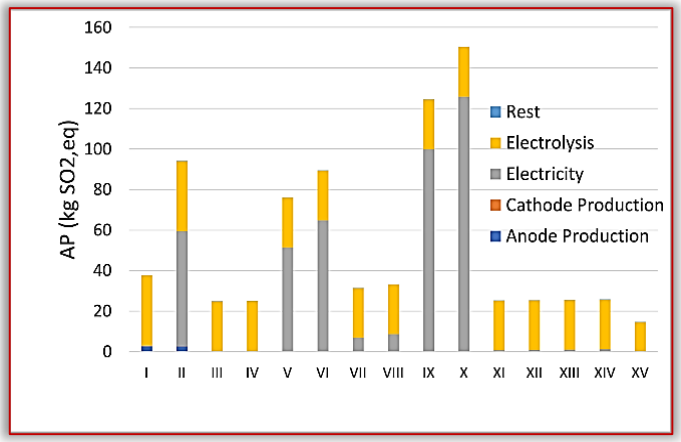

Figure 4. AP for the fifteen scenarios

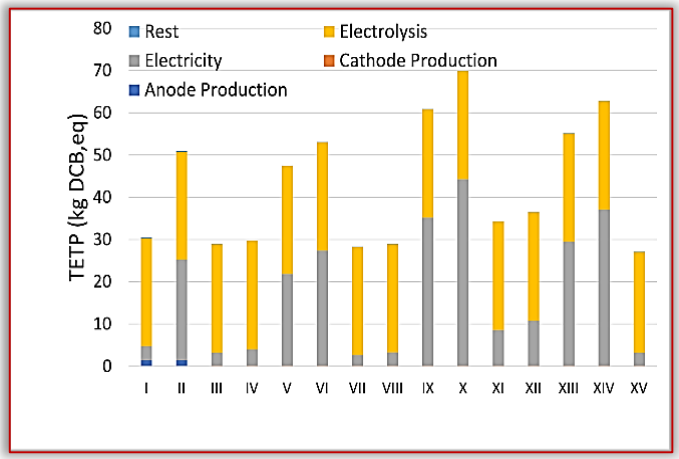

Figure 5. TETP for the fifteen scenarios

Freshwater Use

In Figure 6, the freshwater use for the Hall–Heroult process and the IMA scenarios is displayed. The highest freshwater use is 141,460,827 kg H_2O per tonne Al for Scenario IV (inert, 17 kWh, hydro) and the lowest freshwater use is 4,769,210 kg H_2O per tonne Al for Scenario VII (inert, 13.5kWh, gas).

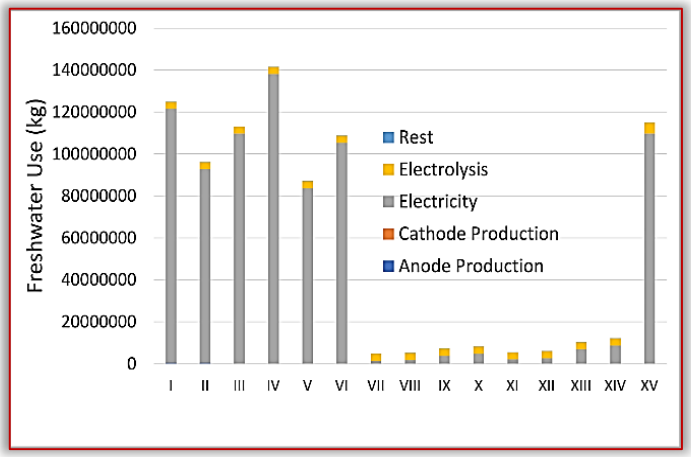

Figure 6. Freshwater use for the fifteen scenarios

DISCUSSIONS

Global Warming Potential

As expected, the transition to inert anodes offers significant $CO_{2,\,eq}$ emissions savings when the appropriate energy mix is used. Powering electrolysis with hydropower, much of the GWP in the HH process comes from anode production, direct emissions from the electrolysis process, and upstream emissions related to alumina production. Although the IMA process maintains these alumina–related emissions, the carbon emissions in the anode production and direct emissions from electrolysis are essentially eliminated. As relates to anode production, although the IMA technology this study is based upon require iron, nickel, and copper (metals not used in comparable quantities in the Hall–Heroult process) and so include in their LCA the corresponding production processes, this effect overall is quite small due to the anodes' long lifetimes and recyclability. The increase in energy requirement modeled in Scenario IV does little to alter these results when the energy source is Icelandic hydropower.

Using global energy mixes – Scenarios V and VI – alters these conclusions significantly. In Scenario V, GWP is still saved with a switch to IMA when the power requirement is 13.5 kWh per kilogram Al. As in Scenarios III and IV, this is primarily due to the reduction of emissions from the anode production and electrolysis processes. However, with the 17 kWh power requirement of Scenario VI, the GWP of HH and inert production become almost equal, with the HH process at 16,500 kg $CO_{2,\,eq}$ per tonne Al and the IMA process at 16,100 kg $CO_{2,\,eq}$. Scenarios VII to XIV display predictable results with coal–powered electricity producing the highest GWP, followed by natural gas, geothermal, and nuclear. Scenario XV displays the "best case scenario" for aluminum production, specifically for the case of alumina refinement in South America and smelting in Europe. These results were achieved by embedding hydropower data into the alumina refinement process, as well as maintaining the conditions from Scenario III. With a GWP of 820 kg $CO_{2,\,eq}$, Scenario XV represents an 81.4% GWP savings from Scenario I and a 64.0% GWP savings from Scenario III.

Primary Energy Demand

Following a similar trend to GWP, most of the PED savings offered by IMA come from the anode production stage. The fossil–based composition of carbon anodes adds significant chemical energy to the HH LCA and is eliminated in the IMA LCA, resulting in a 23.0% PED savings between Scenarios I and III. This percentage rises to 31.3% when the electrolysis portion of production is isolated by neglecting alumina refinement. For other scenarios, a general trend of PED due to energy source can be seen with coal as the highest, followed by nuclear, then global mix, then geothermal. Hydropower offers the lowest PED per tonne Al.

Human Toxicity Potential

The carbon anodes in the HH process are the primary cause of the sulphur and perfluorocarbon compounds

that affect HTP. Due to this, Scenario III shows a 68.7% reduction in HTP over Scenario I. In this impact category, the electrolysis process appears as the most significant factor as Scenario II tops even Scenario X. However, fluoride present in the electrolyte is the source of hydrofluoric acid emissions and electrolyte composition and interaction for IMA electrolysis is still a point of continued research.

Thus, reliable estimates of the HTP reduction requires further study. For IMA Scenarios VII to XIV, energy source again determines the trend with coal followed by nuclear, then natural gas, then geothermal.

Acidification Potential

Again due to sulphur compounds present in carbon anodes, IMA are able to offer AP savings over the HH process, with Scenario III having 34.2% less AP than Scenario I. Even with a global mix energy source – Scenarios II and V – IMA offers a 19.3% reduction. Other energy sources cause a decreasing trend with respect to coal, natural gas, geothermal, and nuclear.

Terrestric Toxicity Potential

As with other impact categories, the lack of carbon anodes in the IMA process leads to a reduction potential in TETP. Between the hydropower scenarios I and III there is a 5.3% TETP reduction and a 7.0% TETP reduction between the global mix scenarios II and V.

Other scenarios are listed in terms of decreasing TETP according to their energy mix: coal, geothermal, nuclear, natural gas.

Freshwater Use

Common trends for other impact categories are slightly altered for freshwater use, as hydropower uses substantial amounts of freshwater to generate electricity. For this reason, scenarios that include hydropower production – I, II, III, IV, V, VI, and VX – are significantly higher than all other energy mix scenarios.

Sensitivity Analysis

When focusing on GWP100 as the main environmental indicator, it was found that the source of electricity had the most significant impact on the results. When the global mix energy input was varied by 50% against a default energy source of hydropower, it produced an 18.3% effect on the results. Although the variance of alumina input also had an impact – 5.18% variance of the results with a 50% variation – this can be viewed as a sub–case of power source variation, already identified as the most significant contributor to GWP.

Finally, the electrode input amount had an extremely insignificant effect on the results. This is not surprising, as the longer lifetime and recyclability of the anodes allow their effect to be minimized in the LCA.

LCA Limitations and Future Research

Although LCA software and databases such as GaBi and ecoinvent attempt to consider all production streams and potential variations, capturing all these perfectly is unlikely, especially in the face of future prediction. Since IMA technology is still not in use at an industrial level, this LCA relies on the validity of current datasets to be accurate in the future, a reasonable assumption for most industrial processes but one that can never be fully verified.

Additionally, there is certain knowledge that can be added to this LCA as it becomes available to extend its accuracy. Continued research is needed specifically on possible direct emissions from IMA electrolysis, anode lifetime, and anode recycling processes.

CONCLUSION

Although the Hall–Heroult process has been the only industrial option for aluminum production since the 1890s, inert anodes represent the future of this industry. For this reason, it is crucial to fully understand their effect on the environment and climate.

When electricity production for aluminum electrolysis comes from renewable sources, such as is the case in Iceland, and power requirements for smelting can be limited to 13.5 kWh per kilogram of pure aluminum, IMA offer over a 90% GWP savings from the Hall–Heroult process, as well as over a 30% reduction in PED. At this power requirement, IMA also offer significant GWP savings using global energy data, although this result is cancelled out if power requirements rise to 17 kWh.

Note: This paper was presented at DEMI 2023 – 16th International Conference on Accomplishments in Mechanical and Industrial Engineering, organized by Faculty of Mechanical Engineering, University of Banja Luka (BOSNIA & HERZEGOVINA), co–organized with the Faculty of Mechanical Engineering University of Niš (SERBIA), Faculty of Mechanical Engineering University of Podgorica (MONTENEGRO), Faculty of Engineering Hunedoara, University Politehnica Timişoara (ROMANIA) and Reykjavik University (ICELAND), in Banja Luka (BOSNIA & HERZEGOVINA), in 01–02 June, 2023

References

[1] Brown, C. (2001). Next generation vertical electrode cells. JOM, vol. 53, no. 5, p. 39–42

[2] Gunnarsson, G., Óskarsdóttir, G., Frostason, S., & Magnússon, J. (2019). Aluminum Electrolysis with Multiple Vertical Non–consumable Electrodes in a Low Temperature Electrolyte. Light Metals, p. 803–810

[3] Haupin, W., Kvande, H. (2000). Thermodynamics of Electrochemical Reduction of Alumina. Light Metals, vol. 2

[4] Kovács, V., Kiss, L. (2015). Comparative Analysis of the Environmental Impacts of Aluminum Smelting Technologies. Light Metals, p. 529–534

[5] Kvande, H., Drabløs, P. A. (2014). The Aluminum Smelting Process and Innovative Alternative Technologies. Journal of Occupational and Environmental Medicine, vol. 56, no. 5 p. S23–S32

[6] Padamata, S. K., Singh, K., Haarberg, G. M., & Saevarsdottir, G. (2022). Wettable TiB2 Cathode for Aluminum Electrolysis: A Review. Journal of Sustainable Metallurgy, vol. 8, no. 2, p. 613–624

[7] Padamata, S. K., Yasinskiy, A., & Polyakov, P. (2018). Progress of Inert Anodes in Aluminium Industry: Review. Journal of Siberian Federal University. Chemistry, vol. 11

[8] Saevarsdottir, G., Kvande, H., & Welch, B. J. (2020). Aluminum Production in the Times of Climate Change: The Global Challenge to Reduce the Carbon Footprint and Prevent Carbon Leakage. JOM, vol. 72, no. 1, p. 296–308

[9] Huglen, R., Kvande, H. (2016). How to Minimize the Carbon Footprint from Aluminum Smelters. Global Considerations of Aluminium Electrolysis on Energy and the Environment p. 948–955

[10] de Nora, V., Sekhar, J. A. (1994). Anode–Cathode Arrangement for Aluminum Production Cells. Moltech Invent S.A., Luxembourg, Patent, no. 5,362,366.

[11] La Camera, A. F., Tomaswick, K. M., Ray, S. P., Ziegler, D. P. (1995). Process and Apparatus for Low Temperature Electrolysis of Oxides. Aluminum Company of America, Pittsburg, USA, Patent, no. 5,415,742.

[12] (2017). Life Cycle Inventory Data and Environmental Metrics for the Primary Aluminium Industry. International Aluminium Institute. LCA.

ISSN: 2067-3809

ACTA TECHNICA CORVINIENSIS – BULLETIN OF ENGINEERING
TOME XVI [2023] | FASCICULE 4 [OCTOBER – DECEMBER]

[1.]Mladen TOMIĆ, [2.]Predrag ŽIVKOVIĆ, [3.]Jovan ŠKUNDRIĆ,
[1.]Miroslav KLJAJIĆ, [1.]Borivoj STEPANOV, [1.]Željko VLAOVIĆ

PERFORMANCE ANALYSIS OF A BIOMASS–FIRED STEAM BOILER WITH FGR USING AGRICULTURAL RESIDUE STRAW AS FUEL

[1.] University of Novi Sad, Faculty of Technical Sciences, Trg Dositeja Obradovića 6, Novi Sad, SERBIA
[2.] University of Niš, Faculty of Mechanical Engineering, Aleksandra Medvedeva 14, Niš, SERBIA
[3.] University of Banja Luka, Faculty of Mechanical Engineering, Vojvode Stepe Stepanovića Blvd. Banja Luka, Banja Luka, BOSNIA & HERZEGOVINA

Abstract: This paper presents an analysis of a biomass–fired steam boiler with capacity of 14 MW which produces saturated steam at pressure of 14 bar using agriculture residue straw as fuel. The boiler operates with flue gas recirculation rate of 20%, a common technique to improve the efficiency of the combustion process and reduce emission. Data from the PLS sensors were collected to evaluate the boiler's performance. Thermal calculations were performed to analyze the heat transfer rate, heat loss, and combustion efficiency of the boiler. Three different cases were considered: flue gas recirculation after the bag filters, recirculation after the flue gas channel exit, and without the recirculation. Parallel, the emission of NOx for all scenarios was discussed. The analysis of the results shows that for both cases flue gas recirculation yields almost the same efficiency. However, the efficiency for lower flue gas recirculation is increased, and without flue gas recirculation was the highest according to both the model and calculations. This suggests that while flue gas recirculation can be an effective way to improve combustion efficiency and reduce emissions, it may not always be the most optimal solution. The findings of this study provide valuable insights into the biomass–fired steam boilers performance and the impact of flue gas recirculation on their efficiency and NOx emission. These insights can be useful for optimizing the design and operation of similar biomass–fired steam boilers and for promoting the use of renewable energy sources in industrial processes.

Keywords: biomass, FGR, NOx, steam boiler

INTRODUCTION

Steam boilers are widely used in various industries for producing steam, which is used for different purposes, such as power generation, heating, and industrial processes. Biomass steam boilers are one of the sustainable alternatives to fossil fuel boilers, and they have gained attention in recent years due to their potential to reduce greenhouse gas emissions and their low–cost fuel source [1].

The combustion of biomass in the boiler generates flue gases, which contain pollutants, including particulate matter (PM), sulphur dioxide (SO_2), nitrogen oxides (NO_x), and carbon monoxide (CO), which have adverse effects on the environment and human health [2,3]. The reduction of these emissions is of great importance, and the use of flue gas recirculation is a commonly used technique for this purpose.

Flue gas recirculation (FGR) is process where a part of the flue gas is returned to the combustion chamber to lower the combustion temperature. FGR is a possible way to improve combustion and decrease the emissions of carbon monoxide CO, particulate matter PM, and nitrogen oxides NOx in order to fulfil emission requirements, for NOx in [3]. The amount of flue gas recirculation depends on the boiler design, fuel characteristics, and emission regulations.

Summarized, the use of flue gas recirculation is commonly used technique to reduce emissions and increase the biomass steam boilers combustion efficiency [3,4].

In this paper, we investigate the performance of a 14 MW steam boiler which produces saturated steam at the pressure of 14 barg, which combusts agriculture residue straw, and operates with flue gas recirculation at a rate of 20%, working on 80% of the maximal power, i.e. 12.57 barg. The aim of this study is to compare the boiler efficiency with flue gas recirculation after the bag filters, flue gas recirculation after the exit from the flue gas channel, and without flue gas recirculation.

Data from PLS sensors, including temperatures at the steam generator furnace exit, after the water heater–economizer 4, and at the last flue gas channel exit, were utilized in this study. The excess air ratio calculation was enabled by measuring oxygen concentration at one point. Additionally, temperature after the bag filter, feed water, and water temperature after the economizer 4 were measured. The efficiency of the boiler was calculated for each case. The results indicated that the highest efficiency, according to both the model and calculations, was achieved without flue gas recirculation.

PERFORMANCE EVALUATION OF A BIOMASS–FIRED STEAM BOILER

Biomass is being combusted on a moving grate. The flue gases released transfer their heat to screens placed in the furnace. Downstream, the flue gases leave the furnace through an opening in the rear screen and enter the flue gas duct, which is inclined downward. Screen tubes are placed in the flue gas duct to transfer heat. After leaving the flue gas duct, the flue gases turn 180° and flow upward through a duct in which an evaporator and an economizer – ECO 4 are placed for heat exchange. After passing through ECO 4, the flue gases change direction again, flow downward, and transfer heat to the economizers ECO 3, ECO 2, and ECO 1 before leaving the flue gas duct and entering the cyclone and filter sections. Part of the flue gas is redirected back to the furnace for recirculation.

The stem boiler technical data are:

Boiler thermal power:

- 14 MW (saturated steam)

Water/steam parameters:

- working pressure – 14 bar
- feedwater temperature – 105°c
- saturated steam temperature – 195°c
- flue gas temperature at the boiler outlet: 170°C

Fuel type – Corn straw:

- LHV: 16 MJ/kg
- designed moisture content: 15%
- ash content on a dry mass: < 8%
- designed fuel ash melting point: < 750°c
- designed fuel nitrogen content: <0.3%
- designed fuel chlorine content: <0.3%
- designed fuel sulfur content: <0.1%

Based on the data provided for corn straw, its composition was adopted for the steam boiler thermal design. The calculations were carried out using the procedure described in various books on steam boiler thermal design [5–7].

These books provided the necessary equations and methodologies for determining the convective and radiant heat transfer coefficients in the steam boiler. The convective and radiant heat transfer coefficients are crucial parameters for evaluating the heat transfer process between the hot flue gases and the water/steam in the boiler. In the thermal design of steam boilers, it is important to accurately determine these coefficients to optimize the boiler's efficiency.

The criteria equations for convective heat transfer and radiant heat transfer were also compared in the calculation process. The results showed the difference < 10% between the criteria equations and also radiant heat transfer fluxes [5–8]. This indicates that methods provide accurate results and can be used interchangeably in the thermal design of steam boilers. However, it is important to note that the choice of the appropriate method may depend on the specific characteristics of the steam boiler and the operating conditions. Therefore, it is recommended to consult with experienced professionals in the field to select the most appropriate methodology of the steam boiler thermal design.

The adoption of air excess ratio is a crucial step of the steam boilers calculation. For the presented case, the excess air ratio was chosen according to the literature recommendations, which dictate a value of 1.2 in the furnace and 1.25 at the exit. The excess air ratio for the first flue gas channel was chosen to be equal to the value at the exit from the furnace, as determined by calculations. However, after the water heater economizer 4, the air excess ratio was found to be 1.345, and thus adopted as such in the calculation.

Similarly, for the two heat exchanger units further calculations were performed to determine the excess air ratio after the evaporator, economizer 3, and economizer 1. Assuming the same rate of growth, the excess air ratio was found to be 1.2975 after the evaporator, 1.3925 after economizer 3, and 1.4875 after economizer 1 at the exit. The excess air ratio was increased for 0.2 after the cyclone and filter to the value of 1.6875, in accordance with literature recommendations.

After thorough analysis and energy balance calculations, the flame adiabatic temperature was determined to be 1324°C. The temperature at the exit of the combustion chamber was found to be 744.6°C, which is consistent with previous findings in the literature. The temperature after economizer 4 was calculated at 366.3°C, and temperature at the exit from the flue gas channel at 181.5°C. These temperatures were calculated for each unit in the steam boiler, ensuring that the heat transfer energy balance between the heat exchanger and flue gases was within +–1%:

- for the flue gases

$$\dot{Q} = \dot{b} \cdot (I'' - I'), \quad (1)$$

- for the heat exchanger

$$\dot{Q} = k \cdot F \cdot \Delta\theta, \quad (2)$$

and in case of water heaters also the comparison with water side was considered:

$$\dot{Q} = \dot{m}_w \cdot c_w \cdot \Delta t_w. \quad (3)$$

The comparison with provided data is presented in the following Figure 1 and Figure 2.

The average RMS between the calculated and the obtained data was found to be 33°C.

The water feed temperature adopted according to the available data was 105.3°C and the temperature at the Economizer 4 outlet was 191.5°C. The calculated water temperature at the economizer outlet (evaporator inlet) was 193.6°C of steam with quality of 0.4%. The difference occurs because in the moment for which the data were presented the water drum was filled to the required level,

so the water flow was larger and valued 18.6 t/h. This gives the total heat power of the economizer line 1 to 4 of 1911 kW, compared to the calculated 1990 kW, which gives the total difference of 4%.

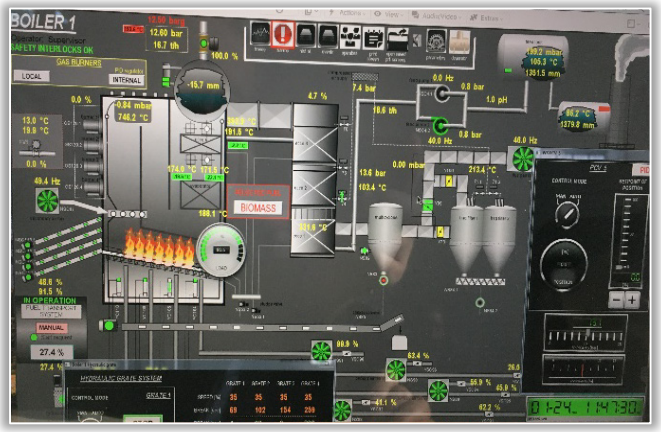

Figure 1. Temperature, pressure and mass flow readings

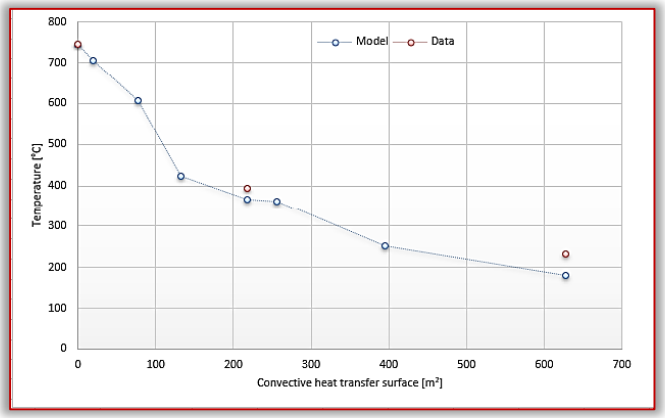

Figure 2. Comparison of temperature measurements and modelled temperatures

THE IMPACT OF FGR ON BOILER PERFORMANCE

The FGR technique involves the flue gas portion recirculation back to the combustion process. This results in a reduction of the flame temperature and the oxygen concentration, which leads to a decrease of the nitrogen oxides (NO_x) and other pollutants formation. However, this technique can also result in lower combustion efficiency, as the recirculated gas pollutes the combustion air and reduces the oxygen concentration.

According to the methodology presented above, the power and efficiency for the flue gas recirculation (FGR) from the filters and at the boiler outlet were calculated, as well as the case without FGR. In this analysis, the influence of the lower efficiency of the combustion process without FGR was considered. The results of the comparison are presented in the Table 1.

The calculations were performed with the methodology described above, and the results were compared for the cases with and without FGR. Table 1 shows that the power output and the efficiency were slightly lower for the FGR case, as expected. However, the difference in power output was only 1.5%, while the difference in efficiency was over the 4%. Temperatures at the combustion chamber and at the outlet are presented in the Table 2.

As expected, there is no significant difference for the cases where FGR is 20%. However, for reduced FGR, an increase in both efficiency and combustion temperature is observed.

Table 1. Thermal power in [kW] and the efficiency of steam boiler, in [%], for different scenarios

Exp no.	FGR– filter (20%)	FGR– exit (20%)	FGR– filter (10%)	Without FGR
Furnace	5670	5816	6421	6946
Exh. manif.	660	661	626	605
Flue gas ch.	968	962	866	755
Evaporator	1625	1613	1363	1146
Ecco 4	442	435	370	323
Turn chmb.	42	39	31	28
Ecco 3	977	950	844	750
Ecco 1–2	572	477	402	289
Net power	10996	10953	10924	10842
Eff.	84.4%	84.5%	86.6%	89.2%

Table 2. Adiabatic temperatures of the flame and flue gas temperature at the exit

Exp no.	FGR– filter (20%)	FGR– exit (20%)	FGR– filter (10%)	Without FGR
Adiabatic temp. of the flame	1324.31	1354.36	1440.50	1698.04
Flue gas temp. at the exit	182.0	185.5	166	170.0

NO_X FORMATION ANALYSIS

The concentration of "thermal NO_x" is controlled by the nitrogen and oxygen molar ratios and the combustion temperature. Combustion at temperatures well below 1,300°C forms much smaller ratios of thermal NO_x. For the obtained main species composition (N_2, H_2O, O_2, CO_2) the thermal equilibrium for NO_x is calculated for the adiabatic flame temperature. The concentration was calculated with help of Gasqe Chemical Equilibrium Software [9,10]. Gasqe is using the Lagrange Method of Undetermined Multipliers for minimization of the Gibbs free energy of the system to find the equilibrium state/ composition. Several different types of problems can be solved using this software from which the several different types of problem can be solved, from which the composition at a defined temperature and pressure was investigated.

The results presented in the Table 3 are in a good agreement with results of Sartor et al. [11] for small and medium sized combined heat and power biomass plants as they found emissions for wheat straw and whol crop to be in the range 500 to 1030 ppm, while for some biomass fuels it can be significantly over 1300 ppm. As it could be

expected the higher temperatures lead to higher values and concentrations of NO_x in the combustion products.

Table 3. NOx concentration for different conditions per kg of fuel

Exp no.	FGR– filter (20%)	FGR– exit (20%)	FGR– filter (10%)	Without FGR
Adiabatic temp. of the flame	1324.31	1354.36	1440.50	1698.04
NOx [kmol/kg]	2.950e–4	3.064e–4	3.705e–4	6.466–4
r_{NOx}	9.71e–4	9.06e–4	1.24e–3	2.49e–3
r_{NOx} [ppm]	971	906	1240	2490

RESULTS AND DISCUSSION

To determine the optimum FGR rate, we need to consider both the boiler efficiency and NO_x emissions. Based on the efficiency the NO_x emissions decrease as the FGR rate increases.

To determine the optimum FGR rate, we need to consider both the boiler efficiency and NO_x emissions, with a weight of *X* given to NO_x emissions reduction. Based on the information available:

- Efficiency for FGR 0% = 89.2%,
- Efficiency for FGR 10% = 86.6%,
- Efficiency for FGR 20% = 84.4%.

This means that the efficiency decreases as the FGR rate increases.

NOx emissions for:

- FGR 0% = 6.466e–4 kmol/kg,
- FGR 10% = 3.705e–4 kmol/kg,
- FGR 20% = 2.950e–4 kmol/kg.

This means that the NO_x emissions decrease as the FGR rate increases.

To find the optimum FGR rate, we need to find the point at which the decrease in NO_x emissions balances out with the decrease in efficiency, with the (arbitrary) weight of 5 given to NO_x emission reduction relative to efficiency. We can calculate the weighted efficiency as:

$$\text{Weighted Efficiency} = \text{Efficiency} - (X \cdot NO_x \text{ Emission Reduction}),$$

where NO_x Emission Reduction is the relative reduction in NO_x emission compared to FGR 0%. For example, for FGR 10%:

$$NO_x \text{ Emissions Reduction} = (NO_x \text{ Emissions for FGR 0\%} - NO_x \text{ Emissions for FGR 10\%}) / NO_x \text{ Emissions for FGR 0\%}.$$

As we can see from the table, the optimum FGR rate changes to 0% when using a weighted efficiency of 1. This means that if reducing NOx emissions is equally important as improving efficiency, then FGR should not be used at all. If we increase the weight for NOx reduction to 5, the highest weighted efficiency is still achieved at 0% FGR rate, but the difference between the weighted efficiency at 0% and 10% FGR rate has decreased compared to the previous table.

Table 4. Analysis of FGR Rate on NOx Emissions and Efficiency, with Weighted Reductions 1

FGR Rate	NOx Emissions [kmol/kg]	Efficiency	NOx Emissions Reduction	Weighted Efficiency
0%	6.466–4	89.2%	89.2%	89.2%
10%	3.705e–4	86.6%	81.3%	–4.7%
20%	2.950e–4	84.4%	73.2%	–26.8%

Table 5. Analysis of FGR Rate on NOx Emissions and Efficiency, with Weighted Reductions 5

FGR Rate	NOx Emissions [kmol/kg]	Efficiency	NOx Emissions Reduction	Weighted Efficiency
0%	6.466–4	89.2%	0%	89.2%
10%	3.705e–4	86.6%	42.6%	81.3%
20%	2.950e–4	84.4%	54.4%	79.3%

CONCLUSIONS

Flue gas recirculation (FGR) is an effective and cost–efficient technique for reducing NOx emissions from burners in certain applications. It is predicted that recirculating up to 20% of the flue gases through the burner can reduce NOx emissions by as much as 55%. However, this may also reduce the steam boiler's efficiency by almost 5%. To determine the optimum FGR rate, an analysis was performed to find the point at which the decrease in NOx emissions is balanced with the decrease in efficiency.

The analysis revealed that the FGR rate should be around 10% depending on the weight of emissions compared to efficiency. It is worth noting, though, that this analysis is based on a simplified model, and the actual optimal FGR rate may vary depending on the specific conditions of the boiler and local emission regulations. If energy stability is a priority, then higher efficiency is preferred over NOx emissions.

Nomenclature

$\dot{b}$	fuel flow, [kg·s^{-1}]
c_w	water heat capacity, [J·kg^{-1}·K^{-1}]
F	heat transfer area, [m^2]
I	flue gas enthalpy per kg of fuel, [kJ·kg^{-1}]
k	overall heat transfer coefficient, [W·m^2·K^{-1}]
$\dot{m}_w$	water mass flow rate, [kg·s^{-1}]
t_w	water temperature, [°C].
$\Delta\theta$	log mean temperature difference, [K].

Acknowledgement

The authors would like to express their sincere gratitude to Mr. Rade Đurić and Mr. Vladan Petrović for their invaluable contribution to this study. Their generous provision of data, including temperature measurements was crucial to the successful completion of this research.

Note: This paper was presented at DEMI 2023 – 16th International Conference on Accomplishments in Mechanical and Industrial Engineering, organized by Faculty of Mechanical Engineering, University of Banja Luka (BOSNIA & HERZEGOVINA), co–organized with the Faculty of Mechanical Engineering University of Niš (SERBIA), Faculty of Mechanical Engineering University of Podgorica (MONTENEGRO), Faculty of Engineering Hunedoara, University Politehnica Timișoara (ROMANIA) and Reykjavik University (ICELAND), in Banja Luka (BOSNIA & HERZEGOVINA), in 01–02 June, 2023

References

[1] Transparency Market Research. From: https://www.globenewswire.com/news–release/2023/01/09/2584969/0/en/Biomass–Boiler–Market–to–grow–at–a–CAGR–of–18–1–during–the–forecast–period–from–2022–to–2031–TMR–Study.html, accesed on: April 25, 2023.

[2] Monks, P. et al., (2017). The Potential Air Quality Impacts from Biomass Combustion. Department for Environment, Food and Rural Affairs; Scottish Government; Welsh Government; and Department of the Environment in Northern Ireland, UK.

[3] Polonini, L.F., Petrocelli, D., Lezzi, A.M. (2023). The Effect of Flue Gas Recirculation on CO, PM and NOx Emissions in Pellet Stove Combustion. Energies, vol. 16, no. 2, p. 954–954

[4] Caposciutti, P., et al. (2022). An Experimental Investigation on the Effect of Exhaust Gas Recirculation in a Small–Scale Fixed Bed Biomass Boiler, Chemical Engineering Transactions, vol. 92, p. 397–402.

[5] Brkić, Lj., Živković, T. (1987). Termički proračun parnih kotlova. Mašinski fakultet Beograd.

[6] Bogner, M. (2004). Termotehničar. AGM, Beograd.

[7] Đurić, V., Farmakoski V. (1958). Parni kotlovi –deo I. Naučna Knjiga, Beograd.

[8] Radojković N., Ilić, G., Vukić, M., Stojanović, I., Živković P. (2007). Termodinamika II. Mašinski fakultet Niš, Niš.

[9] Morley Chris. Gaseq. From: http://www.gaseq.co.uk/, accessed on: April 25, 2023.

[10] Tomić, M. et al., The pollutant emissions assessment from personal vehicles in the republic of Serbia, 1st International conference on advances in science and technology – COAST 2022, Herceg Novi, Montenegro, p. 248 – 254.

[11] Sartor, K. et al. (2014). Prediction of SO_x and NO_x emissions from a medium size biomass boiler. Biomass and Bioenergy, vol. 65, p. 91 – 100

ISSN: 2067–3809

Fascicule 4
[October – December]
tome XVI
[2023]

ACTA Technica CORVINIENSIS
BULLETIN OF ENGINEERING

ISSN: 2067-3809

ACTA TECHNICA CORVINIENSIS – BULLETIN OF ENGINEERING
TOME XVI [2023] | FASCICULE 4 [OCTOBER – DECEMBER]

[1.]Ivan GRUJIC, [1.]Nadica STOJANOVIC, [1.]Miroslav PETROVIC

THE INFLUENCE OF THE HYDROGEN INJECTION PARAMETERS ON THE COMBUSTION PROCESS OF IC ENGINE

[1.]University of Kragujevac Faculty of Engineering, Sestre Janjic 6, 34000 Kragujevac, SERBIA

Abstract: In order to determine the best injection parameters of hydrogen, an experimental work was performed. The test engine was equipped with the installation for the hydrogen supply, and it was tested how the injection timing and number of injection influence on the combustion process. As the control parameters were taken the engine working stability, as well as the indicating efficiency. It was determined that the injection parameters, significantly influence on the engine working cycle, as well as on the combustion process. The adequate injection timing as well as the adequate number of injections, is crucial, for maintaining the stable work oof the IC engine, as well as for indicating efficiency. In order to provide the stable engine work, with the satisfying indicating efficiency, it is necessary provide multiple injections, more accurate two injections, where one serves to provide the adequate amount of fuel for the working cycle, while the second serves to slowdown the combustion process.

Keywords: IC engine, hydrogen, combustion process, injection parameters

INTRODUCTION

The global concern about the ecology, as well as about the fuel crisis, have forced the engineers to think about the alternatives, which can be used instead the crude oil. In most cases, the electric vehicles are presented as the future of the people mobility. However, the electrification of the entire vehicle park of the world, still has many obstacles, which should overcome. First obstacle is the potential of the production of the electric energy, necessary for the supply and charge of the electric vehicle batteries, as well as necessary infrastructure for this. Second is the recycling of the batteries materials. Then we have the question, do we have enough materials, necessary for the production of the electric vehicle's components. These obstacles impose the question, how can provide the sustainability of the IC engines. The answer is quite simple, it should give more attention to the alternative fuels, which are more ecologically friendly, and to see the possibility of their usage. Many substances can be successfully used as the substitution for the conventional fuels, and that:

- natural gas;
- petroleum gas;
- alcohols;
- biofuels;
- reformulated fuels;
- hydrogen;

Fuel which in most cases is presented as so–called the fuel of the future is hydrogen. The hydrogen is present in the entire universe, but almost never in free form, as the single chemical element. The main advantage of the hydrogen is its chemical composition, that is, the hydrogen doesn't have carbon in its chemical composition, how the other fuels have. This theoretically means, that is impossible the appearance of harmful components, such are the carbon–monoxide (CO) and unburnt–hydrocarbons (HC).

Because of the mentioned, many researchers work on the subject of hydrogen use as the fuel for IC engines. In most cases, the main problem of hydrogen use, are the high temperatures caused by the high combustion speed [1], and some of the solutions for this undesirable phenomenon are the Exhaust Gas Recirculation (EGR), water injection, blending biodiesel and ignition delay. It is important to say, that more and more researches are focused on the hydrogen direct injection. The main reason for this are the many limitations of the port fuel injection [2], such are pre–ignition, knocking, backfiring, low volumetric efficiency and compression loss problems. All these limitations cause the limitation of engine achievable load and efficiency. Also, many times, the hydrogen use is considering as the fraction of mixture with different fuels. For example, the addition of the hydrogen as the additive, significantly can be influenced on the engine performances [3]. By increment of the hydrogen volume fraction, the knock resistance is enhanced because of the hydrogen high knock resistance and high octane number. Also, this increase causes and the increment of the peak of the heat release rate and of the cylinder pressure. One of the main reasons, why hydrogen in most cases is considered as the additive, and not as the only fuel, is it influence on the formation of nitric–oxygens (NOx). The

high amount of hydrogen in mixture leads to the increment of the NOx [4]. This happens due to the high combustion speed, and by this due to the high combustion temperature. So, the main idea is to use mixture, where other fuel will decrease this undesirable phenomenon. By considering many factors such are trend of mitigating climate change worldwide, the contribution of a widespread, reliable and affordable propulsion technology like the IC engine is, it can be said that the future use of IC engines can be very significant, once when the usage of conventional fuels reduces, with the increased use of alternative fuels such is hydrogen. However, it still stays to see how to resolve some of most important things, and that are the availability and production of hydrogen, as well as its safe storage and use [5].

The aim of this paper was to investigate how the injection parameters influence on the combustion process and by that on the IC engine working cycle of the fueled only by hydrogen.

EXPERIMENTAL WORK

In order to see how the injection parameters influence on the IC engine combustion process, the experimental work was conducted. For the investigation, it was modified the experimental test engine. The basic variant of test engine was diesel engine. For the experimental work, engine was equipped with the ignition system. Also, it was equipped with the gas installation, which scheme and main components can be seen on the Figure 1.

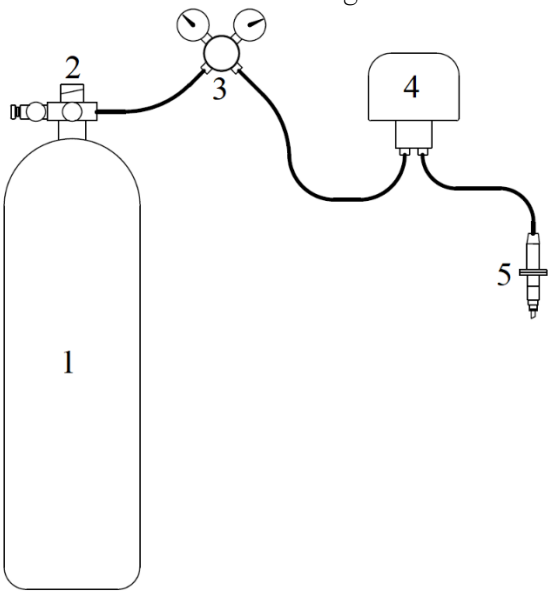

1 – gas tank	3 – valve	4 – pressure regulator
4 – flow meter	5 – prechamber	

Figure 1. Gas installation

The main part of the gas installation is the prechamber, which was made to have the same overall dimensions as the diesel injector, so it was mounted instead the diesel injector. In the prechamber were mounted the spark plug, as well as the Gasoline Direct Injection (GDI) injector, which was used for the injection of the hydrogen. The reason for the use of the prechamber, was the idea to stratify the mixture, in order to reduce the combustion speed of the hydrogen. This was made, because of the fact, that the hydrogen combustion speed is the greatest for the case of the stochiometric mixture, while lean and rich mixture decrease the hydrogen combustion speed significantly [6]. So, by the use of the prechamber, and injection into it, the mixture in prechamber will be always rich, while the mixture in the cylinder will be always lean. By the addition of the prechamber, it was increased the compression volume, and decreased the compression ratio. The compression ratio was first reduced at 13.3:1, but it was found that this value is too high, and due to this, it was replaced and piston so the compression ratio was reduce to 10.4:1. The scheme of the modified engine is shown on the Figure 2, while the engine specifications before and after modifications are given in Table 1.

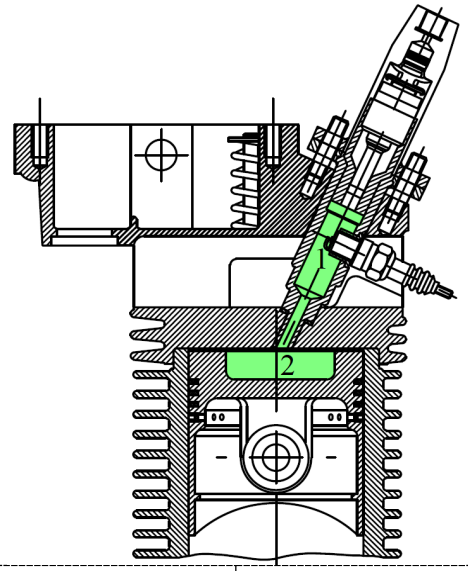

1 – prechamber volume	2 – cylinder

Figure 2. Modified engine working space

Table 1. Test engine specifications

Name	Value before modification	Value after modification	Unit
Engine bore	85	85	mm
Engine stroke	80	80	mm
Number of cylinders	1	1	–
Displacement	454	454	cm^3
Compression ratio	17.5:1	10.4:1	–

In order to see, how the injection parameters influence on the combustion process, a several injection strategies were tested, and that:

- Injection during the intake stroke;
- Simultaneous injection and combustion;
- Dual–stage injection;

The exact injection parameters are given in Table 2.

Table 2. Injection parameters

Test no.	First injection start, °BTDC	First injection duration, ms	Second injection start, °BTDC	Second injection duration, ms
1	344	12	–	–
2	30	12	–	–
3	200	7.2	30	4.8

RESULTS AND DISCUSSION

After the conducted experimental work, from the cylinder pressure it was calculated the heat release rate, Figure 3, which also represents and combustion speed.

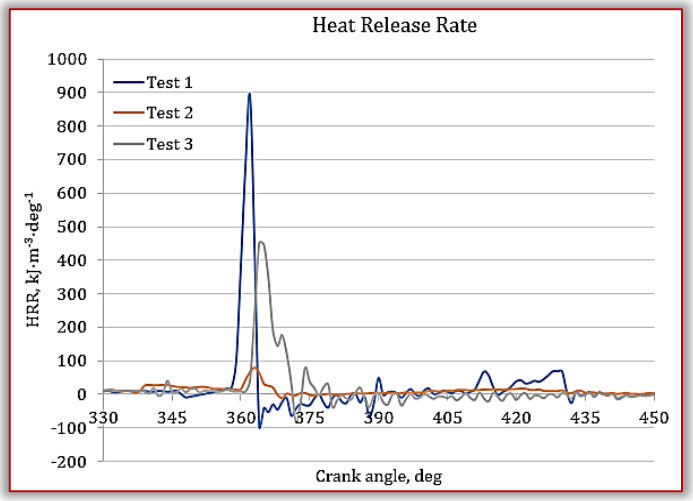

Figure 3. Heat release rate

It was found that the injection parameters, significantly influence on the combustion process. By observing the Figure 3, it can be said that by earlier injection of hydrogen, rises the combustion speed. The reason for this is the formation of more homogenous mixture. The higher combustion speed is followed with better performances due to the higher maximal pressures in the cylinder. However, also it has its negative sides. First of all, during the Test 1 (injection during the intake stroke), it was very hard to start engine with this approach.

The reason for this is a slow engine speed, which allows enough time for the formation of the explosive mixture, which in several case have turned the engine direction, end caused engine stop. Also, during this test, quite often was present the backfire. The reason for this is because was opened the intake valve, and hydrogen exited into the intake port, after which the HHO gas was formatted, which exploded in intake port. Every explosion was followed with pressure wave, which have disabled the intake of air for next cycle, and this caused the unstable engine work.

The Test 2 (simultaneous injection and combustion) have shown as the worst one. During this test, it was impossible to achieve engine load as well as stable regime. Also, the combustion was stretched, what can be seen and from the cumulative heat release, Figure 4.

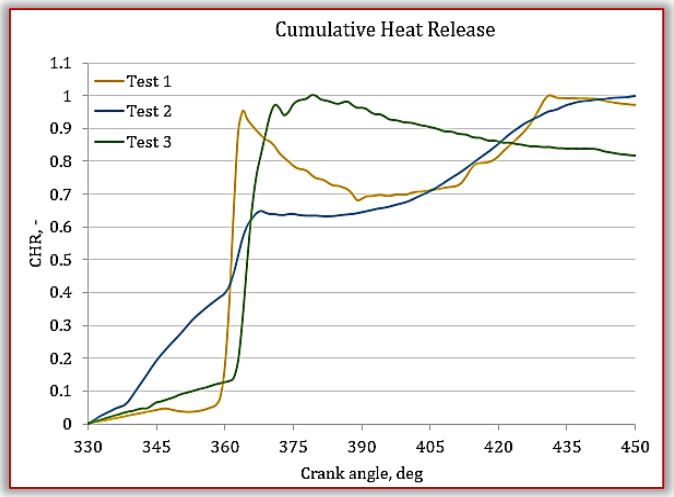

Figure 4. Cumulative heat release

The stretched combustion is specific by low indicating efficiency, which in this case was 22%, while in other two cases was 36% for Test 1, and 34% for Test 3. It can be seen that the center of the combustion (50% of burned mass) is closest to the Top Dead Centre for the Test 1, and due to this, this Test gave the best indicating efficiency.

However, as the best injection parameters, can be ranked the injection parameters used during the Test 3. In this case, the greatest part of the first injection was during the compression stroke, when the intake valve was closed, so in this way, it was avoided the appearance of backfire, and by this was maintained the stable engine work. The role of the second injection was to slow down the combustion, and this was achieved. By slowing down the combustion, are avoided extreme pressure rises ratios, as well as great combustion temperatures. Which means, that this approach is good and from the side of the performances, as well as from the side of the emission, because high temperatures are followed with the rise of NOx, which is the main pollutant in the case of the hydrogen use.

CONCLUSION

It was conducted the experimental investigation of the combustion process, during the engine work with a hydrogen as only fuel. It was found that the injection parameters significantly influence on the combustion process, and by that on the engine work. The best performances can be achieved by early injection, but this can lead to the unstable work, and great mechanical loads. Simultaneous injection and combustion is not recommendable, because doesn't exist enough time for mixture formation, which leads to the stretched combustion and low efficiency. The best solution is multiple injection, where one injection should be during the compression stroke, in order to avoid the backfire, while the second should be defined around the TDC, in order to enrich the mixture, and to slow down the combustion.

Acknowledgement

This paper was realized within the framework of the project "The research of vehicle safety as part of a cybernetic system: Driver–Vehicle–Environment", ref. no. TR35041, funded by the Ministry of Education, Science and Technological Development of the Republic of Serbia.

Note: This paper was presented at DEMI 2023 – 16th International Conference on Accomplishments in Mechanical and Industrial Engineering, organized by Faculty of Mechanical Engineering, University of Banja Luka (BOSNIA & HERZEGOVINA), co–organized with the Faculty of Mechanical Engineering University of Niš (SERBIA), Faculty of Mechanical Engineering University of Podgorica (MONTENEGRO), Faculty of Engineering Hunedoara, University Politehnica Timișoara (ROMANIA) and Reykjavik University (ICELAND), in Banja Luka (BOSNIA & HERZEGOVINA), in 01–02 June, 2023

References

[1] Aggarwal, A., Yadav, S., Singh, K., Verma, A.S., Chhabra, S. (2022). Study of utilization of hydrogen as fuel in internal combustion engine. CIRP Annals – Manufacturing Technology, vol. 64, no. 3, p. 1211–1216

[2] Yip, H.L., Srna, A., Yin Yuen, A.C., Kook, S., Taylor, R.A., Yeoh, G.H., Medwell, P.R., Chan, Q.N. (2019). A review of hydrogen direct injection for internal combustion engines: towards carbon–free combustion. Applied Sciences, vol. 9, no. 22, p. 4842

[3] Fu, Z., Li, Y., Chen, H., Du, J., Li, Y., Gao, W. (2022). Effect of hydrogen blending on the combustion performance of a gasoline direct injection engine. ACS Omega, vol. 7, no. 15, p. 13022–13030

[4] Ali, G., Zhang, T., Wu, W., Yhou, Y. (2020). Effect of hydrogen addition on NOx formation mechanism and pathways in MILD combustion of H2–rich low calorific value fuels. International Journal of Hydrogen Energy, vol. 45, no. 15, p. 9200–9210

[5] Onorati, A., Payri, R., Vaglieco, B.M., Agarwal, A.K., Bae, C., Bruneaux, G., Canakci, M., Gavaises, M., Günthner, M., Hasse, C., Kokjohn, S., Kong, S.C., Moriyoshi, Y., Novella, R., Pesyridis, A., Reitz, R., Ryan, T., Wagner, R., Zhao H. (2022). The role of hydrogen for future internal combustion engines. International Journal of Engine Research, vol. 23, no. 4, p. 483–695

[6] Gong, C., Jang, M., Bai, X.S., Liang, J.J., Sun, M.B. (2017). Large eddy simulation of hydrogen combustion in supersonic flows using an Eulerian stochastic fields method. International Journal of Hydrogen Energy, vol. 42, no. 2, p. 1264–1275

ISSN: 2067–3809

ACTA TECHNICA CORVINIENSIS – BULLETIN OF ENGINEERING
TOME XVI [2023] | FASCICULE 4 [OCTOBER – DECEMBER]

[1.]Vidosava VILOTIJEVIĆ, [1.]V. NIKOLIĆ, [1.]Uros KARADŽIĆ,
[1.]Vuko KOVIJANIĆ, [2.]Ivan BOŽIĆ

ASSESSMENT OF THE TECHNICAL JUSTIFICATION AND PROFITABILITY OF THE NEWLY BUILT SHPP–S IN MONTENEGRO

[1.] University of Montenegro, Faculty of Mechanical Engineering, Podgorica, MONTENEGRO
[2.] University of Belgrade, Faculty of Mechanical Engineering, Belgrade, Belgrade, SERBIA

Abstract: Basic approach to small hydro power plant (SHPP) design implies techno–economic analysis, which determines the SHPP installed parameter more precisely by using the following criteria: the annual electricity production, the annual revenue of the HPP, net present value (NPV), internal rate of return (IRR) and payback period (PB). The SHPP installed parameter represents the ratio of the design flow and the average perennial flow obtained from the flow duration curve at the location of the intended water intake. The main goal of the current research is to compare the 27 newly built SHPPs in Montenegro with the developed methodology, and provide an assessment of their technical justification and profitability. According to the conducted analyses, it can be concluded that 82% of them are designed properly and 18% have serious shortcomings.

Keywords: small hydro power plant, design flow, installed capacity, techno–economic parameters

INTRODUCTION

The construction of small hydropower plants in the Western Balkans in recent years has been followed by many controversies related to environmental, social, hydrological and hydro energetic issues. One of the main problems faced by hydropower engineers was the lack of reliable hydrological data. During 2010 and 2011, flows on 65 small watercourses were measured under the project named the Registry of Small Rivers and Potential Locations of SHPPs at Municipality Level for Central and Northern Montenegro, and relevant flow duration curves (FDCs) have been obtained [1]. This Registry was enhanced during 2018 and 2019 [2]. Location for SHPPs in Montenegro are characterized by relatively low average annual flows and high gross heads. The proper determination of the design flow also proved to be a challenge in terms of technical and economic justification. Due to all of the above mentioned, a methodology was developed for determining the SHPP installed parameter [3, 4]. The methodology takes into account technical (installed capacity, annual electricity production) and economic parameters (the annual revenue of the HPP, NPV, IRR and PB). The application of techno–economic parameters when determining design flow with different approaches can be found in the literature [5 ÷ 12]. The main goal of the current research is to compare the 27 newly built SHPPs in Montenegro with the developed methodology, and provide an assessment of their technical justification and profitability.

METHODOLOGY

This paper investigates 27 (twenty–seven) small watercourses on the territory of Montenegro where small hydropower plants of different capacities have already been built. The SHPP installed parameter is defined as the ratio of the design flow and averaged perennial flow according to the following equation,

$$K_i = \frac{Q_d}{Q_{av}}. \quad (1)$$

The annual gross income of the small power plant is calculated from the generated energy based on the FDCs and the incentive energy prices (Table 1).

Table 1. Electricity prices depending on the capacity of the power plant [13]

Hydro power plant capacity [MW]	Incentive price [c€/kWh]
$P_{SHPP} < 1$ MW	10.44
$1 \leq P_{SHPP} < 3$ MW	$10.44 - 0.7 \cdot P_{SHPP}$
$3 \leq P_{SHPP} < 5$ MW	$8.87 - 0.24 \cdot P_{SHPP}$
$5 \leq P_{SHPP} < 8$ MW	$8.35 - 0.18 \cdot P_{SHPP}$
$8 \leq P_{SHPP} \leq 10$ MW	6.8

The net present value (NPV) is defined as the value of the net cash flow during exploitation period of SHPP discounted back to its present value, and it is calculated according to the next equation [10,14].

$$NPV = \sum_{t=1}^{T} \frac{R(t) - C(t)}{(1+d)^t} \quad (2)$$

where are: R – annual net income of the SHPP, C – annual costs of the SHPP (in the first year this implies total investment costs of the project and in all next years the operation and maintenance costs), d – discount rate (d = 8% for Montenegro), T – the time of cash flow, equal to concession period of 30 years. The internal rate of return (IRR) is the discount rate that reduces the present value of the net project cash flow to zero in a discounted cash

flow analysis and can be calculated from eq. (3), as the value of *d* corresponding to a NPV = 0 [10,14].

The payback period (PB) is the period it takes to recover the cost of an investment and it is obtained by dividing total investment costs with net annual income of SHPP.

RESULTS AND DISCUSSION

Based on hydrological data (flow duration curves and characteristic flow durations), calculations were made to select the optimal K_i on 27 watercourses on the territory of Montenegro. These results were compared with the designed values on these constructed plants and the results are shown in Table 2.

Table 2. Values of SHPP installed parameter (K_i – obtained by methodology, K_i^* – constructed)

	SHPP Name	K_i / K_i^*	NPV (kEUR)	IRR (%)	PB (year)	Annual electricity production (GWh)
1	Jezerštica	2.2	1431.92	15.69	6.56	3.04
		2.1	1402.08	15.63	6.59	3.00
2	Bistrica	1.0	8810.63	22.00	4.37	17.44
		1.2	8992.72	20.96	4.64	19.45
3	Orah	1.4	951.00	11.38	9.93	3.54
		1.4	951.00	11.38	9.93	3.54
4	Spaljevići	2.2	422.70	10.43	10.98	2.17
		1.7	303.96	9.89	11.71	1.96
5	Šekular	1.0	1146.78	11.17	10.21	4.42
		1.7	781.74	9.77	12.14	5.51
6	Jelovica 1	1.2	5149.83	22.11	4.33	8.82
		1.7	5217.91	19.93	4.92	10.36
7	Jelovica 2	1.1	−116.56	7.32	17.12	1.78
		1.4	−175.25	7.08	17.91	1.91
8	Vrelo	1.8	1630.62	16.64	6.10	3.22
		1.3	1336.12	15.82	6.48	2.83
9	Piševska	2.5	523.94	11.28	9.92	2.11
		3.0	557.97	11.33	9.88	2.21
10	Temnjačka	1.9	8484.88	25.97	3.57	15.36
		1.3	7461.46	27.57	3.32	12.53
11	Treskavička	1.9	4350.62	23.59	3.99	7.63
		1.1	3894.91	25.04	3.71	6.08
12	Babinopoljska	1.5	5041.42	23.43	4.03	8.60
		1.5	5041.42	23.43	4.03	8.60
13	Bistrica Majstorovina	1.0	7086.93	21.29	4.55	12.52
		1.6	6457.47	17.52	5.79	14.92
14	Bradavac	1.0	2710.11	22.57	4.19	4.07
		0.9	2580.22	22.25	4.26	3.92
15	Šeremet	1.7	2605.95	22.45	4.21	3.94
		1.7	2605.95	22.45	4.21	3.94
16	Ljevak	1.5	2290.21	18.31	5.43	4.04
		1.0	1653.47	16.86	6.00	3.22
17	Kutska 1	1.0	5044.77	23.62	4.00	7.95
		1.2	5300.22	23.06	4.12	8.65
18	Kutska 2	1.3	2083.14	17.71	5.66	3.81
		1.2	2016.71	17.63	5.69	3.71
19	Mojanska 1	1.1	2801.65	15.80	6.63	6.23
		1.5	3006.11	15.39	6.83	7.15
20	Mojanska 2	1.3	1690.36	14.29	7.44	2.35
		1.6	1417.61	12.84	8.52	4.35
21	Mojanska 3	1.5	670.34	11.86	9.33	2.35
		2.0	723.35	11.69	9.53	2.59
22	Bistrica Lipovska	1.3	2383.78	18.42	5.39	4.17
		1.3	2383.78	18.42	5.39	4.17
23	Paljevinska	1.0	−16.97	7.90	15.56	1.75
		1.3	−69.33	7.63	16.32	1.93
24	Pecka	2.1	563.35	10.07	11.60	3.17
		2.0	543.97	10.03	11.61	3.13
25	Vrbnica	1.3	10338.05	33.56	2.65	16.23
		2.1	10926.19	29.64	3.06	19.83
26	Štitska	2.2	730.09	11.73	9.49	2.59
		2.0	685.91	11.57	9.65	2.53
27	Mišnića	1.9	365.72	10.71	10.53	1.77
		1.0	124.27	9.12	12.80	1.38

Few typical results are shown in the next figures.

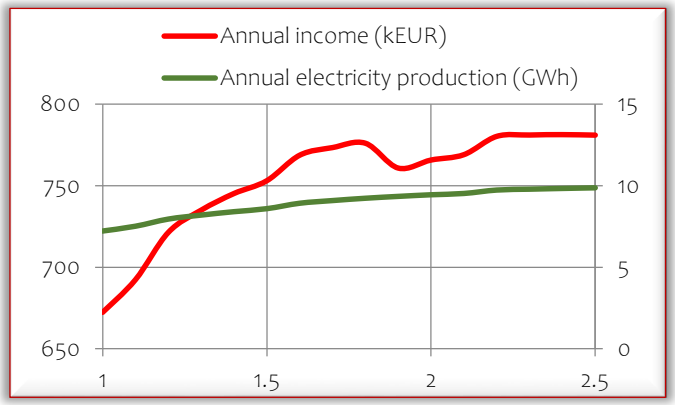

Figure 1. Annual electricity production and income– SHPP Babinopoljska

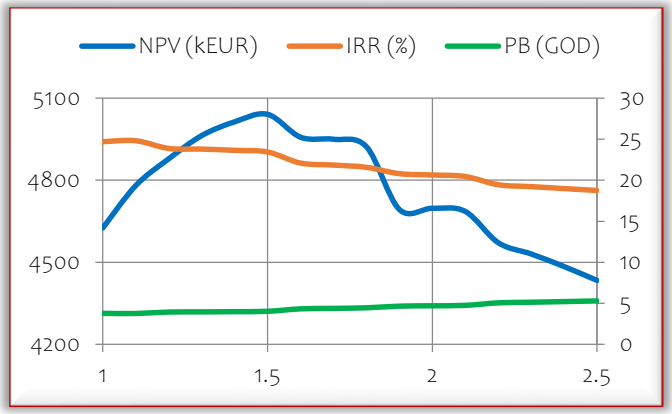

Figure 2. NPV, IRR and PB–SHPP Babinopoljska

The maximum value of annual production and income for SHPP Babinopoljska is obtained for K_i = 2.5 (Figure1). From Figure1 it can also be seen that the annual income is constantly increasing up to K_i = 1.8, after which due to the increase in installed capacity over 3 MW and the reduction of the incentive price it decreases to K_i = 1.9 after which it constantly increases until the end of the range. The maximum values for NPV (5041.42 kEUR) and IRR (24.8%) were obtained for K_i = 1.5 and K_i = 1.2. Designed values of K_i on constructed SHPP Babinopoljska is 1.5. For this value annual electricity production is 8.60 GWh, annual income is 753.12 kEUR, NPV is 5041.42 kEUR, IRR is 23.43% and PB is 4.03 years. Comparing the results obtained by applying the developed methodology with the designed parameters it gives the same parameter values. This designed solution seems to be well chosen if the economic aspect is to be observed.

For SHPP Vrelo the maximum value of annual production 3.58 GWh is obtained for K_i = 2.5, while the maximum value of annual income 350.51 kEUR is obtained for K_i = 1.9. The maximum values for NPV (1702.64 kEUR) and IRR

(16.64%) were obtained for K_i = 1.9 and K_i =1.8, (Figure4). Designed value of K_i on constructed SHPP Vrelo is 1.3. For this value, annual electricity production is 2.83 GWh, annual income is 295.52 kEUR, NPV is 1336.12 kEUR, IRR is 15.82% and PB is 6.48 years.

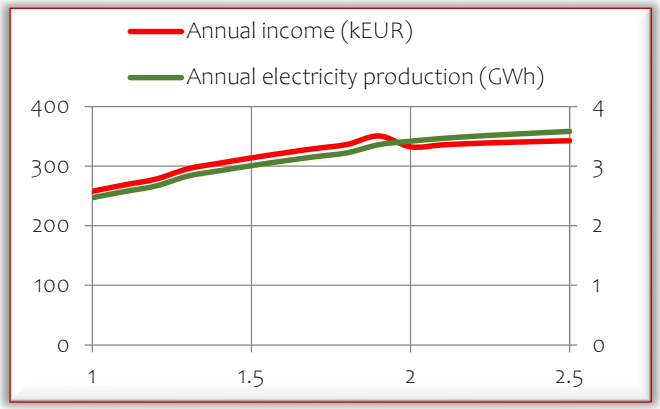

Figure 3. Annual electricity production and income– SHPP Vrelo

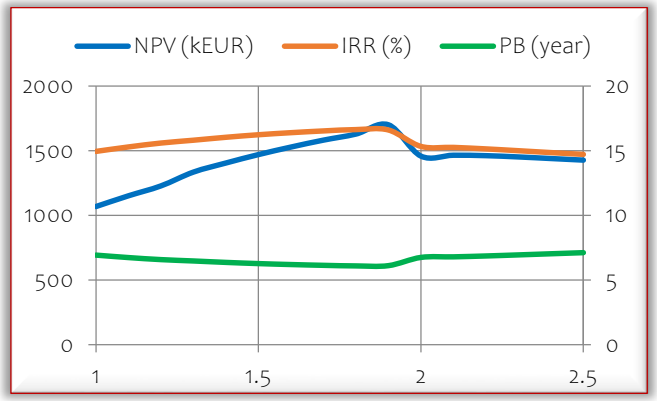

Figure 4. NPV, IRR and PB– SHPP Vrelo

For SHPP Jelovica 2, the maximum value of annual production 2.09 GWh is obtained for K_i = 2.5, while the maximum value of annual income 213.05 kEUR is obtained for K_i = 2.3. The maximum values for NPV (–116.56 kEUR) and IRR (7.32%) i.e. the corresponding PB (17.12 years) were obtained for K_i = 1.1. Designed value of K_i on constructed SHPP Jelovica 2 is 1.4. For this value, annual electricity production is 1.91 GWh, annual income is 199.27 kEUR, NPV is –175.25 kEUR, IRR is 7.08% and PB is 17.91.

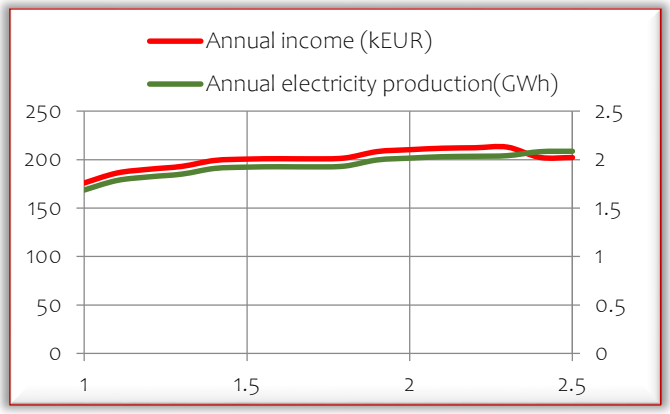

Figure 5. Annual electricity production and income– SHPP Jelovica 2

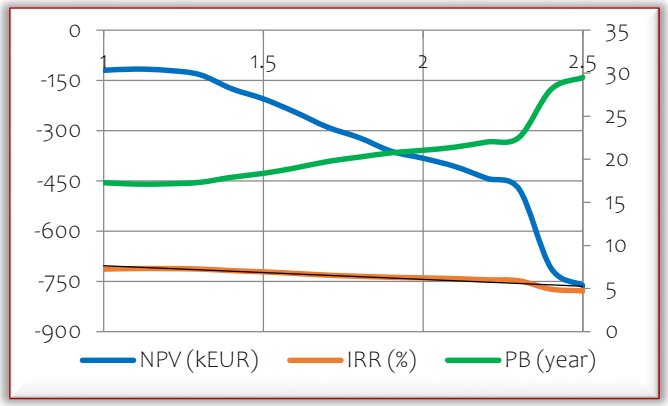

Figure 6. NPV, IRR and PB– SHPP Jelovica 2

Based on the obtained results, it can be noted that the NPV has a negative value for the entire K_i range, which indicates that this SHPP was not designed properly or was designed with wrong input data. Also, the maximum IRR value of 7.32% is lower than the adopted discount rate of 8%, which means that the project is not feasible. The normalized values of NPV and IRR are used for a precise comparison of the results obtained by the methodology and the constructed SHPP solution. Normalized values were obtained by dividing calculated values with optimal ones given with chosen K_i for every plant. With relative values, we are able to check results on the same level and compare different plants. Vertical lines mean constructed K_i and cross points with NPV or IRR lines give constructed NPVs or IRRs. Table 3 shows the criteria for evaluating the validity of the constructed solution.

Table 3. Criteria for evaluating the validity of the constructed solution

Criteria
Optimal solution – (0.85–1.0)
Good solution – (0.6–0.85)
Far from optimal solution – (0.3–0.6)
Bad solution – (0–0.3)

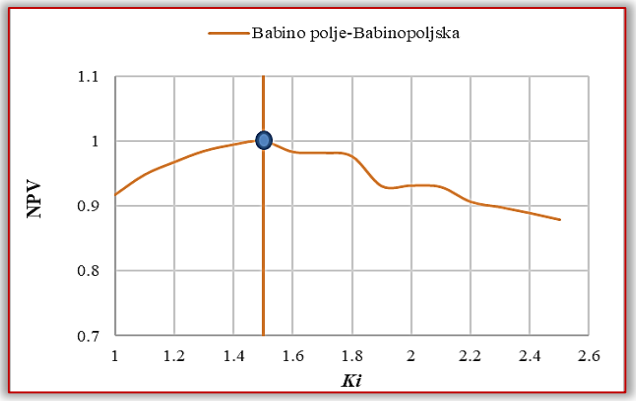

Figure7. Normalized values of NPV – SHPP Babinopoljska

For SHPP Babinopoljska (Figure7), the solution obtained by the methodology is the same as the constructed solution. Considering the above, the constructed SHPP installed parameter (NPV=1) is the optimal solution.

Figure8 shows normalized values of IRR for SHPP Vrelo. By comparing the constructed SHPP installed parameter

and the SHPP installed parameter obtained by the methodology, it can be observed that slightly better results of all considered parameters are provided by the optimal solution. However, the constructed value of the SHPP installed parameter (IRR=0.95) is the optimal solution.

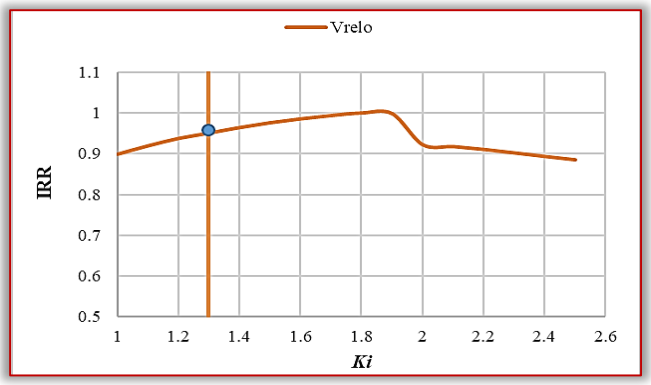

Figure 8. Normalized values of NPV – SHPP Vrelo

Bearing in mind that for SHPP Jelovica 2, NPV has a negative value and that the maximum IRR value is lower than the adopted discount rate, it can be concluded that this power plant was built as a bad solution.

CONCLUSION

The research subject in this paper is 27 small hydropower plants that were built in the period from 2014 to 2023 on the territory of Montenegro. Based on hydrological data (flow duration curves and characteristic flow durations), calculations were made to select the optimal SHHP installed parameter. By comparing the obtained with the constructed results, a conclusion can be drawn as to whether the designed solutions are optimal, good, far from optimal, or bad.

Table 4. Evaluation of the validity of the implemented solutions of SHPPs built in Montenegro

Optimal solution	20 SHPPs
Good solution	3 SHPPs
Far from optimal solution	1 SHPP
Bad solution	3 SHPPs

In all cases, it was found out that choosing the optimal K_i value depending on the annual income and annual electricity production leads to an increase in the annual income, but also to an increase in the price of the investment. From the research it is also concluded that the difference in the investment between the highest income and the maximum NPV and IRR is several times greater than the difference in income. It proves that in all cases NPV and IRR are more influential parameters for choosing the SHPP installed parameter compared to the annual income and annual electricity production. Finally, the developed methodology can serve as a guide for designers and investors of small hydropower plants.

Note: This paper was presented at DEMI 2023 – 16th International Conference on Accomplishments in Mechanical and Industrial Engineering, organized by Faculty of Mechanical Engineering, University of Banja Luka (BOSNIA & HERZEGOVINA), co–organized with the Faculty of Mechanical Engineering University of Niš (SERBIA), Faculty of Mechanical Engineering University of Podgorica (MONTENEGRO), Faculty of Engineering Hunedoara, University Politehnica Timișoara (ROMANIA) and Reykjavik University (ICELAND), in Banja Luka (BOSNIA & HERZEGOVINA), in 01–02 June, 2023

References

[1] Vodni zdroje, a.s., Blom, Sweco Hydroprojekt CZ, a.s., Sistem doo, HMZCG. (2011). Registry of Small Rivers and Potential Locations of SHPPs at Municipality Level for Central and Northern Montenegro. European Bank for Reconstruction and Development (EBRD) and Ministry of economy, Podgorica, Montenegro.

[2] Vodni zdroje as, Sweco Hydroprojekt CZ as. (2019). Enhancement of Registry of Small Rivers for Small Hydropower Projects Potential of up to 10 MW. European Bank for Reconstruction and Development (EBRD) and Ministry of economy, Podgorica, Montenegro.

[3] Vilotijević, V., Karadžić, U., Vujadinović, R., Kovijanić, V., Božić, I. (2021). An Improved Techno–Economic Approach to Determination of More Precise Installed Parameter for Small Hydropower Plants, Water, vol. 13.

[4] Vilotijević, V., Karadžić, U., Kovijanić, V., Božić, I., Vujadinović, R. The techno–economic analysis of small hydropower plants installed parameters for three different mountain watercourses. International Conference Power Plants 2021, November 2021, Belgrade, Serbia.

[5] Božić, I. (2022). Renewable Energy Sources – Small Hydro Power Plants. University of Belgrade, Faculty of Mechanical Engineering, Belgrade, Serbia. (in Serbian)

[6] Lopes de Almeida, J.P.P.G., Nenri Lejeune, A.G., Sa Marques, J.A.A., Conceição Cunha. M. (2006). OPAH a model for optimal design of multipurpose small hydropower plants, Advances in Engineering Software, vol. 37, p. 236–247.

[7] Anagnostopoulos, J.S., Papantonis, D.E. (2007). Optimal sizing of a run–of–river small hydropower plant. Energy Convers. Manag., vol. 48, p. 2663–2670.

[8] Karlis, A., Papadopoulos, D. (2000). A systematic assessment of the technical feasibility and economic viability of small hydroelectric system installations. Renewable Energy, vol. 20, p. 253–262.

[9] Montanari, R. (2003). Criteria for the economic planning of a low power hydroelectric plant. Renewable Energy, vol. 28, p. 2129–45.

[10] Kaldellis, J., Vlachou, D., Korbakis, G. (2005). Techno–economic evaluation of small hydropower plants in Greece: a complete sensitivity analysis. Energy Policy, vol. 33, p. 1969–1985.

[11] Santolin, A., Cavazzini, G., Pavesi, G., Ardizzon, G., Rosetti, A. (2011). Techno–economical method for the capacity sizing of a small hydropower plant. Water Resources and Management, vol. 52, p. 2533–2541.

[12] Mishra, S., Singal, S., Khatod, D. (2012). A review on electromechanical equipment applicable to small hydropower plants. Int. J. Energy Res, vol. 36, p. 553–571.

[13] Government of Montenegro. (2015). Regulation on the Tariff System for Determining the Feed Cost of Electricity from Renewable Energy Sources and High–Efficiency Cogeneration. Podgorica, Montenegro.

[14] Basso, S., Botter, G. (2012) Streamflow variability and optimal capacity of run–of–river hydropower plants. Water Resources Research, vol. 48 .

ISSN: 2067–3809

[1.] Arinola Bola AJAYI, [2.]Muritala Bamidele ADISA, [3.]Adeshola Oluremi OPENIBO, [4.]Victor Ugochukwu ANIKE

DEVELOPMENT OF SOLAR BAKING OVEN WITH SENSIBLE HEAT STORAGE

[1,2,4.]Mechanical Engineering Dept., University of Lagos, Lagos, NIGERIA.
[3.]Mechanical Engineering Dept., Lagos State University, Epe, Lagos State, NIGERIA

Abstract: This paper presents the design and development of a solar baking oven with sensible heat storage material which is essentially for baking dough and other confectionaries. Bread is one of the staple foods in sub–Saharan Africa after rice. The increase in the prices of loaves of bread sparked the Arab Spring in Tunisia in 2010. Bread is normally baked in a fossil-fuel-fired oven in most cases. Sometimes, electric ovens are used as well but most of the electricity used to power these ovens is from non–renewable energy sources that pollute the environment. Renewable energy sources are abundant in Sub–Saharan Africa, they are clean and they do not pollute the environment. The baking oven was developed to produce a heating effect without the burning of charcoal, firewood, or other fossil fuels thus reducing the carbon footprint of this activity. Baking using non–renewable fossil fuels has its side effects such as high cost of energy, emission of greenhouse gases, and the possibility of choking by the operator resulting from inhaling of smoke. The system is made up of a solar box oven, solar reflector, heat storage, and insulating materials. Design and sizing of the baking oven and solar reflector are provided. Solar energy incidents on the solar reflector and reflected into the oven cavity through the glass which provides the greenhouse effect in preventing convective heat loss, this then leads to the accumulation of heat in the oven chamber which is used in the baking process. A dough of bread of mass 150 g was baked in 3 hours with the highest temperature of 96.75°C achieved in the oven. The oven was able to retain heat over a long period of time due to granite stones incorporated as sensible heat retention materials.

Keywords: Solar box oven. Reflector. Fossil fuel. Greenhouse effect. Heat storage materials

INTRODUCTION

Sub–Saharan Africa is blessed with renewable energy resources in abundance which include but are not limited to solar energy, biomass, wind energy resources, large hydropower potentials, great potential for hydrogen and hydrogenated fuel, geothermal energies as well as ocean energies. These renewable energies are largely untapped due to a lack of appropriate technology and neglect. The major impediments in the development and penetration of technologies for the exploitation and utilization of renewable energy resources in the region include also, the lack of appropriate policies, regulations, and institutional framework and the lack of the will to stimulate investments in the sector. Electricity generation and penetration in Nigeria is low. Ajao et al, (2011) [1] noted that about 60 percent of Nigeria's population are not served with electricity. Per capita consumption of electricity in Nigeria is approximately 100 kWh as against 1379 kWh, 1934 kWh, and 4500 kWh in China, Brazil, and South Africa, respectively. The Sun's energy is radiated at the rate of 3.8 x 10^{23} kW per second. This energy is propagated radially and reaches the edge of the earth's atmosphere at about 1.5 kW/m^2. The downside of solar energy is that it is not concentrated like fossil fuels but the daily energy received by Nigeria from the Sun is in the range of 5.08 x 10^{12} kWh and with appropriate appliances to harvest the solar energy at an efficiency of just 5 % in an area of about 1 % of Nigeria's surface area, electrical energy in the range of 2.54 x 10^6 MWh can be obtained daily. This electrical energy is the equivalent of 4.66 million barrels of crude oil per day. Some applications of these solar energies can be in drying, cooking, heating, distillation, cooling, refrigeration, and also in electricity generation in thermal power plants (Ajao, et al) [1]. Baking is an essential process as it serves as one of the major food processing and preserving methods. The most commonly utilized method for baking is by firewood and other fossil fuels which are causes of environmental pollution and depletion of forest resources. An oven is a device that is used for baking or cooking as a result of its thermally insulated internal chamber. The first recorded use of an oven dates back to around 29,000 BC in Central Europe. These ovens were made in the form of pits used to cook food such as mammoth meat. From 20,000 BC, Ukrainians used pit ovens with hot coals. The Greeks were credited by culinary historians for developing the art of bread baking after they were able to build front–loaded bread ovens (Ohajianya et al, 2014) [2].

The high concern for the depletion of ozone layer and activities to reduce carbon footprint in human activities led to the invention of this new means of baking which subjects the environment to less or no danger i.e. it brings about a clean environment, this new means of baking uses the renewable solar energy to heat up and bake

substances through the reflection of the sunlight on a solar reflector which then transfer heat to the food substance that is contained in the inner chamber of the solar box oven. The need to develop another means of baking that will reduce or eradicate the menace of the present use of fossil fuel in baking is essential. A new type of baking system is developed where solar energy is used as a power source (Hassen, et. al 2011) [3].

The development of a solar baking oven with heat storage material enables the baking of food both during the day and at night without affecting the depletion of the ozone layer as a result of the usage of clean energy in cooking which ultimately prevents the release of harmful emissions into the atmosphere. The basic reason for solar cooking is to heat up food to the required temperature without burning fossil fuel. Solar energy can be used to cook, bake, or fry food items. A solar box can cook because the interior of the box is heated by the sun's radiation through the glass top, direct and reflected sunlight enters the solar box. When the sun's radiation is absorbed by the black absorber plate and cooking pots inside the oven, it is converted into heat energy. As a result of this heat input, the temperature within the solar box cooker rises until the heat loss of the cooker equals the solar heat gain. This phenomenon causes warmth in confined rooms where the sun shines through a clear material like glass. Visible light shines readily through the glass, where it is absorbed and reflected by the materials (aluminum foil) within the enclosed enclosure. The reflected light is either absorbed by other materials in the box or, because it does not change wavelength, it is reflected and travels back out through the glass. The heat absorbed by the black metal absorber plate and pots is transferred via those materials, to bake the food. Heat retention materials can be added to the solar box. The ability of a solar box cooker to store heat improves as the density and weight of the heat retention materials within the insulated box increase. There are basically two types of storage materials which are:

(1) sensible heat energy storage, and

(2) phase change energy storage.

In sensible heat storage, such as rocks, there is an increase in the temperature of the material without the material changing phase. In latent heat storage, the material absorbs heat that is added and goes through a change of phase from solid phase to liquid phase at a certain constant temperature (Saxena and Goel, 2013) [4]. Heat energies are stored in materials that are closely packed which can be rocks, ores, or an enclosed phase change material (PCM), a container, and the transfer of heat through the voids of the bed. There are different ways heat can be transferred to and through the materials. This may be done through convective, conductive, or radiant heat transfer (Sarada et al, 2013) [5].

Many researchers have worked on different types of cookers and ovens that are powered by solar energies [6 – 26]. Some reviews have also been carried out on solar cookers and ovens by many researchers [6 – 10]. Some of these ovens are without any form of heat storage for use when the sun is down [11 – 19] while some are with heat storage devices incorporated in them [20 – 23] and these cookers can still be used after the Sun must have gone down. Domanski, et al (1994) [20] carried out a study to investigate off sunshine hours cooking using phase change materials as storage material in their experiment. They used stearic acid (melting point of 67 – 69 °C) or magnesium nitrate hexahydrate (melting point of 89 °C) as phase change material (PCM). It was discovered that the performance of the cooker was strongly dependent on the intensity of the Sun, the mass of the cooking medium, and the thermo–physical properties of the phase-change materials. Budhi and Sahoo (1995) [21] designed and fabricated a solar cooker with latent heat storage material. They observed that cooking in the evening was feasible by using a solar cooker with latent heat storage. It was observed that the plate temperature was at 57.2 °C during a midnight cooking. Sharma et al (2004) [22] using an evacuated tube solar collector that was equipped with phase change material (PCM) storage, studied the heat performance of a prototype solar cooker. The design comprised two different parts which were energy collection and cooking coupled with a PCM storage unit. The energy from solar is stored in the PCM storage compartment during the time of sunshine and is used for cooking in the evening or at night when the sun is down. They noted that cooking at the noon had no effect on the evening cooking. They also discovered that using PCM heat storage to cook in the evening was faster than cooking at noon. Xie et al (2018) [23] did research on the incorporation of phase change material with the aid of a solar vacuum collector. They obtained a result that shows the effectiveness of PCM usage, which showed that adding phase change material enables the oven's inner temperature to achieve a temperature of 30°C – 80°C higher than the usage of the oven without storage material. The performance of heat storage materials shows that the heat storage layer has a certain heat storage capacity in all seasons and the daily heat storage is about 2718 kJ. Mahfoudi et al (2014) [24] did a simulation on the use of sand as a heat storage material. The setup has a cubic configuration with embedded charging tubes which were used to store solar energy with sand. It was discovered in their results that sand has an important thermal inertia. They observed that the sand bed charging time was about 5 hours and the temperature distribution in the sand bed led to higher

energy efficiency of the sand bed. The objective of this work is to develop a solar baking oven with material for heat retention for the purpose of extended use after sundown. This oven aims to prevent pollution of the environment compared to the conventional mode that uses fossil fuel. It is also economical since there is no consumable fuel cost associated with its use and the use cannot be subjected to fluctuation of prices.

MATERIALS & METHODS

Materials

Some of the materials used for the work are given in this section:

— Solar reflector

The reflector, Figure 1, reflects the sun rays into the oven in other to increase heat transfer into the oven. The solar reflector is made of galvanised steel which has two of its sides raised at 67° to one end of it as shown below, a reflective material of 98% reflection is pasted on the inner surface of the structure to enhance reflection. It is used to reflect the light coming from the sun to the baking element which passes through the glass cover on the solar box.

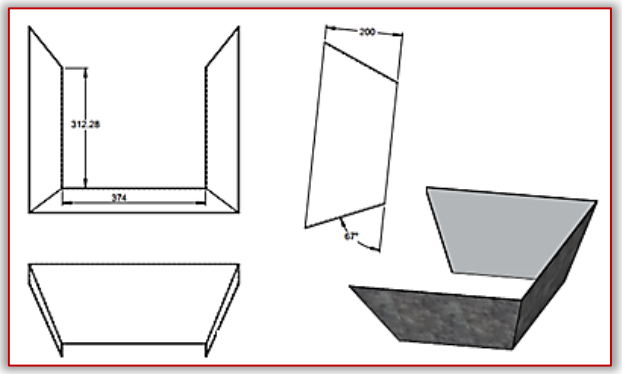

Figure 1a: Design of the solar collector

Figure 1b: 3–side solar reflector

— Solar box oven

The solar box oven is a square-shaped box that is made of three different compartments which are the inner box, the heating storage material compartment (for granite), and an insulating compartment. and the insulating material which is 40 mm thick to prevent heat loss. The entire solar box oven is made of three different boxes, the inner box is of size 250 mm x 250 mm x 150 mm (this is actually the oven cavity). The inner box is the space where the dough is kept for the baking process. It is made of stainless steel in other to enhance proper heating of the food substance and prevent food contamination. The outer shell (casing) of dimensions 400 mm x 340 mm x 150 mm in size, the space between these two casings is where the granite painted black is stored, and the oven is enclosed within another box of dimension 480 mm x 380 mm x 240 mm, the outer cavity is enclosed with fibre glass to minimize convective and conductive heat losses to the environment. Plane glass of 4 mm thickness and dimensions of 400 mm x 340 mm is placed at the top of the oven which allowed inflow of solar insolation and minimized convective heat losses from the cavity.

— Granite

Granite stones, Figure 2, is used as the heat storage material. It is formed and found below the surface of the Earth as a result of volcanic magma eruptions and hardening. The granite used is painted black for good heat absorption and dissipation.

Figure 2: Granite stones painted black

— Glass cover

The glass cover is the medium through which solar insolation passes into the solar box for heat absorption and heating of the cooker and its contents. It also serves as a prevention of the radiant energy from leaving the box cooker thereby creating a process known as the greenhouse effect. This process heats up the oven's inner chamber and the heat storage materials. The glass cover is 3 mm thick.

Experimental setup

After the fabrication of every aspect of the baking oven, the different components were coupled together as shown in Figure 3, and Figure 4. The test was carried out using bread dough to achieve baking.

The temperature of the day was recorded against the time of the day. Thermocouple Temperature Sensor, Figure 5a, MAX 6675 K–Type was used to measure the temperature. The temperature probe was placed inside the oven for the instantaneous temperature readings. Arduino Uno microcontroller board, Figure 5b, was used in this experiment to take the temperature readings of the oven. Jumper wires, Figure 5c were used to connect the thermocouple sensor to the Arduino module.

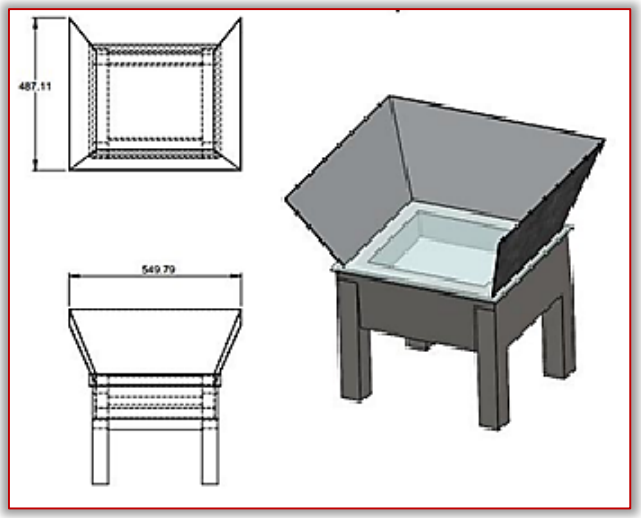

Figure 3. Assembly of the solar box oven

Figure 4: Experimental setup of the solar box cooker

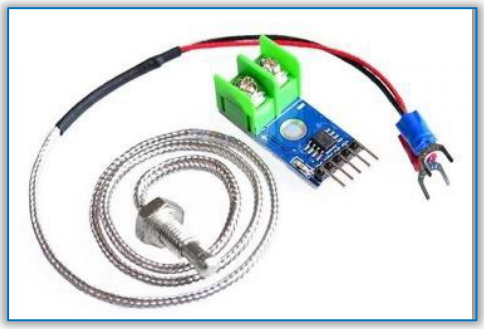

Figure 5a: K–type thermocouple and Max 6675 temperature sensor

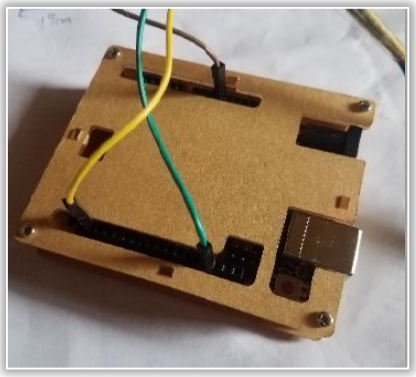

Figure 5b: Arduino Uno module

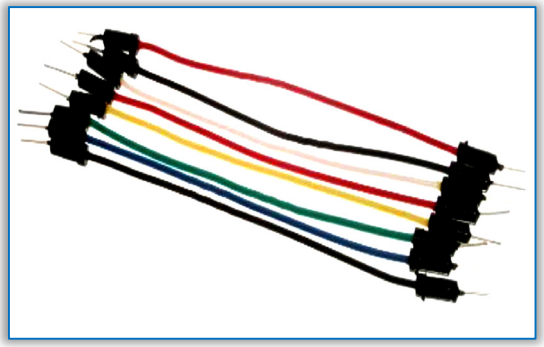

Figure 5c: Jumper wires

Figure 6a is bread dough before baking and Figure 6b is the loaf of bread baked in the oven.

Figure 6a: Dough of bread before baking

Figure 6b: Loaf of bread after baking

RESULTS AND DISCUSSIONS

The solar oven was tested at the Faculty of Engineering, University of Lagos, Lagos Nigeria (6.517985, 3.399527). The temperature obtained during testing was plotted against time in an interval of 15 minutes is shown in Figure 7.

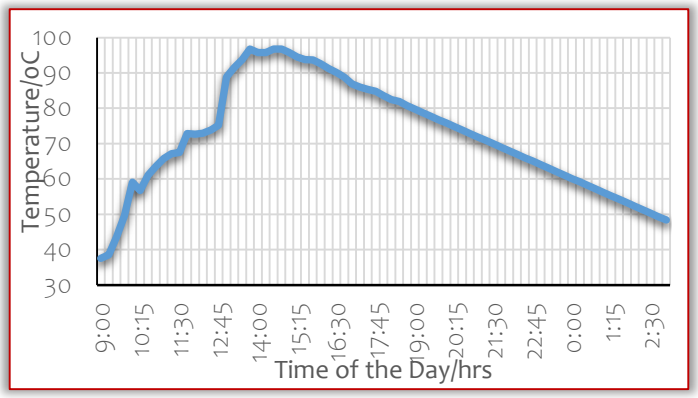

Figure 7: Baking oven Temperature against time of the day

From Figure 7, it was observed that the temperature increased steadily as the sun rose and heated up the chamber and the granites in the chamber. As the sun approached the peak temperature of the day and then the temperature started dropping after the peak temperature was attained. It was also observed from the graph that the oven retained heat for a long period after the sun had gone down which was the purpose of adding heat retention materials. The maximum temperature that was obtained during the day was between the hours of 12:30 pm and 2:30 pm.

CONCLUSION

In this paper, the design and development of a solar baking oven with sensible heat storage material which is purposefully for baking dough and other confectionaries has been presented. It was discovered during the course of the experiment that the time taken to achieve baking is highly dependent on the intensity of the Sun (Solar irradiation). Less intensity of the sun will prolong the time taken to achieve the baking process while the high intensity of the sun will shorten the time taken to achieve the baking process. The heat was retained in the oven for a long time due to the inclusion of heat retention materials and this is also dependent on solar irradiation during the day. This oven can be used even in the rural areas away from power grids. It does not pollute because it uses the energy from the sun which is renewable. The project also incorporates the solar reflector for more effective capture of the Sun energy, which will always aid temperature rise in the oven and fast-track the baking process.

References

[1] Ajao, K.R., Oladosu, O.A., popoola, O.T. (2011). Cost–benefit Analysis of Hybrid Wind–Solar Power Generation by Homer Power Optimization Software. Journal of Applied Science and Technology, 16(1–2), 52 – 57.
[2] Ohajianya, A., Abumere, O. E., Osarolube, E., & Madu, C. A. (2014). Construction and testing of one reflector solar oven for solar panel lamination. IOSR Journal of Applied Physics 6(6), 24 – 31.
[3] Abdulkadir AH, Demiss AA, Ole NJ. (2011). Performance investigation of solar-powered Injera baking oven for indoor cooking. ISES Solar World Congress proceedings, Kassel, Germany; 186–96
[4] Abhishek Saxena, Varun Goel, (2013). "Solar Air Heaters with Thermal Heat Storages", Chinese Journal of Engineering, Article ID 190279, 11 pages.
[5] Kuravi, S., Trahan, J, Goswami, D.Y., Muhammad, M. R., Stefanakos, E. S. (2013). Thermal energy storage technologies and systems for concentrating solar power. Progress in Energy and Combustion Science, 39(4), 285 – 319
[6] Jurinak, J.J., Abdel–Khalid, S. I., (1978), Sizing phase–change energy storage units for air–based solar heating systems, Solar Energy, 22, 355 – 359.
[7] Nkhonjera, L.K, Bello–Ochende, T., John, G., King'ondu, C.K. (2017). A review of thermal energy storage designs, heat storage materials and cooking performance of solar cookers with heat storage. Renewable and Sustainable Energy Reviews. 75, 157 –167.
[8] Joshi, S.B., & Thakkar, H.R. (2017). Solar Cooker – A Review. Proceedings of Solar Cooker International, 6th SCI World Conference, 2017. At: Muni Seva Ashram, Goraj, dist. Vadodara, Gujarat, India. 1 – 9.
[9] Sarbu, I., Sebarchievici, C. (2018). A Comprehensive Review of Thermal Energy Storage. Sustainability, 10(1), 191.
[10] Sharma, A., C.R. Chen, V. V. S Murty, & Anant Shukla. (2009). Solar cooker with latent heat storage systems: A Review. Renewable and Sustainable Energy Reviews, 13(6–7). 1599 –1605.
[11] Shou–Ling, W. (1988). Solar Energy food Oven. Advances In Solar Energy Technology, Proceedings of the Biennial Congress of the International Solar Energy Society, Hamburg, Federal Republic of Germany, 2703–2707
[12] Stone, L. (1997). Solar Baking Under the Sonoran Sun. Home Power, 59, 50–53
[13] G. Hernandez–Luna, & G. Huelsz. (2008). A solar oven for intertropical zones: Evaluation of the cooking process. Energy Conversion & Management. Energy Conversion and Management 49(12), 3622 – 3626.
[14] Tesfay, A. H., Mulu , B. K., & Ole Nyda, J. N. (2014). Design and Development of Solar Thermal Injera Baking: Steam Based Direct Baking. Energy Procedia 57, 2946 – 2955.
[15] Jebaraj, S., Srinivasa. R. P. (2015). High–efficiency solar oven for tropical countries. ARPN Journal of Engineering and Applied Sciences. 10(2), 10213 – 10217.
[16] Abdulkarim, H. T., Nasir, A., & Jiya, J. Y. (2016). Solar Energy for Cooking and Power Generation: An Analysis. International Research Journal of Engineering and Technology (IRJET). 3(6), 1728 – 1734.
[17] Nayak, J., Sahoo, S. S., Swain, R. K., Mishra, A., Chakrabarty, S. (2016). Construction of box type solar cooker and its adapability to industrialized zone. Materials Today: Proceedings, 4(14), 12565 – 12570.
[18] Weldu, A., Zhao, L., Deng, S., Mulugeta, N., Zhang, Y., Nie, X., Xu, W. (2019). Performance evaluation on solar box cooker with reflector tracking at optimal angle under Bahir Dar climate. Solar Energy. 180, 664 – 677.
[19] Zafar, H. A., Badar, A. W., Butt, F. S., Khan, M. Y., Siddiqui, M. S. (2019). Numerical modeling and parametric study of an innovative solar oven. Solar Energy. 187, 411–426.
[20] Domanski, R., El–Sebaii, A. A., Jaworski, M. (1994). Cooking during off–sunshine hours using PCMs as storage media. Energy, 20(7), 607 – 616.
[21] Budhi, D., Sahoo, L. K. (1997). Solar cooker with latent heat storage: Design and experimental testing. Energy Conversion and Management. 38(5), 493–498.
[22] Sharma, S. D., Iwata, T., Kitano, H., Sagara, K. (2005). Thermal performance of a solar cooker based on an evacuated tube solar collector with a PCM storage unit. Solar Energy. 78(3), 2005, 416 – 426.
[23] Xie, S., Wang, H., Wu, Q., Liu, Y., Zhang, Y., Jin, J., Pei, C. (2018). A study on the thermal performance of solar oven based on phase–change heat storage. Energy Exploration & Exploitation. 37(5), 014459871879549.
[24] Mahfoudi, N., Moummi, A., Ganaoui, M.E. (2014). Sand as a Heat Storage Media for a Solar Application: Simulation Results. Applied Mechanics and Materials, 621, 214 – 220.
[25] Tiwari, G. N., Meraji, M., Khan, M. E., Azhar, Md. (2021) Modified Hottel–Whillier–Bliss Equation for Active Solar Distillation System for Higher Yield and Thermal Efficiency. Journal of Thermal Science and Engineering Applications 14(2):1–26.
[26] Rimstar.org (2023) How to design solar reflectors for solar cookers. Online resouces. rimstar.org/renewnrg/how_design_solar_cooker_sun_reflector.htm (Accessed on 27th March, 2023)

ISSN: 2067-3809

Fascicule 4
[October – December]
tome XVI
[2023]

ACTA Technica CORVINIENSIS
BULLETIN OF ENGINEERING

ISSN: 2067-3809

[1.] Andreea–Cătălina Cristescu, [2.] Filip ILIE

A WAY TO DETERMINE THE CAR BRAKING SYSTEM EFFICIENCY IN CORRELATION WITH THE TRAVEL SPEED, THE TIME, AND DISTANCE OF BRAKING

[1–2.]Department of Biotechnical Systems, Polytechnic University of Bucharest, Spl. Independentei 313, 060042 Bucharest, ROMANIA

Abstract: The importance of utilizing an optimal and efficient braking system is emphasized in this study. Braking system optimization and efficiency were practically determined through successive tests on the brake dynamometer, according to road safety regulations. Subsequently, the results were correlated with practical tests involving consecutive braking at different speeds, tracking both the time and distance of braking. The coefficient of friction (COF) was established for each braking instance by utilizing the braking force measured on the brake dynamometer. This paper aims to highlight the genuine impact of the braking system by measuring and establishing its braking efficiency depending on the car's speed, time, and distance of braking.

Keywords: braking efficiency; braking distance; braking time; coefficient of friction; car breaking system

INTRODUCTION

The braking system of a car has a pivotal role in ensuring road safety. The capacity of a vehicle to swiftly decelerate and come to a complete halt within a certain distance is realized by the braking system and is commonly known as braking. During the braking process, the vehicle's kinetic energy is transformed into thermal energy, even one in the contact area between the tires and the road surface [1].

However, the braking force and deceleration are the main braking parameters of a car. Practical, the parameters most commonly utilized are braking time and distance, through their values. The vehicle's traction parameters can be refined through activities such as driving across diverse road surfaces, investing in new tires with substantial tread depth, and even adjusting the vehicle'weight distribution—especially when it is being loaded or unloaded. Factors, like the height of the center of mass, load distribution across axles, and the contact area between the road surface and the tires, can be influenced by variations in the car's load. It's important to note that changes in tire load do not alter the braking factors, a principle given by the fundamental laws of physics [1].

The COF when braking is significantly influenced by changes in velocity and the temperature of the brake disc–pads interface. The COF when braking is significantly influenced by changes in velocity and the temperature from the brake disc–pads interface (COF decreased with temperature and sliding speed). Any vehicle with a friction–based braking system exhibits wear of the disc–brake pads system when the COF noticeably decreases as a result of temperature variations [2–4].

In other words, the factor affecting braking system (brake disc–pads) wear is the tribological state of the braking parts when they are in operation. A number of variables, such as the load, speed, temperature, sliding time, and materials composition in contact commonly affect the tribological properties of the contact surfaces (here brake disc–pads). There is verified evidence that the COF, force and speed of braking, temperature are all in direct relation. Was proven as the COF varies depending on the car mass and is inversely proportional to travel speed [5].

Vehicle braking parameters are routinely evaluated using mathematical models. However, in real–world situations, the braking and deceleration parameter values are always unpredictable [6].

Yin et al. [7] after analyzing the braking process and using testing methods have identified five main parameters (COFs between the discs and the brake pads, and also between the tire and road surface, braking command and control system, driver physical effort, car mass) that have influenced the braking process. The braking ability of the brake discs was then studied under harsh circumstances by Rashid [8] and Sharip [9]. As a result, they contend that brake discs need to transfer heat more effectively (superior thermal conductivity), friction good properties, friction high resistance, and mechanical, and thermal shock strength [10]. Additionally, it must have low weight, and there should not be any noticeable changes in terms of wear or modification of the braking system components [11], and all of these depend on the constructive variant selected. Therefore, as demonstrated

by Volkov et al. [12], the regulations that must be adhered to by braking systems vary continuously, and the performance criteria continue to improve. As a result, several investigations and studies have been conducted [6–11] to enhance the performance and dependability of braking systems [13].

Also, continue to improve the materials used, redesign the braking system assembly (with all components), simulations regarding the behavior of the braking system over time, field testing, as well as studies and research to improve the braking systems performance of motor vehicles [1, 2, and 13].

As more vehicles share the same road space, traffic congestion becomes a common occurrence, especially in urban areas. This situation often leads to frequent braking due to the need for maintaining safe following distances, navigating through congested traffic, and adhering to traffic signals and road signs. The frequent use of the braking system in such congested environments poses significant challenges to the overall efficiency and performance of a vehicle's braking system. Continuous stop–and–go movements result in increased wear and tear on the brake components, potentially leading to decreased braking efficiency in a shorter period of time. This underscores the necessity for vehicles to be equipped with robust and responsive braking systems that can handle the demands of urban traffic and frequent braking scenarios.

In light of these considerations, the correlation between the rising number of cars intensified traffic conditions, and the increased use of the braking system is evident. The design, maintenance, and performance of braking systems become critical factors in ensuring road safety.

For this, it was necessary a series of successive tests on a vehicle with the purpose of monitoring the wear tendency of the brake pads, even of the brake discs along with the measurement of braking distance and time to evaluate the braking system's efficiency. The tests were conducted both on the brake dynamometer stand and in traffic to establish the effectiveness of the braking system in relation to the travel speed, time, and distance of braking. Thus, the coefficient of friction had been determined with the following mathematical relationship:

$$\mathrm{COF} = \frac{\text{Breaking Force (F)}}{\text{Normal Force (N)}}, \quad (1)$$

and the braking force had been measured by testing the vehicle on the dynamometer, while the normal force is determined by the following equation/relation:

$$\mathrm{N} = \mathrm{m} \times \mathrm{g} \quad (2)$$

where: m – vehicle mass (kg); g – gravitational acceleration (9.81 m/s^2).

Then, starting from the definition of the vehicle braking system efficiency, η, as being the percentage braking force, F, from the total weight of the vehicle, m, and given by the relation/equation [14]:

$$\text{Braking efficiency } (\eta, \%) = \frac{\text{Braking force (F)}}{\text{Vehicle weight (m)}} \times 100. \quad (3)$$

Through successive replacements, considering that the car's initial kinetic energy, $E = (m \cdot v^2)/2$ (v – initial braking speed) must be equal to the mechanical work, $W = F \cdot S$, done from the moment of braking, until the movement complete stop (vehicle final velocity, $v_f = 0$ and S – braking distance) by the vehicle's braking system, the equation/relation (3) becomes:

$$\text{Braking efficiency } (\eta, \%) = \frac{\text{Square of the initial braking speed (v,m/s)}}{2 \times \text{gravitational acceleration (g,m/s)} \times \text{braking distance (S,m)}} \times 100. \quad (4)$$

It can be seen that in equation/relation (4), the measured parameters appear (in braking distance, $S = v \cdot t - (d \cdot t^2)/2$ in m, with t – stopping/braking time (braking application duration, in s), and d – vehicle deceleration, in m/s^2.

Thus, measuring the braking time and distance depending on travel speed, and the friction coefficient made it possible to the verification/evaluation and validation of the braking system efficiency of the tested vehicle (car).

MATERIALS AND METHODS

To measure the parameters necessary to establish the braking efficiency, both on the brake dynamometer and in the field (in urban traffic conditions), a real car was used, when the brake pedal is operated frequently, and the braking system is heavily stressed. Brake systems can be tested in a simulated environment using a brake dynamometer. Brake dynamometers can be used at any time to measure the performance of a brake system over the course of its lifetime [15].

Brake dynamometers can replicate the forces that a vehicle would face in addition to measuring performance. The wheels are rotated and stopped by the brake dynamometer to simulate driving situations. This is done with an electric motor with 75 to 200 CP. The motor is managed by a computer that can simulate various vehicle inputs.

The motor generates torque that causes the wheel to turn, simulating the kinetic energy of a moving object. In other words, it causes the brake system to rotate at the required speed, or at an interval of "n" rot/min (rpm) [15–18]

The vehicle put through testing was driven in urban locations with heavy traffic, subjecting the braking system to severe stress and requiring frequent use of the brake pedal, also it was driven at constant speeds in rural locations, with little bit or no use of the braking system.

It is mentioned as when is creating or reverse engineering an application, manufacturers of brake pads for the aftermarket, frequently avoid testing on a real car. It costs money and takes time to do this kind of testing. Results can also be affected by human factors.

The tested car (provided with braking assisting devices) has a disc and pad braking system, both on the front and rear axles. Thus, that car uses unventilated discs at the back axle, and the ventilated discs are used at the front axle, as presented in Figures 1(a) and 1(b).

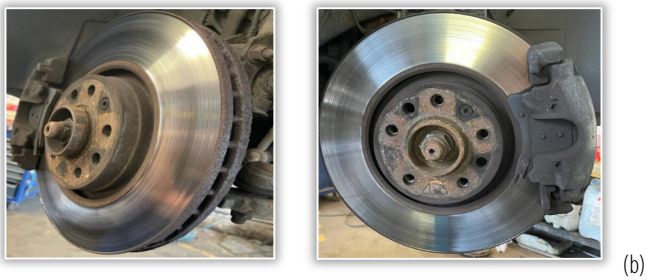

(a) (b)

Figure 1. Brake disc–pads with ventilated brake discs (a); unventilated brake discs (b)

Tested car technical specifications are presented in Table1:

Table 1. The car's technical specifications

Parameter	Valors
Engine power	88 kW
Engine capacity	1910 cm^3
Maximum allowed mass	1865 kg
Vehicle mass	1375 kg

To establish the car braking system efficiency, along with the braking force was used the Nussbaum VISIO brake dynamometer, version 2.0.1.4 STD, equipped with a BT110/410 model roller set (3.5 kW, 6.0 kN, 5.0 km/h) [12], to measure the braking system parameters of the tested car and simplified it is illustrated in Figure 2.

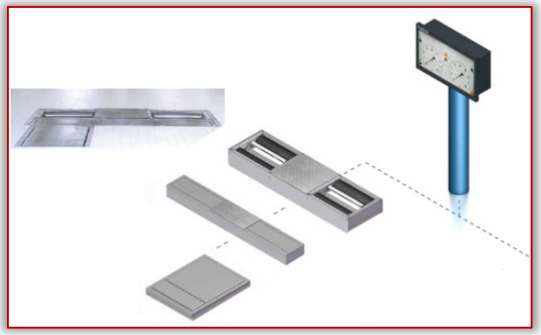

Figure 2. Nussbaum VISIO dynamometer [12]

This dynamometer type is employed for the braking system testing of cars and light commercial vehicles, with the following component parts and technical specifications: axle load of 4 tons, with a maximum braking force of 6 kN; galvanized roller set; electronic measurement system with strain gauges; start protection for braking rollers; control unit; large–scale indicators for braking values (diameter 350 mm); differential indicator and automatic lamp; splash–resistant motors; roller set with premium plastic corundum coating; cable set with a length of 15 meters [12].

The modern software system (Figure 3) has several features and a two–tier interface that makes it typically user–friendly and simple to understand.

Users can set up the program such that the brake force graphs are displayed visually in either analog or column format. By driving the car onto the testing track, the test can start. The software's ability to configure two or more sequences makes it possible to choose the testing method that best satisfies the requirements [12].

Figure 3. Monitoring parameters by the software application

The testing stand detects if a vehicle is positioned on the rollers with all of its wheels when the dynamometer rollers are in motion (Figure 4). The testing stand then automatically switches to an erratic left–right rolling. The force sensor for the brake pedal (Figure 5) is yet another crucial part. Either a wire or remote control can be used to connect the device. This makes it possible to compare braking forces using the force of the brake pedal. On the LCD screen or printed in the testing report, the differential in brake force can be seen.

Figure 4. Dynamometer rollers in motion, testing the braking efficiency

Figure 5. Brake pedal force measurement sensor [12]

Most countries use a test speed of 5 km/h for measuring brake efficiency, while loaded vehicles commonly utilize the maximum braking force range of up to 8 kN. For the purpose of calculating brake efficiency, a weighing device that measures the weight of the vehicle being tested must be positioned beneath the rollers or, in the case of a testing track, on the testing stand [12]. The technical

characteristics of the dynamometer rollers used for testing are presented in Table 2.

Table 2. Technical characteristics of the dynamometer rollers, BT 110/410

Characteristics	Max. allowed value
Permissible axle weight (t)	4
Measurement range (kN)	6
Test speed (km/h)	5
Roller diameter (mm)	204
Roller surface	Welding
Test surface width (mm)	800–2200
Motor power (kW)	3.5
Roller set dimensions (mm)	2332 x 668 x 265
Control panel dimensions (mm)	582 x 500 x 210

A series of successive tests were conducted in the field to determine braking time and distance depending on the vehicle's velocity, in urban traffic conditions. The car had a mass of 1516 kg at the time of performing these tests. Additionally, were used for the testing also following instruments: stopwatch; tape measure; mobile radar; brake pedal activation reference points.

RESULTS AND DISCUSION

To ascertain the braking system parameters as closely to real values as possible, the vehicle was weighed on the testing stand equipped with a scale. The technical parameters of the tested vehicle are presented in Table 3.

Table 3. Parameters of the tested car

Parameter	Measure unit	Front axle	Rear axle	Measured value
Static weight of the left wheel	kg	484	274	
Static weight of the right wheel	kg	484	274	
Axle weight	kg	968	548	
Total weighed mass of the vehicle	kg	1516		

A set of brake system tests were carried out for both axles after, the vehicle's parameters were established. The car was placed on the brake dynamometer rollers to simulate a 5 km/h speed. For the most precise results, the brake was applied repeatedly. A sensor for measuring the brake pedal force and another sensor for calculating the braking force differential were also added. The results can be observed in Table 4.

The experimental tests in urban traffic (of land) conditions were done at different speeds, which were varied in two ranges. In the first range, the speed varied between 37–40 km/h, and in the end, the speed varied between 50–51 km/h. It is mentioned that the experimental tests at these speed ranges were done after the brake pads had been used for 13,083 km, and the brake discs were reused.

For a speed ranging from 37 to 40 km/h, the experimental results are presented in Table 5, and the braking time and braking distance vs. speed graphs for the speed range of 37–40 km/h can be found in Figure 6. At the desired speed, the braking system was acted upon when reaching brake pedal activation reference points.

Table 4. Braking system parameters of the tested car on the brake dynamometer

Parameter	Measure unit	Front axle	Rear axle
Left wheel braking force	kN	2.93	1.84
Right wheel braking force	kN	3.54	1.75
Axle braking force	kN	6.47	3.59
Difference between braking forces	%	17	5
Left wheel friction	kN	0.13	0.10
Right wheel friction	kN	0.14	0.07
Friction force on the road	kN	0.27	0.17
Axle ratio	%	69	68
Dynamic wheel mass	kg	1058	592
Maximum difference on the right	kN	2.93	1.84
Maximum difference on the left	kN	3.54	1.75
Total service brake force	kN	10.06	–
Total parking brake force	kN	–	2.71
Service brake force difference	%	30	17
Service brake efficiency relative to total car mass	%	50	63
Parking brake efficiency relative to total car mass	%	16	18
Service brake force difference	%	30	17
Coefficient of friction	–	~ 0,44	~ 0.24

Table 5. Braking time, distance, and efficiency for the speed range of 37 – 40 km/h

Nr. crt.	Travel speed [km/h]	Braking time [s]	Braking distance [m]	Braking efficiency [%]
1	37	1.56	3.81	63.16 %
2	38	1.93	4.30	59.03 %
3	37	1.80	4.20	57.67 %
4	38	1.46	4.36	58.22 %
5	40	2.34	4.50	62,50 %
6	39	2.20	4.36	61.32 %
7	40	2.36	4.66	60.35 %

The braking system efficiency was established in percentage, based on the relationship/equation (4) depending on the car velocity, time, and distance of braking. For example, using the relation/equation (4) the braking efficiency, η will be:

$$\eta\,[\%] = \frac{\left(\frac{37}{3.6} - 0.325 \cdot \frac{37}{3.6}\right)^2}{2 \cdot 10 \cdot 3.81} \times 100 = 63.16\ \%.$$

Note: Since the initial braking speed is considered to be 30–35% lower than the vehicle's moving speed (here 37 km/h = (37/3.6) m/s), the average value (32.5%) of the interval was considered in the calculation, and the gravitational acceleration, g was rounded to 10 m/s^2, and the value, η = 63.16% was obtained.

Analyzing Table 5 and Figure 6, it can be observed that the maximum braking time and distance are reached at a velocity of 40 km/h, and the minimum braking time at a velocity of 38 km/h, while the minimum braking distance at a velocity of 37 km/h. Therefore, at the highest speed of the range considered, the longest braking time and distance result, respectively at the intermediate speed (38 km/h, and the second test series) the shortest braking time results.

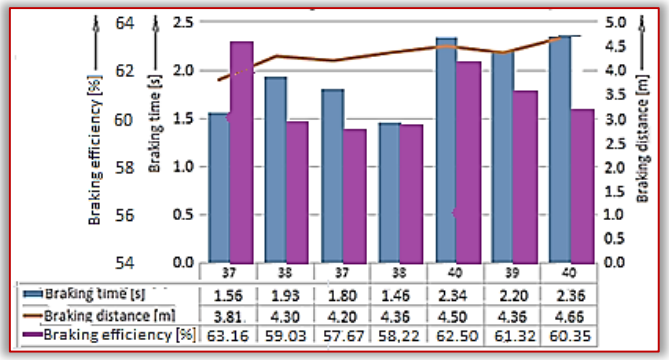

Figure 6. Braking time, distance and efficiency based on vehicle speed (37– 40 km/h)

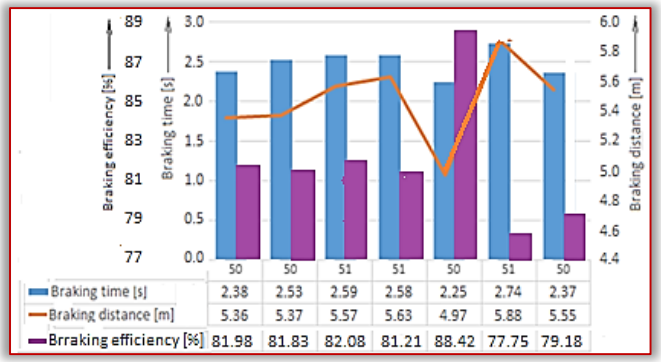

Figure 7. Braking time, distance, and efficiency based on vehicle speed (50–51 km/h)

The explanation would be the better adaptation of the brake pads–disc contact surface (the contact areas have increased, the possible increase in temperature or humidity on the contact surfaces, etc.). Instead, the shortest braking distance is at a velocity of 37 km/h. Hence, it can say that there is a relative correlation between travel speed, time, and braking distance.

It was also observed that testing at the same travel speed and the same braking system (used brake discs–pads), the braking time and distance increased, due to the change in the stroke of the brake pedal, as a result of the wear of the brake disc–pad brake system (especially the brake pads). Then, at the same travel speed, after one or two repetitions, both the time and the braking distance differ from one test to another, with lower values in the second tests series for braking time (see 38 km/h from Table 5 and Figure 6), respectively with higher for braking distance values (see at 38 km/h in the first series of tests and 40 km/h in the second series of tests). This is due to the wear of the elements of the braking system, the environmental and traffic conditions, as well as the way the brake pedal is actuated by the driver, hence the difference between the time and distance of braking at the same velocity.

For the speeds from the range of 50–51 km/h, the experimental results are presented comparatively in Table 6 and their graphs can be seen in Figure 7. A series of braking had been executed while trying to keep a steady speed and braking point.

Table 6. Braking time, distance, and efficiency for the speed range of 50 – 51 km/h

Nr. crt.	Travel speed [km/h]	Braking time [s]	Braking distance [m]	Braking efficiency [%]
1	50	2.38	5.36	81.98 %
2	50	2.53	5.37	81,83 %
3	51	2.59	5.57	82.08 %
4	51	2.58	5.63	81.21 %
5	50	2.25	4.97	88.42 %
6	51	2.74	5.88	77.75 %
7	50	2.37	5.55	79.18 %

Note: Here, the braking efficiency was established on the same principle as the example presented in Table 6.

From the analysis of Table 6 and Figure 7, and in this case (car travel velocity in the range of 50–51 km/h) the findings from the previous case are valid, with the observation that in the third test (at a speed of 50 km/h), both the time and the braking distance had a sudden drop (especially the braking distance, see Figure 7). This was possible, possibly due to the increase in the friction temperature and the degree of humidity in the brake disc–pads contact area, even the degree of tire wear. Also, in each individual case, an oscillatory variation of both the braking time (but with relatively smaller amplitudes) and the braking distance (but with relatively larger amplitudes) is observed.

It is observed that the efficiency of the service brake is over 43.5% (as the minimum accepted point of the efficiency of the braking system, for both travel speed ranges), under the conditions of the normal vehicle load of 1,515 kg (see Tables 5 and 6, as and Figures 6 and 7). This limit of 43.5 % for the braking efficiency was established according to the North American Standard and with U.S.A federal regulations accepted and by European Community.

Thus, it was observed a braking system efficiency of about 60.32 %, for the range of 37–40 km/h, respectively of about 81.78 %, for the range of 50–51 km/h, as an average value. It is important to specify that first the experimental tests were performed in the range of speeds 50–51 km/h and then in the range of 37–40 km/h.

Braking efficiency results (60.32 %, as the average value) show for the range 37–40 km/h, the need to replace in a much shorter time period of some braking system elements (especially the brake pads), than the recommended one. Instead, for the range 50–51 km/h, the braking efficiency being over 21 % bigger, it proves that the lifetime of the braking system approaches with much to the recommended interval.

It seems that the explanation would be: the experimental tests were realized after ones from the speed range of 50–51 km/h, respectively the car was used in urban/intense traffic conditions, which has led to more accelerated wear of the brake pads and even of the discs.

At the same time, it seems that the degree of humidity, the road condition, even also the degree of tire wear, as well as the heat evacuation being slower at lower speeds led to this difference.

This is also confirmed by the evolution of the braking efficiency (through the values in Table 5, but also the graph in Figure 6). An oscillatory evolution is observed, its increase at the speed of 37 km/h, followed by a decrease at the increased speed (38 km/h), even at the same speed (of 37 km/h), in the second test. Then, with the increase in travel speed (to 40 km/h), the braking efficiency increases again (but below the first value from 37 km/h), after which it continues to decrease with the decrease in speed to 39 km/h and even to 40 km/h, on the second test. In the case of the speed interval 50–51 km/h, an oscillatory evolution of the braking efficiency with relatively small amplitude is also observed (see Table 6 and Figure 7), but it starts from lower values (relatively close, with small alternations, both at a velocity of 50 km/h and at a velocity of 51 km/h). After that it has a relatively sudden increase at a velocity of 50 km/h (from the third test), followed by a sudden decrease at a velocity of 51 km/h (also on the third test) and then a relatively small increase at a velocity of 50 km /h (also on the third test). These observations show the influence of the alternation of traffic conditions (the road, the degree of humidity and cooling of the braking system, the steering wheel, and the driver's mode of operation).

However, in both cases (the range 37–40 and 50–51 km/h), the braking system efficiency was well above the allowed limit of 43.5%, respectively it was observed that the parameters (the time and distance of braking/stopping, measured) for the braking efficiency establishment have increased with increasing car velocity (from 37 to 50 km/h). At the same time, the wear of the brake pads and discs was monitored, in relation to the initial velocity, to highlight the need for the replacement more frequent of some braking system elements, especially, in heavy traffic conditions.

CONCLUSIONS

The correlation between braking efficiency and braking distance/time highlights the crucial role a functional braking system plays in mitigating potential accidents and ensuring the safety of passengers and pedestrians alike.

The experimental results have been validated by experimental methods of testing, as close as possible to operational reality, and have shown that the recommendations regarding the replacement frequency of brake pads and discs (less) are inconsistent with the braking system's actual wear.

The results obtained from the analysis of braking times and distances emphasize the importance of maintaining an efficient braking system. It is imperative to address any discrepancies in braking time/distance and ensure that the braking system is optimized for maximum efficiency.

A high–performance braking system, well maintained and operated, can greatly reduce the risks associated with unexpected stops and collisions. It follows that continuous monitoring, maintenance, and improvement of the braking system are essential elements for improving road safety and preventing potential accidents.

After conducting the experimental tests, a larger reduction in the efficiency of the braking system was found, for the velocity range of 37–40 km/h and with much less for the velocity range of 50–51 km/h in urban traffic conditions.

The braking system efficiency has been around 60%, for the range of lower speeds (37–40 km/h) and around 82% for the range of higher speeds, on average. By comparison with the allowed limit value (43.5%) for the braking system, these results suggest the need to replace (usually, first the brake pads,) some braking system elements, at a much shorter interval (for the lower speed range) and much longer (for the higher speed range), than the recommended one.

Because, in these conditions, it has been shown that the braking system efficiency decreases faster, it is essential, to carry out new studies to determine the braking system wear, to ensure the safety of all traffic participants.

Therefore, it is necessary to continue research on the braking system behavior in urban traffic conditions and also at other velocity ranges, even other conditions. The results obtained will be followed the braking system wear tendency by simulations, based on a statistical calculation model.

Moreover, the study has shown that heavy/urban traffic has a psychological effect on drivers, who tend to behave much more aggressively, which proves the need for an effective braking system.

Acknowledgements: This work has been funded by the European social fund from the sectorial operational programmer human capital 2014–2020, through the financial agreement with the title "training of PhD students and postdoctoral researchers in order to acquire applied research skills – smart", contract no. 13530/16.06.2022 – smis code: 153734.

References

[1] D. Berjoza , I. Dukulis, V. Pirs, I. Jurgena, Testing Automobile Braking Parameters by Varying the Load Weight, Proceeding of 7th International Conference on Trends in Agricultural Engineering 2019 (TAE 2019), Prague, Czech Republic, 51–58.

[2] P. Greibe, Braking distance, friction and behaviour. Findings, analyses and rec–ommendations based on braking trials, Trafitec, Scion–DTU 2007, Lyngby, Denmark.

[3] *** National Highway Traffic Safety Administration (NHTSA), Consumer Braking Information, 2003, https://www.nhtsa.gov/document/woodspdf.

[4] K. Parczewski, Effect of tyre inflation preassure on the vehicle dynamics,", Eksploatacja i Niezawodnosc –Maintenance and Reliability, Eksploatacja i Niezawodnosc –Maintenance and Reliability 2013, 15(2), 134–139.

[5] Y. Zhang, X. Jin, M. He, L. Wang, Q. Wang, L. Wang, Y. Wu , The convective heat transfer characteristics on outside surface of vehicle brake disc, International Journal of Thermal Sciences 2017, 120, 366–376

[6] A. Demira, A. Oz, Evaluation of vehicle braking parameters by multiple regression method, Scientia Iranica B 2019, 6(26), 3334–3355
[7] Y. Yin, J. Bao, J. Liu, C. Guo, T. Liu, Y. Ji, Brake performance of a novel frictional–magnetic compound disc brake for automobiles, The Proceedings of the Institution of Automobile Engineers, Part D: Journal of Automobile Engineering 2018, 233(10).
[8] A. Rashid, Overview of Disc Brakes and Related Phenomena – a review, International Journal of Vehicle Noise and Vibration 2014, 10(4), 257–301
[9] S. Sharip, Design Development of Lightweight Disc Brake for Regenerative Braking – Finite Element Analysis, International Journal of Applied Physics and Mathematics 2013, 3(1), 52 – 58
[10] F. Ilie, A.C. Cristescu, Experimental Study of the Correlation between the Wear and the Braking System Efficiency of a Vehicle, Applied Sciences 2023, 3(14), 8139
[11] R.M. Firdaus, B Supriyo, A. Suharjono, Analysis of braking force efficiency measurements for various braking strategy applied for vehicle tested on roller brake tester, Journal of Physics: Conference Series 1517 2020, 012079, 1–6
[12] Nussbaum, Break Test Standas, Test Lanes and Headlight Testers. Passenger Cars and Transporters 2016
[13] F. Ilie, A.C. Cristescu, Tribological Behavior of Friction Materials of a Disk–Brake Pad [Braking System Affected by Structural Changes—A Review, Materials 2022, 15(14), 4745
[14] P.R. Childs, Mechanical Design Engineering Handbook, Chapter 13 – Clutches and Brakes 2014, Butterworth–Heinemann, 513–564
[15] A. Markel, The Real Cost of Installing Cheap Brake Pads, 2022, https://www.brakeandfrontend.com/the–real–cost–of–installing–cheap–brake–pads/.
[16] Anasiei Ioana, Mitrica Dumitru, Badea Ioana–Cristina, Șerban Beatrice–Adriana Storz Andreas, Carcea Ioan, Olaru Mihai Tudor, Burada Marian, Constantin Nicolae, Matei Alexandru Cristian, Popescu Ana–Maria Julieta, Characterization of Complex Concentrated Alloys and Their Potential in Car Brake Manufacturing, Materials, 16, 2023
[17] Ioana, A., Constantin, N., Istrate, A., Paunescu, L., Pasare, V., Possibilities of Physical–Chemical Sensors' Use for Optimizing the Processing of Metallurgical Melting Based on Computer Systems, Sensors, 23, 8, 2023
[18] Ciurdas, M., Arina Gherghescu, I., Ciuca, S.,Cotrut, C., Heat treatment influence on the corrosion resistance of a Cu–Al–Fe–Mn bronze, Revista de Chimie, 2018, 69(5), pp. 1055–1059

ISSN: 2067-3809

Fascicule 4
[October – December]
tome XVI
[2023]

ACTA Technica CORVINIENSIS
BULLETIN OF ENGINEERING

ISSN: 2067-3809

ACTA TECHNICA CORVINIENSIS – BULLETIN OF ENGINEERING
TOME XVI [2023] | FASCICULE 4 [OCTOBER – DECEMBER]

[1.]Kolawole Adesola OLADEJO, [2.]Nurudeen Olatunde ADEKUNLE, [3.]R. ABU,
[4.]Damilare Vincent ADIASOR, [5.]Ayoola G. TIKAREWA

A CONTACT STRESS AND FAILURE PITTING OF STRAIGHT BEVEL GEARS

[1, 5.]Department of Mechanical Engineering, Obafemi Awolowo University, Ile–Ife, Osun, NIGERIA
[2, 4.]Department of Mechanical Engineering, Federal University of Agriculture, Abeokuta, NIGERIA
[3.]Department of Mechanical Engineering, University of Ibadan, NIGERIA

Abstract: Bevel gears find application in transmitting motion between shafts that are not aligned, typically forming a 90° angle relative to each other. Some of the several types that are available commercially are the straight bevel, the Zerol bevel, the spiral bevel and the hypoid. Stainless steel, gray cast iron, titanium alloy and structural steel were used for the behavioural assessment. The design and modelling of the straight bevel gears were carried out using SolidWorks 2015, while ANSYS 18.2 was employed for simulating the stress and deformation of the gears. The 3D solid model generated using SolidWorks was imported into ANSYS, where the analysis was conducted using the finite element software, ANSYS Workbench. Stress distribution plot, deformation plot, and equivalent strain plot were generated. The highest stress, measuring 73.16 MPa, became evident as the load concentrated near the base of the gear teeth. The finite element analysis revealed a minimal likelihood of gear failure, and the least deformation was observed in the structural steel configuration, resulting in a deformation of 8.2354 x 10^–3 mm. Consequently, the gear pair is capable of successfully transmitting 6 kW of power without experiencing any failures with a good factor of safety.

Keywords: bevel gears, contact stress, translational displacement, pitting, bending stress

INTRODUCTION

Bevel gears have their teeth intricately carved onto the frustum of a cone, diverging from the conventional cylinder–shaped teeth found in spur and helical gears. In order for two such cone–frustum–shaped gears to engage seamlessly without any slipping, they require a shared apex, necessitating careful alignment of bevel gears on their respective shafts. This alignment ensures that the gear teeth elements converge to form a singular apex point. This, in turn, guarantees that the pitch surfaces of the engaged bevel gears remain proportionate to their distance from the common apex, facilitating a state of pure rolling motion between them.

Due to the conical nature of the pitch surfaces on bevel gears, the thickness and height of the teeth vary from the front end (toe) to the back end (heel), the larger extremity of the bevel gear. Conventional practice in bevel gear technology involves precisely defining the size and configuration of the tooth profile at the gear's back end.

Bevel gears fall into distinct categories based on their geometry:

- Straight bevel gears exhibit conical pitch surfaces, with their teeth following a straight and tapering pattern toward s the apex.
- Spiral bevel gears feature curved teeth set at an angle, enabling gradual and smooth tooth engagement.
- Zerol bevel gears closely resemble standard bevel gears, differing primarily in their curved teeth structure: the tooth ends lie on a common plane with the gear axis, while the middle portion of each tooth sweeps circumferentially around the gear. Zero level gears can be seen as a variation of spiral bevel gears, sharing curved teeth but having a spiral angle of zero, aligning the tooth ends with the gear axis.
- Hypoid bevel gears resemble spiral bevel gears, but their pitch surfaces follow a hyperbolic shape rather than a conical one

The validation of performance of the bevel gears occurred through a comparison between the outcomes of the Algorithm's computations and those generated by the software (Oladejo and Bamiro, 2009; Akinnuli, et al., 2015; Abu, et al., 2016). The efficacy of Bevel CAD was affirmed, attributing slight dissimilarities in the outcomes to approximation inaccuracies. Bevel CAD enhances efficiency while alleviating the tedium associated with extensive calculations, thus positioning it as a recommended instrument for both industrial and tertiary settings engaged in bevel gear design. Bevel gears are commonly situated on shafts with a 90–degree separation, although they can be customized to function effectively at varying angles (Rufus, et al., 2016; Oladejo and Ogunsade, 2014). These gears possess a pitch surface in the form of a cone. When two bevel gears mesh together, it is referred to as bevel gearing. Within this gearing system, the pitch cone angles of the pinion and gear depend on the angle of the shafts' intersection. The

applications of bevel gears are extensive, including their use in locomotives, marine vessels, automobiles, printing presses, cooling towers, power plants, steel plants, and railway track inspection machines.

The modeling application enables the manipulation of a generated 3D gear model using pre–defined parameters that rely on geometric relationships and constraints (Ramana–Rao, et al., 2013; Ligata and Zhang, 2011). Altering these parameter values leads to modifications in the ultimate shape of the gear. This rapid parameter–driven model creation facilitates swift analysis of forces and stress through an analytical approach. The modeling methodology and functionality, illustrated through a specific example, hold potential applicability in the realm of cone crushers. Modify the software to enable the calculation of contact stress and acceleration variations in the driven wheel during the meshing process (Dong, et al., 2011; Oladejo, et al., 2018). This calculation is instrumental in directing the adjustments made to the spur bevel gear. The simulation outcomes demonstrate that tooth modification significantly influences the stress distribution on the gear surface. This modification proves instrumental in mitigating issues such as load concentration, agglutination, and pitting, effectively preventing their occurrence.

Assessment of the stress distribution at the tooth root of the bevel gear is conducted across diverse load scenarios, encompassing both uniformly varying loads and concentrated loads at the pitch point (Mohan and Jayaraj, 2013; Ligata and Zhang, 2011); Oluwole, et al., 2014). This study further delves into the load dispersion along the pitch line and examines stress patterns within the root fillet region.

This objective is effectively accomplished by recalculating the gear blanks, while keeping the flank geometry and tooth–cutting process unaltered (Karlis, et al., 2014; Jadeja et al., 2013; Edward and Lucky, 2018; Raj, and Jayaraj, 2013; Osakue and Anetor, 2017). Consequently, the optimized tooth ends of the gear pair can be machined without disrupting the standard tooth–cutting procedure. To substantiate this notion, an illustrative recalculation example is presented. These enhancements yield heightened tooth strength, streamline the gear blank geometry, align with contemporary machining practices, and lead to a reduced outer gear diameter.

Bevel gears find application in differential drives, enabling the transfer of power to two axles that rotate at varying speeds (Patil, et al., 2014; Gupta, et al., 2016; Oladejo et al., 2021). Examples include cornering automobiles and hand drills, where they redirect the shaft's orientation, or in cases like shifting power from a horizontal gas turbine engine to a vertical rotor. This study undertook a comparison between the Lewis equation and ANSYS Workbench, yielding closely aligned results.

Assessing the fitness of each individual through Monte Carlo simulation relies heavily on the quantity of samples used, which directly impacts accuracy (Jean–Yves, et al., 2008),. A higher volume of samples enhances precision but escalates computational expenses. To mitigate the computational burden associated with Monte Carlo simulation and genetic algorithm–based optimization, a strategy involves applying varied fitness levels. This entails introducing different sample quantities during the optimization process within our algorithms. Standards have been established to govern the design, analysis, and production of bevel gears (Ratnadeepsinh, et al., 2013; Shan and Zhang, 2012). The equation for calculating bending stress in the teeth of bevel gears is derived from the Lewis bending stress equation applied to beams. This equation yields bending stress values for various types of bevel gears, including spiral bevel gears, straight teeth bevel gears, and zerol bevel gears. To compare the analytical values with those obtained through ANSYS Workbench 14.0, the bending stress values for the aforementioned gears are evaluated. The application of parametric design to bevel gears could serve as a foundation for subsequent finite element stress analysis or assembly procedures (Shan and Zhang, 2012; Kurlapkar, et al., 2016). In this study, a set of bevel gears generated through the execution of macros was successfully assembled, demonstrating a precise meshing of the gears

Albert, et al. (2006) delved into the investigation of failure in a crown wheel and pinion set. Through the application of established metallurgical methods, a fractured gear underwent a comprehensive analysis aimed at determining the root cause of the failure. The findings of the study point to the failure being attributed to the manufacturer's decision to compromise the raw material composition. This compromise becomes evident in the notably elevated manganese content, coupled with the absence of nickel and molybdenum. As a consequence, the core hardness significantly increased, ultimately triggering the premature failure of the pinion. In the work by Alexander (2003), an engineering approach is outlined, aimed at harmonizing the bending stress distribution within both the pinion and the gear. Typically, these components possess distinct tooth profiles and widths, often comprising varying materials. The study introduces an equation that ensures equivalent bending safety factors for the highest bending stresses encountered in both the pinion and the gear. The objective is to establish teeth of equal strength for both the pinion and the gear.

Hasan et al. (2006) conducted a comprehensive analytical examination of elastic–plastic stress distribution within a rotating orthotropic annular disc. This disc is composed of a metal matrix infused with curvilinear reinforced steel fibers. Varied angular velocities were employed in the study to facilitate the observation of plastic region

separation. The outcomes revealed pronounced differences, with the inner surface of the disc exhibiting greater values for both radial displacements and plastic flow compared to the outer surface. Suggested are a pair of dynamic models designed to explore the interplay between surface wear on a gear and its dynamic behaviour (Ahmad and Ahmet, 2007; Oladejo, et al., 2018). These models encompass the impact of worn surface profiles on dynamic tooth forces and transmission error, along with the effect of dynamic tooth forces on wear profiles. Explored was the application of an asymmetric toothed gear to enhance bending–related fillet strength (Kumar, et al., 2008; Abu et al., 2016). Additionally, an examination of the maximum fillet stress was undertaken to aid in enhancing this bending–related capacity. The study employed a non–standard asymmetric rack cutter for both the pinion and the gear. The findings indicated that employing an asymmetric gear configuration augments the fillet load–bearing capability of both the pinion and the gear, particularly at higher–pressure angles

Presenting a gear model derived from analytical simulation, followed by experimental tests using strain gauges, and subsequently comparing the outcomes with numerical results (Michele, et al., 2005); Yi and Chia, (2011); Oladejo and Bamiro, 2009). Strain gauge measurements were conducted on a modified bevel gear, disregarding alignment with the model's nodes. Consequently, stress estimation at corresponding strain gauge positions was unfeasible within the experiment. The primary objective revolves around the design and analysis of straight bevel gears, encompassing two key aspects:

- Creation of a 3D model for a Straight Bevel Gear utilizing SolidWorks.
- Execution of simulations on the 3D model, entailing an examination of bending stress, strain, and deformation across diverse materials such as Structural Steel, Stainless Steel, Gray Cast Iron, and Titanium Alloy.

MATERIALS AND METHODS

The purpose of this study is to design and analyse a straight bevel gear, create a 3D model using Solidworks, run stress simulations on the generated model and compare the simulation result to the numerical analysis result. Assessment of the behaviour of different materials under certain loading conditions will be done. The materials that will be used for the behavioural assessment of the bevel gear (Figure 1) under certain loading conditions include: Gray cast iron, Stainless steel, Structural steel, and Titanium alloy, and their properties are stated in Table 1.

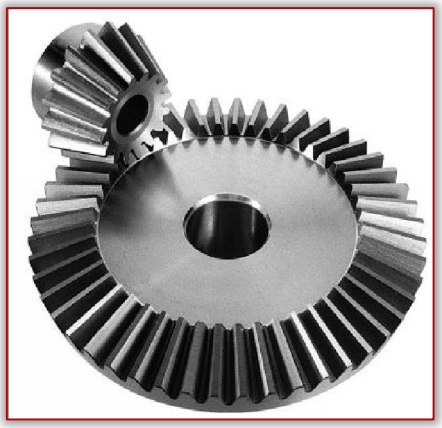

Figure 1: Bevel Gear Profile

Table 1: Material Properties for Behavioural Assessment

Parameter	Gray cast iron	Stainless steel	Structural steel	Titanium alloy	Unit
Young's Modulus	1.1×10^5	1.93×10^5	2×10^5	96000	MPA
Specific Heat	4.47×10^5	4.8×10^5	4.34×10^5	5.22×10^5	mJ/kg·℃
Ultimate Tensile Strength	240	586	460	1070	MPA
Density	7.2×10^{-6}	7.75×10^{-6}	7.85×10^{-6}	4.62×10^{-6}	Kg/mm^3

Design Equations

For the design of the bevel gear, a nomenclature is defined for the gear in Figure 2 and the parameters and formulae for its design are stated in Tables 2 and 3

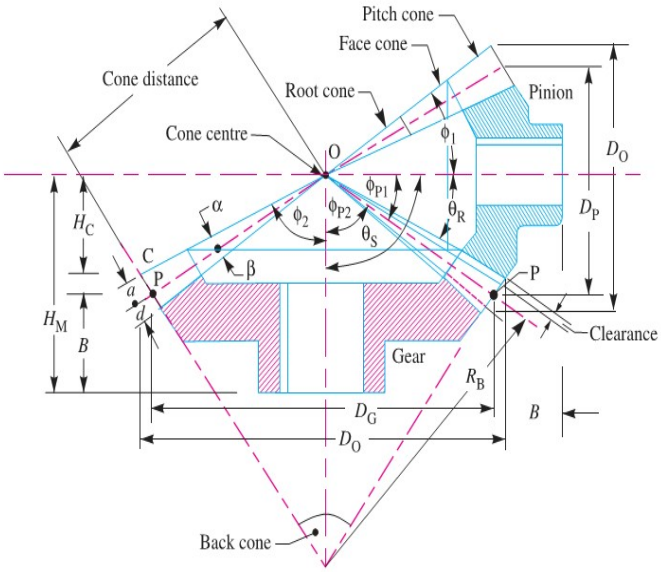

Figure 2: Bevel Gear Nomenclature (Khurmi and Gupta, 2005)

Table 3: Design Parameters

Parameters	Pinion	Gear	Unit
Power	6	6	kW
Number of teeth	20	30	No.
Pitch circle diameter	100	150	mm
Module	5	5	mm
Pressure angle	20°	20°	Deg.

Table 2: Bevel Gear Design Equations (Khurmi and Gupta, 2005)

Parameter	Formula
Velocity ratio or Gear ratio	$V.R = \frac{D_g}{D_p} = \frac{T_g}{T_p} = \frac{N_g}{N_p}$
Pitch angle of pinion	$\theta_{P1} = \tan^{-1}\left(\frac{1}{V.R.}\right) = \tan^{-1}\left(\frac{D_P}{D_G}\right) = \tan^{-1}\left(\frac{T_P}{T_G}\right) = \tan^{-1}\left(\frac{N_G}{N_P}\right)$
Pitch angle of gear	$\theta_{P2} = \tan^{-1}(V.R.) = \tan^{-1}\left(\frac{D_G}{D_P}\right) = \tan^{-1}\left(\frac{T_G}{T_P}\right) = \tan^{-1}\left(\frac{N_P}{N_G}\right)$
Addendum	a = 1m
Deddendum	d = 1.2m
Clearance	c = 0.2m
Working Depth	w = 2m
Thickness of tooth	t = 1.5708m
Face width	b = 0.25 x OC
Mean Pitch Diameter	$D_m = D - b\sin\theta_p$
Circumferential velocity on the Mean pitch circle	$V_m = \frac{\pi D_m n}{6000}$
Nominal tangential load on the Mean	$F_t = \frac{P}{V_m}$ pitch circle
Bending Stress	$\sigma_b = \frac{F_t}{b\,m\,j} K_v K_o K_m$

2.2 Bending Stress in Bevel Gear

As per the AGMA, the bending stress in bevel gear is calculated by the Equation (1).

$$\sigma_b = \frac{2T}{d}\frac{Gr}{FmJ}\frac{K_a K_m K_s}{K_v K_x} \quad (1)$$

Load Calculation

The load calculation involves calculating torque and tangential load acting on the bevel gear. Consider a bevel gear with the following:

The speed of bevel gear (n) = 500 rpm, and

Power transmitted = 6 kW

$$\text{Torque transmitted } (M_t) = 9.5488 \times \frac{\text{Power(w)}}{\text{speed(rpm)}} \quad (2)$$

$$M_t = 9.5488 \times \frac{6\times1000}{500}$$

M_t = 114.586 Nm = 114586 Nmm

Tangential component,

$$P_t = \frac{2\times M_t}{d} \quad (3)$$

$$P_t = \frac{2\times114586}{100} = Pt = 2291.72\ N$$

Bending Stress

$$\sigma_b = \frac{P_t}{m\times b\times y\left(1-\frac{b}{A_o}\right)} \quad (4)$$

where

$\left(1-\frac{b}{A_o}\right)$ = Bevel Factor

$$A_o = \sqrt{\left(\frac{D_p}{2}\right)^2 + \left(\frac{D_g}{2}\right)^2}$$

$$A_o = \sqrt{\left(\frac{100}{2}\right)^2 + \left(\frac{150}{2}\right)^2} = 90.139\ mm$$

B = A_o / 3 = 30.05 mm

$$\sigma_b = \frac{2291.72}{5\times30.05\times0.32\left(1-\frac{30.05}{90.139}\right)} = 71.50\ N/mm^2$$

MODEL DEVELOPMENT PROCESS USING SOLIDWORKS

A three–dimensional solid model of a bevel gear using SolidWorks was developed. The development involves the following steps.

Sketch the Gear Profile:

Sketch the gear profile as shown in Figure 3 and produce the solid model as shown in Figure 4. Use sketch tools to draw a tooth profile of the bevel gear as shown in Figure 5. Create a tooth as shown in Figure 6.

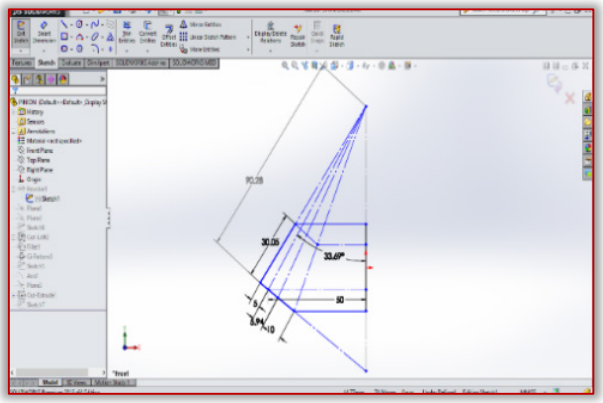

Figure 3: Sketch of the bevel gear

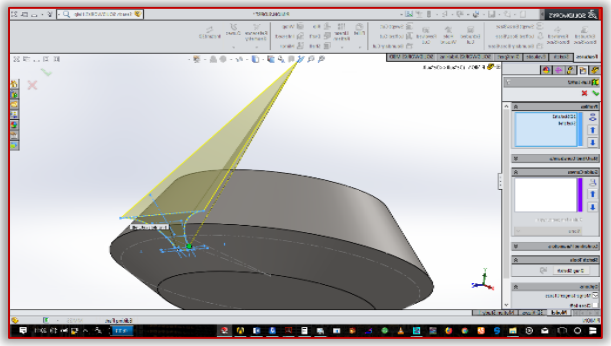

Figure 4: Solid model of the bevel gear

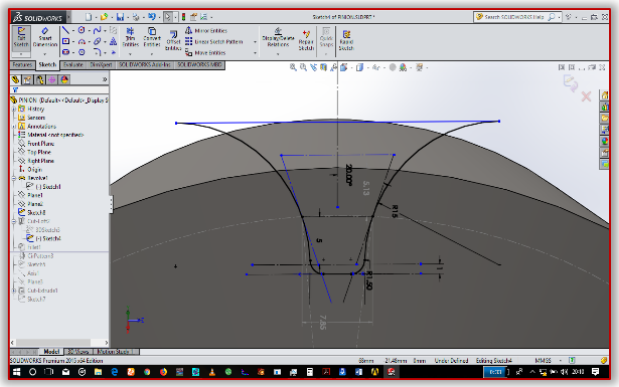

Figure 5: Using sketch tools to draw the tooth profile

Revolve the Tooth Profile:

Use the "Revolve Boss/Base" feature. Select the sketch profile as the profile to revolve and specify the axis of rotation (centerline of the gear). Set the angle to 360 degrees to obtain the profile shown in Figure 7.

Create the Bevel Gear Teeth:

The subtract tool in the "Combine" feature was used to create the teeth as shown in Figure 8.

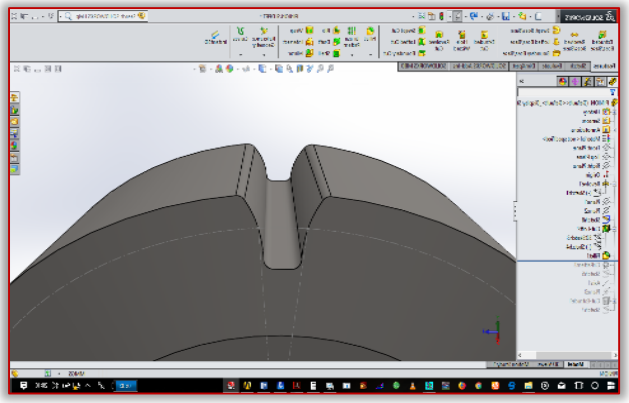

Figure 6: Development of a tooth profile

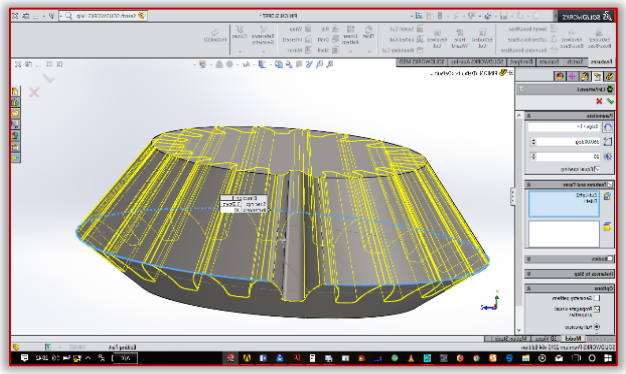

Figure 7: Revolving the tooth profile

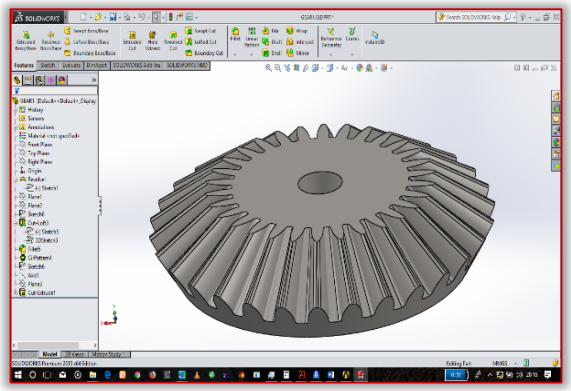

Figure 8: The developed 3D model of the gear

Add the Second Bevel Gear (Pinion):

Similar steps were followed to create the second bevel gear (Figure 9) which is pinion.

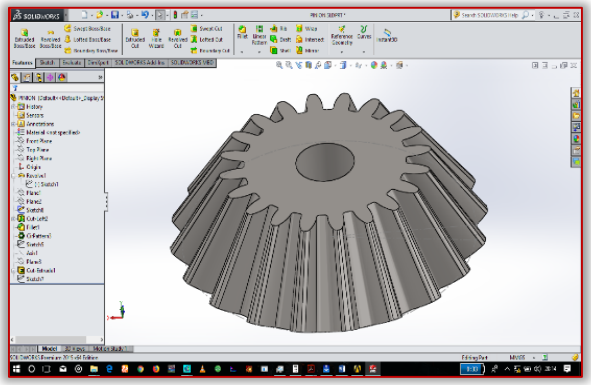

Figure 9: The developed 3D model of the gear

Combine Gears in an Assembly:

An assembly file was opened and the two gears were inserted into the assembly. The "Mate" tool was used to define the relationship and movement between the gears (Figure 10).

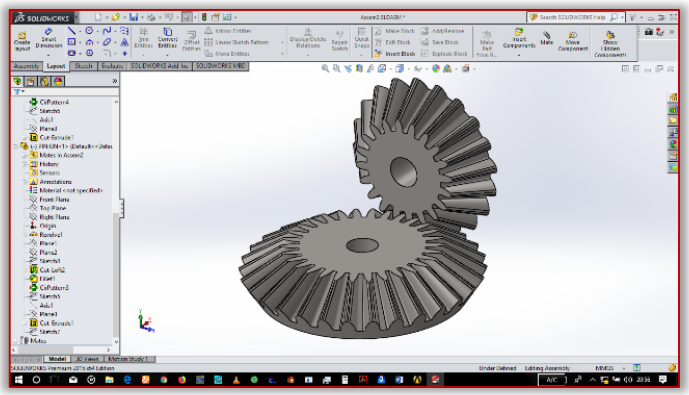

Figure 10: Assembling of Pinion and Gear

Save:

The SolidWorks file is save in "IGES" format for export to finite element analysis (FEA) software

ANALYSIS OF 3D MODEL OF THE BEVEL GEARS

Finite Element Model

The SolidWorks software was utilized to generate a comprehensive three–dimensional solid model, which was subsequently imported into ANSYS. The subsequent analysis involved the application of the finite element (FE) program, ANSYS Workbench 19.1. The initial 3D solid model constitutes an assembly comprising two interlocking gears, as depicted in Figure 11. This assembly consisted of a total of 598,289 elements. The subsequent step encompassed a stress analysis of the solid model, with the primary objective being the determination of both normal and shear stresses.

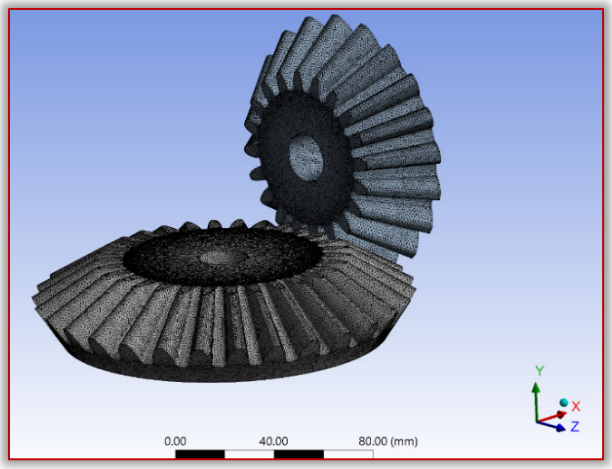

Figure 11: Meshing of Gear Pair

Loading and Boundary Conditions

The load is exerted as a moment, with a magnitude of 114,586 Nmm, acting upon both faces of the pinion. The pinion's bore is supported without friction, while the gear is affixed with fixed support. The frictionless support on

the bore enforces a normal constraint across the entire surface. This arrangement permits translational movement in all directions except perpendicular to the supported plane.

RESULTS AND DISCUSSION

The results of a mechanical analysis conducted on bevel gears using the ANSYS Workbench software on evaluating the bending stress, strain, and deformation of the gears made from different materials (structural steel, stainless steel, gray cast iron and titanium alloy) were obtained. Figure 11 presents a visual representation of the equivalent stress distribution across the bevel gears. It indicates that the highest stress occurs near the root of the teeth, and the maximum stress value observed is approximately 73.16 MPa.

Table 4 displays the numerical outcomes of the material analysis individually. The bending stress values resulting from the applied loads span a range of approximately 73.05 MPa to 73.54 MPa across various materials (depicted in Figures 12 to 15), with structural steel exhibiting the lowest stress level. Regarding strain values, they vary from around 4.2453 x 10^{-4} to 8.795 x 10^{-4} mm/mm among the different materials, with structural steel again demonstrating the least strain. The deformation measurements encompass a range of approximately 8.2354 x 10^{-3} to 1.7466 x 10^{-2} mm across diverse materials, with structural steel registering the lowest deformation.

Figure 11: Bending Stress analysis of Bevel Gears in ANSYS Workbench

Table 4: Bending Stress, Strain and Total Deformation of Bevel Gears in ANSYS

Materials	Bending Stress (N/mm^2)	Strain (mm/mm)	Deformation (mm)
Structural Steel	73.16	4.2453 x 10^{-4}	8.2354 x 10^{-3}
Stainless Steel	73.216	4.3954 x 10^{-4}	8.5613 x 10^{-3}
Gray Cast Iron	73.055	7.732 x 10^{-4}	1.4875 x 10^{-2}
Titanium Alloy	73.536	8.795 x 10^{-4}	5.1x 10^{-2}

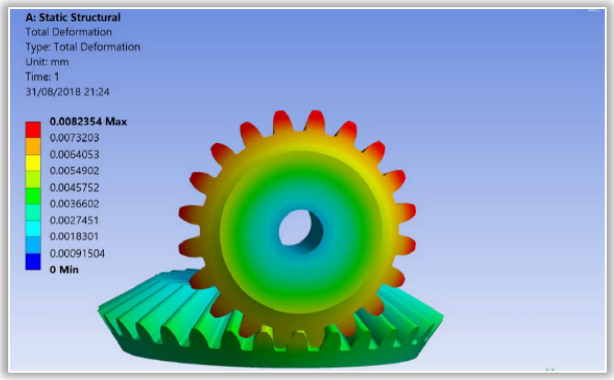

Figure 12: Deformation of Bevel Gears in ANSYS Workbench (Structural Steel)

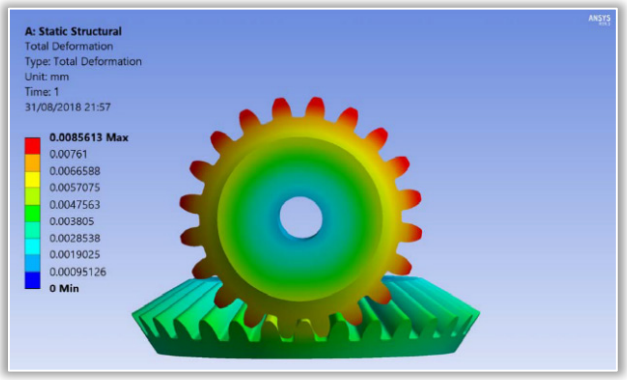

Figure 13: Deformation of Bevel Gears in ANSYS Workbench (Stainless Steel)

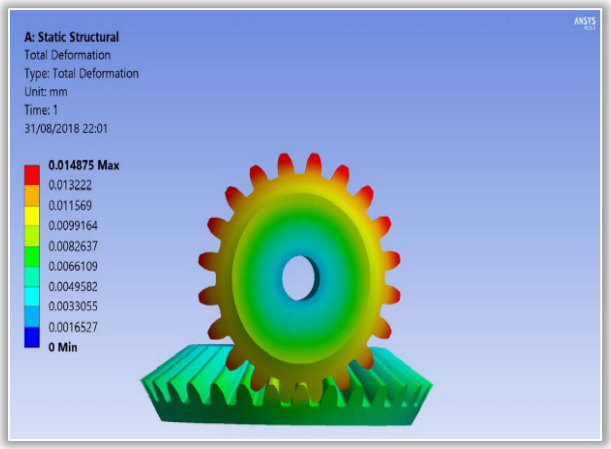

Figure 14: Deformation of Bevel Gears in ANSYS Workbench (Gray Cast Iron)

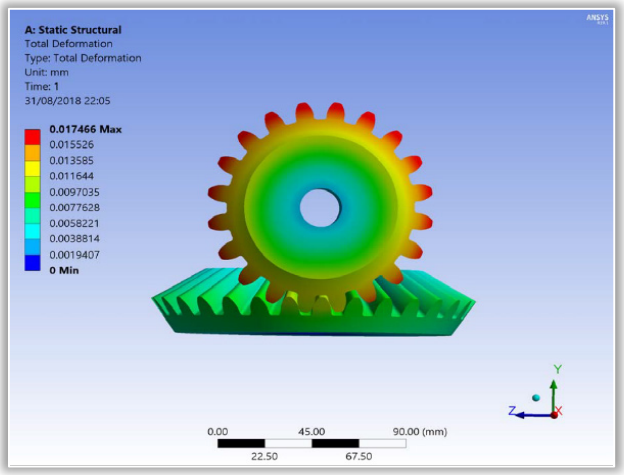

Figure 15: Deformation of Bevel Gears in ANSYS Workbench (Titanim Alloy)

CONCLUSIONS

The design of bevel gears results in thrust forces away from the apex. With the bearing limitations, the gears have to be carefully designed to ensure that they are not thrown out of alignment as they are loaded. Bending stress as a criterion of bevel gear capacity can be defined as the ability of the gear set to withstand repeated or continued operation under design load without the fracture of the teeth by fatigue bending. It is a function of the bending stresses in a cantilever beam and is directly proportional to the applied tooth load. It also involves the fatigue strength of the gear materials and shape of the teeth.

Pitting resistance as a criterion for wear failure on straight–bevel gear capacity can be defined as the ability of the gear set to withstand repeated operation under design load without suffering destructive pitting of the tooth surfaces. Destructive pitting progresses widely to destroy the geometry of the tooth surfaces and ultimately leads to failure.

In the present work, static structural analysis for bending strength by ANSYS Workbench has been done and the equivalent stress, total deformation and equivalent strain plots obtained. Finite element analysis manifests a minimum chance of gear failure. The material with the least deformation is Structural Steel with a maximum deformation of 8.2354 x 10^{-3}mm. The gear pair can be used to transmit the 6 kW power without failure of gear and with a good factor of safety.

These findings can guide material selection and design decisions for optimizing the gears' performance in various applications.

Acknowledgment

The authors would like to acknowledge Department of Mechanical Engineering, Obafemi Awolowo University, and Federal University of Agriculture, Abeokuta and Nigeria, for supporting the present work through Research Fund. The authors declare no conflict of interest.

NOMENCLATURE

T Torque,
d Diameter of gear,
F Face width,
m Module,
Gr Gear ratio
J Geometry factor of gear
Ka Application factor = 1
Km Load distribution factor 1.6
Ks Size factor = 1
Kv Dynamic factor = 1
Kx Gear geometry factor = 1 for straight teeth bevel gear, = 1.15 for spiral bevel gear and zerol bevel gear.
Y Lewis form factor,
M Module,
b Face width,

References

[1] Akinnuli, B. O., Agboola, O. O. and Ikubanni, P. P., (2015), Parameters Determination for the Design of Bevel Gears Using Computer Aided Design, British Journal of Mathematics and Computer Science, 9(6): 537–558

[2] Oladejo, K. A. and Bamiro, O. A, (2009), Technical Survey of Gear–drives Design and Manufacturing Practices in Some Selected States in Nigeria, 1st Faculty of Technology Conference, OAU, Nigeria, Vision 20: 2020, (RETAV), pp. 69 – 73.

[3] Abu, R., Oluwafemi, J. A. and Oladejo, K. A., (2016), Development of Computer–Based Model for Gear Design and Analysis, International Conference of Mechanical Engineering, Energy Technology and Management, IMEETMCon2016–007, pp. 92 – 113, Nigeria.

[4] Rufus, O. C., Samuel, I. U, Abdulrahim, A. T. and Benjamin, I. C, (2016), Design, Modeling, Application and Analysis of Bevel Gears, Int. Journal of Engineering Research and Applications, Vol. 6, Issue 4, (Part – 3), pp.44–52, www.ijera.com.

[5] Oladejo, K. A. and Ogunsade, A. A, (2014), Drafting of Involute Spur–Gears in AutoCAD–VBA Customized Environment, Advancement in Science and Technology Research,(ASTR), Vol. 1 (2), p. 18–26, http://www.netjournals.org/z_ASTR_14_026.html.

[6] Ramana–Rao, A.V., Bhanu–Prakash, C. H., and Sivaram, K. M., (2013), Parametric Modelling of Straight Bevel Gearing system and Analyze the Forces and Stresses by Analytical Approach, International Journal of Engineering Trends and Technology, (IJETT), Vol. 4, Issue. 9, http://www.ijettjournal.org

[7] Ligata, H. and Zhang, H. H., (2011), Geometry Definition and Contact Analysis of Spherical Involute Straight Bevel Gears, IAJC–ASEE, International Conference, pp: 163, ENG 107

[8] Dong, Y, Huanyong, C, Xijie, T, Qingping, Z, and Pengfei, Xu, (2011), Research on Tooth Modification of Spur Bevel Gear, The Open Mechanical Engineering Journal, 5, 68–77.

[9] Oladejo, K. A, Abu, R, Oriolowo, K. T., Adetan D. A. and Bamiro, O. A., (2018), Development of Computer–Based Model for Design and Analyses of Worm Gearing Mechanism, EJERS, European Journal of Engineering Research and Science, Vol. 3, No. 12, December 2018

[10] Mohan, R. N. and Jayaraj, M., (2013), Design of Contact Stress Analysis in Straight Bevel Gear, International Journal of Computational Engineering Research, Vol. 03, Issue. 4, 145 – 148, www.ijceronline.com.

[11] Oluwole, O, Oladejo, K. A. and Abu, R, (2014), Literacy across Scientific Curriculum–Case for Regular across Board Curriculum Enhancement by Standardization Boards using Stakeholders, International Journal of Scientific and Engineering Research, (IJSER), Vol. 5(3): pp. 380–388.

[12] Karlis, P, Arturs, I, and Toms, T, (2014), Spiral Bevel Gears with Optimised Tooth–End Geometry, Procedia Engineering, 69, 383 – 392

[13] Edward, E. O. and Lucky, A, (2018), Design of Straight Bevel Gear for Pitting Resistance, FME Transactions, 46, 194–204

[14] Oladejo K. A, Oriolowo K. T, Abu R. and Ibitoye O, (2021), Analysis for Involute Spur Gears, the Bendings and Pittings Stress on Gears, Applied Engineering, 5(2): 51–59, http://www.sciencepublishinggroup.com/j/ae

[15] Jean–Yves, D, Jerome, B, Jean–Paul V. and Regis, B, (2008), Vectorial tolerance allocation of bevel gear by discrete optimization, Mechanism and Machine Theory, 43, 1478–1494, www.elsevier.com/locate/mechmt

[16] Oladejo, K. A, Adetan, D. A, Ajayi, S. A, and Aderinola, O. O, (2017), Finite Element Simulation of Bending Stress on Involute Spur Gear Tooth Profile, International Journal of Engineering Research in Africa, Vol. 30, pp 1–10

[17] Osakue, E. E., Anetor, L. (2017A), Helical Gear Contact Fatigue Design by Spur Gear Equivalency, Int'l Journal of Research in Engineering and Technology, Vol. 06, Issue 02.
[18] Raj, N. Mohan and Jayaraj, M., (2013): Design of Contact Stress Analysis in Straight Bevel Gear, International Journal of Computational Engineering Research, Vol–03, Issue–4.
[19] Mott, R. L., (2004), Machine Elements in Mechnical Design, 4th Ed. SI, Pearson Prentice Hall, New York.
[20] Stadtfeld, H. J, (2001), The Basics of Spiral Bevel Gears, Gear Technology, pp. 31 – 38.
[21] Joshi, H. D. and Kothari, K. D., (2014), Mode and cause of failure of a Bevel gear–A review, Int'l Journal of Advance Engineering and Research Development (IJAERD), Volume 1 Issue 2, March 2014.
[22] Shigley, J. E and Mischke, C. R., (1996), Standard Handbook of Machine Design, McGraw– Hill, New York.
[23] Norton, R. L., (2000), Machine Design: An Integ– rated Approach, 2nd. Ed., Prentice–Hall, Upper Saddle River, New Jersey.
[24] Dudley, D. W. (2009), Handbook of Practical Gear Design, CRC Press, Baca Raton.
[25] Ratnadeepsinh, M. J, Dipeshkumar M. C, and Jignesh, D. L, (2013), Bending Stress Analysis of Bevel Gears, International Journal of Innovative Research in Science, Engineering and Technology, Vol. 2, Issue 7.

ISSN: 2067-3809

[1.] Csaba Imre HENCZ

THE INTERPRETATION OF THE QUALITY OF LOGISTICS INFORMATION

[1.] Széchenyi István University, Audi Hungaria Faculty of Automotive Engineering, Department of Logistics and Transportation, Gyor, HUNGARY

Abstract: The use of high–quality information in a warehouse and the operational results achieved through it is not a novel research topic. Numerous studies have already shown that good information enhances competitiveness. The correlation clearly points out that decision–makers, when armed with good information, are capable of making good decisions. However, acquiring good, accurate information poses challenges. While members of an organization tend to favor communication channels from which the accuracy of received information can be verified over time, this is by no means a guarantee of the information's quality. This is because it consists of a multitude of non–reproducible, intuitive decisions. Modeling information as a warehouse resource is, therefore, a challenging task. During such studies, we continually encounter difficulties, as the verifiability of this in a certain – undefined – environment is simply not achievable. My goal is to create a model that can support decision–making in warehousing.
Keywords: information value, information interpretation, corporate resource

INTRODUCTION

Based on my research, in the case of microeconomic models describing warehouse operations, there is an opportunity to objectively handle processed information, provided that we assign it some value. I intend to characterize the degree of truthfulness of the utilized information with a goodness factor, which I consider to be an expression of its objectivity. I interpret this factor with an efficiency–type characteristic between 0 and 1, making it mathematically manageable. In cases where it is not possible to determine the relationship of the information to objectivity, the processor of the information should be aware of it. Currently, information is not being treated at this level in warehouse management. Of course, the process of approximating probable reality is not unknown to science. However, in a warehousing environment, probability theory examines the occurrence of predefined, statistically not entirely independent events, which naturally follow certain regularities.

Such examinations can only be carried out and applied in an environment where reality is reproducible. Statisticians, for example, are familiar with the concept of the value of reality, and in many cases, they refer to it as a margin of error in statistical terms. However, based on my current research, there has been no application of this concept in the field of warehouse systems.

REALITY AND ITS KNOWABILITY

Logistics is an interdisciplinary field that fundamentally involves engineering, natural sciences, and social sciences. In engineering and the natural sciences, there exists an objective reality, meaning there is knowable information. If we do not consider it this way, there would be no such thing as engineering science. Researchers in these fields have the opportunity to understand objective reality. In the social sciences – in our case, economics – which is of paramount importance in logistics, the possibility needed to reproduce reality no longer exists. However, when we examine explicitly mathematical models in economics, such as those describing utility and costs, we once again move closer to objectivity.

Therefore, in the field of logistics, under certain conditions, we have the opportunity for objectivity, but only in the case of microeconomic models describing warehouse operations

Spatiotemporal Knowability

As highlighted in László Duma's doctoral dissertation, production and logistics processes are typically planned based on uncertain demand forecasts. This entails the risk that products are not manufactured or stored in the right quantity or composition [3]. In his work published this year, M. Christopher also drew attention to the increasing risk of relying on demand forecasts [4].

Therefore, the sole tool for risk management is to postpone decisions until better–founded forecasts are available. However, by delaying decisions, one of the most critical factors, time, is taken away from the procurers. As a result, they are likely unable to achieve the goals set by Szegedi and Prezenszki, namely:

1. Achieving optimal quality.
2. Minimizing total costs.
3. Identifying, selecting, and evaluating suppliers.
4. Contributing to low inventory levels and continuous product flow.
5. Collaborating and integrating with other organizational units [5].

If the risk of uncertain demand forecasts is significant and persistent, procurers have no choice but to ensure continuous production with high inventory levels, constant replenishments, or consignment inventories (The essence of consignment inventory is that the seller's stock is stored in the buyer's warehouse. The goods remain the property of the seller until they are used.), to meet customer demands quickly and cost–effectively [6].

On the other end of the spectrum, which is becoming increasingly common in the warehouse sector with the development of information societies, is that decision–makers have too much irrelevant information at their disposal alongside useful information. Typically, this occurs with the use of Radio–Frequency Identification (RFID) technology, which generates a large amount of data with "a push of a button." Without proper information management, decision–making time further increases [7].

Can it be asserted that the utilization of forecasted information leads to increasingly accurate information, remaining within tolerance levels?

Exploring the Internal Logic of Data Structures

The likelihood of information can be increased through statistical analysis and/or an analysis of the internal logical structure. Managing information as a resource also entails continually enhancing its real value.

This means that within the information environment, data should not be treated as a static factor but rather as an ongoing data management process, ensuring that these values are always as appropriate as possible.

To form a judgment about something, it is necessary to have some level of connection with the relevant process in space and time. Working in a physical or engineering system is only possible when our work is based on mathematically reproducible values. Since the acquisition of information is achieved through comparison with something similar, and this comparison can be precisely defined, the following conditions must be met for objective information to be acquired:

— We are either in the same place or in different places. We are talking about events in the past, present, or future.

Practical example

— We are either in the same place at the same time, providing us an opportunity for direct understanding.

Example: Our own inventory

— We are in the same time frame but in different locations, allowing for indirect (logical) understanding.

Example: Inventory in transit

— We are talking about a future event happening in the same location, but we can only understand it indirectly.

Example: Year–end inventory

— We are talking about a future event happening in different locations, but we can only understand it indirectly.

Example: Year–end customer demands

— We are talking about a past event that occurred in the same location, and we have the opportunity for direct understanding.

Example: Last year's orders

— We are talking about a past event that occurred in different locations, allowing for indirect (logical) understanding.

Example: Changes in customer demands

If you wish to determine a future expected event, you can only do so logically or based on past data. In this approach, what matters to us is whether the information was correct or incorrect.

— In the case where we can determine the expected consumption using mathematical methods based on past data, and this value matches the actual consumption value, we are talking about information that is both real and logically correct.

— However, if there is a discrepancy between the value of expected consumption determined based on past data and the actual consumption value, we can speak of a logically correct inference, but unfortunately, it is still an inaccurate value. In this case, the information derived from the inference triggers incorrect actions within the logistics organization. Therefore, incorrect, erroneous, or information with zero factual content cannot be considered as information in a warehouse environment.

However, it is essential to recognize that the use of the true (1) and false (0) values is not sufficient. Warehouses operate as dynamically changing environmental elements, and these changes induce their preparedness for future events. (They cannot operate a model that does not provide results if it cannot provide an exact value.) To ensure that the warehouse goes from the logically deduced expected value to the actual value, it is advisable to continuously review forecasts and logical inferences and supplement them with an expected "goodness value."

CHANGES IN THE QUALITY OF INFORMATION OVER SPACE AND TIME

Based on my observations, the factual content of data found in warehouse management systems is often known only to those who input it, and even they may not have a complete understanding. Meanwhile, users of the system often lack the ability to question the data within the system.

In an industrial environment, determining the daily production plan is a critical task. There are well–established methods for this, such as the minimum stock and minimum constant production strategy, which are

used to determine the aggregated production plan almost automatically. Based on these, the master production schedule (MPS) is created.

To reach this point, basic mathematical methods are sufficient, but determining the necessary input data for the model's continuous operation is far from simple. The accuracy of demand forecasts determines the operation of the entire system. However, there is no need to worry because there are well–established subjective and objective methods for this.

Regardless of the method we use, whether it's estimation, expert consultation, Delphi method, time series analysis, etc., we still cannot predict the future. This means that anomalies can occur, where calculations proceed as planned, conclusions are correct, but due to unexpected disruptions (a supplier is delayed, a machine breaks down, a worker gets injured, etc.), the warehouse cannot produce the desired product.

While it's impossible to prepare for or model these events, and modeling them is even more challenging, the fact that the possibility of their occurrence always looms over a given warehouse means that there must be provisions for resource transformation capabilities (I will delve into this in more detail in a later section of my paper).

These models should not only serve the static analysis of the specific system but also provide for dynamic assessments capable of directly sensing vulnerabilities and pointing to necessary improvements [8]. The need for improvement reflects the importance of the element and its associated satisfaction level [9].

In my experience, the main problem lies in the disconnect between continuously performed demand forecasts and the resulting actual production outcomes.

In current warehouse systems, there is no requirement, and often not even a recommendation, for establishing a connection between forecasts made at different points in time, such that, upon later review, past values increasingly align with actual needs.

The quality of information should not be considered a constant value; it needs to be continually managed in the warehouse environment. The aim should be for this value to consistently increase, not decrease. It should reach a level that is certainly sufficient for the organization to make appropriate decisions. Until this is achieved, decisions made in the ongoing process should be continuously reviewed and revised.

Preconditions

Mathematically, it can be best expressed as follows:

- When the probability variable has a value of p=1, then objective reality is confirmed.
- When the probability variable has a value of p=0, we have no evidence to suggest whether the data we are handling is objectively real or not.

In practical terms, if at the moment of placing an order for a product or service, the assumed fulfillment probability is p=0.1, then when examining the expected probability of fulfillment at the moment of fulfillment, it should be greater than p=0.1.

In modern logistics systems, we are compelled to continuously review forecasting values. However, in one of the warehouse systems I examined, this type of "reprocessing" review does not function, and no one verifies these values.

Automating such a statistical verification process and incorporating it into warehouse operations is not inconceivable.

MEASUREMENT OF WAREHOUSE INFORMATION QUALITY

On the contrary, perhaps for this very reason, researchers emphasize the integrity of the represented information. In other words, research is restricted to the transmission of information where it can be clearly stated that its operation is considered appropriate only if the input signal passes through the system without distortion and can be transformed back to its original form.

Since the above theories largely avoid examining the objective value of input signals, modern decision support systems need to incorporate such approaches.

As is known, information and data are not the same. Just because I can reinterpret signals into meaningful data, it does not guarantee the desired actions that I intend to stimulate through the transmission of information. In the current economic environment, we consider information to be acquired "real" and "necessary" knowledge that prompts logical and intentional actions, or has the potential to do so for the organization.

From this perspective, disinformation does not carry the desired effect of promoting the interests of the warehouse, as although it prompts action, it cannot be clearly considered useful or usable information for the logistics organization.

In Werner Gitt's work titled "Information", he defines the value of information in terms of its usability. He distinguishes between valuable and worthless information [10].

As I mentioned earlier, in the business world, I can only consider information that prompts acquiring knowledge leading to actions that enable the organization to achieve its goals under specific circumstances. Therefore, in the diagram above, I assign value exclusively to information in the useful category. However, I want to go even further with this approach because, in a warehouse environment, useful information must also be necessary. This approach is based on the reality of the relationship between information and logistics in this field.

Approaching information management in this way cannot be considered trivial. On one hand, there is information that is measurable, has determinable units of

measurement, while on the other hand, this value is based on an understanding, during which an event becomes a sum of properties, and we make assertions about these properties through their understanding. Hence, we need to narrow down the scope we intend to examine, focusing only on the properties of reality that can be made objective through their understanding!

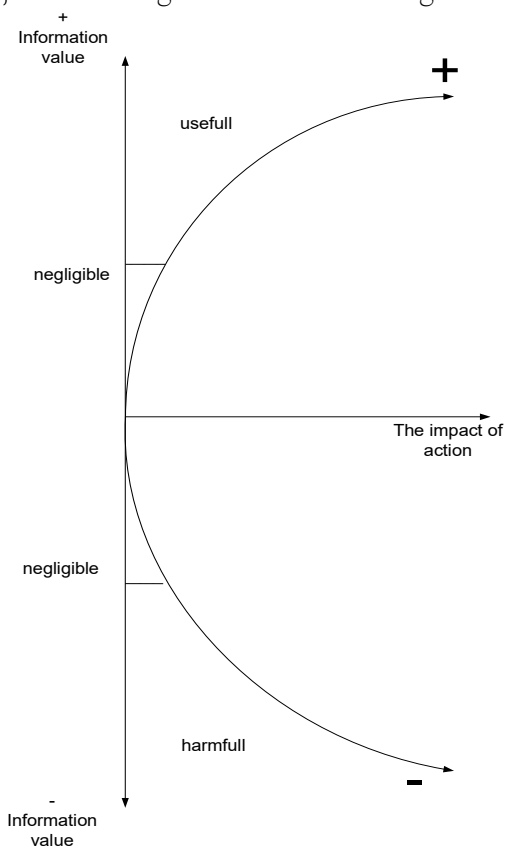

Figure 1. Werner Gitt's redefined diagram–based methods for evaluating information (self–edited).

CONCLUSIONS

The value of information's quality is determined by how necessary and real it is for the warehouse.

By "necessity", I mean the set of information that is indispensable for warehouse operations or can be substituted at a cost by involving other resources.

For me, the necessity of information in a warehouse environment can be interpreted within the range of 0 and 1, where 0 represents unnecessary and 1 represents necessary.

Under the value of "reality", I refer to the degree of closeness to the probable reality.

The determination of the degree of closeness should rely solely on objective procedures. This means that the event being evaluated:

— Must be replicable at any time,
— Must have occurred in the past (at least once), or
— I have no means of establishing its relation to objectivity.

For me, the reality of information in a warehouse environment can be interpreted within the range of 0 and 1, where 0 represents not real and 1 represents real.

$$V_{I_{gdn}} = I_r \cdot I_c \qquad (5.1)$$

Therefore, based on the above, I make the following statement to determine the value of goodness:

where:

V_{Igdn} = Value of Information goodness
I_r = Necessity of information (required)
I_c = Concreteness of information (concrete)

So, in a warehouse environment, the value of information goodness is given by the product of the necessity and concreteness of the given information.

If we do not have relevant information available and we have no means of objectively understanding reality, then the only option is to compensate for the missing information by introducing something extra into the information acquisition process, so that the non–existent or superficial data can be brought at least approximately to an appropriate value.

References

[1] A. M. Porat, J. A. Haas: Information effects on decision making. Behavioral Science, (1969) pp. 98–104.
[2] Streufert, S. C.: Effects of information relevance on decision making in complex environments, Memory and Cognition, 1, (1973) pp. 224–228.
[3] Duma L.: A logisztikai üzleti modellek és értékelési módszerek a hálózati gazdaságban, Doktori értekezés, Budapest (2005)
[4] M. Christopher: Logistics and Supply Chain Management FT, Prentice Hall, Pearson Education (2005)
[5] Szegedi Z., Prezenszki J.: Logisztikamenedzsment, Kossuth Kiadó (1995)
[6] R. Saibal, E. M. Jewkes: Customer lead time management when both demand and price are lead time sensitive, European Journal of Operational Research 153. (2004) pp. 769–781.
[7] Cs. I. Hencz, T. Hartványi: NFC Applications in the Tracking Systems, Advanced Logistic Systems: Theory And Practice (ISSN: 1789–2198) 7: (2) pp. 41–48. (2013)
[8] Dyer J S.: Remarks on the Analytical Hierarchy Process. Management Science; 36; (1990) pp. 249–258
[9] Perez J.: Some Comments on Saaty's Analytic Hierarchy Process. Management Science; 41; (1995) pp. 1091–1095
[10] Werner Gitt: In the Beginning Was Information, Master Books (2006)

ISSN: 2067-3809

ACTA TECHNICA CORVINIENSIS – BULLETIN OF ENGINEERING
TOME XVI [2023] | FASCICULE 4 [OCTOBER – DECEMBER]

[1.] U.J. ETOAMAIHE, [2.]C. DIRIOHA, [3.] T. PAUL, [4.] K.O. UMA

EFFECT OF SPEED AND BAFFLE SIZE ON THE DEGREE OF MIXING OF TUMBLE DRUM FEED MIXER USING RESPONSE SURFACE METHODOLOGY

[1,2,3]Department of Agricultural Engineering, Michael Okpara University of Agriculture, Umudike, Umuahia, Abia State, NIGERIA
[4]Department of Animal Production, Michael Okpara University of Agriculture, Umudike, Umuahia, Abia State, NIGERIA

Abstract: The effects of speed, number of baffles and baffle lengths of a developed tumble drum mixer as they relate to the degree of mixing of feed in the mixer were investigated. Results showed that the degree of mixing of the tumble drum mixer was influenced by the linear effects of the number of baffles, also the interactions of the number of baffles and baffle lengths of the mixer at 5% probability. These factors accounted for about 94.37% of the variations in the degree of mixing of the mixer. The highest degree of mixing of 79.21% was obtained when the number of baffles were 9 and baffle length was 20cm.
Keywords: drum, mixer, baffles, response, surface, methodology, degree, mixing

INTRODUCTION

Feed production for livestock and aquatic animals involve processing operations like grinding, mixing pelleting and drying (Okafor, 2015). Mixing operation is very important because through it different ingredients of the feed are mixed in such a way to get the desired balanced feed formulation (Balami *et al.*, 2013). Mixing is known to be the process by which feed or food ingredients are stirred together to give a uniform mixture (Adeleke *et al.*, 2020). Mixers are generally designed to mix varieties of free flowing materials for feed and food formulation. Hence, to have a well–balanced diet with all the required nutrients, mixing is necessary, providing a uniform mixture by the stirring of two or more ingredients together (Pastukhov and Dogan, 2014). The main purpose of mixing is to blend ingredients (formulation) into a compound such that each unit of the sample (given mass) has the same ingredient composition as the designed formula (Okwabi, 2016).

Feed mixing operations can either be mechanical or manual. According to Adebukola and Patrick (2019), manual method of mixing food/feed involves using hand or shovel to mix up the feed's constituents into one another on open space for proper blending. However, the manual mixing of feed ingredients is usually characterized by low output, low efficiency and drudgeries can be hazardous and unsafe to the health of intending consumers. The mechanical method of mixing on the other hand involves the use of mechanized mixers for mixing/blending while eliminating the drudgeries in manual mixing. Tumble barrel mixers are generally mechanized mixers that engage the principle of rotating barrel and internal baffles/stirrers to properly mix feed/food homogeneously inside a barrel. The total mixing of constituents and elimination of unmixed spots in the mixing barrel due to the tumbling actions of the mixer is an advantage (Chikelu, 2015).

MATERIALS AND METHODS

The tumble drum feed mixer was developed in Agricultural and Bioresources Engineering Department, Michael Okpara University Umudike, Abia State. The tumble barrel mixer which consists of a cylindrical stainless steel drum of length 0.99m and diameter of 0.5m mounted on a rigid steel frame work, powered by a 3Hp variable speed gear motor (Etoamaihe *et al.*, 2022). The frame is 0.6m in height, 1.8m length and 0.54m width. The driving shaft length was 1.9m and the cylindrical drum was slanted 30° to the horizontal to aid mixing. The mixer had a feed opening at the topmost part of the drum and a discharge point at the bottom. Stirrers are fixed on the driving shaft inside the drum. There are also baffles by the sides of the drum located below and above the stirrers on the driving shaft. The mixer was designed to operate in batches. The isometric and orthographic drawings of the machine are shown in Figs 1 and 2, while the developed machine is shown Fig.3.

The response surface methodology (RSM) is important in formulating, designing, developing, and analyzing new scientific studies and products. It is also efficient in the improvement of existing studies and products (Khurmi and Gupta, 2005; Oni *et al.*, 2009). The most common applications are in food science, physical and engineering science, industrial, biological and clinical science and social science.

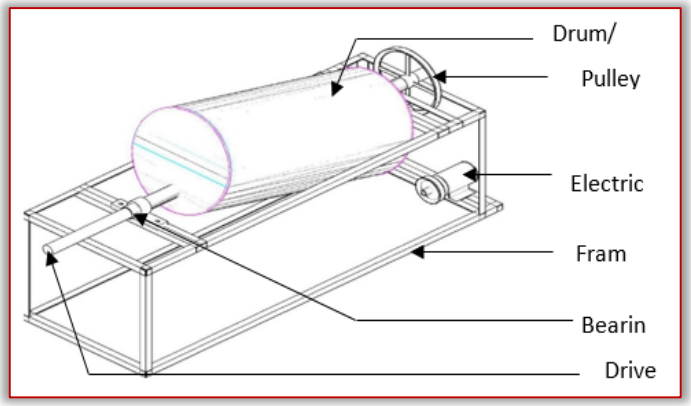

Figure 1: Isometric View of the Tumble Drum Mixer

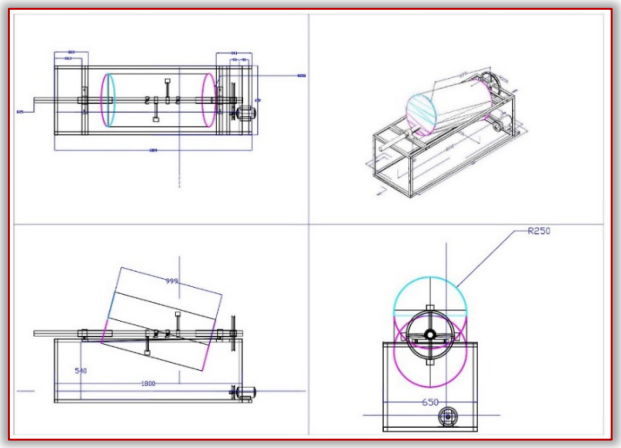

Figure 2: Orthographic view of the tumble drum mixer

Figure 3: The developed tumble drum mixer

According to Myers and Montgomery (2002), response surface methodology is an experimental design that employs the use of first–degree polynomial model to approximate the response variable. However, the model is simply an approximation, but it is easy to estimate and apply, even when little is known about the process. Response surface methods are designs and models for working with continuous treatments when finding the optima or describing the response (Agriga and Iwe 2008). Firstly, the goal of response surface method is to evaluate the optimum response. When there is more than a response then it is important to find the optimum that does not optimize only one response (Jau *et al.*, 2009; Rosell and Collar, 2009). When there are constraints on the design data, then the experimental design has to meet requirements of the constraints. Further goal is to understand how the response changes in a given direction by adjusting the design variables. In general, the response surface can be visualized graphically. The graph is helpful to see the shape of a response surface; hills, valleys, and ridge lines (Yeng and Yu, 2011; Paul *et al*, 2021). According to Deniz and Ismail (2007), response surface is the most popular optimization method used in recent years because of the ease of application and least number of experimental runs needed to evaluate the process (Okwabi, 2016).

The performance tests for the tumble drum mixer was carried out according to the standard test procedure for farm batch mixers which was developed by ASAE (2006). In the tests, 100kg of ground corn and 2.8kg of shelled corn were put into the mixer before operation. Three speeds of the machine which are 100, 150 and 200 rpm were tested for the three different number of baffles 3, 6 and 9 and three baffle lengths of 10, 15 and 20cm of the machine to determine their various percentage degrees of mixing (DM). Each of the tests were carried out for a period of 5 minutes mixing duration in all cases. At the end of each test run, ten samples of 500g each were drawn from the mixed components and analysed.The coefficient of variation among the blended samples and level of mixing were computed using the expressions developed by Ibrahim and Fasasi (2004).

$$CV = \frac{SD}{Y} \times 100 \quad (1)$$

$$Y = \frac{\sum yi}{n} \quad (2)$$

$$SD \equiv \sqrt{\frac{(Y - yi)^2}{n - 1}} \quad (3)$$

$$DM = 100 - \%CV \quad (4)$$

where, CV = percent coefficient of variation, *DM* = degree of mixing (percent), *SD* = standard deviation

Y = mean, *yi* = individual sample analysis results, *n* = total number of samples

A faced centred response surface methodology (RSM) using central composite design (CCD) was used to design the experiments (NIST/SEMATECH, 2012). This method is useful because it uses very few experimental runs to describe how the test variables affect the response. (Agriga, 2008; Etoamaihe, 2015). RSM helps to determine the inter–relationships among test variables on the response and also helps to describe the combined effects of all the test variables on the response (Agriga and Iwe 2008). A 3 factor, 3 level central composite design of RSM was used in this study and the design is suitable for exploring quadratic response surfaces and evaluation of second order polynomial model thereby optimizing the process using a small number of experimental runs (Myers and Montgomery, 2002; Arocha *et al.*, 2021). A total of 20

experimental runs were used. The nonlinear model of response surface methodology is given as:

$$Y = bo + \sum_{i} biXi + \sum_{i} biiXi^{2} + \sum \sum_{ik(k<j)} bjkXjXk \quad (5)$$

where Y= response variable

bo = intercept

Xk, Xj, Xi = independent variables.

bii, bjk, bi= regression coefficients of the model.

In the tests, the three factors considered are speed, number of baffles and baffle lengths of the tumble drum mixer, these were investigated as they affect the degree of mixing of the machine. The regression analysis was carried out with Minitab 16 software, while the response surface graphs were plotted with Matlab R2015a software. In the design the linear, interactive and quadratic effects of the factors (independent variables) were studied as they affect the response percent degree of mixing (DM) of the mixer. Three levels of each of the factors were studied. They are listed as follows: Three different speeds of the machine, namely; 100rpm, 150rpm and 200rpm. Different number of baffles in the machine, namely; 3, 6 and 9. Three different baffle lengths of the machine namely; 10cm, 15cm and 20cm.

RESULTS AND DISCUSSIONS

The experimental variables and coding are shown in Table 1, while the experimental results with the independent variables are shown in Table 2.

Table 1: Experimental Variables and Coding Used in the Design

Independent Variables	Variable Levels		
Speed of mixer, X1	100rpm	150rpm	200rpm
Number of Baffles, X2	3	6	9
Baffle Lengths, X3	10cm	15cm	20cm
Code Designation	–1	0	1
Dependent Variable (Response)			
Degree of Mixing (%) Y			

Table 2: Experimental Results of Independent Variables and Response in Coded Terms

Runs	X1	X2	X3	Y
1	1	1	1	73
2	–1	–1	–1	74
3	0	–1	0	75
4	–1	–1	1	54
5	0	0	1	74
6	0	0	0	64
7	0	0	0	63
8	0	0	0	63
9	0	0	0	64
10	0	1	0	62
11	1	0	0	68
12	1	–1	1	64
13	1	1	–1	36
14	0	0	–1	59
15	1	–1	–1	85
16	0	0	0	64
17	0	0	0	65
18	–1	1	–1	56
19	–1	1	1	81
20	–1	0	0	62

The estimated regression coefficients for the degree of mixing versus speed, number of baffles and baffle lengths of the mixer are shown in Table 3, while the analysis of variance associated with the regression are shown in Table 4. From Table 3, the linear effects of number of baffles, the interactions of speed and number of baffles and also the interactions of the number of baffles and baffle lengths were significant to the degree of mixing of the tumble drum mixer at 5% probability ($P \leq 0.05$). These factors accounted for about 94.37% of the variations in the degree of mixing of the machine. The analysis of variance Table 4 also fully confirms the stated results. From the response surface curve in Fig. 4, the highest Degree of Mixing of 66.49% was obtained when the number of baffles were 9 and the speed was 60rpm while in Fig. 5 the highest degree of mixing of 68.51% was obtained when the baffle length was 20cm and the speed was 200rpm. In Fig 6, the overall highest degree of mixing of 79.21% was obtained when the baffle length was 20cm and the number of baffles were 9.

Table 3: Response Surface Regression: Y versus X1, X2, X3

Term	Coef	SE Coef	T	P
Constant	64.8455	1.182	54.874	0.000
X1	–0.1000	1.087	–0.092	0.929
X2	–4.4000	1.087	–4.048	0.002
X3	3.6000	1.087	3.312	0.008
X1*X1	–1.3636	2.073	–0.658	0.525
X2*X2	2.1364	2.073	1.031	0.327
X3*X3	0.1364	2.073	0.066	0.949
X1*X2	–6.1250	1.215	–5.040	0.001
X1*X3	1.3750	1.215	1.131	0.284
X2*X3	12.8750	1.215	10.594	0.000

S = 3.43746 PRESS = 1152.97

R–Sq = 94.37%;R–Sq (pred) = 45.05% ;R–Sq (adj) = 89.30%

The regression equation:

$$Y=64.85–0.1X_1–4.4\ X_2+3.6\ X_3–1.36\ X_1^2+2.14\ X_2^2+0.136\ X_3^2–6.13\ X_1\ X_2+1.38\ X_1\ X_3+12.88\ X_2\ X_3$$

Table 4: Analysis of Variance for Y

Source	DF	Seq SS	Adj SS	Adj MS	F	P
Regression	9	1980.04	1980.04	220.00	18.62	0.000
Linear	3	323.30	323.30	107.77	9.12	0.003
X1	1	0.10	0.10	0.10	0.01	0.929
X2	1	193.60	193.60	193.60	16.38	0.002
X3	1	129.60	129.60	129.60	10.97	0.008
Square	3	15.36	15.36	5.12	0.43	0.734
X1*X1	1	0.00	5.11	5.11	0.43	0.525
X2*X2	1	15.31	12.55	12.55	1.06	0.327
X3*X3	1	0.05	0.05	0.05	0.00	0.949
Interaction	3	1641.38	1641.38	547.13	46.30	0.000
X1*X2	1	300.13	300.12	300.12	25.40	0.001
X1*X3	1	15.13	15.13	15.13	1.28	0.284
X2*X3	1	1326.13	1326.13	1326.13	112.23	0.000
Residual Error	10	118.16	118.16	11.82		
Lack–of–Fit	5	115.33	115.33	23.07	40.70	0.000
Pure Error	5	2.83	2.83	0.57		
Total	19	2098.20				

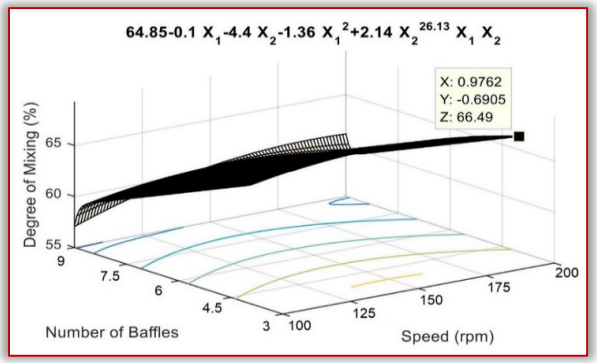

Figure 4: Response Surface Curve of the Effects of Number of Baffles and Speed on the Degree of Mixing of the Mixer

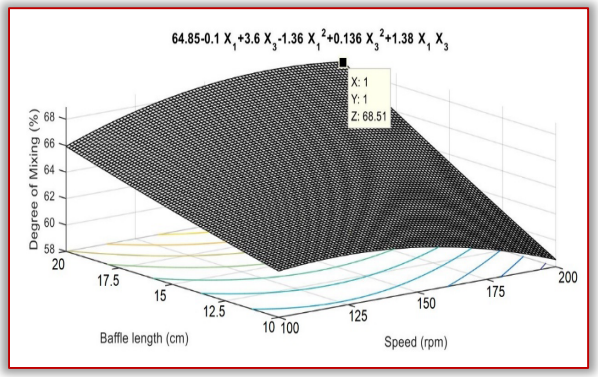

Figure 5: Response Surface Curve of the Effects of Baffle Lengths and Speed on the Degree of Mixing of the Mixer

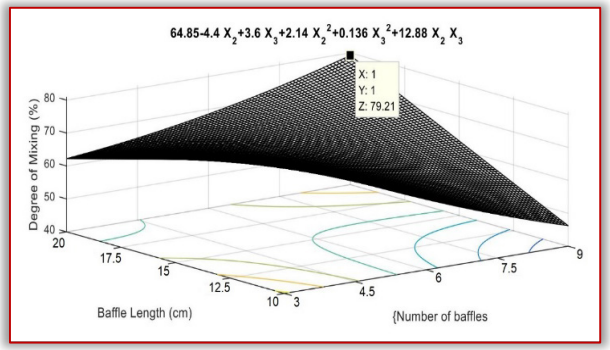

Figure 6: Response Surface Curve of the Effects of Baffle Lengths and Number of Baffles on the Degree of Mixing of the Mixer

CONCLUSIONS

From experimental results and analysis, the following conclusions can be drawn from this study. The degree of mixing of the tumble barrel mixer was influenced by the linear effects of the number of baffles, also the interactions of the number of baffles and baffle lengths of the mixer at 5% probability. These factors accounted for about 94.37% of the variations in the degree of mixing of the mixer. The overall highest degree of mixing of 79.21% was obtained when the number of baffles were 9 and baffle length was 20cm.

References

[1] Okafor B. E (2015). Design of Power Driven Dough Mixing Machine. Int'l Journal of Engineering and Technology 5(2): 71–74.
[2] Balami, A. A., Adgidzi, D, and Muazu, .A (2013). Development and Testing of an Animal Feed Mixing Machine, International Journal of Basic and Applied Sciences 1(3): 491–503.
[3] Adeleke A.E, Oni O.K, Ogundana T.O, Satimehin A.A and Oyelami S. (2020). Development and performance evaluation of a dough mixing machine. Journal of Engineering and Environmental Sciences. 2 (2): 30–41.
[4] Pastukhov A. and Dogan H. (2014). Studying of Mixing speed and Temperature impacts on rheological properties of wheat flour dough using Mixolab. Agronomy Research 12(3): 779–786.
[5] Okwabi R. (2016). Design and construction of a hand operated mixer machine for food fortification. International Research Journal of Engineering and Technology. 3(9): 6 –15.
[6] ASAE Standards (2006). ASAE S380 R2006. Test Procedure to Measure Mixing Ability of Portable Farm Batch Mixers, pp 261–262.
[7] Adebukola A.A and Patrick O.A (2019). Development and Evaluation of a Fish Feed Mixer. Agric Eng. Int: CIGR Journal Open Access. 21(3): 43–56.
[8] Chikelu C.C, Ude M.U, Onyekwere D.C, Eze N.N and Ukwuani S.T (2015). Design and development of a cross ribbon dough mixer. International Journal of Adavnced Engineering Research and Scieence. 7 (2): 24–27.
[9] Etoamaihe U.J., Dirioha, N.R., Uma K.O and Oluwaseun Babalola, (2022). Development and Performance Evaluation of a Motorized Tumble Barrel Feed/Food Mixer. Scientific Journal of Agricultural Engineering, Faculty of Agriculture, University of Belgrade.No.4 pp 15– 27.
[10] Oni, O. K. Alakali J. S and Akpapumam M. A (2009). Design, Fabrication and Performance
[11] Gupta J. K (2005). A Textbook of Machine Design. Eurasia publishing house Ltd, New Delhi.
[12] Myers, R.H., and Montgomery, D.C. Response Surface Methodology. Process and Product Optimization Using Designed Experiments. 2nd Edition, John Wiley and Sons New York.
[13] Agriga A.N. and Iwe M.O (2008). Physical Properties of Cookies Produced from Cassava, Groundnut–Corn Starch Blend. A Response Surface Analysis. Nigerian Food Journal 26(2) 83–96.
[14] Jau, K.W., Hua, S. C, and Ching, S.H (2009). Optimization of the Medium Components by Statistical Experimental Methods to Enhance Nattokinase Activity. Fooyin Journal of Health Sciences 1(1)21–27.
[15] Rosell C.M and Collar C. (2009). Effect of Temperature and Consistency on Wheat Dough Performance. International Journal of Food Science and Technology. 6(2): 52–64.
[16] Yeng Y.T and Yu C.H (2011). Flow Characteristics in Mixers Agitated by Helical Ribbon Blade Impeller. Engineering Applications of Computational Fluid Mechanics 5(3): 416–429.
[17] Paul .T, Adejumo B.A, Nwakuba N.R and Ehiem J.C (2021). Proximate composition of packaged freeze dried cheeses in storage. Agricultural Engineering international. 23 (2): 264–272.
[18] Deniz, B. and Ismail, H.B (2007). Modelling and Optimization: Usability of Response Surface Methodology. Journal of Food Engineering. 78(3):836–845.
[19] Fasasi M.B (2004). Design and Development of a Portable Feed Mixer for Small Scale Poultry Farmers. Proceedings of NIAE 26 Ilorin.
[20] NIST/SEMATECH (2012). Handbook of Statistical Methods http://www.itl.nist.gov/div 898, Accessed 17th January 2023.
[21] Etoamaihe, U.J, (2015). Effects of Additives and Briquetting on the Calorific Values of Cassava Peels Using Response Surface Methodology. ASABE Annual International Meeting 152186792. (doi:10.13031/aim.20152186792).
[22] Agriga, A.N (2008). Development and Evaluation of Cassava–Groundnut Bars Using Corn–Starch as Binder. A Response Surface Analysis. Unpublished M.Sc. Thesis. Dept of Food Science and Technology. Michael Okpara University of Agriculture Umudike pp 38–43.
[23] Arocha C.G, Simonyan K.J and Paul .T (2021). Performance evaluation of a motorized ginger rhizomes peeling machine. Agricultural Engineering. 46 (4): 84–96.

ISSN: 2067-3809

[1.] Kristián PÁSTOR, [1.] Miroslav BADIDA, [1.] Tibor DZURO, [1.] Miroslava BADIDOVÁ

DIAGNOSTICS OF SOUND QUALITY IN THE INTERIOR OF A HYBRID CAR USING PSYCHOACOUSTIC MEASUREMENTS

[1.] Technical University of Kosice, Faculty of Mechanical Engineering, Institute of Industrial Engineering, Management, Environmental Engineering and Applied Mathematics, Department of Business Management and Environmental Engineering, Kosice, SLOVAKIA

Abstract: In recent years, sound design has become one of the most important research topics in sound quality technology. Sound quality research, which focuses on how people perceive and evaluate sound, has gained attention especially in the automotive, transportation, and electrical appliance industries worldwide. This article focuses on the description of the methods used to evaluate sound quality and the application of an objective evaluation method. The subject of the measurements was a vehicle with a hybrid drive, and psychoacoustic parameters were measured at different vehicle speeds. With the development of noise monitoring technologies, sound quality research has gained attention, especially in the fields of automotive, transportation, industry and electrical appliances worldwide. The concept of product sound was strongly influenced by the automotive industry's need to design the sounds generated by vehicles to give the impression of high quality in every respect. The sounds generated by the car indicate certain aspects of how it works and these positive sounds are enhanced to compete with other car brands.
Keywords: Sound quality, psychoacoustics, hybrid vehicle, psychoacoustic parameters

INTRODUCTION

With the development of noise monitoring technologies, sound quality research has gained attention, especially in the fields of automotive, transportation, industry and electrical appliances worldwide. Intensive theoretical and experimental work on human perception of sound quality in the automotive industry has been carried out by companies such as Honda, Delphi, Ford, GM etc. Many car companies have optimized their product designs based on this research data. Researchers also discuss the impact of sound quality on airplanes, trains, and Maglev trains. Studies are also focused on air conditioners, refrigerators, washing machines, mobile phones, etc. [1][2]

Marketing studies have shown that customers pay close attention to sound quality not only in situations where sound is the primary object of interest, but also when sound is just a side effect of the product's operation.[3]

Sound quality studies in the automotive industry also focus on sounds such as the sound of a car door closing. Even this sound can contribute to the overall impression of the car, which is very important, because closing the door is one of the operations that the customer can perform when viewing the car in the dealer's hall. Etienne Parizet, Erald Guyader and Valery Nosulenko focused on the sound of the door closing in the article Analysis of car door closing sound quality. They analyzed the perception of the sound emanating from a car door closing, focusing on the image of the quality of the car that the listener might have in mind with this sound.[4]

SOUND QUALITY AND PSYCHOACOUSTICS

Noise can be defined as a disturbing or unpleasant sound. This subjective definition does not exclude any sounds, as essentially any sound can be distracting depending on many factors related to the listener. Noise as such is also interesting in the context of sound quality and also in the context of psychoacoustics. [5]

Blauert and Jekosh [6] define the sound quality of a product as "adequacy of sound in the context of a specific technical goal and/or task". For all products that produce perceptible sound, the sound quality of the product is assessed each time it is used.

The concept of product sound was strongly influenced by the automotive industry's need to design the sounds generated by vehicles to give the impression of high quality in every respect. The sounds generated by the car indicate certain aspects of how it works and these positive sounds are enhanced to compete with other car brands. In addition to engine sounds, product sounds for cars include sounds generated when various parts of the vehicle are used, such as windows opening, seat movements, sunroof opening, and button presses. Sounds and audio–tactile interaction when getting into the car are very important: unlocking the lock, using the door handle and closing the door create both auditory and tactile perception, which creates an impression of the quality of the car's finishing. The sound of the engine that is audible in the interior of the car should be designed so that it is not intrusive, although it must be audible over other sounds in the cabin, as it provides information about the operation of the engine. [7][8]

The most popular approaches to determining the sound quality of a product can basically be divided into two areas: subjective and objective evaluation [9][10].

The first of them emphasizes that sound can be subjective and sensitive for a person; the latter expresses sound in terms of an objective numerical value, such as physical acoustics and psychological acoustics [11].

ASSESSMENT OF CAR SOUND QUALITY

Sound engineering in research, development, but also in the production of cars represents a connecting link between physics (design characteristics, such as excitation, transmission, etc.) and psychology, which presents acoustic comfort, but also a feeling of health and well–being. The driving comfort of a particular car is understood as the perception of the effect of comfort features through one or several channels of perception in each person: visual (sight), auditory (hearing), haptic (tactile), olfactory (smell).

The individual perception of a person is very subjective, and therefore it can only be described incompletely using purely physical and objectively measured quantities. It depends both on the characteristics of the car that is being observed, on the specific experienced situation, but also on the socialization of the evaluating person and the surrounding environment in which the evaluation process takes place. Each car is characterized by its typical acoustic properties, which are e.g. the sounds of a stationary car (interior and exterior sound), engine sounds during different driving modes (slow, fast, interrupted, smooth driving, etc.) also play an important role in the so–called functional sounds (sound of rear–view mirror adjustment, window lowering sound, seat adjustment sound, sunroof opening sound and more). The comfort of driving a car is also affected by spontaneously occurring sounds (e.g. whistling, rattling, screeching, etc.), which together create a qualitative impression of the well–being of driving a car (driving comfort), which is perceived by the car crew. [12][13]

Subjective evaluation methods

The goal of psychoacoustics research is man and his perception of sound. Unlike general acoustics, where data is obtained using microphones or other devices that are calibrated, psychoacoustics uses the person as the only instrument ("measuring instrument"). However, a person cannot be calibrated in the same way as e.g. microphone. In the case of the application of psychoacoustic listening tests, the emphasis is placed on the answers of people (evaluators) and it is worked as if calibrated microphones were not available. In data analysis, statistical analysis plays an important role, and for testing purposes it is always required that a statistically significant (relevant) sample of evaluators be available. [14]

The subjective perception test is a basic procedure for obtaining the sound quality character of sound events and for developing parametric models that describe sound quality quantities. Two methods are commonly used. The Semantic Differential Method, developed by Osgood in 1957, offers a quick way to measure people's attitudes and emotional connotations of concepts. A range of indices of semantic differential were studied, including safe–dangerous, satisfied–dissatisfied, quiet–noisy, friendly–hostile, close–distant, and happy–sad. This method has been applied to various problems in marketing, personality measurement, clinical psychology, intercultural communication, and auditory perception of sound signals. The Paired Comparison method offers a simple way to present people's attitudes using a sequence of pairs of sounds A and B. For each pair, people have to decide which sound they prefer. [15] [16]

Objective evaluation methods

In recent times, for the purposes of psychoacoustic measurements, technical means are also being increasingly promoted. They are highly sophisticated systems, developed to measure selected psychoacoustic parameters with highly specialized software support. Perceiving sound through two ears is called binaural hearing. It is the ability to hear sounds from the left ear and the right ear in parallel and the ability to locate the direction of the incoming sound. This type of hearing strongly depends on the geometric parameters of the human body (ears, head and trunk). [17][18]

Important and highly effective technical means for measuring psychoacoustic parameters include the so–called "artificial head" (or psychoacoustic head). (Figure. 1) It is an identical figure with a human head. The psychoacoustic head has two microphones that are installed in the ears. It is characterized by the same acoustic and auditory properties as the human head. The goal is to achieve a state so that the evaluator of the quality of the sound event, who listens to the audio recordings obtained from the psychoacoustic head, has the impression that he is part of the space of the acoustic event. [19]

Various feelings or perceptions can be displayed as using psychoacoustic parameters of perception, as well as using auditory thresholds of perception, which can be determined using psychoacoustic methods. Psychoacoustic parameters such as roughness, loudness, tonality, sharpness and fluctuation of strength are referred to as "classical" psychoacoustic parameters. Other parameters related to hearing are also known, such as height, color, subjective duration and others. [20]

Figure 1. Psychoacoustic head

PSYCHOACOUSTIC EXPERIMENT – MEASUREMENT OF SELECTED PSYCHOACOUSTIC PARAMETERS IN THE INTERIOR OF A HYBRID VEHICLE

The aim of the measurements carried out using a binaural measuring device, the so–called psychoacoustic head, was to determine the values of selected psychoacoustic parameters under conditions of different car speeds. The subject of the research was the vehicle Suzuki Vitara Hybrid. (Figure 2.)

Figure 2. Suzuki Vitara Hybrid

The psychoacoustic head was placed in the interior of the vehicle in the position of the passenger on the front seat. The location of the psychoacoustic head in the test vehicle is shown in Figure 3.

Figure 3. Placement of the psychoacoustic head in the vehicle

Measurements were performed at speeds of 30 km/h, 50 km/h, 90 km/h and 130 km/h. The section of the road where the measurements were taken is shown in Figure 4.

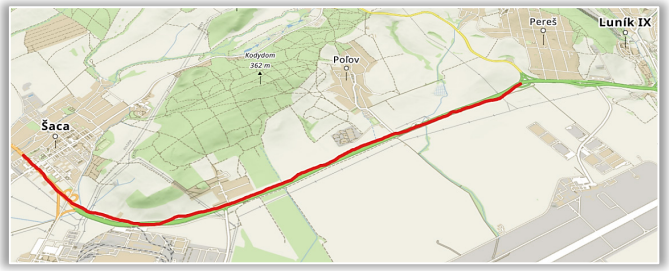

Figure 4. The section of the road where the measurements were performed

RESULTS OF MEASUREMENTS

The obtained results of measurements of psychoacoustic parameters at specified speeds for the right and left ear together with their average values for vehicle Suzuki Vitara are shown in Table 1.

The results show a difference in values between the left and right ears, with the values in the right ear being higher than those in the left ear. These differences can be attributed to the location of the psychoacoustic head in the vehicle, which was placed on the passenger seat, and thus her right ear, in which the values were higher, was closer to the surrounding environment than the left ear, which faced the interior of the vehicle.

Table 1. Results of measurements of psychoacoustic parameters

Speed	Microphone	Fluctuation of strength	Average L-R	Loudness	Average L-R
30 km/h	Left mic.	0,0199	0,02055	10,4	10,8
30 km/h	Right mic.	0,0212		11,2	
50 km/h	Left mic.	0,0232	0,02335	15	15,45
50 km/h	Right mic.	0,0235		15,9	
90 km/h	Left mic.	0,0298	0,03035	21,2	22
90 km/h	Right mic.	0,0309		22,8	
130 km/h	Left mic.	0,032	0,03255	31,3	32,15
130 km/h	Right mic.	0,0331		33	

Speed	Microphone	Roughness	Average L-R	Sharpness	Average L-R	Tonality	Average L-R
30 km/h	Left mic.	0,0302	0,03045	0,597	0,6015	0,245	0,3165
30 km/h	Right mic.	0,0307		0,606		0,388	
50 km/h	Left mic.	0,0358	0,0379	0,789	0,791	0,222	0,1865
50 km/h	Right mic.	0,04		0,793		0,151	
90 km/h	Left mic.	0,0492	0,0495	0,968	1,009	0,15	0,12185
90 km/h	Right mic.	0,0498		1,05		0,0937	
130 km/h	Left mic.	0,0541	0,0562	1,3	1,375	0,239	0,187
130 km/h	Right mic.	0,0583		1,45		0,135	

In Figure 5, we can see the graphs of the total values of individual psychoacoustic parameters.

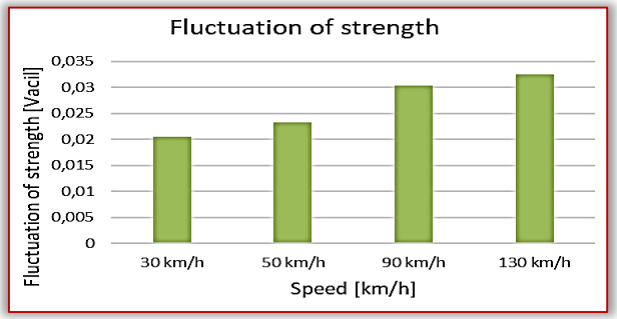

(a)

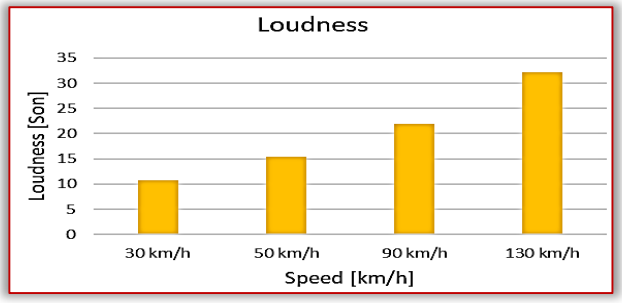

(b)

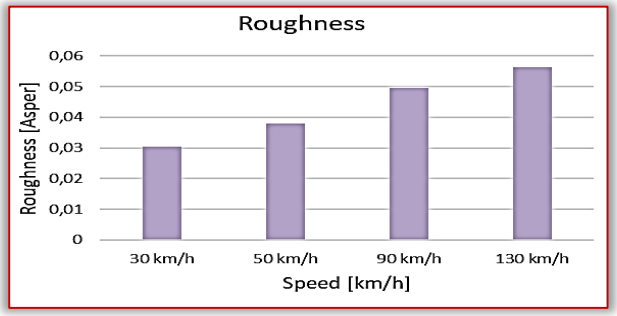

(c)

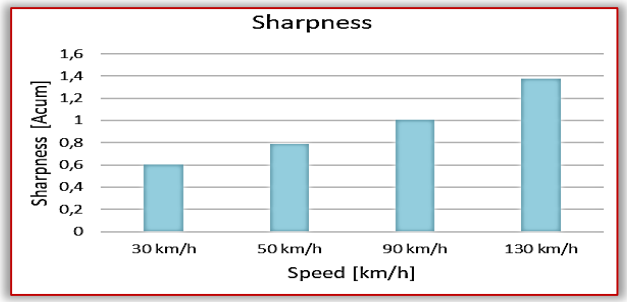

(d)

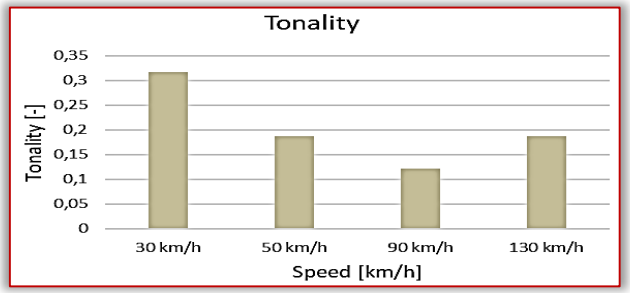

(e)

Figure 5. Graphs of the total values of individual psychoacoustic parameters

Based on the measured results, we can see that the values of most monitored parameters grew with increasing speed. The exception in this case was the Tonality parameter. Here we can see that this parameter even decreased up to a certain speed and started to rise suddenly only at a speed of 130 km/h.

CONCLUSIONS

The overall perception of the quality of the car is significantly influenced by its characteristics regarding noise in the interior. Therefore, it is important to find a balance between "pleasant" and "dynamic" sound that meets the customer's requirements with regard to the brand and class of the vehicle. The driver, passenger or customer perceives the car interactively and also through several senses in parallel. Customers, drivers and passengers form their perception of the quality of a particular car as a result of sensory impressions that are inextricably linked. Car sound assessment is currently taking on another new dimension, that of interactively influencing the sound. The effort is to arrive at the conceptual formation of vehicle acoustics (active sound design). Psychoacoustics can be considered a very suitable tool for assessing and optimizing the acoustic properties of various products. When applying objective methods during the experimental measurement of psychoacoustic parameters, it was found that the psychoacoustic parameter values are influenced by the speed of the vehicle in the vehicles that were the subject of the research. For most parameters, psychoacoustic parameter values increase with increasing speed. These values are also influenced by the location of the psychoacoustic head in the vehicle, when different values can be seen between the left and right ear.

Acknowledgement

This contribution was created based on the solution of the project project KEGA 013TUKE–4/2022, project VEGA 1–0485–2022, project UNIVNET 0201/0082/19 and project 009TUKE–4/2021.

References

[1] JIAO FL, LIU K. Sound quality in noise control: Subjective assessment. In: Proceedings of 2003 national conference environmental acoustics; 2003
[2] Jiguang, J., Yun, L.: Review of active noise control techniques with emphasis on sound qualityenhancement. In: Applied Acoustics, č.136, 2018, p.139–148,
[3] Badidová, A. 2011. Návrh metodiky posudzovania kvality zvuku v interiéri automobilu psychoakustickými metódami [Doctoral dissertation]. Košice: technická univerzita v Košiciach [s. n.], 2020. 187 p.
[4] Etienne, P., Erald, G., Valery N.; Analysis of car door closing sound quality. Applied Acoustics, Elsevier, 2008, 69, pp.12–22.
[5] Pástor, K., et al.; Analysis of the sound of selected automobile powertrains using psychoacoustic methods In: Novus Scientia 2023: 20th International Scientific Conference of Doctoral Students of Engineering Faculties of Technical Universities and Colleges: Proceedings of the 20th International Scientific Conference of Doctoral Students of Engineering Faculties of Technical Universities and Colleges. – Košice (Slovakia): Technical University in Košice p. 199–204, ISBN 978–80–553–4369–3
[6] BLAUERT, J., JEKOSCH, U.; A layer model of sound quality. J. AudioEng. Soc., 2012, 60(1/2), 4–12 p.
[7] BLAUERT, J.; JEKOSCH, U.: Sound – quality evaluation: A multi – layered problem. Acta Acustica United with Acustica, 99 (1), 1977, 1 – 13 p.
[8] Badidová, A.; Sobotová, L.; Badida, M.; Psychoakustika v technickej diagnostike, 2020.In: Strojárstvo/Strojírenství = Engineering Magazine. – Žilina (Slovensko) : Media/ST Vol. 24, No. 10 (2020), pp. 60–61
[9] Rychtáriková, M.: Psychoakustické testy v stavebnej akustike. Monee, IL, USA, 2020
[10] Zwicker, E.: Psychoakustik. Springer Verlag, Berlin, Heidelberg, 2020, 198 p.
[11] Pástor, K., et al.; Analýza zvuku automobilov s fosílnym a elektrickým pohonom psychoakustickými metódami 2023. In: Noise and vibration in practice. 26:peer–reviewed scientific proceedings, Bratislava (Slovensko):Spektrum STU s.63–68, ISBN 978–80–227–5303–6
[12] MORAVEC, M.; Sound quality subjective and objective assessment methods of domestic appliances: ANNALS of Faculty Engineering Hunedoara – International Journal of Engineering, 2019, p.91–94, ISSN 1584 – 2665
[13] DENGFENG, Wang, ZONG–WEI, Liu, JIE, Liang. Subjective evaluation experiments and objective quantificational description of vehicle interior noise quality: J Jilin Univ (Engineering and Technology) 2006; 2: 343–53.
[14] ROSSI, F., NICOLINI, A., FILIPPONI, M.: An index for motor vehicle passengers acoustical comfort: The 32nd international congress and exposition on noise control engineering Korea; 2003.
[15] OSGOOD CE, TANNENBAUM PH, SUCI GJ. The measurement of meaning: Urbana: University of Illinois Press; 1957.
[16] David HA. The method of paired comparisons, 2nd ed. London: Chapman and Hall; 1988
[17] MORAVEC, M., et al.; Application of the psychoacoustics and binaural measurement for the valuation of the sound quality, 2015. In: Global Management and Economics. No. 1 (1) (2015), p. 85–90. – ISSN 2413–9823
[18] MORAVEC, M., et al.; Assessment of the washing machines sound quality by the binaural measurement systems, 2017, In: Technical sciences and technologies. Vol. 7, no. 1 (2017), p. 161–166. – ISSN 2411–5363
[19] N. Radic, C. Novak and H. Ule, Experimental evaluation of vehicle cabin using subjective and objective psychoacoustic analysis techniques, In: Canadian Acoustics, vol. 39, No. 4, pp. 27 – 36. 2011.
[20] IPAR, P., et.al.: Psychoacoustic approach used for developing the model of sound pleasantness of vacuum cleaners and suction units based on objective and subjective analysis. In: 5th Congress of Alps–Adria Acoustics Association, September 2012

ACTA TECHNICA CORVINIENSIS – BULLETIN OF ENGINEERING
TOME XVI [2023] | FASCICULE 4 [OCTOBER – DECEMBER]

[1.] Sejal J. PATEL, [2.] G. M. DEHERI

SLIP EFFECT ON SHLIOMIS MODEL BASED MAGNETIC FLUID LUBRICATION OF A SQUEEZE FILM IN CIRCULAR CYLINDER NEAR A PLANE

[1.] Department of Mathematics, Sheth M. N. Science College, Patan, Gujarat, INDIA
[2.] Department of Mathematics, Sardar Patel University, Vallabh Vidyanagar, Anand, Gujarat, INDIA

Abstract: An endeavor has been made to study the performance of a ferrofluid based squeeze film in circular cylinder near a plane resorting to Shliomis model, considering slip velocity. The stochastic model of Christenson and Tonder has been brought in here to evaluate the effect of surface roughness. The associated stochastically averaged Reynolds type equation is solved to obtain the pressure distribution. Then load bearing capacity has been calculated. The results show that Shliomis model based ferrofluid lubrication is relatively better as compared to the Neuringer– Rosensweig model for magnetic fluid lubrication of this type of bearing system, even if the slip is higher. The adverse effect of roughness can be reduced considerably at least in the case of negatively skewed roughness with a suitable choice of curvature parameters. It is observed that this type of bearing system supports some amount of load even when there is no flow, unlike the case of conventional lubricants. Some of the results presented here establish that the adverse effect of slip velocity can be minimized with suitable magnetic strength, irrespective of the fact that the roughness induces adverse effect.

Keywords: circular cylinder, squeeze film, roughness, slip velocity, magnetic fluid, load bearing capacity, shliomis model

INTRODUCTION

It is recorded that hydraulic dampers, gears, braking units, synovial joints, and skeletal bearing use for a purpose of squeeze film mechanism. Generally, an electrically conducting fluid with high thermal and electrical conductivity is applied as a lubricant for squeeze film to work under such extreme circumstances. Also, an exploit of external magnetic field then advances the performance of lubrication.

Neuringer and Rosensweig [1964] proposed a quite simple model where the effect of magnetic body force was measured under the supposition of magnetization vector being parallel to the magnetic field vector. However, Shliomis [1972] consigned on a different formulation. He analyzed that the magnetic particles in the fluid had Brownian motion and their rotation affected the motion of magnetic fluids. Thus, Shliomis promoted the equation of motion for ferrofluids by considering internal angular momentum by cause of the self– rotation of particles. After that many researchers (Kumar et al. [1992], Singh and Gupta [2012], Patel and Deheri [2012], Lin et al. [2012], Lin [2013], Patel and Deheri [2013], Patel and Deheri [2014], Patel and Deheri [2014]) dealt with the model of Shliomis to examine the performance of different bearing's characteristics. All the above investigations analyze the steady state characteristics of the bearings lubricated with magnetic fluids, resorting to the flow model estimated by Shliomis.

The review of Shliomis [1974] discussed briefly the methods of preparation and stability problems of magnetic colloids. This review paper summarized the results of theoretical and experimental investigations of the effect of a magnetic field on the equilibrium conditions and on the character of the motion of the suspensions. Consideration was given to various effects caused by rotation of the particle, anisotropy of the viscosity and of the magnetic susceptibility, entrainment of the suspension by a rotating field and dependence of the kinetic coefficients on the field intensity.

Many investigations have been made regarding Circular cylinder (Bearman and Zdravkovich [1978], Zdravkovich [1985], Kawamura et al. [1986], Trahan et al. [1999], Price et al. [2002], Dipankar and Sengupta [2005], Lin et al. [2013], Patel and Deheri [2016]).

Stochastic model of Tzeng and Saibel [1967] was developed by Christensen and Tonder [[1969a, 1969b, 1970] to study the effect of surface roughness. Various techniques were deployed to measure the roughness effect. The effect of roughness has been studied in various squeeze film bearing systems (Tseng and Seibel [1967], Kawamura et al. [1986], Deheri et al. [2005], Abhangi and Deheri [2012], Patel et al. [2019]).

Beavers and Joseph [1967] constructed a simple theory to replace the effect on the boundary layer, with a slip velocity proportional to the exterior velocity gradient. The result obtained from this theory was found to be in good agreement with the experimental results. Various squeeze

film bearing systems have been studied considering the effect of slip velocity (Wu [1972], Sparrow et al. [1972], Prakash and Vij [1976], Patel [1980], Thakkar et al. [2008], Patel and Deheri [2011], Patel and Deheri [2013], Patel and Deheri [2014 a], Patel and Deheri [2014 b], Patel and Deheri [2014 c], Barik et al. [2016], Acharya et al. [2017], Patel and Patel [2020], Patel et al. [2022]).

The effect of porosity has been examined in various squeeze film bearing systems (Wu [1971], Prajapati [1992], Bhat and Deheri [1993], Patel and Deheri[2003], Deheri and Patel [2006], Patel et al. [2011], Naduvinamani et al. [2012], Shimpi and Deheri[(2013], Patel and Deheri [2014], Shimpi and Deheri [2015], Patel et al. [2018], Shah [2022]).

Patel and Deheri [2016] considered combined effect of slip velocity and transverse surface roughness on the performance of a squeeze film for a circular cylinder near a plane. Therefore, in the present article it has been mooted to study the combine effect of slip velocity and transverse surface roughness on the Shliomis model based magnetic fluid lubrication of a squeeze film for circular cylinder near a plane.

ANALYSIS

The following figure presents the bearing configuration.

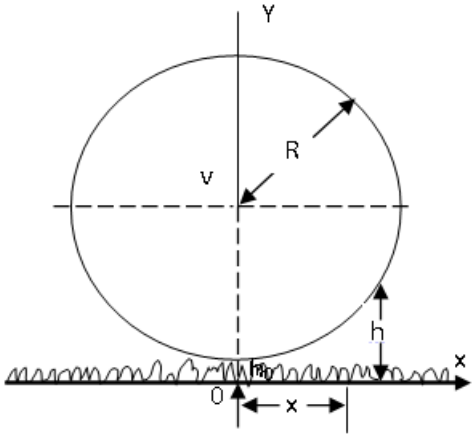

Figure 1. A Cylinder Near a plane

Majumdar informs that the Reynolds equation concern in an isoviscous incompressible fluid is given by

$$\frac{\partial}{\partial x}\left(h^3\frac{\partial p}{\partial x}\right)+\frac{\partial}{\partial z}\left(h^3\frac{\partial p}{\partial z}\right)=-12\,\eta_a V \qquad (1)$$

where V is the squeeze velocity $-\frac{dh}{dt}$ and $\eta_a=\eta(1+\tau)$ is the viscosity of the lubricant.

The length of the cylinder is assumed to be large as compared to the radius of the cylinder, so that the side leakage can be neglected. Equation (1), then reduced as to

$$\frac{d}{dx}\left(h^3\frac{dp}{dx}\right)=-12\,\eta(1+\tau)V \qquad (2)$$

The film thickness h is determine by the relation

$$h=h_0+R-\sqrt{R^2-x^2}$$

which approximately equals

$$h_0+\frac{1}{2}\frac{x^2}{R}$$

considering the series expansion.

Following Christensen and Tonder (1970), the thickness $h(x)$ of the lubricant film is considered to be

$$h(x)=\bar{h}(x)+h_s \qquad (3)$$

Here, $\bar{h}$ is the mean film thickness and h_s is the deviation from the mean film thickness characterizing the random roughness of the bearing surfaces. h_s is assumed to be stochastic in nature and governed by the probability density function $F(h_s)$, which is defined by

$$F(h_s)=\begin{cases}\frac{32}{35c}\left(1-\frac{h_s^2}{c^2}\right)^3 & ;-c\le h_s\le c\\ 0 & ;\text{otherwise}\end{cases} \qquad (4)$$

The following relationships decide the mean α,the standard deviation σ and the measure of symmetryεrespectively, while Estands for the expected value define by equation (6).

$$\alpha=E(h_s);\ \sigma^2=E[(h_s-\alpha)^2];\ \varepsilon=E[(h_s-\alpha)^3] \qquad (5)$$

$$E(R)=\int_{-c}^{c}R\,F(h_s)dh_s \qquad (6)$$

The details can be seen from Christensen and Tonder [1969(a),1969(b), 1970]. In order to describe the steady flow of magnetic fluids in the presence of slowly changing magnetic fields a mathematical model was proposed by Neuringer–Rosensweig in1964. This model and related aspects has been widely discussed in Bhat [2003].

Christensen and Tonder [1969(a), 1969(b), 1970] augmented the method of Tzeng and Seibel [1967] and described the surface roughness in terms of a random variable having non zero mean, variance and skewness. Using the model of Christensen and Tonder and the procedure given in Gupta and Deheri, equation (2) transform to

$$\frac{d}{dx}\left(g(h)\frac{dp}{dx}\right)=-12\,\eta(1+\tau)V \qquad (7)$$

where

$$g(h)=h^3+4(\sigma^2+\alpha^2)h+2\alpha^2h+2\alpha^3+3\sigma^2\alpha+\varepsilon$$

It is found that the role of standard deviation is much more as compared to the other two parameters and therefore one gets

$$g(h)\cong h^3+4\sigma^2h$$

Lastly, making use of (Beavers and Joseph, 1967) slip model one arrives at the stochastically averaged Reynolds' type equation, governing the film pressure, in dimensionless form as

$$\frac{d}{dx}\left(\left(\frac{4+\bar{S}}{2+\bar{S}}\right)(\bar{h}^3+4\bar{\sigma}^2\bar{h})\frac{dP}{dx}\right)=-12(1+\tau) \qquad (8)$$

wherein the dimensionless quantities are

$$\bar{S}=s\bar{h},\ P=\frac{ph^3}{\eta V R},\ \bar{\sigma}=\frac{\sigma}{h}$$

The non–dimensional boundary conditions associated with the bearing system are

$$\frac{dP}{d\bar{x}}=0\ \text{at}\ \bar{x}=0 \qquad (9)$$

where

$$\bar{x} = \frac{x}{R}$$

Solving equation (8) with the aid of boundary conditions (9) one gets the expression for non–dimensional pressure distribution:

$$\bar{P} = -\frac{3(1+\tau)}{\left(\frac{4+\bar{S}}{2+\bar{S}}\right)\bar{\sigma}^2}\log\left[\frac{\bar{h}}{\sqrt{\bar{h}^2+4\bar{\sigma}^2}}\right] \qquad (10)$$

Then, the load carrying capacity of the bearing system in non–dimensional form is found to be

$$\bar{W} = \frac{(1+\tau)}{\left(\frac{4+\bar{S}}{2+\bar{S}}\right)}\left[\log 4\bar{\sigma}^2 + \frac{1}{4\bar{\sigma}^2} + \frac{1}{12\bar{\sigma}^2}\left(\frac{C_0}{h_0}\right)^2\left(\frac{h_0}{R}\right) + \frac{1}{80}\left(\frac{C_0}{h_0}\right)^4\left(\frac{h_0}{R}\right)^2\frac{1}{\bar{\sigma}^2}\right] \qquad (11)$$

where $\bar{W} = \frac{{h_0}^3 w}{\eta V R L C_0}$

L being the length of the bearing.

RESULTS AND DISCUSSION

The magnetization enhances viscosity of the lubricant, which results in increased load bearing capacity. Mathematically also this can be seen clearly as the expression (10) is linear with respect to τ. The sharp increase in load carrying capacity can be seen from figures 2–3.

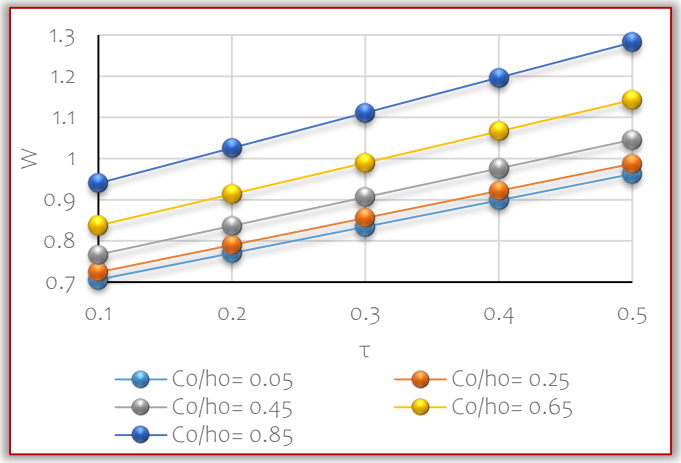

Figure 2. Variation of Load carrying capacity with respect to τ and C_0/h_0.

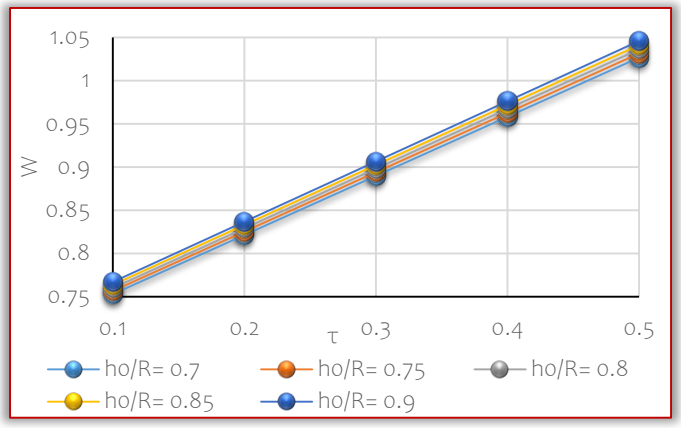

Figure 3. Variation of Load carrying capacity with respect to τ and h_0/R.

The profile of load carrying capacity with respect to the standard deviation presented in the Figures 4–6 asserts the load carrying capacity gets lowered. But, the influence of h_0/R on the variation of load carrying capacity with respect to $\bar{\sigma}$ stays nominal.

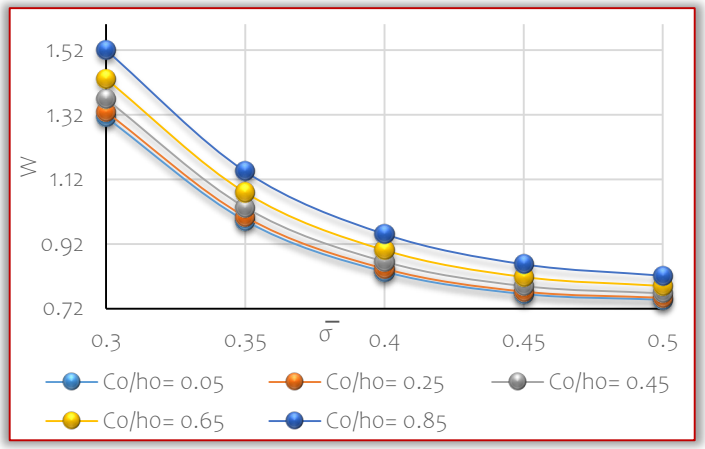

Figure 4. Variation of Load carrying capacity with respect to $\bar{\sigma}$ and C_0/h_0.

In fact the effect of h_0/R on the load bearing capacity with respect to standard deviation is almost negligible. At the same time the initial values of C_0/h_0 registers a negligible effect.

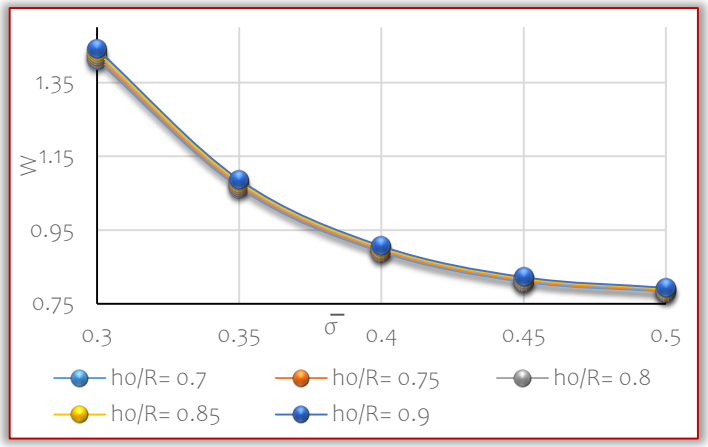

Figure 5. Variation of Load carrying capacity with respect to $\bar{\sigma}$ and h_0/R.

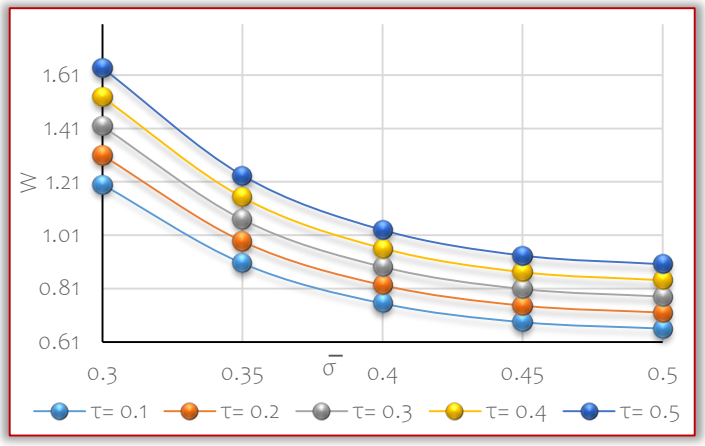

Figure 6. Variation of Load carrying capacity with respect to $\bar{\sigma}$ and τ.

Lastly, it is observed from Figures 7–10 that for a better performance, the slip is required to be kept at low level.

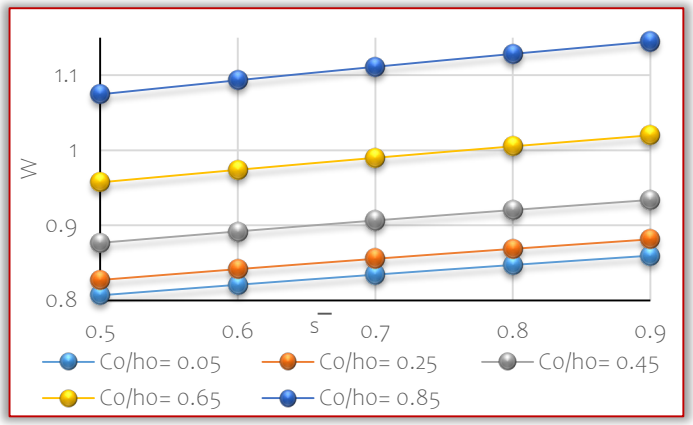

Figure 7. Variation of Load carrying capacity with respect to $\bar{s}$ and C_0/h_0.

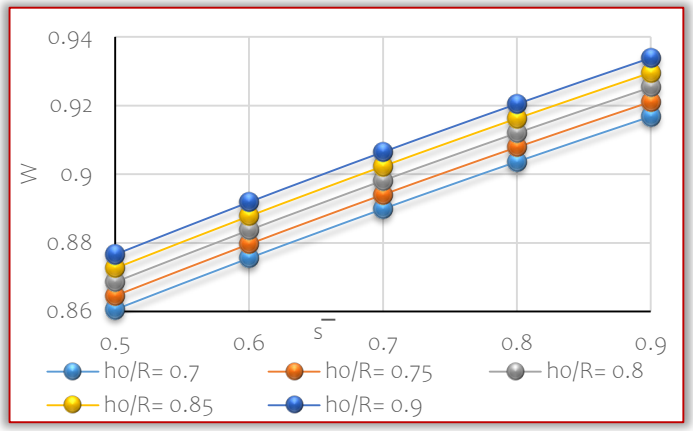

Figure 8. Variation of Load carrying capacity with respect to $\bar{s}$ and h_0/R.

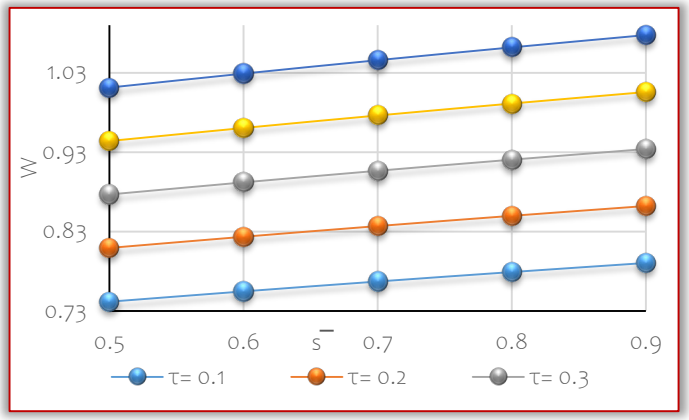

Figure 9. Variation of Load carrying capacity with respect to $\bar{s}$ and τ.

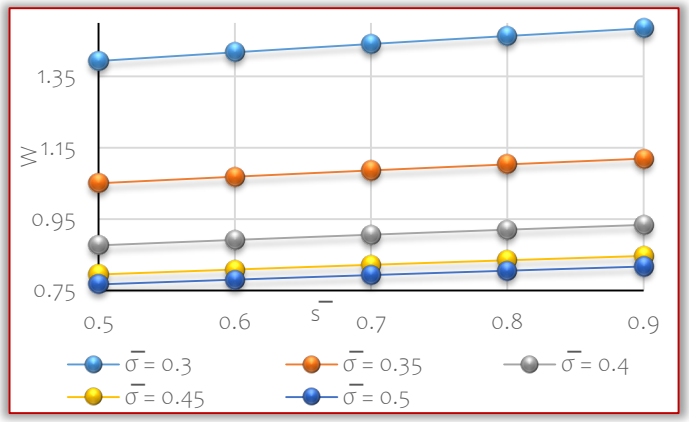

Figure 10. Variation of Load carrying capacity with respect to $\bar{s}$ and $\bar{\sigma}$.

CONCLUSION

This investigation opines that the Shliomis model is relatively suitable for this type of bearing system in comparison with the Neuringer–Rosensweig model. The graphical results mandate that the roughness–slip need to be given priority while designing the system, even if the slip is at reduced level. It is seen that some amount of load remains present in the absence of fluid flow, which does not happen in conventional lubricant.

References:

[1] Abhangi ND, Deheri GM: Numerical modeling of squeeze film performance between rotating transversely rough curved circular plates under the presence of a magnetic fluid lubricant, ISRN Mechanical Engineering, 2012, Article ID 873481, 2012.

[2] Acharya AS, Patel RM, Deheri GM: Ferro Fluid Squeeze Film in Rough Porous Circular plates considering the effect of viscosity variation and velocity Slip, International Journal of Theoretical and Applied Mechanics, 12 (4), 797–804, 2017.

[3] Barik M, Mishra SR, Dash GC: Effect of sinusoidal magnetic field on a rough porous hyperbolic slider bearing with ferrofluid lubrication and slip velocity, Pages, Tribology–Materials, Surfaces & Interfaces, 10 (3), 131–137, 2016.

[4] Bearman PW, Zdravkovich MM: Flow around a circular cylinder near a plane boundary, Journal of Fluid Mechanics, 89 (1), 33–47, 1978.

[5] Beavers GS, Joseph DD: Boundary conditions at a naturally permeable wall, Journal of Fluid Mechanics, 30(01), 197, 1967.

[6] Bhat MV: Lubrication with a magnetic fluid, Team spirit Pvt. Ltd., India, 2003.

[7] Bhat MV, Deheri GM: Magnetic–fluid based squeeze film in curved porous circular discs, Journal of Magnetism and Magnetic Materials, 127 (1–2), 159–162, 1993.

[8] Cameron A: Basic Theory of Lubrication, John Willy & Sons, New–York: Ellis Harwood Limited, Halsted Press, 1972.

[9] Christensen H, Tonder KC: The hydrodynamic lubrication of rough bearing surfaces of finite width, ASME–ASLE lubrication conference, paper No.70–Lub–7, 1970.

[10] Christensen H, Tonder KC: Tribology of rough surfaces: Parametric study and comparison of lubrication models, SINTEF, Report No. 22/69–18, 1969 a.

[11] Christensen H, Tonder KC: Tribology of rough surfaces: Stochastic models of hydrodynamic lubrication, SINTEF, Report No. 10/69–18, 1969 b.

[12] Deheri GM, Andharia PI, Patel RM: Transversely rough slider bearings with squeeze film formed by a magnetic fluid, Int. J. of Applied Mechanics and Engineering, 10 (1), 53–76, 2005.

[13] Deheri GM, Patel RM: Squeeze film based magnetic fluid in between porous circular disks with sealed boundary, Int. J. of Applied Mechanics and Engineering, 11(4), 803–812, 2006.

[14] Dipankar A, Sengupta TK: Flow past a circular cylinder in the vicinity of a plane wall, Journal of Fluids and Structures, 20(3), 403–423, 2005.

[15] Kawamura T, Takami H, Kuwahara K: Computation of high Reynolds number flow around a circular cylinder with surface roughness, Fluid Dynamics Research, 1(2), 1986.

[16] Kumar D, Sinha P, Chandra P: Ferrofluid squeeze film for spherical and comical bearings, Int. J. Engg. Sci. 30(5), 645–656, 1992.

[17] Lin JR: Fluid inertia effects in ferrofluid squeeze film between a sphere and a plate, Applied Mathematical Modeling, 37(7), 5528–5535, 2013.

[18] Lin JR, Lin MC, Hung TC, Wang PY: Effects of fluid inertia forces on the squeeze film characteristics of conical plates—ferromagnetic fluid model, Lubrication Science, 429–439, 2012.

[19] Lin JR, Lu RF, Lin MC, Wang PY: Squeeze film characteristics of parallel circular disks lubricated by ferrofluids with non–Newtonian couple stresses, Tribology International, 61,56–61, 2013.

[20] Naduvinamani NB, Hanumagowda BN, Fathima ST: Combined effects of MHD and surface roughness on couple–stress squeeze film lubrication between porous circular stepped plates, Tribology international, 56, 19– 29, 2012.
[21] Neuringer JL, R.E. Rosensweig RE: Magnetic Fluid, Physics of Fluids, 7(12) 19–27, 1964.
[22] Patel HP, Deheri GM, Patel RM: Combined effect of magnetism and roughness on a ferrofluid squeeze film in porous truncated conical plates: effect of variable boundary conditions, Italian Journal of Pure and Applied Mathematics – n. 39 (107–119), 107, 2018.
[23] Patel HP, Deheri GM, Patel RM: Numerical Modeling of Hydromagnetic Squeeze Film in Conducting Longitudinally Rough Annular Plates, International Journal of Research and Analytical Reviews, 6 (2), 2019 (E–ISSN 2348–1269, P– ISSN 2349–5138).
[24] Patel JR, Deheri GM: Effect of various porous structures on Shliomis model based magnetic fluid lubrication of a squeeze film in rough Porous circular plates upper one being Curved, Journal of Tribology and surface engineering; Hauppauge, 3(3–4), 137–160, 2012.
[25] Patel JR, Deheri GM: Shliomis model based magnetic fluid lubrication of a squeeze film in rotating rough curved circular plates, Carib.j.SciTech, 1, 138–150, 2013.
[26] Patel JR, Deheri GM: Combined effect of surface roughness and slip velocity on Jenkins model based magnetic squeeze film in curved rough circular plates, International J. of computational mechanics, 2014, 9 pages, 2014.
[27] Patel JR, Deheri GM: Effect of slip velocity and roughness on the performance of Jenkins model based on magnetic squeeze film in curved rough circular plates, J. of Serbian society for computational mechanics, 8(1), 45–63, 2014.
[28] Patel JR, Deheri GM: Shliomis model–based magnetic squeeze film in rotating rough curved circular plates: a comparison of two different porous structures, Int. J. of Computational Materials Sci. and Sur. Eng. 6 (1), 29– 49, 2014.
[29] Patel JR, Deheri GM: Theoretical study of Shliomis model based magnetic squeeze film in rough curved annular plates with assorted porous Structures, FME Transactions, 42 (2), 56–66, 2014.
[30] Patel JR, Patel ND, Deheri GM: Influence of slip and roughness on a ferrofluid squeeze–film between a sphere and flat porous plate, Materials Today: Proceedings, 50 (5), 1308–1314, 2022.
[31] Patel KC: The hydromagnetic squeeze film between porous circular disks with velocity slip, Wear, 58 (2), 275–281, 1980.
[32] Patel NC, Patel JR: Magnetic fluid–based squeeze film between curved porous annular plates considering the rotation of magnetic particles and slip velocity, Journal of the Serbian Society for Computational Mechanics, 14(2), 69–82, 2020.
[33] Patel ND, Deheri GM: Effect of Surface Roughness on the Performance of a Magnetic Fluid Based Parallel Plate Porous Slider Bearing with Slip Velocity, Journal of the Serbian Society for Computational Mechanics, 5 (1), 104–118, 2011.
[34] Patel RM, Deheri GM: A study of magnetic fluid based squeeze film behaviour between porous circular plates with a concentric circular pocket and effect of surface roughness, Industrial Lubrication and Tribology, 55(1), 32–37, 2003.
[35] Patel RM, Deheri GM, Patel HC: Effect of surface roughness on the behavior of a magnetic fluid– based squeeze film between circular plates with porous matrix of variable thickness, Acta Polytechnica Hungarica, 8(5), 171–190, 2011.
[36] Patel RU, Deheri GM: Effect of Slip Velocity on the Performance of a Short Bearing Lubricated With a Magnetic Fluid, Acta Polytechnica, Journal of Advanced Engineering, 53(6), 2013.
[37] Patel SJ, Deheri GM: Ferrofluid lubrication of a squeeze film in rough porous parallel circular disks, considering slip velocity, Journal of Mechanical and Industrial Engineering Research, 3 (2), 9–24, 2014.
[38] Patel SJ, Deheri GM: Combined effect of slip velocity and transverse surface roughness on the performance of a squeeze film for a circular cylinder near a plane, Annals of the faculty of engineering Hunedoara – International Journal of engineering, 14(3), 231–236, 2016.
[39] Patel SJ, Deheri GM, Patel JR: Combined Effect of Slip Velocity and Surface Roughness on a Magnetic Squeeze Film for a Sphere in a Spherical Seat: A Comparison of Two Different Porous Structures, Advances in Natural and Life Sciences, United Scholars Publications, USA, Vol. 2, pp. 190–229, 2016.
[40] Prajapati BL: Squeeze film behavior between rotating porous circular plates with a concentric circular pocket: Surface roughness and elastic deformation effects, Wear, 152(2), 301–307, 1992.
[41] Prajapati BL: On certain Theoretical Studies in Hydrodynamic and Electro–magneto–hydrodynamic Lubrication, Ph.D. Thesis: Sardar Patel University, Gujarat, 1995.
[42] Prakash J, Vij SK: Effect of velocity slip on the squeeze film between rotating porous annular discs, Wear, 38 (1), 73–85, 1976.
[43] Price SJ, Sumner D, Smith JG, Leong K, Paidoussis MP: Flow visualization around a circular cylinder near to a plane wall, Journal of Fluids and Structures, 16(2), 175–191, 2002.
[44] Shah RC: Ferrofluid lubrication of porous–rough circular squeeze film bearings, The European Physical Journal Plus, 137, Article number: 190, 2022.
[45] Shimpi ME, Deheri GM: Ferrofluid lubrication of rotating curved rough porous circular plates and effect of bearing's deformation, Arab. J. Sci. Eng., 38(10), 2865–2874, 2013.
[46] Shimpi ME, Deheri GM: Surface Roughness and Deformation Effects on the Behaviour of a Magnetic Fluid Based Squeeze Film in Rotating Curved Porous Circular Plates, American Journal of Marine Science, 3 (1), 1–10, 2015.
[47] Shliomis MI: Effective viscosity of magnetic suspensions, Sov. Physics JETP, 34(6), 1291–1294, 1972.
[48] Shliomis MI: Magnetic Fluids, Soviet Physics Uspekhi, 17(2), 153, 1974.
[49] Singh UP, Gupta RS: Dynamic performance characteristics of a curved slider bearing operating with ferrofluid, Advances in Tribology, Article Id 278723, 2012.
[50] Sparrow EM, Beavers GS, Hwang IT: Effect of Velocity Slip on Porous–Walled Squeeze Films, Journal of Tribology, 94(3), 260–264, 1972.
[51] Thakkar SB, Patel HC, Deheri GM, Patel RM: Effect of transverse surface roughness on the performance of squeeze film behavior between rotating porous circular plates having concentric circular pocket with velocity slip, International Colloquiam Tribology, Lubricants, Materials and Lubrication Engineering, 31 pages, 2008.
[52] Trahan JF, Hussey RG, Roger RJ: The velocity of a circular disk moving edgewise in quasi–steady Stokes flow toward a plane boundary, Physics of Fluids, 11, 1999.
[53] Tzeng ST, Saibel E: Surface roughness effect on slider bearing lubrication, Trans. ASLE 10, 334–342, 1967.
[54] Wu H: Effect of velocity–slip on the squeeze film between porous rectangular Plates, Wear, 20 (1), 67–71, 1972.
[55] Wu H: The Squeeze film between rotating porous annular disks, Wear, 18(6), 461–470, 1971.
[56] Zdravkovich MM: Forces on a circular cylinder near a plane wall, Applied Ocean Research, 7(4), 197–201, 1985.

ISSN: 2067–3809

Fascicule 4
[October – December]
tome XVI
[2023]

ACTA Technica CORVINIENSIS
BULLETIN OF ENGINEERING

ISSN: 2067-3809

ACTA TECHNICA CORVINIENSIS – BULLETIN OF ENGINEERING
TOME XVI [2023] | FASCICULE 4 [OCTOBER – DECEMBER]

[1.]Mihai APOSTOL, [2.]Constantin Stelian STAN, [3.]Mihai CHIŞAMERA,
[4.]Georgian CABEL, [5.]Codrut CARIGA

A TECHNICAL ANALYSIS OF THE EVOLUTION OF COIN AND MEDAL MINTING METHODS

[1–5.]University Politehnica of Bucharest, Faculty of Materials Science and Engineering, 313 Splaiul Independenței, 6 District, Bucharest, ROMANIA

Abstract: The history of coin and medal minting methods spans millennia, reflecting the advancement of technology and the changing needs of societies. This technical analysis explores the evolution of coin and medal minting techniques, from ancient civilizations to modern industrial processes. By examining the key innovations and methodologies employed throughout history, this study sheds light on the fascinating journey of numismatic craftsmanship. The study begins by delving into the earliest forms of coin and medal production, highlighting the techniques used by ancient civilizations such as the Greeks, Romans, and Chinese. It explores the manual methods of hand–striking coins and casting medals, shedding light on the intricacies of engraving and die–making. As we progress through history, this analysis identifies pivotal developments. The transition from manual labor to mechanized minting processes revolutionized the precision and efficiency of coin production. Furthermore, this analysis investigates the emergence of modern coin and medal minting techniques, including the use of computer–aided design (CAD), digital engraving, and advanced metallurgical processes. These innovations have allowed for greater intricacy in design, increased durability, and enhanced security features, meeting the demands of contemporary economies and collectors. Additionally, the study addresses the environmental and ethical concerns associated with coin and medal production, including the use of sustainable materials and responsible sourcing. The evolution of minting methods also includes the development of eco–friendly practices to minimize the environmental impact of coin and medal production. Ultimately, this technical analysis provides a comprehensive overview of the evolution of coin and medal minting methods, demonstrating the intricate balance between tradition and innovation. By understanding this evolution, we gain insights into the cultural, technological, and economic shifts that have shaped the world of numismatics, offering valuable perspectives for collectors, historians, and scholars alike.

Keywords: coins, medals, die, manufacturing

INTRODUCTION

The history of coinage and medal production is a testament to human ingenuity and technological advancement. Coins and medals have not only served as mediums of exchange and symbols of honor but also as windows into the evolution of metallurgy, engineering, and artistic craftsmanship. This technical analysis embarks on a journey through time to explore the fascinating evolution of coin and medal minting methods, from ancient civilizations to the cutting–edge technologies of the modern world.

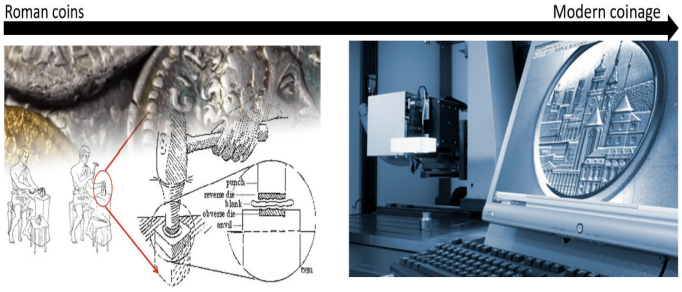

Figure 1. Evolution of the coins manufacture

The ancient Romans crafted their coins from flat, round metal discs or 'mints' using a method we now refer to as minting – a term still associated with wealth today! Unlike today's automated factory processes, Roman minted coins were entirely handcrafted within a workshop space resembling a blacksmith's forge. In the early 200s BCE, these coins were primarily composed of bronze, but over time, the Roman coin–making process evolved to incorporate silver, gold, and copper. The most iconic and widely circulated coin throughout the Roman Empire was the denarius, produced through the pressing of silver. Remarkably, the denarius remained in circulation for an astounding five centuries. In the creation of their coins, the Romans employed two distinct techniques on metals – cold striking and hot striking.

Coins and medals have played pivotal roles in economies and societies across the globe. They have been used to facilitate trade, commemorate important events and individuals, and serve as artifacts that reveal the cultural, political, and economic landscapes of their respective eras. As these roles evolved, so did the techniques and technologies used in their creation. This study aims to dissect the progression of minting methods, offering insights into the technical intricacies that underlie the creation of these tangible pieces of history. By examining the evolution of coin and medal minting, we gain a deeper appreciation for the artistry, craftsmanship, and innovation that have shaped this field over centuries. Our exploration begins by examining the origins of coin and medal production, where rudimentary techniques

involving hand–crafted dies and manual striking processes dominated the landscape. As we journey through time, we encounter the monumental shifts brought about by the Renaissance and the Industrial Revolution, which heralded the era of mechanized minting and mass production. In the modern era, the integration of computer–aided design (CAD), digital engraving, and advanced metallurgical processes has transformed the art of coin and medal minting. These technological advancements have not only enhanced the precision and quality of these numismatic objects but have also introduced novel security features to combat counterfeiting. Moreover, this analysis does not stop at the technical aspects of minting methods; it also delves into the ethical and environmental considerations surrounding coin and medal production. Responsible sourcing of materials and sustainable practices have become integral aspects of the minting industry, reflecting society's growing awareness of the environmental impact of industrial processes. As we navigate this historical and technical terrain, we will uncover the rich tapestry of innovations, challenges, and societal shifts that have shaped coin and medal minting methods. By understanding the evolution of these techniques, we gain a deeper appreciation for the integral role that numismatics plays in documenting our shared history. In this paper we want to focus on the technical processes and artistic achievements that have defined the world of coin and medal minting, linking past and future through the lens of craftsmanship and innovation.

ANALYSIS OF CURRENT COIN MINTING PROCEDURES USED TO CREATE MEDALS

A metal shaping process known as coining plays a pivotal role in the production of coins and medallions. The conventional method of manufacturing medallions necessitates a pressing demand for expediting production, cost reduction, and the minimization of material wastage. In order to streamline the manufacturing process and curtail production expenses, contemplation of an alternative coining technique becomes imperative. Coining, essentially, signifies a form of metal forming wherein the material undergoes a minute displacement relative to the part's overall volume. Within minting facilities, the conceptualization of medallion and coin designs conventionally commences with the creation of hand–rendered sketches on paper. Subsequently, these designs traverse through a series of intermediary processes before being transcribed onto the dies.

This study encompasses a comprehensive scrutiny of the coining process, the introduction of an alternative approach that integrates Computer–Aided Design and Computer–Aided Manufacturing (CAD/CAM) applications into the design and production phases, as well as the proposal of modular die designs tailored for both blanking and coinage dies.

Figure 2. Plaster and silicone model

Figure 3. Silicone and acrylic model

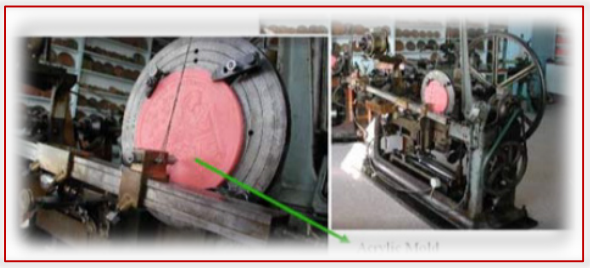

Figure 4. Clasic reduction machine

To initiate this creative endeavor, the Art Workshop embarks on a preliminary investigation, wherein the sculptor and a dedicated design team delve into historical contexts and pertinent aspects of the specific event or gather essential information pertaining to the individual for whom the coin or medallion is intended. Once preparatory groundwork reaches its culmination, the sculptor proceeds to delineate the design on paper, amplifying its scale to a certain magnitude. The design team, in turn, undertakes the task of discerning the optimal design configuration, considering anarray of alternatives for the impending coin or medallion project. Subsequently, sculptors commence the meticulous refinement of the positive plaster model, ensuring that every intricacy is meticulously attended to. Following the completion of the positive plaster model, a corresponding negative silicone model is meticulously crafted. This is done with the explicit purpose of facilitating the transfer of intricate details onto an acrylic model, which constitutes a robust thermoplastic sign material characterized by its relative toughness. The subsequent phase entails the replication of the negative silicone

model onto the acrylic substrate, effectively generating a positive mold. Secondly, within the Die/Mold workshop, the relief design undergoes a laser reading process via an engraving machine. It is worth noting that the traditional engraving machines are mechanical in nature, functioning by proportionally reducing the dimensions, height, and intricacies of the relief through the coordinated movement of a mechanical probe and tool. Depending on the specific dimensions and level of detail required for the mold, this process an extend over a duration of at least 36 hours. One notable challenge arises from the necessity for the dies utilized in the production of the master die to maintain precise alignment with the original part throughout the manufacturing process. As a result, achieving the desired level of tolerance within the relief design becomes a formidable task.

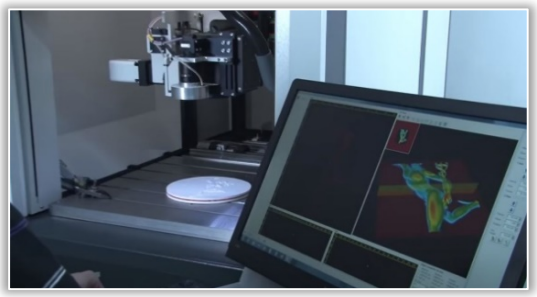

Figure 5. A view of 3D laser scanning

The engraving of the die can also be executed through the application of state–of–the–art technology. The process involves a series of steps commencing with the initial phase of 3D scanning of the plaster model. Subsequently, the processed file is seamlessly transitioned into CNC programming. This, in turn, facilitates the utilization of either mechanical engraving or laser engraving machines to realize the desired die.

Mechanical engraving using a CNC machine for coining die

Mechanical engraving, employing a CNC machine, represents a precise and versatile method for the creation of coining dies. This advanced technique harnesses the power of automated control systems to intricately carve out the required relief patterns and designs on the die surface. CNC machines, guided by precise coordinates, offer exceptional accuracy and repeatability, ensuring that the resulting coining dies meet the exacting standards necessary for the production of coins and medallions. This method not only streamlines the manufacturing process but also allows for the realization of intricate and finely detailed coin designs with a high degree of precision and consistency.

Figure 6. A view of mechanical engraving using a CNC machine

Laser engraving using a CNC machine for coining die

This innovative method leverages the precision of laser technology to etch intricate relief patterns and designs onto the die's surface. Guided by digital instructions and precise coordinates, CNC–controlled laser engraving machines offer unparalleled accuracy, repeatability, and flexibility in producing coining dies of exceptional quality. The benefits of laser engraving in coining die production are multifaceted. Firstly, it allows for the creation of highly detailed and fine relief designs with remarkable intricacy, which is particularly advantageous for crafting coins and medallions that demand intricate artwork. Additionally, laser engraving is a non–contact process, reducing wear and tear on the machinery and extending its operational lifespan.

Figure 7. A view of laser engraving using CNC machine

Manual polishing of coin dies

Manual polishing of coin dies is a fundamental and meticulous process within the coin minting industry. Coin dies are essential components responsible for imprinting intricate designs and details onto coins. The quality of these dies directly affects the final appearance and precision of the coins produced. In the world of coin minting, manual polishing of coin dies is a labor–intensive yet indispensable process. It ensures that coin dies maintain their quality and longevity, ultimately leading to the production of coins with sharp and well–defined designs. While automation has made strides in this field, the artistry and skill of manual polishing remain integral to achieving exceptional coin quality.

Figure 8. Manual polishing of coin dies

The heat treatment of coin dies

The heat treatment of coin dies represents a critical metallurgical process integral to the enhancement of their durability and performance within the coin minting process. This procedure involves a series of carefully controlled heating and cooling cycles, each meticulously calibrated to achieve specific metallurgical transformations and desired mechanical properties.

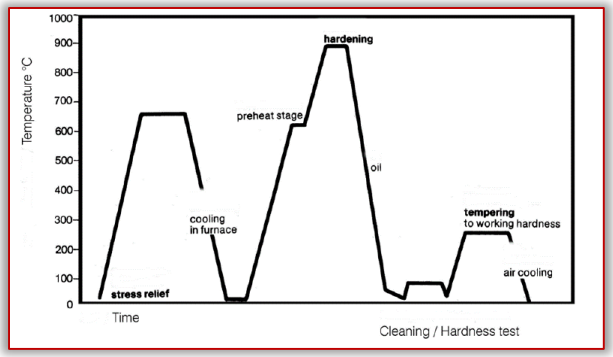

Figure 9. K 455 steel heating and tempering diagram

Hard chromium plating of coin dies

An electroplating procedure is systematically employed to administer a deposition of hard chromium onto the die's surface. This strategic intervention serves a twofold purpose: the mitigation of wear during the coining process and the consequential extension of the operational lifespan of the dies.

Figure 10. A view of the chrome plating process of the dies

Blanking process

To begin with, within the minting facility, an alloy material is cast and subsequently processed through rolling operations to achieve the desired thickness. Subsequently, blanks are meticulously cut from the rolled metal alloy. These alloys typically comprise a blend of base metals, and their composition undergoes rigorous and precise control measures.

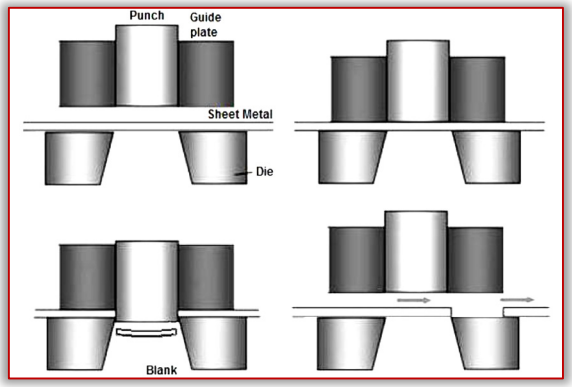

Figure 11. Punching of blanks used to obtain coins

The amount of cutting clearance between the punch and the die is of great importance in all sheet metal work. It is usually given as a percentage of the thickness of cut material, as shown in the next Table.

Table 1. The tolerance of the cutting space between the punch and the cutting die depending on the thickness of the cut material

Material	Hardness HV	Clearence as a % of thickness
Mild Steel	94-144	5-10
70/30 Brass	77-110	0-10
Copper	64-93	0-10
Zinc	61	0-5
Aluminum	21-28	0-5

During the rolling, work hardening is naturally applied to the blank metal. Before the coinage, the blanks need to be softened slightly in a furnace by bring blanks up to a certain temperature and then cooling them again. This provides metal to relieve thermal stresses. After annealing, the blanks are burnished to make their surface brighter, remove any discoloration and in some cases apply a minute amount of lubricant to assist in coining. In the burnishing machine, surfaces of blanks are etched and polished by tumbling inside a mixture of small steel balls and ceramic media combined with special chemicals. After burnishing, the blanks are dried with hot air.

The volume of the metal and the volume of the enclosure between the dies when they are confined should remain the same. Excessive loads that developed inside the dies do not damage the press and dies themselves unless the metal volume exceeds the space between upper and lower dies when closed. In order to ensure that volume of the blank remain constant, the weight, which is easily measured and converted to volume should be carefully controlled.

Coining is a metal forming process that cannot be considered as a simple process because the process can be characterized by entirely 3–D material deformation and continuously changing boundary conditions.

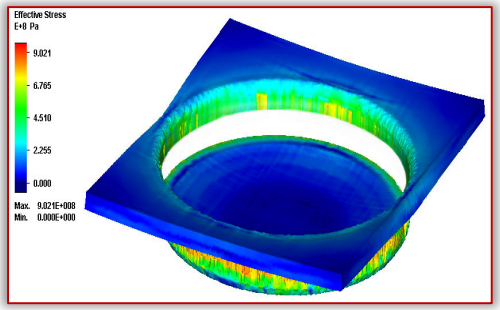

Figure 12. Effective Stress Distribution for Blanks

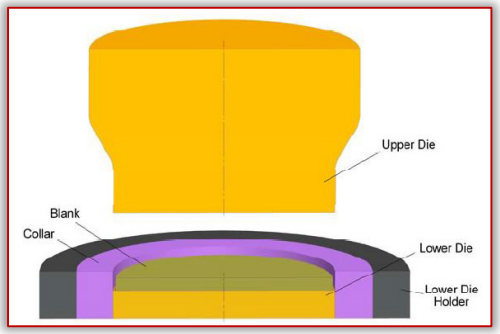

Figure 13. A simulation of the process of pressing a coin

Therefore, production of a full solution requires experienced and challenging people who perform the simulation in relatively short calculation times. In order to predict the flow of metal, stress, strain and temperature distributions, accurate and robust algorithms are required.

Figure 14. Effective Stress Distribution in the coin with a Diameter of 89mm

After both of the upper and lower dies are mounted, alignment of them is checked with few test shots when the press is in unloaded position.

Figure 15. A view of Assembled Upper Die Set

After it is ensured that the alignment of the upper and lower dies is done appropriately, the upper die set is brought to the upper dead centre so that shut height can be adjusted for the coining process.

Figure 16. A view of Die Sets before the Coinage

Taking into consideration that the diameter and weight of a coin are predetermined prior to the commencement of the design phase, the thickness of the semi–finished coin blanks is meticulously calculated using specialized 3D software. This calculation is aimed at ensuring that an adequate quantity of material is utilized, thereby facilitating the faithful replication of all intricate details incorporated into the coin's design.

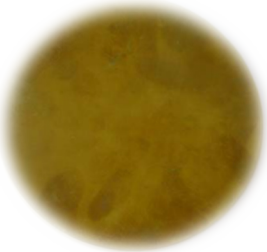

Figure 17. Circular Blanks before minted

The blank is carefully placed within the lower supporting die, a pivotal step in the coin minting process that initiates the transformation of the blank into a finished coin. This precise positioning is fundamental, as it ensures that the blank aligns perfectly within the die, setting the stage for subsequent operations that will impart the coin's unique design and features.

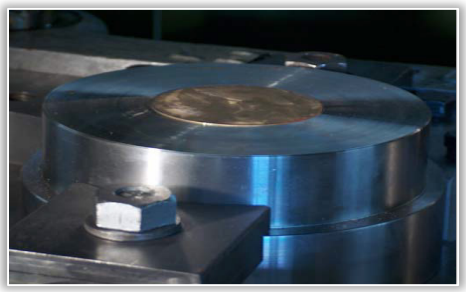

Figure 18. A view of the Blank on the Lower Supporting Die

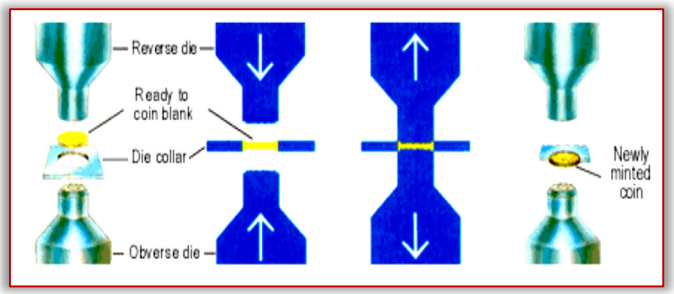

Figure 19. The process of punching blanks and pressing coins

Figure 20. Minted coin

Following the coining process, a meticulous assessment of both the design and technical specifications is undertaken. This post–production evaluation is crucial to ensure that the minted coins meet the intended standards and that all aspects, from the visual elements to the precise technical details, adhere to the desired criteria.

The importance of technical analysis of the evolution of coin and medal minting

The importance of conducting a technical analysis of the evolution of coin and medal minting methods lies in its multifaceted significance across various domains, including history, technology, artistry, economics, and environmental sustainability. Here are several key reasons highlighting the importance of such an analysis:

— Preservation of Cultural Heritage: Coinage and medals serve as important artifacts reflecting the cultural, historical, and political contexts of their times. Analyzing the evolution of minting methods helps preserve and understand the cultural heritage of civilizations through the ages.

— Advancement of Technology: The evolution of minting methods parallels technological progress. Studying these developments provides insights into how societies have advanced in metallurgy, machinery, and automation, which can have broader applications beyond numismatics.

— Artistic Expression: Coins and medals are often miniature works of art, featuring intricate designs and engravings. A technical analysis helps in appreciating the artistic aspects of these pieces, shedding light on the skill and creativity of craftsmen throughout history.

— Economic Significance: Coins are integral to economies. Changes in minting methods impact currency production efficiency, costs, and the quality of coins in circulation. Understanding these changes can provide valuable economic insights.

— Numismatic Research: Numismatists and collectors rely on technical details to authenticate, classify, and value coins and medals. An in–depth analysis aids collectors in accurately assessing the historical and numismatic value of their holdings.

— Security and Counterfeiting: Advances in minting techniques, such as incorporating security features, play a vital role in combating counterfeiting. Understanding these security measures is crucial for maintaining the integrity of currencies and collectibles.

— Environmental Considerations: In the modern era, sustainability is a growing concern. Examining the environmental impact of coin and medal production, as well as exploring sustainable practices, is essential for responsible numismatic manufacturing.

— Education and Outreach: Research on the evolution of minting methods can serve as a valuable educational resource. It helps engage students, historians, and the general public in understanding the complexities of coin and medal production.

— Collector and Investor Knowledge: Collectors and investors in numismatics rely on information about minting methods to make informed decisions. Understanding the technical aspects can guide investment strategies and ensure the acquisition of high–quality coins.

— Interdisciplinary Insights: The analysis of minting methods bridges multiple disciplines, including history, engineering, art, and economics. Such interdisciplinary exploration fosters a holistic understanding of the subject matter.

In summary, a technical analysis of the evolution of coin and medal minting methods is essential for preserving cultural heritage, advancing technology, appreciating artistry, understanding economic implications, supporting numismatic research, enhancing security measures, promoting sustainability, facilitating education, aiding collectors and investors, and fostering interdisciplinary insights. It enriches our understanding of history, technology, and art while addressing contemporary concerns like sustainability and security.

Advanced research on technical analysis of coin and medal

Certainly, in this studies are some key contributions and developments related to the technical analysis of the evolution of coin and medal minting:

— Advanced Metallurgical Techniques: Recent advancements in metallurgy have allowed for the use of new and innovative coin and medal materials. These materials offer improved durability, resistance to wear, and unique aesthetic qualities. For example, the use of bi–metallic or polymer–based coins has become more common in many countries.

— 3D Printing and Additive Manufacturing: The adoption of 3D printing and additive manufacturing technologies has opened up new possibilities for coin and medal design and production. These technologies enable the creation of highly intricate and customizable designs with great precision.

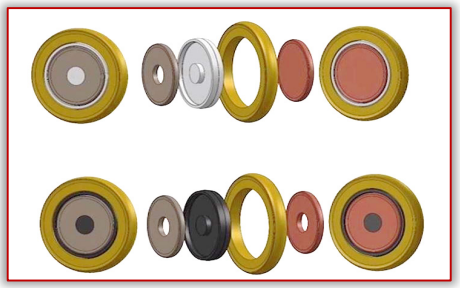

Figure 21. Various combinations through different geometries and material selections of the separators as well as the inserts

— Digital Engraving and Design Software: The use of digital engraving tools and design software has become prevalent in the minting industry. This allows for the creation of detailed and intricate designs that were once difficult or impossible to achieve using traditional methods.

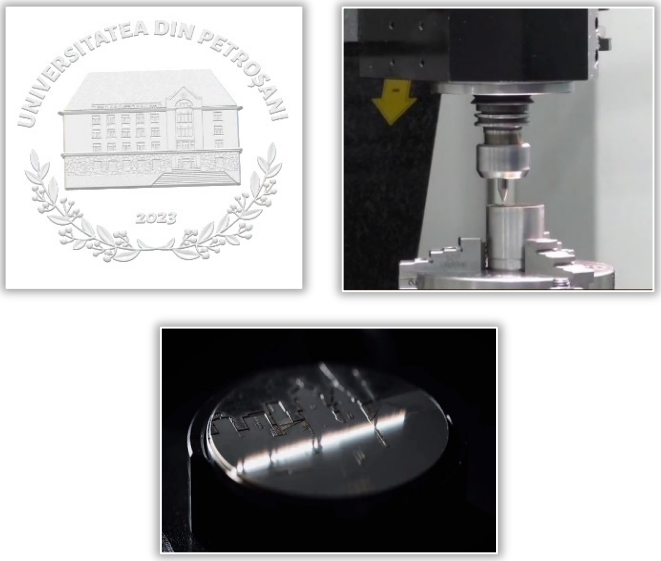

Figure 22. Application of electronic files for the production of moulds using CNC machines

— Anti–Counterfeiting Measures: With the rise of sophisticated counterfeiting techniques, there has been a significant focus on integrating advanced security features into coins and medals. These include microprinting, holograms, color–changing inks, and other covert security features that are challenging for counterfeiters to replicate.

Figure 23. security features using laser micro–engraving

— Minting Automation: Automation has continued to advance, allowing for faster and more efficient coin and medal production. High–speed coin presses, robotics, and automated quality control systems have become integral to modern mints.

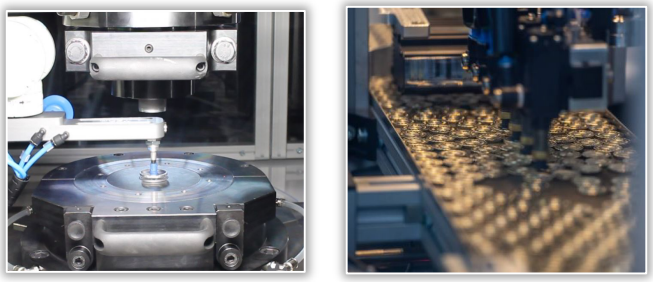

Figure 24. Automation of coin pressing using robot arm

— Digital Minting Technologies: Some mints have embraced fully digital minting processes, where coins and medals are designed, produced, and stored digitally. This allows for greater flexibility, reduced lead times, and the ability to create on–demand or limited–edition pieces.

Figure 25. 3D inspection of coins using 3D optical scanning

— Sustainability and Responsible Sourcing: Increasing awareness of environmental concerns has prompted mints to adopt more sustainable practices. This includes responsible sourcing of materials, recycling, and reducing energy consumption in the minting process.

— Virtual Mint Tours: Mints and numismatic organizations have leveraged technology to offer virtual mint tours and interactive online platforms. These initiatives provide enthusiasts and collectors with insights into the minting process from the comfort of their homes.

— Research and Documentation: Ongoing research and documentation efforts aim to catalog and preserve the history of coin and medal production techniques. This includes the creation of archives, databases, and reference materials for researchers and collectors.

— Education and Outreach: Mints and numismatic organizations are actively engaged in educational outreach, including workshops, seminars, and online resources. This helps disseminate knowledge about coin and medal minting techniques to a wider audience.

These contributions reflect the dynamic nature of the coin and medal minting industry, where technology, craftsmanship, and innovation continue to shape the way coins and medals are produced and appreciated. As technology advances and new challenges arise, the field of numismatics adapts and evolves, ensuring the

continued relevance and fascination of coin and medal collecting.

CONCLUSIONS

The evolution of coin production, from manual coin pressing to the utilization of CNC machines and CAD software, represents a significant transformation in the numismatic industry. Several noteworthy conclusions can be drawn from this evolution:

- Precision and Consistency: The transition from manual coin pressing to CNC machines and CAD software has ushered in an era of unparalleled precision and consistency in coin production. CNC machines can execute intricate designs with pinpoint accuracy, resulting in coins that adhere to exacting specifications.
- Complexity of Designs: CAD software has revolutionized coin design by allowing for the creation of highly intricate and detailed coin motifs that were previously challenging to achieve through manual methods. This has expanded the creative possibilities for coin designers.
- Efficiency and Speed: CNC machines have drastically reduced production times, enabling the rapid minting of coins in comparison to manual techniques. This increased efficiency can be particularly advantageous in meeting high demand.
- Customization and Personalization: The integration of CAD software and CNC machines has made it easier to customize and personalize coins. This is valuable for creating commemorative coins, special editions, or coins for specific events or individuals.
- Quality Control: The use of CNC machines allows for precise quality control throughout the coin production process. Imperfections and defects can be identified and rectified more efficiently, resulting in a higher standard of finished coins.
- Reduced Wear and Tear: CNC machines are less physically taxing on the dies, as they do not require the forceful manual pressing used in traditional methods. This reduction in wear and tear can extend the lifespan of coin dies.
- Technological Advancements: The adoption of CNC machines and CAD software reflects the broader trend of incorporating advanced technology into traditional industries. It showcases how technology can enhance age–old practices while preserving the artistry and craftsmanship associated with coin production.
- Historical Continuity: Despite these technological advancements, coin production retains its historical significance and cultural importance. Modern methods pay homage to the time–honored traditions of coin minting while embracing contemporary tools and techniques.

It can be said, the shift from manual coin pressing to the integration of CNC machines and CAD software marks a pivotal moment in the evolution of coin production. It has brought forth improved precision, efficiency, and creative possibilities, ensuring that coins continue to play a vital role in our society while adapting to the demands of the modern world.

In summary, the technical analysis of the evolution of coin and medal minting methods offers a fascinating journey through time, uncovering the intricate and multifaceted aspects of this age–old craft. From the rudimentary techniques of ancient civilizations to the cutting–edge technologies of the modern era, the study of coin and medal minting methods reveals a rich tapestry of innovation, artistry, and historical significance. Throughout history, coins and medals have served as tangible symbols of culture, power, and economic exchange. Their production methods have mirrored the advancements in technology, metallurgy, and design capabilities of each era. This analysis has illuminated several key findings:

- Historical Significance: Coins and medals are invaluable artifacts that provide invaluable insights into the history and culture of the societies that produced them. The evolution of minting methods parallels the rise and fall of civilizations, making it an indispensable field of study for historians and archaeologists.
- Technological Advancements: From hand–struck coins of antiquity to the precision of modern digital engraving and computer–aided design, the technical sophistication of coin and medal production has continuously evolved. Innovations such as coin presses, automation, and security features have transformed the industry.
- Artistic Expression: The artistry in coin and medal design has flourished over the centuries. Engravings, motifs, and intricate details reflect the artistic sensibilities and cultural influences of their time. Technical advancements have enabled greater artistic freedom and complexity in design.
- Economic Implications: Coinage has played a pivotal role in economies worldwide. Understanding the evolution of minting methods provides insights into the economic stability and challenges faced by societies. It also underscores the importance of efficient, reliable, and secure coin production.
- Environmental Responsibility: The contemporary minting industry recognizes the need for sustainable and responsible practices. This includes ethical sourcing of materials, eco–friendly production methods, and minimizing the environmental footprint of coin and medal minting.

— Numismatic Insights: For numismatists and collectors, technical analysis is essential for authenticating, grading, and valuing coins and medals. It aids in distinguishing genuine pieces from counterfeits and contributes to a deeper appreciation of their collections.
— Interdisciplinary Nature: The study of coin and medal minting methods spans multiple disciplines, from history and metallurgy to engineering and art. It showcases the interconnectedness of these fields in preserving and understanding our past.

In an ever–evolving world, the technical analysis of coin and medal minting methods serves as a bridge between tradition and innovation. It not only preserves our cultural heritage but also propels us forward into the future, where new materials, technologies, and environmental considerations continue to shape the fascinating world of numismatics. As we continue to uncover the secrets of the past through the lens of minting techniques, we are reminded that the story of coins and medals is a testament to human creativity, adaptability, and the enduring value of history.

Acknowledgement

This work has been funded by the European Social Fund from the Sectoral Operational Programme human Capital 2014–202, through the Financial Agreement with the title "Training of PhD students and postdoctoral researchers in order to acquire applied research skills–SMART", Contract no. 13530/16.06.2022–SMIS code:153734.

References:

[1] Library.oapen.org, (2019). Money and Coinage in the Middle Ages [online] Available at: https://library.oapen.org/bitstream/handle/20.500.12657/24386/1005729.pdf?sequence=1&isAllowed=y [Accessed 2.11.2022]
[2] Colcestreasurehunting.co.uk. Identifying British coinage. [online] Available at: http://www.colchestertreasurehunting.co.uk/c/coinhistory.htm [Accessed 3.11.2022]
[3] Muzeydeneg.ru. Coin minting technique [online] Available at: http://muzeydeneg.ru/research/tehnika–chekanki–monet–ch–3–stanochnaya–chekanka–testonov–i–talerov/ [Accessed 3.11.2022]
[4] Vsemedali.ru. A Brief Essay on the History of Medal Art [online] Available at: http://vsemedali.ru/books/item/f00/s00/z0000000/st003.shtml [Accessed 1.11.2022]
[5] Romancoins.info. Roman Numismatic Gallery [online] http://www.romancoins.info/Lydia600BCELTrite.jpg [Accessed 1.11.2022]

ISSN: 2067-3809

Fascicule 4
[October – December]
tome XVI
[2023]

ACTA Technica CORVINIENSIS
BULLETIN OF ENGINEERING

ISSN: 2067-3809

[1.]Anniel Heriberto MARTÍN–DELGADO, [2.]Lorenzo PERDOMO–GONZÁLEZ,
[3.]Norge Isaias COELLO–MACHADO, [4.]Elke GLISTAU

OBTAINING A CERAMIC BY ALUMINOTHERMIA FOR USE AS AN ABRASIVE MATERIAL

[123.]Universidad Central "Marta Abreu" de Las Villas, Santa Clara, CUBA
[4.]Otto von Guericke University Magdeburg, Magdeburg, GERMANY

Abstract: Polishing operations are mandatory in the manufacturing of floors and terrazzo, which are performed with grinding wheels. This study is carried out in two main stages, a laboratory study and later a study in the experimental pilot plant where the obtaining of abrasive materials from the aluminothermic processing of solid industrial wastes and Cuban minerals is approached. Different mixtures composed of mill scale and aluminum chips to which different proportions of limestone are added are studied. As a result of the process, a high hardness ceramic is obtained as the main product and a metal as a byproduct. The results of the process are evaluated on the basis of the metal and slag yields. The behavior of the ceramic as an abrasive material is evaluated by means of scratch tests on glass, as well as the behavior of the powders during setting with p–350 cement. Finally, a real working test of the abrasive obtained is carried out, achieving good results, which justifies the production on a larger scale of the abrasive materials with the objective of substituting the imported abrasive. The proposed technology constitutes a great step towards sustainability, since it would allow to substitute the importation of this product, minimizing its price and using Cuban industrial waste and minerals as raw materials.
Keywords: aluminothermia, ceramics, castings, abrasive wheels, sustainability

INTRODUCTION

An abrasive is a material of a certain hardness and density that allows other materials to be processed by removing the material itself [9]. Hardness, grain size, composition and structure are of fundamental importance [5].

Each of these variables affects the final result. Choosing the right abrasive is essential to achieve the desired result [9]. They can be found on the market in multiple forms (wheels, discs, paper, powders, pastes, etc. [7].

The combination of logistics and quality assurance (management) creates the conditions for a change in production and services [6]. To work in this direction, the country's leadership gives priority to scientific and technological work, which is carried out by increasing university–industry links to obtain concrete results.

Likewise, the choice of the type of infrastructure and the way in which the services provided over it are designed, regulated and operated, determine the price, times and quality of the products [2].

In Cuba, the polishing of floor and terrazzo elements is done with grinding wheels, which are manufactured using abrasive powders imported at high costs in the international market. The absence of an industrial process for obtaining abrasive materials represents a major constraint to the economic development of the island. This makes it necessary to develop an economically feasible alternative for the manufacture of these abrasive materials, since they are used in numerous tasks.

From a mixture consisting of: mill scale, aluminum shavings and the addition of limestone, it is possible to obtain by aluminothermia a ceramic with high alumina content and high hardness, which can be used in the production of grinding wheels. The pyrometallurgical processing is carried out using the energy generated by the redox reactions that take place, being more than 90 % of the materials used industrial waste.

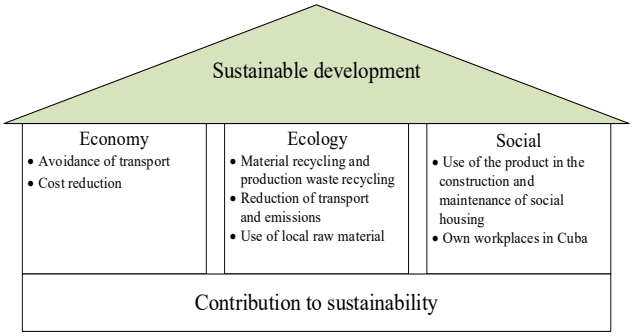

Figure 1. Effects on sustainability through the research results achieved

The proposed methodology constitutes a scientific novelty for the country Cuba, since the process uses Cuban industrial wastes and minerals as raw material [3]. This is also a contribution to sustainability, Figure 1. Sustainability is an essential trend of the present [4]. This leads to the use of waste and reduction of transportation expenses. This technology may be interesting for other countries with similar conditions.

MATERIALS AND METHODS

Figure 2 shows the scientific approach and methods of the work, applied in the research.

RAW MATERIALS

The raw materials used in aluminothermic processing are as follows:

≡ Mill scale, from the company A.
≡ Aluminium shavings, from company B.
≡ Limestone (stone dust), from company C deposit.

Table 1 shows the chemical composition of the raw materials to be reacted.

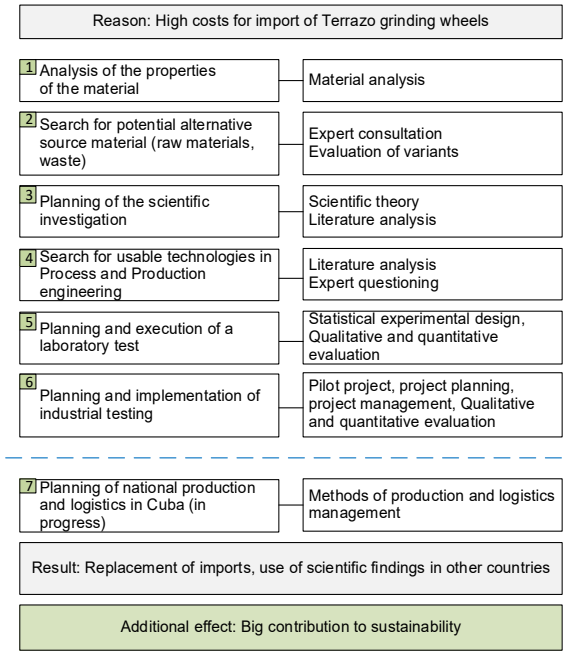

Figure 2. Scientific approach and methods of the research work

Table 1. Chemical composition of the raw materials to be used

Aluminium shavings								
Si	Fe	Mn	Cu	Mg	Zn	Cr	Ti	Al
0,5	0,2	0,1	0,1	0,2	0,2	0,1	0,1	report
Mill scale								
Fe_2O_3	Fe_3O_4	FeO	Fe	Fe	O_2	Impurities		
20–30	40–60	15–20	2–5	70,3	24,1	5		
Limestone								
CaO	MgO	SiO_2	Al_2O_3	Fe_2O_3	Ignition Lose			
55,20	0,68	0,34	0,23	0,17	44,38			

Mill scale is a solid residue generated during hot rolling processes in the steel industry. The iron oxide (mill scale) has a very variable grain size, therefore, it was crushed and sieved until all the residue had a grain size of less than 2 mm.

Aluminothermia requires the use of aluminium with low granulometry, so the shavings used were sieved below 3 mm.

Limestone ($CaCO_3$) is marketed in different grain sizes, according to the requirements for its use, using in this case the fraction called stone dust, which has a grain size of less than 1 mm.

FORMULATION OF THE LOADS AND OBTAINING THE ABRASIVES

— EXPERIMENTAL STUDY

The research strategy consisted of formulating five charges, from 0 to 4, according to the amount of heat generated per unit mass of each charge, so that the amount of heat released by the reactions would be sufficient to ensure the self–sustainability of the process and the adequate separation of the metal from the ceramic. The data are shown in Table 2.

Table 2. Conformation of aluminothermic charges (in g)

	Mill scale	Shavings	Limestone
0	150	52	0
1	150	52	15
2	150	52	30
3	150	52	45
4	150	52	60

Once the melting process is finished, the mixture is left to cool in the reactor for its later extraction in a tray, leaving the metal in the lower part and the ceramic in the upper part, which are separated manually.

Finally, load 1 was selected and reproduced 20 times to obtain a greater quantity of ceramics, which will be evaluated in the manufacture of abrasive materials. Table 3 shows the charge conformation for the large casting.

Table 3. Conformation of the aluminothermic caster large (in g)

Mill scale	Shavings	Limestone
3000	1040	300

The different components of the load, once weighed on a balance technical, are introduced into a drum mixer in increasing order according to their density: aluminium shavings, limestone and mill scale. The components are mixed for 30 minutes. Subsequently, each mixture was preheated in an oven between 250 and 300 °C for one hour, then it was placed, hot, in the graphite reactor, starting the reaction by the action of the electric arc. The process of obtaining the termites is shown in Figure 3.

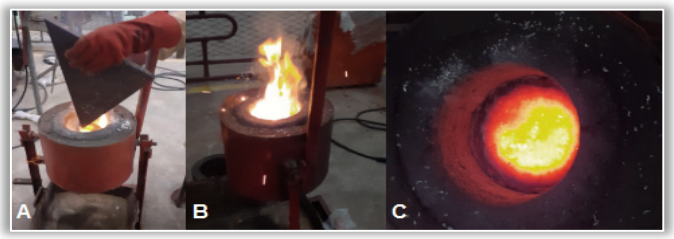

Figure 3. Obtaining of the Termites: A) Reactor feed and ignition of the reaction, B) Self–sustainability of the reaction, C) Cooling of the termite

— STUDY AT THE EXPERIMENTAL PILOT PLANT

In the laboratory study, the best performing mixture was selected, which reproduced at a higher volume and behaved favorably. For the study in the experimental pilot plant, two large–volume mixtures (Table 4) were developed with the objective of obtaining the largest possible amount of ceramic to evaluate them under real working conditions in the factory. The process of obtaining the termites is shown in Figure 4.

Table 4. Forming of two casts in the Pilot Plant (in kg)

Casts	Mill scale	Shavings	Limestone
1	76	26,4	7,6
2	136	46,2	13,3

The reactions developed satisfactorily, the ignition of the process was adequate, guaranteeing that the mixture to react completely in a self–sustaining manner, allowing an adequate metal–ceramic separation.

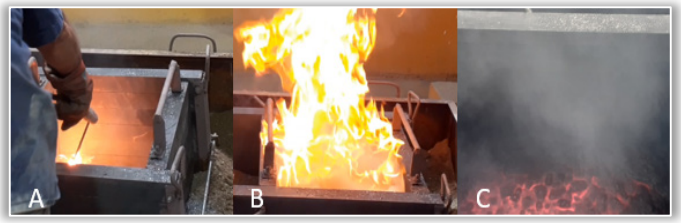

Figure 4. Obtaining oh the termites at the experimental pilot plant level: A) Ignition of the reaction, B) Self–sustainability of the reaction, C) Cooling of the termite

RESULTS AND DISCUSSION

MASS BALANCE

From the charge conformation data shown in Table 2 and 3, the chemical composition of each of the raw materials (Table 1) and the fundamental chemical reaction to occur between Fe_2O_3 and aluminium (Equation 1), a mass balance is performed to estimate the potential outputs of each of the charges, assuming that all the iron present in the scale is in the form of Fe_2O_3.

$$Fe_2O_3(s) + Al(s) \longrightarrow Fe(s) + Al_2O_3(s) \quad (1)$$

The balance is carried out on the basis of the principle of Conservation of Mass, the general expression of which is shown in Equation 2, [1].

$$\text{Accumulation} = \text{Input} - \text{Output} + \text{Generation} - \text{Consumption} \quad (2)$$

From the results obtained in the mass balances, the theoretical quantity of metal, ceramics and gases to be obtained in each of the loads is determined.

CALCULATION OF HEATS OF REACTION

The determination of the heats of reaction allows the assessment of the feasibility of occurrence of the chemical reactions that develop during metallurgical processing [8], results that allow the prediction of the feasibility of self–sustaining the aluminothermic reaction. These results are shown in Tables 5 and 6.

Table 5. Amount of heat generated by the charges in the experimental study (cal/g)

	0	1	2	3	4
Reaction heat	–930,9	–867,2	–811,4	–762,5	–719,19

Table 6. Amount of heat generated by the loads in the study of the experimental pilot plant (cal/g)

	1	2
Reaction heat	–852,9	–859,0

These values for all loads are above 700 cal/g of pyrometallurgical mixture, which guarantees the self–sustainability of the aluminothermic process without the supply of additional external energy, which guarantees the adequate separation between metal and slag [8].

METALLURGICAL TREATMENT RESULTS IN THE EXPERIMENTAL STUDY

— SMALL LOADS

In general, the small casts behaved satisfactorily, the ignition process went smoothly, good ignition of the reaction developed in a self–sustained way until the end of the process. Metal and ceramics are adequately separated, Figure 5.

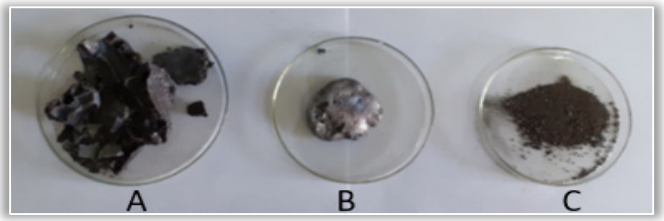

Figure 5. a) slag, b) metal, c) unreacted mixture

The quantitative results of the processing of all small loads in terms of: amount of metal, slag and unreacted mass of mixture are shown in Table 7, also the yield values, which are determined from the ratio between the actual amount obtained and the theoretical amount determined from the mass balance, are also shown.

Table 7. Masses of molten metal, slag and unreacted mixture of small termites

	Metal		Ceramic		Unreacted
	Mass (g)	(%)	Mass (g)	(%)	Mass (g)
0	93	87,5	97	101,4	5
1	91	85,6	108	103,7	6
2	85	79,9	116	103,1	16
3	80	75,2	128	105,7	18
4	58	54,6	131	101,1	47

To evaluate the process on a larger scale, charge 1 is selected because of its good pyrometallurgical behavior, good yield and lower amount of limestone incorporated into the mixture.

— PROCESSING OF THE LARGE CHARGE

The ignition process went smoothly, with a good reaction rate, resulting in metal with a uniform and smooth appearance (Figure 6).

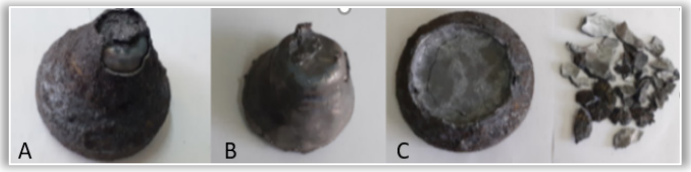

Figure 6. A) Products obtained, B) Metal, C) Slag

The results of the processing of the large charge in terms of metal and slag quantity are shown in Table 8.

Table 8. Results of the processing of large thermite

Product	Theoretical mass (g)	Actual mass (g)	(%)
Metal	2124,9	1995	93,9
Cerámic	2082,8	2120	101,8

Table 8 shows that the aluminothermic processing of the large charge yielded more than 2 kg of ceramic and more than 1,9 kg of metal, which represents 102 and 94 % yield respectively.

Comparing these results with those of casting 1, we find the following:

- with increasing amount of the mixture to be processed, the metallic yield increases significantly and the ceramic yield decreases slightly,
- while at the same time the amount of unreacted mixture decreases significantly.

This leads to an improvement in the results of pyrometallurgical processing.These results make it possible to evaluate the possibility of scaling up the process.

EVALUATION OF ABRASIVES

— VALUATION OF THE SCRATCH TEST

The objective of the test is to evaluate and compare the quality of the ceramics obtained in terms of their hardness. The test consists of scoring a crystal by the action of the abrasive with a constant load of 2 kg, following the principles of tribology [5], see Figure 7.

Figure 7. Abrasive action on glass

As shown in Figure 7, all ceramics have a higher hardness than glass, with the hardness of glass on the Mohs scale being 5.5 [7], which validates their use for the manufacture of abrasive powders.

— PRODUCTION OF GRINDING WHEEL SPECIMENS

When casting 1 was selected as the one with the best results, it was necessary to evaluate the behavior of the different granulometric fractions during setting, as these ceramics will be used for the development of grinding wheels, using P–350 cement as a binder.

The aim of this test is to evaluate the possible reactivity of the abrasive grains (ceramics obtained) with Portland P–350 cement.

Therefore, all of the ceramics obtained in the load large were manually crushed and granulometrically classified. The product obtained was then sorted into 5 fractions so that they could be grouped according to the particle size requirements of the grinding wheels.

Table 9 shows the results of the granulometric classification of the crushed ceramics and the average grain number, according to the granulometry obtained.

Table 9. Results of the granulometric classification process of the crushed ceramics

	Grain size fraction	Number of grain	Mass (en g)	%	Accumulated in %
1	–0,315 +0,21	60	540	30,3	30,3
2	–0,21 +0,16	80	188	10,5	40,9
3	–0,16 +0,08	100	715	40,1	81,0
4	–0,088 +0,05	180	230	12,9	93,9
5	–0,053	240	109	6,1	100

Table 9 shows that it is possible to obtain abrasives with different grain sizes.

This makes it possible to produce abrasive discs required for carrying out grinding and polishing work on floors and terrazzo. When the test specimens shown in Figure 8 were made, it was confirmed that they behaved satisfactorily, and the problems presented in previous studies [10] were not observed.

Figure 8. Test tubes manufactured with the 5 particle size fractions obtained

RESULTS OF METALLURGICAL TREATMENT IN THE STUDY OF THE EXPERIMENTAL PLANT PILOT

The results of the evaluation carried out at the experimental pilot plant level are presented in Table 10, Figure 9 shows a picture of the products obtained.

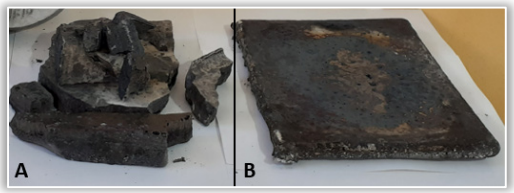

Figure 9. Products obtained at experimental pilot plant level. A) Slag, B) Metal

Table 10. Results of the Pilot Plant scale evaluation

Casts	Metal		Ceramics	
	Mass (kg)	(%)	Mass (kg)	(%)
1	55	104,7	44	87,4
2	94	101,2	80	89,0

Experimental pilot plant scale tests scaling were satisfactory, with a tendency for the metallic yield to increase and the ceramic yield to decrease as the amount of charge processed increases.

Two samples obtained from the crushing and grinding process of the abrasive powders obtained at the Pilot Plant were subjected to a sieving process for ten minutes, obtaining the results shown in Table 11.

Table 11. Results of the sieving of the abrasive obtained in the ball mill and retained between the two large sieves at the company C

Coarse grain (mm)	Retained mass (g)	Retained (%)	Accumulated (g)	Grind	%	%
–1	62	9,2	62	18		
+1 –0,84	109	16,2	171	20		90,4
+0,84 –0,5	348	51,6	519	25; 30; 35	74,2	
+0,5 –0,315	152	22,6	671	40; 45; 50		
+0,315 –0,2	3	0,5	674	60; 70		
Total	674	100				

As can be seen in Table 11, 9 % of the abrasive powder is concentrated between 0.1 and 0,315 mm, of which 74 % is between 0,315 and 0,84 mm, a range that corresponds to a particle size range, with which different grinding wheels can be produced, mainly for roughing, the rest can be used for polishing and finishing operations.

The study of the grinding and sieving process of the abrasives obtained in the plant allows us to affirm that with the appropriate use of the existing equipment in the plant, it is feasible to obtain all the particle size fractions required to cover the demand for grinding wheels used in the roughing and polishing operations of floors and terrazzo. The selected particle size fractions were used for the manufacture of grinding wheels Figure 10, which were

evaluated under real working conditions and their performance was verified.

Figure 10. Abrasive wheels made from the abrasive powders obtained

Once the grinding wheels have been made from the abrasive obtained, the wheel must be left to set for approximately 20 days. Finally, the wheels are used for grinding and polishing operations.

The same were evaluated in real working conditions giving a performance very close to the imported abrasive, even superior in some specific granulometric fractions, in the Figure 11 you can see a series of finished terrazos.

Figure 11. Polished terrazzo tiles available for use

PRODUCTION STRATEGY IN EXPERIMENTAL PLANT

On the basis of the previous studies, an economic evaluation is carried out to determine the techno economic feasibility of the possible setting up of a pilot plant for the manufacture of abrasive powders. The evaluation allows us to determine that it is feasible from an economic point of view to carry out these productions, as all the indicators are favorable.

In order to materialize the research, a technology transfer contract is signed between the companies D and company C for the installation of the Pilot Plant. It is proposed to install a plant with a production capacity of 22,3 t/year of abrasive powders and 14 t/year of metal, for a total of 36,3 t/year of products, obtaining these production levels from the realization of 20 castings per month.

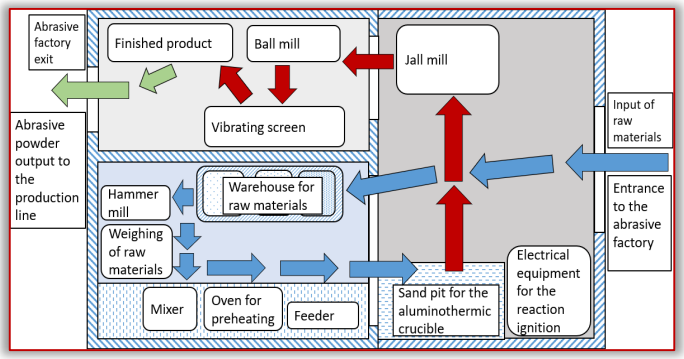

Figure 12. Layout and material flow (intralogistics) used for the manufacture of abrasive powders

Figure 12 shows the layout of the equipment to be used within the plant, which is built in an old building that was refurbished to meet the proposed requirements.

Figure 13 shows the processing scheme of the abrasives plant, which must be complied with for the proper functioning of the process and the production of good quality ceramics.

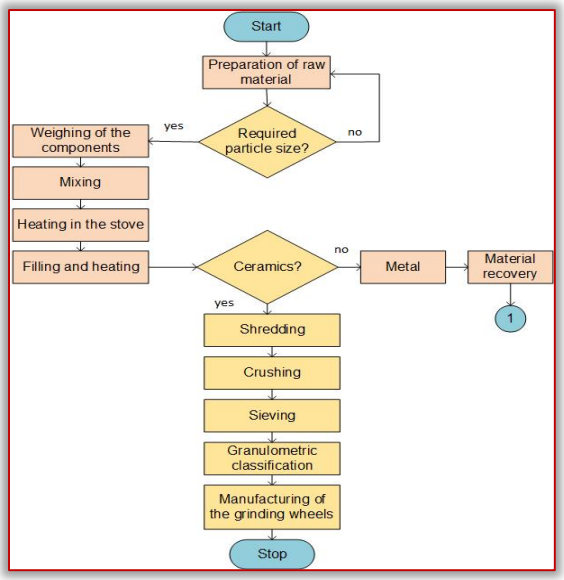

Figure 13. Flow diagram of the process of obtaining abrasive materials at the plant

CONSIDERATIONS ON EXPERIMENTAL PILOT PLANT

— ECONOMIC AND MARKET ASPECTS

Company C manufactures grinding wheels by hand with imported abrasive grains and Portland cement p–350. The new technology that makes it possible to manufacture these products in Cuba with 100% domestic components, guarantees full sovereignty for this production in the future and helps to introduce these products in the national market and also in the Latin American region.

— ASSIMILATION AND DEVELOPMENT CAPACITY

The processing technology does not have a high degree of complexity and can be assimilated by the company's technical staff from the advice offered by the CIS, so that workers and technical staff can be trained in a relatively short time.

— ENERGY

The proposed technology, unlike traditional methods, is based on the energy released by a chemical reaction between a metal oxide and aluminium, which is highly exothermic.

— RAW MATERIALS AND NATURAL RESOURCES

All the raw materials involved in the abrasive powder production process are industrial residues [3] (> 90 %) and Cuban minerals (< 10 %).

— LOCATION OF THE PILOT PLANT

Company C decided to build the experimental pilot plant within a facility of the same, since the powders obtained would be used there minimizing transportation costs, the construction was in the municipality of Cifuentes, Figure

14, since it is located a distance of 32 km from the Central highway, which allows a distribution throughout the whole country.

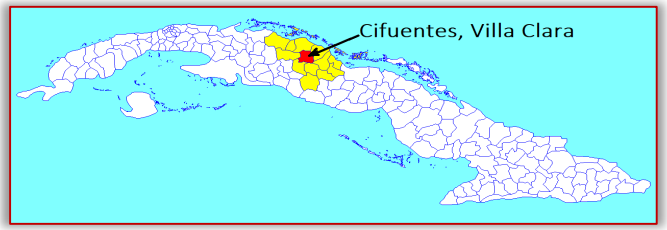

Figure 14. Location of the pilot plant in the municipality of Cifuentes Villa Clara in Cuba

— MANPOWER

As this is a small pilot plant for the manufacture of abrasive powders, in addition to the interlinking of the processes within the plant, only three workers will be employed to carry out all the tasks.

CONCLUSIONS

— The characteristics and chemical composition of the selected raw materials, as well as the proportions in which they were mixed, allow the generation of heat quantities between 719,19 – 930,6 cal/g, which guarantee the self–sustainability of the process and the adequate separation of the metal and the slag, ensuring the proper development of the aluminothermic processing.

— The charges made up of mill scale, aluminium chips and limestone allowed obtaining metal yield values between 54,6 – 87,5 % and slag yield values between 101,1 – 105,7 %, with an adequate technological behavior during pyrometallurgical processing for all the mixtures, where the reproduction of charge 1 (larger volume) allowed considerably reducing the amount of unreacted mixture, obtaining a metal yield of 94 % and slag yield of 102 %, considerably improving the results of the process.

— The abrasiveness tests carried out with the abrasive grains obtained showed that they all have a hardness higher than glass, making it possible to use them to manufacture the grinding wheels used for polishing flats and terrazzo. On the other hand, no deformations were observed in any of the samples evaluated during the setting of the mixtures of abrasive powders with P–350 cement.

— The Experimental Pilot Plant installed in Cifuentes, allows the production of abrasive powders required by Company C, to satisfy its demand for abrasive wheels for polishing floors and terrazzo.

— The technological proposal constitutes an impact on sustainability since it allows savings in the import costs of abrasive materials, also allows to take advantage of industrial and mineral waste to obtain an abrasive material, not generating more polluting waste.

References

[1] Castellanos, J. et al., (2001). Mass and energy balance, classical methods and non–conventional techniques. Edited by María del Carmen Rodríguez Fernández. Publishing house Feijóo, Cuba.

[2] CEPAL, (2019). Trade Facilitation, Trade and Logistics in Latin America and the Caribbean, Logistics for Production, Distribution and Trade. BULLETIN 369, issue 1. ISSN: 1564–4227.

[3] Ecología Verde, (2020). Industrial waste: what it is, examples, types, classification and management. Available at: https://www.ecologiaverde.com/residuos–industriales–que–son–ejemplos–tipos–clasificacion–y–manejo–2714.html

[4] Glistau, E. Coello–Machado, N.I.; Trojahn, S. (2022) Logistics 4.0: goals, trends and solutions. Advanced Logistic Systems – Theory and Practice, Vol. 16, No. 1 (2022), pp. 5–18.

[5] Grote, K; Hefazi, H. (2021): Springer Handbook of Mechanical Engineering. p.1310.

[6] Illes, B; Glistau, E; Coello–Machado, N.I. (2012): Logística y Gestión de la Calidad. Miskolc: p.193.

[7] Ramón, H. M.; Asensio, S. I. (2018): The mohs scale, hardness of minerals. Department: Plant Production, Polytechnic University of Valencia. p.7.

[8] Riss, A.; Khodorovsky, Y. (1975). Production of ferroalloys. Moscow, ed. Foreign languages publishing house. P.278.

[9] Rosver (2023). What are abrasives and what are they used for? Available in: https://www.rosver.com/en/what–are–the–abrasives–and–what–are–they–for/

[10] Saavedra, R. F. (2019). Development of abrasive materials by pyrometallurgical methods. Thesis presented in option to the degree of Mechanical Engineer. Faculty of Mechanical and Industrial Engineering, Center for Welding Studies, Universidad Central "Marta Abreu" de Las Villas. Cuba.

ISSN: 2067-3809

[1.]C.O. OLISE, [1.]Samuel SULE, [1.]Chioma T.G. AWODIJI

RELIABILITY ASSESSMENT OF SUBGRADE SOIL ALONG THE DAWANAU–KAZAURE RAILWAY LINE

[1.] Department of Civil Engineering, University of Port Harcourt, Rivers State, NIGERIA

Abstract: This study investigates the reliability of subgrade soil materials along the Dawanau–Kazaure railway line by analyzing compaction characteristics, including California bearing ratio (CBR), Maximum dry density (MDD), and Optimum moisture content (OMC) derived from field and laboratory data. Statistical information for basic random variables was generated using Minitab 15 software, and limit–state equations were formulated for each compaction characteristic. These limit–state equations are based on regression equations developed from field and laboratory data. The safety of the subgrade material was assessed across a range of coefficient of variation values (from 10% to 100%). The findings revealed that as the coefficient of variation increased, reliability indices generally decreased. For all cases considered, the reliability indices obtained for bearing capacity failure were positive, indicating the subgrade material's overall safety, but did not meet the minimum recommended value of 1.0 set by the Nordic Committee on Building Regulations. Therefore, the subgrade soil requires improvements in its index properties. Specifically, the expected values of the California Bearing Ratio for soaked and unsoaked soil samples were 32.5% and 78%, respectively, with corresponding reliability indices of 0.9275 for soaked CBR and 0.9250 for unsoaked CBR.

Keywords: Subgrade soil reliability, California bearing ratio, Coefficient of variation, Limit–state equations, Railway infrastructure

INTRODUCTION

The construction and maintenance of railway infrastructure are crucial engineering endeavors that demand meticulous attention to detail, especially when it comes to the subgrade – the foundation upon which the tracks are built. The performance and longevity of railway tracks are significantly influenced by the properties of the subgrade soil. Hence, accurate and reliable characterization of subgrade soil properties is essential for ensuring the safety, durability, and cost–effectiveness of railway systems (Kozubal et al., 2022).

Traditionally, subgrade soil properties have been assessed using deterministic methods that rely on point estimates of soil parameters (Ayres, 1997). However, this approach often fails to account for the inherent variability and uncertainties that exist in natural soils. The limitations of the deterministic approach have led to instances of suboptimal designs and unforeseen failures in railway infrastructure.

To address these challenges and enhance the understanding of subgrade soil behavior, engineers and researchers have turned to a more advanced and sophisticated approach known as "Reliability–Based Evaluation" or "Probabilistic Geotechnics." This methodology seeks to quantify the uncertainties associated with subgrade soil properties by incorporating probabilistic methods and data from trial pit investigations. Trial pits represent one of the primary means of gaining direct access to the subsurface layers and are extensively employed in geotechnical investigations for railway projects. These excavations provide a visual representation of the soil profile and enable the collection of in–situ soil samples for subsequent laboratory testing (Gu and Liu, 2021; Zhao et al., 2020). The data obtained from trial pit investigations form the backbone of the reliability–based evaluation process, offering valuable insights into the spatial variability of soil properties.

Numerous studies have explored traditional methods for soil characterization and geotechnical investigation, but a systematic framework for integrating reliability analysis into the evaluation of subgrade soil properties remains lacking (Li and Selig, 1998). Due to the ever–increasing demands on railway infrastructure systems and the need to minimize the risks associated with soil variability, this research gap has been identified (Saha, 2009). This paper aims to explore the concept of reliability–based evaluation of subgrade soil properties using trial pits in the context of railway design and construction.

By considering the inherent uncertainties in soil characteristics, this approach seeks to provide engineers with a more comprehensive understanding of subgrade behavior, enabling the design of safer, more resilient, and economically optimized railway systems (Li et al., 2021; Wu et al., 2022; Phoon and Kulhawy, 2003; Vessia et al., 2020).

This study presents the results of reliability assessments of subgrade soil for a proposed railway line section, spanning from Dawanau to Kazaure in Kano State, Nigeria. The safety level of the subgrade soil was examined using the First–Order Reliability Method. Both field and laboratory

data were leveraged to establish the safety level, ensuring that railway subgrade design is both economically viable and reliable for the intended purpose.

MATERIALS AND METHODS

Location and Accessibility:

The study area is located in Dawanau (about 65 km away from the Kano metropolis) and extends towards Kazaure, Jigawa State. It lies between Easting 438906.732 to 435034.140, and Northing 1338525.942 to 1396008.238, with corresponding chainage between 20+500 and 43+500 and covers about 23.50 km stretch (Figure 1). It is accessible through major roads, namely: Kano–Danbatta–Kazaure–Daura Road, Kazaure–Roni–Ingawa and Kazaure–Shuwaki–Lamba road. There are also numerous networks of footpath throughout the area.

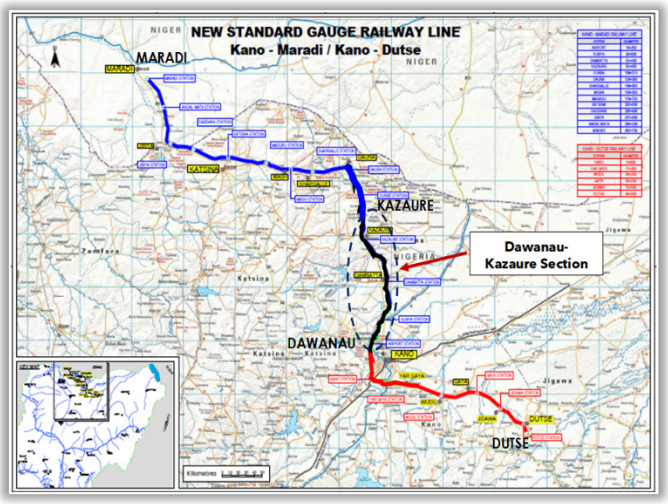

Figure 1. Map Showing Location of the Study Area

The area is typical of Sudan Savanna tropical climatic zone of Nigeria, which is characterized by two distinctive seasons (dry and wet seasons). The dry season begins from October to April and is associated with low humidity, especially during the harmattan period. The wet or rain season commences from May to October, with mean annual rainfall of about 700 – 750 mm per anum. The annual range of temperature is between 27 to 34°C (Kankara 2014). The vegetation pattern is predominantly thorny shrubs with grasses of less than 2m high. The few tall trees are thorn Acacia, Neem and Baobab which are scattered, and normally shed their leaves completely during the dry seasons. They have an average height of 10 to 15 m. It is denser along river courses due to the presence of moisture which allows the vegetation to flourish.

The study area is a part of the basement complex of Northern Nigeria, which has three main lithologic profiles, including older granite complexes from the late Precambrian to lower Paleozoic eras, also known as pan–African granite, and undifferentiated migmatite complex of Proterozoic to Archean origin. The pan–African thermometric event has altered and damaged all of these rocks. Typically, the rock weathers into reddish micaceous sandstone to clay materials. Underlying the research region are rocks and more recent sediments from the Quaternary–aged Chad formation. Surface layers of fine sand that have been pushed into a number of low dunes cover a large portion of the land. The Chad sediments are concealed by sand dunes and the sandy beds are formed over the impervious clays of the Chad Formation and the main source of water in the dry season. These soils are comparatively recent in origin. They are generally sandy at the top, compact at depth with often hard pans. Aeolian deposits from the Sahara Desert form substantial part of the soils. The mixing of the subsoils in these deposits has given rise to clayey subsoil, which dominates the area.

Trial Pit Excavation and Soil Sampling:

Trial pit, also known as Test pit, is a type of intrusive geotechnical site investigation used to determine the ground conditions and soil profile throughout a site. They are cost effective and allow for a rapid inspection of ground conditions in situ, both horizontally and vertically as the pit advances and side walls exposed. Bulk disturbed samples are taken for detailed laboratory examination and testing.

Along the 23.5 km Dawanau–Kazaure Railway Line section investigated (between chainages 20+500 and 43+500), a total of Forty–Seven (47) Trial Pits were excavated at approximately 500–meter intervals. The Trial Pits were excavated to the dimensions: 1.2m x 1.2m x 3m (Figure 2). Bulk disturbed soil samples were collected for proper identification of the various strata formation of the subgrade subsoil and detailed laboratory analyses. The subsurface lithologic profile encountered across the forty–seven data points along the railway section investigated are mostly greyish to reddish brown concretionary laterite and brownish clayey silty sand. Most of the soil types for this section are classified as either A–4, A–2–4 or A–6 based on American Association of State Highway and Transportation Officials (AASHTO) soil classification system.

Figure 2. A typical excavated trial pit for soil sampling and in situ field observation.

Laboratory Testing:

A comprehensive suite of geotechnical laboratory tests on the soil samples obtained from the trial pits. These tests included grain size analysis, Atterberg limits, moisture content, modified proctor compaction test, specific gravity and California bearing ratio test (soaked and unsoaked) to determine the soil properties (Table 1).

Data Analysis and Pre–processing:

The trial pit data and laboratory test results were organized and compiled in a suitable format. Conduct a statistical analysis of the data to identify the mean, standard deviation, and other statistical parameters for each soil property (Table 1).

Uncertainty Quantification:

Determine the uncertainties associated with soil properties obtained from the trial pits and laboratory tests. This involves quantifying the spatial variability of soil properties, measurement errors, and other sources of uncertainty.

Probabilistic Modeling:

Probabilistic modeling in reliability–based evaluation involves choosing an appropriate probability distribution (e.g., normal, log–normal, or uniform) based on the characteristics of the soil property data and then calibrating the distribution's parameters to fit the observed data. This process allows engineers to incorporate uncertainty into their analyses and make more informed decisions in railway design by accounting for the probabilistic nature of subgrade soil properties.

Reliability Analysis:

A reliability analysis model was developed to integrate the probability distributions of soil properties with the loading conditions and design parameters, utilizing the First–Order Reliability Method (FORM) to compute the probability of failure or the reliability index. Let the limit state function in the space of input variables be given by:

$$g(X_1, X_2, \ldots\ldots, X_n) = 0 \quad (1)$$

Also,

Let the input variables be random variables collected in the vector $X = [X_1, X_2, \ldots\ldots, X_n]^T$ with second moment statistics $E(X)$ and $Cov(X, X^T)$. The normalized random variables $Y_1, Y_2, \ldots., Y_n$ are introduced by a suitable one to one linear mapping. $X = L(Y)$ such that $Y = L^{-1}(X)$.

The corresponding space of y is then defined by the transformation:

$$X = L(Y),\ Y = L^{-1}(X) \quad (2)$$

Applying Equation (1) maps Equation (2) into:

$$h(y_1, y_2, \ldots., y_n) = 0 \quad (3)$$

Where the function h is defined by:

$$h(y) = g[L(y)] \quad (4)$$

Equation (2) represents the limit state equation in normalized coordinate. The mean value of y is the origin and the projection of y on the arbitrary straight line through the origin is the random variable with the standard deviation of unity. The geometric reliability index β is then defined as the distance in the normalized coordinate from the origin to the failure surface.

That is:

$$\beta = \min\left\langle \sqrt{\sum y_1^{\,2} + y_2^{\,2} + \ldots.. + y_n^{\,2}} \,\middle|\, h(y_1, y_2, \ldots, y_n) \right\rangle = 0 \quad (5)$$

In matrix notation, Equation (5) can be re–written as:

$$\beta = \min\left\langle \sqrt{y^t y} \,\middle|\, h(y) \right\rangle = 0 \quad (6)$$

where β = reliability index.

The values of the design variables that minimize the reliability index β subject to $h(y_1, y_2, \ldots, y_n) = 0$ are obtained by optimization. Tables 1 and 2 show the results of the laboratory analyses and statistics of the basic random variables respectively.

Sensitivity Analysis:

A sensitivity analysis was carried out by varying the values of coefficient of variation (COV) of the design parameters and output variables between 10% and 100% to identify the most influential soil parameters and loading conditions that affect the reliability of the subgrade soil materials.

RESULTS AND DISCUSSION

The results obtained from the laboratory analysis of soil samples obtained from the different trial pit locations are presented in Table 1. Statistical information for basic random variables obtained are summarized in Table 2.

Table 1: Results of laboratory analysis of trial pit soil samples

Trial Pit No.	EMC (%)	LL (%)	PL (%)	PI (%)	MDD (g/cm3)	OMC (%)	Specific gravity	CBR (%) Unsoaked	CBR (%) Soaked
1.	4	25	16	9	1.92	10.20	2.62	56	11
2.	8	30	20	10	1.88	17.10	2.73	87	36
3.	6	31	21	10	1.86	16.30	2.70	80	32
4.	4	27	18	9	1.90	10.50	2.63	48	12
5.	6	26	19	7	2.12	9.20	2.71	76	29
6.	5	36	18	18	1.89	10.20	2.62	53	16
7.	4	30	21	9	1.93	12.70	2.69	82	29
8.	6	28	16	12	1.98	11.10	2.64	56	17
9.	5	26	17	9	1.96	10.80	2.60	46	13
10.	6	28	18	10	1.92	12.30	2.65	61	22
11.	14	34	16	18	1.78	16.70	2.70	58	23
12.	10	27	19	8	1.93	9.90	2.68	78	25
13.	7	22	17	9	1.96	10.03	2.60	41	8
14.	7	28	18	10	1.91	10.4	2.61	53	13
15.	4	32	20	12	1.89	12.8	2.69	70	25
16.	15	33	17	16	1.95	14.8	2.72	72	27
17.	6	30	20	10	1.96	9.9	2.63	47	10
18.	12	32	21	11	2.04	9.30	2.68	79	27
19.	10	35	23	12	1.83	14.9	2.73	62	23
20.	7	27	17	10	1.99	10.3	2.66	75	26

Table 1: Results of laboratory analysis of trial pit soil samples (continuing)

Trial Pit No.	EMC (%)	LL (%)	PL (%)	PI (%)	MDD (g/cm3)	OMC (%)	Specific gravity	CBR (%) Unsoaked	CBR (%) Soaked
21.	5	31	19	12	1.97	11.1	2.65	86	25
22.	11	32	20	12	1.94	12.3	2.69	80	33
23.	6	30	21	9	2.02	7.6	2.67	51	14
24.	5	29	20	9	1.98	9.2	2.60	49	10
25.	7	28	18	10	1.90	10.5	2.62	52	10
26.	4	32	22	10	1.93	11.6	2.61	45	8
27.	7	28	20	8	1.91	10.40	2.60	42	11
28.	10	29	21	8	1.92	10.80	2.63	53	13
29.	5	27	18	9	1.89	10.60	2.61	45	12
30.	5	26	18	8	1.95	10.40	2.62	37	12
31.	7	30	20	10	1.86	10.80	2.62	42	10
32.	6	31	21	10	1.90	9.90	2.63	39	8
33.	6	30	19	11	1.84	10.10	2.60	43	11
34.	5	30	21	9	1.88	10.70	2.63	48	11
35.	4	28	20	8	1.90	9.90	2.60	45	10
36.	5	32	22	10	1.92	10.30	2.62	47	9
37.	4	29	21	8	2.10	7.20	2.72	85	31
38.	8	28	19	9	1.89	11.10	2.61	50	11
39.	6	30	21	9	1.94	9.80	2.63	46	10
40.	6	31	22	9	1.84	11.1	2.61	47	11
41.	5	28	20	8	1.71	13.1	2.63	42	12
42.	7	29	19	10	1.88	10.1	2.65	49	13
43.	5	34	22	12	1.86	9.4	2.62	43	12
44.	6	30	20	10	1.90	10.3	2.60	38	10
45.	6	32	22	10	1.87	9.7	2.62	41	10
46.	7	28	20	8	1.89	10.0	2.62	37	11
47.	10	30	19	11	1.92	9.9	2.60	40.0	13

Table 2: Statistics of the basic random variables

S/N	Variable	Unit	Type of Probability Distribution	Mean	Standard Deviation	Coefficient of Variation
1	EMC	%	Lognormal	6.681	2.563	0.384
2	LL	%	Lognormal	29.809	2.890	0.084
3	PL	%	Lognormal	19.702	1.793	0.091
4	PI	%	Lognormal	10.106	2.305	0.228
5	MDD	g/cm^3	Lognormal	1.917	0.07042	0.037
6	OMC	%	Lognormal	11.01	2.07	0.188
7	Gs	–	Normal	2.643	0.0403	0.0152
8	CBR (Unsoaked)	%	Lognormal	55.362	15.4	0.278
9	CBR (Soaked)	%	Lognormal	16.57	8.216	0.494

The results of the sensitivity analysis carried out over a range of coefficient of variation between 10% – 100% are displayed in Plots 1 to 8 respectively.

The results of the reliability–based design of subgrade soil analyzed at predefined reliability indices are presented in Table 3.

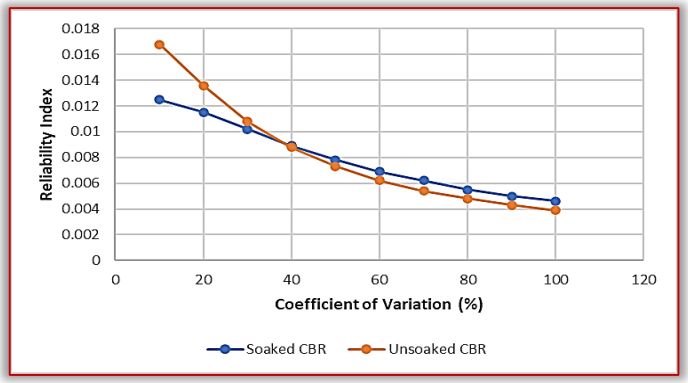

Figure 3. Relationship between Reliability Indices and Coefficient of Variation for Soaked and Unsoaked CBR.

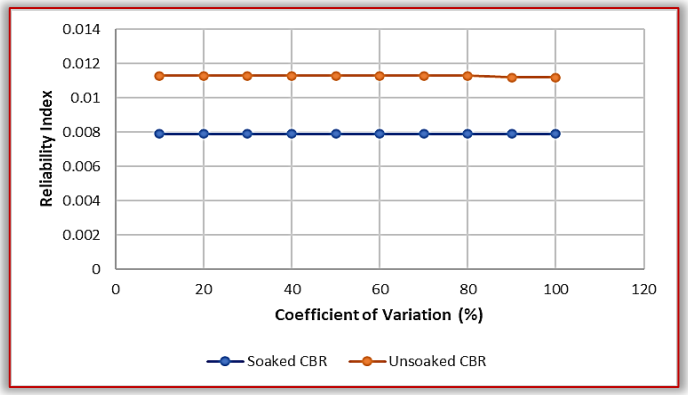

Figure 4. Relationship between Reliability Indices and Coefficient of Variation for Moisture Content.

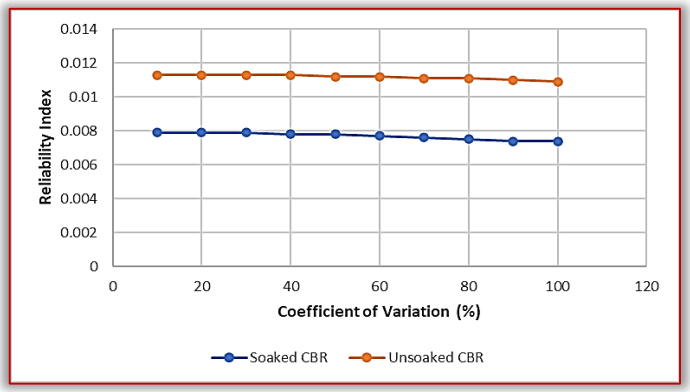

Figure 5. Relationship between Reliability Indices and Coefficient of Variation for Liquid Limit.

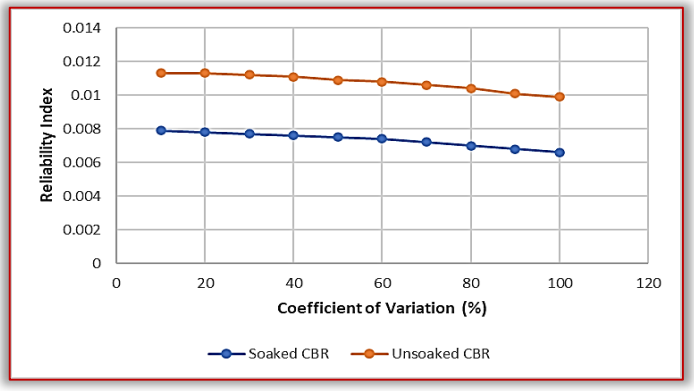

Figure 6. Relationship between Reliability Indices and Coefficient of Variation for Plastic Limit.

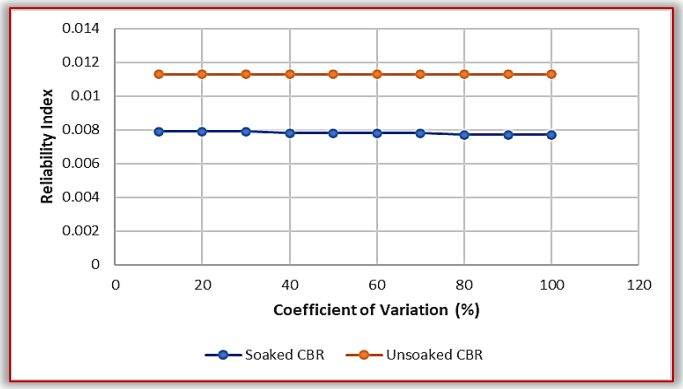

Figure 7. Relationship between Reliability Indices and Coefficient of Variation for Plasticity Index

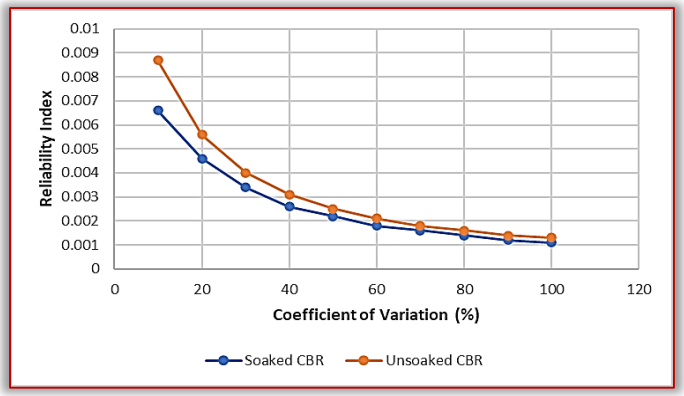

Figure 8. Relationship between Reliability Indices and Coefficient of Variation for Maximum Dry Density

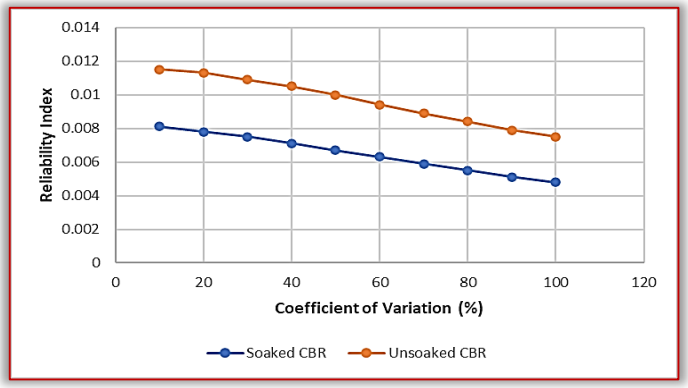

Figure 9. Relationship between Reliability Indices and Coefficient of Variation for Optimum Moisture Content

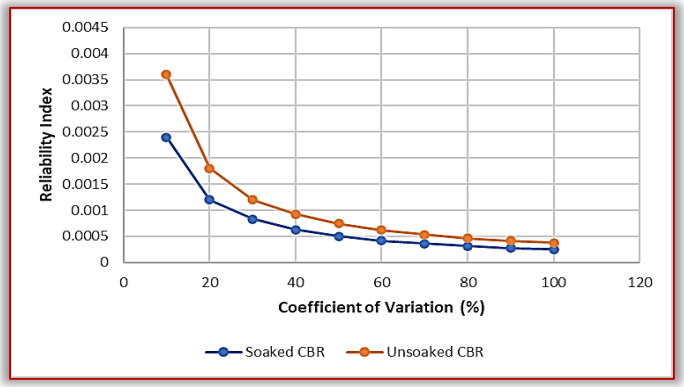

Figure 10. Relationship between Reliability Indices and Coefficient of Variation for Specific Gravity

Table 3: Reliability–Based Design of Subgrade Soil at Pre–defined Reliability Indices

Variables	Soaked CBR (32.5 %) β = 0.9275	Unsoaked CBR (78 %) β = 0.925	Initial Value
EMC	6.6701	6.5646	6.681
LL	24.7616	24.7523	24.53
PL	19.959	19.9691	19.89
PI	9.7065	9.7254	9.745
MDD	1.9267	1.933	1.917
OMC	11.2959	11.3387	11.01
Gs	2.6537	2.6565	2.643

The results of reliability estimate of the subgrade soil along Dawanau–Kazaure proposed railway section based on California Bearing Ratio (CBR) are presented in Figures 3 to 10. The results of the reliability–based design of subgrade soil at target reliability index of 1.0 is presented in Table 3.

Influence of California Bearing Ratio (CBR) on reliability index

Figure 3 displays the results of reliability indices for the California Bearing Ratio (CBR) under both soaked and unsoaked conditions at various coefficient of variation values. It is evident from Figure 3 that the reliability indices exhibit a decrease as the coefficient of variation increases, ranging from 10% to 100%, for both soaked and unsoaked subgrade soil samples. This trend is attributable to the rise in variability in the measured CBR values as the coefficient of variation for CBR (both soaked and unsoaked) increases, leading to a reduction in the reliability index values. The reliability indices range from 0.0046 to 0.0125 for soaked CBR and from 0.0039 to 0.0168 for unsoaked CBR.

These results consistently indicate positive values, signifying the safety of the subgrade soil. However, it is worth noting that the minimum reliability index value of 1.0, as recommended by the Nordic Committee on Building Regulations (NKB, 1978) is not attained within the considered range of coefficient of variation values. This suggests that modifications are required for the subgrade material to enhance its performance, as outlined in Table 3.

Effect of Natural Moisture Content on the Reliability Index

Figure 4 illustrates the influence of natural moisture content (NMC) on the reliability indices of the subgrade soil across a spectrum of coefficient of variation (COV) values, ranging from 10% to 100%.

A notable observation from Figure 4 is the constancy of reliability index values for both soaked and unsoaked soil samples, suggesting that water content has minimal to no discernible impact on the reliability index.

The subgrade soil, in its capacity as subgrade material, maintains consistent reliability index values throughout

this moisture content variation range. It is worth highlighting that all reliability index values within the considered range of COV values are positive.

However, it is essential to note that the minimum reliability index threshold of 1.0, as stipulated in the NKB Report (1978), is not attained. Consequently, the subgrade soils necessitate improvement to enhance their performance and meet the specified reliability standards.

Influence of Liquid Limit on the Reliability Index

The results of the reliability indices at varying values of the coefficient of variation ranging from 10% to 100% are presented in Figure 5. It can be seen from Figure 5 that for both soaked and unsoaked California Bearing Ratio (CBR), the reliability index value is constant for the range of values of the coefficient of variation considered.

The constant value is due to the fact that liquid limit has little or no effect on the reliability indices of the subgrade soils evaluated. However, the minimum value of the reliability index of 1.0 recommenced by the NKB Report (1978), is not met and the subgrade soils therefore need to be improved.

Effect of Plastic Limit on the Reliability index

Figure 6 demonstrates the influence of the Plastic Limit on the Reliability Index for both soaked and unsoaked California Bearing Ratio (CBR).

As depicted in Figure 6, it is evident that the reliability index values remain constant across a range of coefficient of variation values spanning from 10% to 100%, regardless of whether the CBR measurements were taken under soaked or unsoaked conditions. This constancy in reliability index values underscores the limited or negligible impact of the plastic limit on the reliability of the investigated subgrade soils.

Although all reliability index values are positive, indicative of the subgrade soils' general safety, they fall short of the recommended minimum threshold of 1.0. Consequently, the subgrade soils require improvement measures to meet the prescribed reliability standards.

Effect of Plasticity Index on the Reliability Index

The results of the reliability index for coefficient of variation ranging from 10% to 100% for both soaked and unsoaked California Bearing Ratio (CBR) are presented in Figure 7. From Figure 7, it can be observed that the reliability indices maintain constant values within the considered range of coefficient of variation, regardless of whether the CBR measurements were conducted under soaked or unsoaked conditions.

This consistency in reliability index values is attributed to the limited or negligible impact of plasticity index on the reliability indices. While all reliability index values are positive, denoting the overall safety of the subgrade soils, they fall short of the recommended minimum threshold of 1.0 for both soaked and unsoaked CBR, indicating the need for improvement measures to meet the specified reliability standards.

Effect of Maximum Dry Density on the Reliability Index

Figure 8 illustrates the outcomes of reliability indices across a range of coefficient of variation values from 10% to 100% for both soaked and unsoaked California Bearing Ratio (CBR).

As evident from Figure 8, the reliability indices exhibit a consistent decrease as the coefficient of variation increases. This trend is expected because higher coefficient of variation values introduces greater variability in the CBR measurements of soaked and unsoaked soil samples, leading to a reduction in reliability index values.

While all reliability index values are positive, signifying the overall safety of the subgrade materials, they fall short of meeting the recommended minimum threshold of 1.0, indicating that there is no assurance of satisfactory performance in service.

Therefore, improvement measures are necessary for the subgrade materials to meet the required standards.

Effect of Optimum Moisture Content on the Reliability Index

The results of the reliability indices for values of coefficient of variation ranging from 10% to 100% are presented in Figure 9. It can be seen from Figure 9, that the reliability indices decrease as the values of the coefficient of variation decreases for the both soaked and unsoaked soil samples. This is because the variability of the optimum moisture content of the soil is expected to increase and this results to decrease in the values of the reliability indices.

Also, the value of the reliability indices are all positive and this connotes the safety of the subgrade soil. However, the recommended minimum value of the reliability index of 1.0 is not achieved, showing that the subgrade soils require improvement.

Effect of Specific Gravity on the Reliability Index

The results of reliability indices for a range of coefficient of variation values from 10% to 100% are depicted in Figure 10. As observed in Figure 10, both for soaked and unsoaked California Bearing Ratio (CBR), the reliability indices exhibit a consistent decrease as the coefficient of variation values increase. This decline in reliability index values, ranging from 0.0024 to 0.000249 for soaked soil samples and from 0.0036 to 0.000373 for unsoaked soil samples, can be attributed to an escalation in the variability of the specific gravity of the soil samples. Despite the decreasing trend, all reliability index values remain positive, indicating the overall safety of the subgrade soil.

However, it is important to note that these values fall short of the recommended minimum reliability index threshold of 1.0, underscoring the need for improvement

measures for the subgrade soil, as outlined in the NKB Report (1978).

Reliability–Based Design of Subgrade Materials at Target Reliability Index of 1.0.

The essence of reliability–based design is to ensure that structures perform optimally in service. The results of the reliability–based design of subgrade material at minimum target reliability index value of 1.0 are presented in Table 3. The values of the design parameters for both soaked and unsoaked California Bearing Ratio corresponding to their expected values are presented in Table 3.

The expected values of the California bearing Ratio for both soaked and unsoaked soil samples are 32.5% and 78% and their corresponding reliability indices are 0.9275 and 0.925 respectively. This improvement in the index properties of the soil will lead to improved performance.

Limit State Performance Function

The limit state equation with respect to bearing capacity failure for soaked CBR is given by:

$$G(X) = \text{Expected CBR} - (402.8) - 0.031\,EMC + 0.164\,LL + 0.331\,PL - 0.252\,PI + 38\,MDD + 1.242\,OMC + 122.9\,Gs.$$

The limit state equation with respect to bearing capacity failure for unsoaked CBR is given by:

$$G(X) = \text{Expected CBR} - 0.184\,PI - (-740 - 0.475\,EMC + 0.226\,LL + 0.545\,PL - 0.184\,PI + 89.6\,MDD + 2.05\,OMC + 223\,Gs.$$

where: CBR is california bearing ratio, PI is plasticity index, EMC is equilibrium moisture content, LL is liquid limit, PL is plastic limit, MDD is maximum dry density, OMC is optimum moisture content and Gs is specific gravity.

CONCLUSIONS

From the study, the following conclusions are drawn:

- The reliability indices consistently decreased as the coefficient of variation values of the soil parameters increased, regardless of whether the soil samples are soaked or unsoaked.
- Factors such as water content, liquid limit, plastic limit, and plasticity index had minimal to negligible effects on the reliability indices of the subgrade material.
- An increase in the coefficients of variation for maximum dry density, optimum moisture content, and specific gravity of the subgrade soil reduced the reliability indices.
- The considered index properties yielded positive reliability index values, indicating the general safety of the subgrade soil. However, it is important to note that these values fell short of the recommended minimum reliability index threshold of 1.0, underscoring the need for improvement to ensure optimal performance.
- For achieving satisfactory performance of the subgrade soil, the expected values of California Bearing Ratio are determined to be 32.5% and 78%, respectively.
- The MATLAB–Based First Order Reliability Method Program had proved to be a rapid and suitable tool for generating design points and corresponding reliability indices, making it well–suited for highway and structural applications.

References

[1] Kozubal, J. V., Wyborski, P., Tankiewicz, M., & Gisterek, I. (2022). Reliability Assessment Approach for the Quality of Railroad Subgrade. Materials, 15(5)
[2] Ayres, M. J., (1997). Development of a Rational Probabilistic Approach for Flexible Pavement Analysis (3 Volumes), Ph.D. Dissertation, University of Maryland, College Park, Maryland.
[3] Gu, H.; Liu, K. (2021). Influence of Soil Heterogeneity on the Contact Problems in Geotechnical Engineering. Appl. Sci., 11, 4240.
[4] Zhao, L.; Huang, Y.; Xiong, M.; Ye, G. (2020). Reliability and Risk Assessment for Rainfall–Induced Slope Failure in Spatially Variable Soils. Geomech. Eng., 22, 207–217.
[5] EN 1990 (2002). Eurocode–Basis of Structural Design. Comité Européen de Normalization: Brussels, Belgium.
[6] ISO 2394 (2015). General Principles on Reliability for Structures. General Principles on Reliability for Structures: Geneva, Switzerland.
[7] Li, D. and Selig, E. T. (1998a). Method for railroad track foundation design I: development, J. Geotech. Geoenviron. Eng. 124 (4) 316–322.
[8] Li, S.; Ye, Y.; Tang, L.; Cai, D.; Tian, S.; Ling, X (2021). Experimental Study on the Compaction Characteristics and Evaluation Method of Coarse–Grained Materials for Subgrade. Materials, 14, 6972.
[9] Wu, M.; Cai, G.; Wang, C.; Liu, S. (2022). Mapping Constrained Modulus Differences in a Highway Widening Project Based on CPTU Data and Two–Dimensional Anisotropic Geostatistics. Transp. Geotech., 32, 100686.
[10] Phoon, K.K. & Kulhawy, F.H. (2003). Evaluation of model uncertainties for reliability–based foundation.
[11] Vessia, G., D. Di Curzio, and A. Castrignanò (2020). "Modeling 3D soil lithotypes variability through geostatistical data fusion of CPT parameters." Science of the Total Environment 698:134340.
[12] Peter, M., Burrow, N., Ghataora, G. S., & Evdorides, H. (2011). Railway Foundation Design Principles. In Journal of Civil Engineering and Architecture (Vol. 5, Issue 3).
[13] Kankara, I. A. (2014). Geology and Geochemical Characterization of Rocks in Funtua Sheet 78, NE, Scale 1:30, 000, NW Nigeria. An unpublished PhD Thesis submitted to Dept. of Geology, Federal University of Technology, Minna, Nigeria.
[14] ETL 1110–2–547, (1997). "Introduction To Probability and Reliability Methods for use in Geotechnical Engineering", a report to theU.S. Army Corps of Engineers, Washington, DC 20314–1000.
[15] NKB (1978). Structure for Building Regulations, The Nordic Committee on Building Regulations (NKB), Report No. 34, Stockholm.
[16] Saha, Nayan (2009). "Evaluation of subgrade strength and flexible pavement designs for reliability." https://digitalrepository.unm.edu/ce_etds/26. "A mechanistic–empirical subgrade design model based on Heavy Vehicle Simulation.

ISSN: 2067–3809

Fascicule 4
[October – December]
tome XVI
[2023]

ACTA Technica CORVINIENSIS
BULLETIN OF ENGINEERING

ISSN: 2067-3809

[1.]Ştefan ŢĂLU, [2.]Mihai ŢĂLU, [3.]Laura–Catinca LEŢIA

THE INTERNET OF THINGS IN CIVIL ENGINEERING: A REVIEW OF CHALLENGES AND SOLUTIONS IN THE ROMANIAN CONTEXT

[1.] Technical University of Cluj–Napoca, The Directorate of Research, Development and Innovation Management (DMCDI), Cluj–Napoca, ROMANIA
[2.] University of Craiova, Faculty of Mechanics, Department of Applied Mechanics and Civil Engineering, Craiova, ROMANIA
[3.] Technical University of Cluj–Napoca, Faculty of Building Services Engineering, Structures Department, Cluj–Napoca, ROMANIA

Abstract: The Internet of Things (IoT) is the network of physical objects (that contain sensors, actuators, trackers, storage, software, and other technologies) connected with computing systems via wired (for example, Ethernet) or wireless (for example, WiFi, cellular) networks to exchange data and information, merging the digital and physical universes to improve productivity, efficiency, services, etc. At the same time, civil engineering is experiencing a rapid digital transformation changing research frontiers and knowledge base structure towards intelligent tendencies and smart and sustainable infrastructure. The application of IoT in civil engineering assumes new challenges, such as data security and privacy concerns, interoperability issues, and the need for IoT professionals. However, the benefits of IoT in enhancing construction processes, infrastructure management, and sustainability make it a compelling and promising area for the civil engineering industry, making it more efficient, sustainable, and responsive to the needs of modern society. This paper aims to assess the current status of IoT implementation in civil engineering, highlighting its applications, benefits, and potential. Additionally, this article will explore the challenges and difficulties faced by the industry in fully leveraging the capabilities of IoT. By understanding the existing issues, this study intends to offer insights and recommendations to overcome obstacles and optimize the usage of IoT in civil engineering projects in the Romanian context.
Keywords: civil engineering, civil engineering projects, device communication, Internet of Things, IoT challenges, global network

INTRODUCTION

The concept of the Internet of Things (IoT) was first coined by British engineer Kevin Ashton in 1999. Kevin Ashton, while working at Procter & Gamble, used the term "Internet of Things" in a presentation to describe a revolutionary idea where everyday physical objects could be connected to the Internet and communicate with each other. At the time, Kevin Ashton was exploring ways to improve supply chain management and inventory control in retail using RFID (Radio Frequency Identification) technology. He realized that by equipping objects with RFID tags and connecting them to the internet, businesses could gain real–time visibility into their inventory, track products, and automate processes more efficiently. The term "Internet of Things" captured the essence of this vision, emphasizing the interconnectedness of physical objects and their ability to communicate over the Internet without human intervention. The concept quickly gained traction and became a cornerstone in the development of the IoT industry [1].

Following Kevin Ashton's proposal, IoT has grown exponentially, becoming a major driver of innovation in technology and transforming various industries. Today, the IoT ecosystem includes a vast array of devices, sensors, and systems that collect and exchange data, enabling automation, data–driven decision–making, and new levels of efficiency in numerous domains. From smart homes to industrial automation, from healthcare to agriculture, IoT applications have proliferated, making our lives more connected and convenient [2,3].

The Internet of Things (IoT) has a lot of applications in the field of civil engineering (such as buildings, roads, bridges, dams, railways, sewerage systems, etc.), revolutionizing the way infrastructure is designed, constructed, and managed [4]. IoT implementation in buildings aligns with the broader concept of creating smart buildings that are energy–efficient, technologically advanced, and user–centric. By focusing on these aims, IoT technology contributes to sustainable and optimized building management, leading to a positive impact on both occupants and the environment [5,6].

While converting existing buildings into smart buildings is feasible, the complexity and extent of the conversion may vary depending on the building's age, infrastructure, and desired level of smart functionality. In some cases, retrofitting may be straightforward, while in others, it might involve more extensive modifications [7].

By employing this interconnected network of sensors, actuators, and microchips, smart buildings can create an efficient, automated, and adaptive environment. By harnessing the power of IoT and automation, smart buildings offer numerous benefits, including increased energy efficiency, cost savings, improved occupant

comfort, enhanced security, and reduced environmental footprint. The ongoing advancements in IoT technology continue to expand the possibilities and potential for smart buildings in creating more intelligent, sustainable, and connected spaces, to enhance energy efficiency, occupant comfort, security, and overall building performance. As technology continues to advance, smart buildings will likely become more sophisticated, offering even greater benefits and capabilities to building owners, operators, and occupants, making smart buildings an essential component of sustainable and eco–friendly urban development.

Some examples of smart infrastructure in different sectors are smart office buildings, smart transportation facilities, health care facilities and hospitals, educational facilities, smart stadiums, smart parking lots, smart waste management, smart energy grids, smart farming, smart bridges, and roads [8–10].

Modern smart buildings were initially envisioned as sensor–embedded residences with various integrated systems. The concept revolved around using a network of sensors to gather data about the building's environment, such as temperature, lighting levels, occupancy, and energy usage. The key features of such smart buildings include sensor integration, centralized control, remote operation, efficiency and sustainability, interoperability, and data analytics [11–13].

IoT SYSTEM ARCHITECTURE

The Internet of Things (IoT) integrates systems from hardware to software, encompassing numerous technologies and components. The Internet of Things (IoT) system architecture is commonly described as a four–stage process, also known as the IoT data flow, where data is collected from sensors attached to various "things" and then transmitted through a network for processing, analysis, and storage. It involves four main stages:

- Sensing/Perception stage: in this initial stage, sensors, and devices attached to physical objects, often referred to as "things," collect data from the environment. These sensors can measure various parameters, such as temperature, humidity, pressure, motion, and more. The data collected at this stage is often in the form of raw sensor data.
- Communication/Network stage: once the sensors have gathered the raw data, it needs to be transmitted or communicated to a central processing system or data center. This stage involves the use of communication protocols and networks, such as Wi–Fi, Bluetooth, Zigbee, LoRaWAN, or cellular networks, to transfer the data from the sensors to a gateway or directly to the cloud.
- Data processing and analysis stage: after the data is transmitted to the central system or cloud, it undergoes processing and analysis. This stage involves various data processing techniques, such as filtering, aggregation, normalization, and analytics. The goal is to extract meaningful information and insights from the raw data. Data processing can occur either at the edge (edge computing) or in the cloud, depending on the specific use case and requirements.
- Cloud/Storage stage: in the final stage, the processed and analyzed data is stored in a cloud–based data center or storage system. Cloud storage provides scalability, accessibility, and the ability to store vast amounts of data generated by numerous IoT devices. The data stored in the cloud can be further used for real–time monitoring, historical trend analysis, predictive analytics, and other applications.

The four–stage IoT system architecture enables the seamless flow of data from the physical world (things and sensors) to the digital world (cloud and data center), where valuable insights can be derived, and appropriate actions can be taken based on the analysis results. This process is fundamental to the functioning and effectiveness of IoT solutions in various industries and applications [14].

APPLICATIONS OF IoT IN CIVIL ENGINEERING

The Internet of Things (IoT) has a wide range of applications in civil engineering, transforming the way infrastructure is designed, built, and managed [15–23]. Some examples of IoT applications in civil engineering include:

- Structural health monitoring: IoT sensors can be integrated into buildings, bridges, and other infrastructure to monitor their structural health in real time. These sensors can detect vibrations, stresses, strains, and temperature changes, providing early warnings of potential structural issues and allowing for timely maintenance and repair. Benefits of structural health monitoring using IoT sensors:
- Enhanced safety: Structural health monitoring using IoT sensors helps identify potential structural issues early, minimizing the risk of catastrophic failures and ensuring the safety of occupants and the public;
- Predictive maintenance: Continuous monitoring allows for predictive maintenance, leading to cost savings and reduced downtime due to unscheduled repairs;
- Data–Driven decision making: Real–time data from IoT sensors enables data–driven decision–making for structural maintenance and repairs;
- Increased lifespan: Proactive maintenance and early detection of structural issues contribute to extending the lifespan of buildings and infrastructure;
- Structural performance optimization: Continuous monitoring and analysis allow engineers to optimize

structural designs and materials for improved performance and efficiency.

- Smart construction sites: IoT–enabled devices and sensors can be deployed on construction sites to monitor equipment, materials, and workers. This enables better project management, optimized resource allocation, improved safety, and reduced downtime. Benefits of IoT in smart construction sites:
  - Improved productivity: IoT–driven data insights enable optimized resource allocation and streamlined workflows, enhancing construction site productivity;
  - Enhanced safety: IoT–based safety monitoring reduces risks and helps in early detection of potential hazards, ensuring a safer working environment;
  - Cost savings: Predictive maintenance and efficient resource management lead to cost savings on equipment repairs and operational expenses;
  - Real–Time decision making: Real–time data from IoT devices empowers project managers to make prompt and data–driven decisions;
  - Environmental compliance: IoT environmental monitoring ensures construction sites comply with environmental regulations, mitigating environmental impacts;
  - Better project management: IoT data provides project managers with a comprehensive view of construction site activities, enabling more effective planning and execution.
- Smart infrastructure management: IoT can be used to monitor and manage various aspects of infrastructure, such as smart lighting systems that adjust brightness based on occupancy, smart water management systems for leak detection and conservation, and intelligent traffic management systems for real–time traffic control. Benefits of IoT in smart infrastructure management:
  - Improved Efficiency: IoT–driven smart infrastructure management optimizes resource usage, reduces operational costs, and enhances overall efficiency;
  - Real–Time Insights: IoT sensors provide real–time data, enabling quick response to changing conditions and immediate intervention when needed;
  - Enhanced Safety and Resilience: Continuous monitoring and predictive maintenance enhance the safety and resilience of critical infrastructure;
  - Data–Driven Decision Making: Data analytics from IoT devices support data–driven decision–making for infrastructure planning and management;
  - Sustainability: IoT–driven smart infrastructure management contributes to sustainability goals by reducing energy consumption and resource waste.
- Environmental monitoring: IoT sensors can be employed to monitor environmental conditions in and around construction sites or infrastructure. This includes monitoring air quality, water quality, noise levels, soil conditions, wildlife monitoring, and urban environmental monitoring, which helps in assessing the environmental impact and ensuring compliance with regulations. Benefits of environmental monitoring using IoT Sensors:
  - Real–Time insights: IoT sensors provide real–time data on environmental parameters, allowing for immediate action or response in case of pollution or environmental risks;
  - Data–Driven decision making: Environmental data collected from IoT sensors enable data–driven decision–making for environmental management and policy development;
  - Early detection of environmental issues: IoT–based monitoring allows for early detection of pollution events, enabling timely interventions and minimizing environmental impacts;
  - Cost–Effective solutions: IoT–based environmental monitoring systems can provide cost–effective solutions compared to traditional monitoring methods;
  - Environmental conservation: Environmental monitoring using IoT sensors contributes to better conservation and protection of natural resources and ecosystems.
- Smart waste management: IoT–based smart waste management systems use sensors to monitor waste levels in bins, optimizing waste collection routes, smart collection vehicles, reducing operational costs, and promoting sustainability. Benefits of IoT–based Smart Waste Management:
  - Cost savings: Optimized waste collection routes and schedules lead to reduced fuel costs and operational expenses for waste management companies and municipalities;
  - Waste reduction: Efficient waste collection minimizes overflowing bins and litter, leading to a cleaner and more aesthetically pleasing environment;
  - Environmental impact: Smart waste management helps reduce carbon emissions and contributes to environmental sustainability by optimizing waste collection processes;
  - Real–Time insights: Real–time monitoring provides instant feedback on waste bin fill levels and collection status, allowing for immediate response to any sudden changes or emergencies;
  - Improved efficiency: IoT–based smart waste management streamlines waste collection operations and improves overall efficiency, ensuring a more reliable and consistent waste collection service.

- Geotechnical monitoring: IoT devices can be installed in the ground to monitor soil conditions and slope stability, providing crucial data for geotechnical engineers to make informed decisions during construction and maintenance projects. Benefits of Geotechnical Monitoring using IoT:
  - Enhanced safety: Geotechnical monitoring helps identify potential geotechnical hazards, enabling timely interventions and ensuring the safety of structures and individuals;
  - Improved design and construction: Real–time data on soil conditions allows engineers to optimize their designs, select appropriate construction methods, and make informed decisions during construction projects;
  - Cost savings: Early detection of geotechnical issues can prevent costly damages and delays, ultimately saving resources during construction and operation;
  - Predictive maintenance: Geotechnical monitoring enables predictive maintenance, ensuring that structures and foundations are regularly inspected and maintained to prevent failures;
  - Data–Driven decision making: Geotechnical data collected from IoT sensors facilitate data–driven decision–making for construction, infrastructure planning, and risk management.
- Energy efficiency and building automation: IoT can be used to create smart buildings with automated systems that optimize energy usage. This includes smart thermostats, lighting controls, and energy management systems, leading to energy savings and reduced carbon footprint. Benefits of IoT in Energy efficiency and building automation:
  - Energy savings: IoT–enabled building automation optimizes energy usage, leading to significant energy savings and reduced operating costs;
  - Enhanced comfort: Building automation systems provide occupants with a comfortable and personalized environment, adjusting settings based on their preferences and needs;
  - Sustainability: Smart buildings contribute to environmental sustainability by reducing energy consumption and greenhouse gas emissions;
  - Improved operational efficiency: IoT–based automation streamlines building operations, leading to increased efficiency in maintenance, energy management, and facility management;
  - Data–Driven decision making: Data analytics from IoT sensors help building managers make data–driven decisions for optimizing operations and energy usage;
  - Remote control: IoT allows for remote monitoring and control of building systems, facilitating easier management of multiple properties from a centralized location.
- Asset tracking and management: IoT–based asset tracking systems allow civil engineering firms to monitor the location and condition of equipment, tools, and materials, ensuring better inventory management and reducing the risk of theft or loss. Benefits of IoT in Asset tracking and management:
  - Improved asset visibility: Real–time tracking provides businesses with comprehensive visibility into the location and status of their assets, leading to better resource management;
  - Enhanced security: IoT–based asset tracking systems deter theft and improve asset security by enabling rapid recovery and accurate identification of lost or stolen assets;
  - Increased efficiency: Automation and real–time data enable businesses to optimize asset utilization, streamline workflows, and reduce operational costs;
  - Predictive analytics: IoT–generated data allows for predictive analytics, helping organizations identify patterns and trends related to asset usage and performance;
  - Regulatory compliance: IoT–based asset tracking systems assist in meeting regulatory compliance requirements by providing accurate records of asset movement and condition;
  - Streamlined maintenance: Predictive maintenance and condition monitoring ensure that assets are well–maintained, reducing the risk of unexpected breakdowns.
- Disaster management: IoT technologies have an important role in disaster management by providing real–time data on weather conditions, water levels, and potential hazards. This data helps in early warning systems and disaster preparedness planning. Benefits of IoT in Disaster management:
  - Early detection and timely response: IoT technologies enable early detection of disasters and rapid response, saving lives and minimizing property damage.
  - Data–Driven decision making: Real–time data from IoT sensors helps disaster management authorities make informed decisions and allocate resources more effectively;
  - Resilient communication: IoT–based communication systems ensure uninterrupted communication channels during disasters when traditional networks may be compromised.
  - Improved situational awareness: IoT devices provide detailed situational awareness, helping responders assess the severity of the disaster and plan their actions accordingly.
  - Faster recovery and reconstruction: IoT data aids in efficient post–disaster recovery efforts, expediting the rebuilding process.

- Remote monitoring and maintenance: IoT enables remote monitoring and maintenance of infrastructure, reducing the need for physical inspections and facilitating predictive maintenance practices. Benefits of IoT–enabled Remote monitoring and maintenance:
  - Cost savings: Remote monitoring reduces the need for frequent site visits, saving time and travel costs for maintenance personnel;
  - Increased efficiency: Real–time monitoring and predictive maintenance optimize asset performance, reducing downtime and maximizing productivity;
  - Improved safety: Remote monitoring minimizes the exposure of maintenance personnel to potentially hazardous environments;
  - Enhanced asset lifespan: Proactive maintenance based on real–time data helps prolong the life of assets and equipment;
  - Data–Driven decision making: Data analytics provide valuable insights for making informed decisions related to asset management and maintenance;
  - Scalability: IoT–based remote monitoring systems are easily scalable, allowing businesses to monitor and maintain multiple assets or facilities efficiently.

The integration of IoT in civil engineering offers numerous benefits, including enhanced safety, improved efficiency, cost savings, and more sustainable infrastructure development and management. As the technology continues to evolve, the potential for IoT in civil engineering applications is expected to expand further.

RESEARCH METHODOLOGY

The primary method of data collection in this research was through a questionnaire survey. By using questionnaires, the researchers aimed to collect data on various variables of interest related to the civil engineering industry in Romania, such as attitudes, perceptions, experiences, or practices of the construction practitioners to gain a better understanding of their perspectives, challenges, and potential areas for improvement in the industry. This could include topics such as construction methods, safety practices, project management, sustainability, and more.

Using the method of random sampling, the findings from the selected 60 participants (CEOs, managers, and various experts from various levels in the technical and economic fields, 48 men and 12 women in senior positions) can offer valuable data–driven insights that may inform policy decisions, industry practices, and future research endeavors related to the Romanian construction sector.

All participation in the studies was voluntary. All participants received information about on study aims and confidentiality. Semi–structured interviews allow for a balance between having some predetermined questions while also allowing participants the freedom to elaborate on their responses and provide additional insights.

The following questions were addressed to the participants:

- Q1) Are there parts/devices/machines/installations in your company that can be operated via the Internet?
- Q2) When did you implement these parts/devices/ machines/plants in your company?
- Q3) Can you provide a list of these parts/devices/ machines/installations?
- Q4) How many types of these parts/devices/machines/ installations are there in your company?
- Q5) Do you know how to operate these parts/devices/machines/installations in your company?
- Q6) How has the integration of internet–operated parts/ devices/machines impacted your work or the company's operations?
- Q7) What is the reliability of these devices/machines/ installations in the IoT system?
- Q8) Do you receive any training or support to operate these internet–connected parts/devices/machines effectively and securely? If yes, could you provide the period of time?
- Q9) Do you know the advantages and disadvantages of using these parts/devices/machines/installations in your company?
- Q10) Are you planning to implement modern IoT solutions in your company in the future period?
- Q11) How do you ensure the security and privacy of internet–operated systems within the company?
- Q12) What do you think would be the risks and challenges in the next 5 years for implementing these IoT solutions?

Most of the participants are civil engineers (70 %), 80 % of participants obtained a diploma, and 20% held master's and PhD. It's interesting to note that 50% of the participants have less than ten years of experience in the field, 40% of participants have less than 20 years of experience, and 10% of participants have less than 40 years of experience.

SPSS Software version 22.0 has been used for the data analysis. The correct application of the semi–structured interviews was verified by analyzing the credibility of the obtained results.

RESULTS

During June 1st – July 31th, 2023, 60 semi–structured interviews were conducted, and all of them were considered valid.

Question Q1 finds that the participants in these interviews demonstrated the following level of understanding of these subjects:

- very well: 50% of participants;
- well: 30% of participants;
- enough: 15% of participants; and

- not enough: 5% of participants.

The overall average certainty level was 85% on a scale from 0 to 100 which indicates a relatively high level of certainty among the respondents about these subjects.

The answers to questions Q2 and Q3 find that the participants knew the period of implementation of these parts/devices/ machines/plants in their company as follows:

- very well: 40% of participants;
- well: 30% of participants;
- enough: 25% of participants; and
- not enough: 5% of participants.

It is noted that for questions Q4 and Q5, the following results were recorded:

- very well: 45% of participants;
- well: 35% of participants;
- enough: 15% of participants; and
- not enough: 5% of participants.

It was found that for questions Q6 and Q7, the following results were obtained:

- very well: 50% of participants;
- well: 30% of participants;
- enough: 15% of participants; and
- not enough: 5% of participants.

For question Q8 it was found that respondents confirmed the training or support to operate these internet–connected and the period of time as follows:

- very well: 50% of participants;
- well: 30% of participants;
- enough: 15% of participants; and
- not enough: 5% of participants.

Question Q9 finds that the participants knew the advantages and disadvantages of using these parts/devices/machines/installations in their company as follows:

- very well: 55% of participants;
- well: 35% of participants;
- enough: 5% of participants; and
- not enough: 5% of participants.

Furthermore, it was found that the respondents' dissatisfaction with IoT devices is not directly influencing their interest or willingness to adopt more IoT solutions in the company (this finding can have several implications: dissatisfaction with IoT devices, separation of concerns, potential for improvement, and varied factors influencing implementation).

The answers to question Q10 find that the participants planning to implement more IoT solutions in their company in the future as follows: 95% of participants, and only 5% participants are not sure.

For question Q11 it was found that respondents knew that the IoT introduces new challenges and risks for the security and privacy of data and devices and it is very important to ensure that IoT network is protected from unauthorized access, malicious attacks, and data breaches, as follows: 95% of participants knew, and only 5% participants are not sure. They agree to use the best practices to follow, such as:

- choosing reliable IoT devices;
- encrypting and authenticating your IoT data;
- implementing access control and monitoring;
- updating and backup the IoT system.

On the other hand, they specified correctly some of the common types of vulnerabilities that affect IoT devices, such as:

- the use of default or weak credentials (failing to change default passwords can leave devices vulnerable to unauthorized access);
- the insecure network protocols (IoT devices may use weak or unencrypted communication protocols, making them susceptible to eavesdropping and data interception);
- the lack of updates or patches (failure to apply these updates can leave devices exposed to known security flaws);
- the inadequate access control (weak access controls can allow unauthorized users to gain access to sensitive data or control IoT devices);
- and the poor data protection (insufficient encryption or data protection measures can expose sensitive data to unauthorized access or tampering).

Furthermore, regular security assessments, employee training, and staying informed about emerging threats can further strengthen their IoT security posture. The results for question Q12 regarding respondents' opinions about the risks and challenges in implementing IoT solutions over the next 5 years were: 90% of participants knew about the risks and challenges associated with implementing IoT solutions in the next 5 years; only 10% of participants were not sure about the risks and challenges. It is highlighted that understanding the risks and challenges associated with IoT implementation can lead to better decision–making, risk management, and resource allocation. It enables organizations to take necessary precautions and implement measures to mitigate potential problems before they escalate.

CONCLUSIONS

A comprehensive literature review on technology adaptation in civil engineering can provide valuable insights into the current state of research, trends, challenges, and potential solutions in this field. Designing a smart civil engineering structure requires interdisciplinary collaboration among civil engineers, architects, IoT experts, and technology providers.

By analyzing existing studies and publications, researchers can identify gaps in knowledge, emerging technologies, and best practices for improving technology adoption in civil engineering.

On the other hand, the study's comprehensive examination of IoT in civil engineering from Romania contributes valuable knowledge to the field and offers actionable insights for businesses, researchers, policymakers, and other stakeholders. It has the potential to influence decision–making, promote growth, and drive positive advancements in the IoT landscape in Romania based on the following reasons:

- understanding perception and use: The study provides valuable insights into the perception of IoT technologies in Romania. Understanding how these technologies are perceived and utilized by businesses and industries can help identify opportunities and challenges for their adoption and implementation.
- identifying barriers and risks: by highlighting the barriers and risks associated with IoT adoption, the study offers essential information for businesses and decision–makers. Recognizing these obstacles allows organizations to develop strategies to overcome challenges and mitigate potential risks.
- industry and support services focus: focusing on the industry and support services sectors in Romania, the study narrows down its scope to specific domains, making the findings more relevant and actionable for businesses operating in these sectors.
- providing insights for development: the study's exploration can serve as a foundation for future planning and investment decisions; this can guide policymakers, industry stakeholders, and academia in creating supportive environments for IoT growth.
- bridging business–academia gap: research that addresses real–world industry challenges can bridge the gap between academia and the business world. The findings can be valuable for academia to refine their curricula, foster collaboration with businesses, and conduct further research in relevant areas.
- informing policy and strategy: the study's findings can inform policymakers about the current state and potential of IoT in Romania. It can influence the formulation of policies that promote innovation, infrastructure development, and regulatory frameworks to support IoT growth.
- driving innovation: understanding the existing landscape of IoT in Romania can inspire innovative ideas and solutions. The study may spark innovations, product developments, and service offerings to address the identified needs and challenges.
- fostering collaboration: the study can serve as a basis for collaboration between businesses, academia, and government agencies. It encourages stakeholders to work together to address challenges, share knowledge, and drive the development of IoT solutions in Romania.

References

[1] T. Kramp, R. van Kranenburg, and S. Lange, "Introduction to the Internet of Things". In: Bassi, A., et al. Enabling Things to Talk. Springer, Berlin, Heidelberg. 2013

[2] A. Nazarov, D. Nazarov, and Ş. Ţălu, "Information security of the Internet of Things". In: Proceedings of the International Scientific and Practical Conference on Computer and Information Security – INFSEC, SCITEPRESS – Science and Technology Publications, Lda, vol. 1, pp. 136–139, 2021. Eds.: Nazarov D. and Nazarov A. International Scientific and Practical Conference on Computer and Information Security (INFSEC 2021) Yekaterinburg, Russia, April 5th–6th, 2021.

[3] R. Dallaev, T. Pisarenko, Ş. Ţălu, D. Sobola, J. Majzner, and N. Papež, "Current applications and challenges of the Internet of Things". New Trends In Computer Sciences, vol. 1, issue 1, pp. 51–61, 2023

[4] G. Manisha, "A review on the internet of things in civil engineering: enabling technologies, applications and challenges", E3S Web of Conferences, 309, 01209, 2021

[5] M. Mishra, P.B. Lourenço, and G.V. Ramana, "Structural health monitoring of civil engineering structures by using the internet of things: A review", Journal of Building Engineering, vol. 48, 103954, 2022

[6] D. Nazarov, A. Nazarov, and Ş. Ţălu, "BIM–technologies for a smart city". AIP Conference Proceedings, vol. 2657, 020050, pp. 1–4, 2022. Eds.: Zakharova G. and Semenov A. IV International Scientific and Practical Conference "New Information Technologies In the Architecture and Construction" (NITAC 2021), Ekaterinburg, Russia, November 2–3, 2021.

[7] M. Jia, A. Komeily, Y. Wang, and R.S. Srinivasan, "Adopting Internet of Things for the development of smart buildings: A review of enabling technologies and applications", Automation in Construction, vol. 101, pp. 111–126, 2019

[8] K.M. Karthick Raghunath, M.S. Koti, R. Sivakami, V.V. Vinoth Kumar, G. NagaJyothi, and V. Muthukumaran, "Utilization of IoT–assisted computational strategies in wireless sensor networks for smart infrastructure management". Int J Syst Assur Eng Manag, 2022.

[9] G. Swetha Shekarappa, M. Sheila, R. Saurav, and B. Manjulata, "Chapter Nineteen – Smart transportation based on AI and ML technology". In: Artificial Intelligence and Machine Learning in Smart City Planning, Elsevier, Eds. V. Basetti, C.K. Shiva, M.R. Ungarala, S.S. Rangarajan, 2023, pp. 281–299.

[10] A. Woll, and J. Tørresen, "What is a Smart Hospital? A Review of the Literature". In: Duffy V.G., Lehto M., Yih Y., Proctor R.W. (Eds.) Human–Automation Interaction. Automation, Collaboration, & E–Services, vol. 10, 2023. Springer, Cham.

[11] C. Pathmabandu, J. Grundy, M.B. Baruwal Chhetri, and Z. Baig, "Privacy for IoT: Informed consent management in Smart Buildings", Future Generation Computer Systems, vol. 145, pp. 367–383, 2023

[12] M. Willetts, and A.S. Atkins, "Application of data mining to support facilities management in smart buildings". In: Marques G., Saini J., Dutta M. (Eds.) IoT Enabled Computer–Aided Systems for Smart Buildings. EAI/Springer Innovations in Communication and Computing. 2023, Springer, Cham

[13] K. Gong, J. Yang, X. Wang, C. Jiang, Z. Xiong, M. Zhang, M. Guo, Lv Ran, S. Wang, and S. Zhang, "Comprehensive review of modeling, structure, and integration techniques of smart buildings in the cyber–physical–social system". Front. Energy, vol. 16, pp. 74–94, 2022

[14] M. Mansour, A. Gamal, A.I. Ahmed, L.A. Said, A. Elbaz, N. Herencsar, and A. Soltan, "Internet of Things: A comprehensive overview on protocols, architectures, technologies, simulation tools, and future directions". Energies, vol. 16, 3465, 2023

[15] R.C.Y. Lam, A. Junus, W.M.Y. Cheng, X. Li, and L.C.H. Lam, "IoT Application in Construction and Civil Engineering Works", 2017 International Conference on Computational Science and Computational Intelligence (CSCI), Las Vegas, NV, USA, pp. 1320–1325, 2017
[16] F. Lamonaca, P.F. Sciammarella, C. Scuro, D.L. Carnì, and R.S. Olivito, "Internet of Things for Structural Health Monitoring", 2018 Workshop on Metrology for Industry 4.0 and IoT, Brescia, Italy, 2018, pp. 95–100
[17] D. Abruzzese, A. Micheletti, A. Tiero, M. Cosentino, D. Forconi, G. Grizzi, G. Scarano, S. Vuth, and P. Abiuso, "IoT sensors for modern structural health monitoring. A new frontier", Procedia Structural Integrity, vol. 25, pp. 378–385, 2020
[18] S.G. Szentesi, L.D. Cuc, R. Lile, and P.N. Cuc, "Internet of things (IOT), challenges and perspectives in Romania: a qualitative research", The Amfiteatru Economic journal, Academy of Economic Studies – Bucharest, Romania, vol. 23(57), pp. 448–448, 2021.
[19] Y. Gamil, M.A. Abdullah, I.A. Rahman, and M.M. Asad, "Internet of things in construction industry revolution 4.0: Recent trends and challenges in the Malaysian context", Journal of Engineering, Design and Technology , vol. 18, no. 5
[20] M.M. Mijwil, K.K. Hiran, R. Doshi, and O.J. Unogwu, "Advancing construction with IoT and RFID technology in civil engineering: a technology review", Al–Salam Journal for Engineering and Technology, 2023
[21] L. Shuai, "Application analysis of Internet of Things technology in civil engineering construction", Proc. SPIE 12625, International Conference on Mathematics, Modeling, and Computer Science (MMCS2022), 126252Y (1 June 2023)
[22] M. Zhang, N. Ghodrati, M. Poshdar, B.C. Seet, and S. Yongchareon, "A construction accident prevention system based on the Internet of Things (IoT)", Safety Science, vol. 159, 106012, 2023
[23] D.T. Patil, and A. Bhaumik, "Efficiency of Internet of Things (IoT)–enabled systems in reducing construction cost", 2023 International Conference on Computational Intelligence and Knowledge Economy (ICCIKE), Dubai, UAE, pp. 408–413, 2023

ISSN: 2067-3809

ACTA TECHNICA CORVINIENSIS – BULLETIN OF ENGINEERING
TOME XVI [2023] | FASCICULE 4 [OCTOBER – DECEMBER]

[1.]Yosra MLOUHI, [2.]Mohamed Najeh LAKHOUA, [3.]Jamel BEN SALEM,
[4.]Imed JABRI, [5.]Taher BATTIKH

METHODOLOGY OF ANALYSIS AND INFORMATION SYSTEM DEVELOPPMENT OF ENERGY METERS CONSUMPTION

[1.]Research Laboratory Information and Communication Technologies & Electrical Engineering, LATICE, National Superior School of Engineering, University of Tunis, TUNISIA
[2,3]Research Laboratory Smart Electricity & ICT, SEICT, National Engineering School of Carthage, ENICarthage, University of Carthage, TUNISIA
[4,5.]Research Laboratory Information and Communication Technologies & Electrical Engineering, LATICE, National Superior School of Engineering, University of Tunis, TUNISIA

Abstract: Because of the difficulty and kindliness of the analysis and modeling of reading of the energy meters consumption of the Information System (IS) will use the OOPP technique (Oriented Objectives Project Planning), that is a comprehensive system modeling tool to analyze a difficult condition by breaking it down from and decreasing it to elementary conditions leading to elementary operational planning. The aim of this work is to offer a methodology of analysis of the energy meters consumption and to develop an IS of reading of the energy meters consumption. Then, we present an applied operation for the reading of the energy meters consumption. This operation will permit energy dispensers to advance the business service by offering an exact and an instantaneously billing.

Keywords: Energy consumption, energy meters, reading techniques

INTRODUCTION

Toward to manage the reading of the energy consumption, energy suppliers have realised a lot of reading tools allowing to follow-up the energy consumption by offering an exact and an instantaneously billing. Then, these tools can decrease appreciated reading exclusion faults of billing, complaints regarding the exalted invoices and invoices arrangements [1-3].

The concept of this paper deal with in a proposal of an applied operation let energy dispensers to advance the clientele business by offering an exact and an instantaneously billing [4-6].

In this situation, we accomplished an applied operation allowing the automatic reading of the index of meters on the basis of a Datalogic Portable Terminal providing mobile professionals by the better applicable aspects required to act in critical status [7-11].

The aim of this article consists in a proposal of a methodology of analysis and IS development of the energy meters consumption by reading the meters index of electric energy and gas, the habilitation and the constructed knowledge administration.

PRESENTATION OF THE ENERGY METERS TECHNOLOGY

A meter is an element allowing to determine the capacity consumed of electric energy or gas. The electricity suppliers and gas use it to note the energy consumption to the customer. Then, a meter can be electromechanical, electronic nature or gas [12-16].

The electronic meters measures the current and tension, and resolve through an intern analysis the comparable energy. They are in durable evolution, contributing regularly increased performance. The elemental fundamental consists in promising the communication of information iconcerning to act a management of the efficient load.

The electronic meters replace the older electromechanical meters as they are used in the numbering of fluids (electricity, gas, water) [17-20]. In fact, many different designs of gas meters are in familiar use, depending on the volumetric flow rate of gas to be measured, the range of flows anticipated, the type of gas being measured and other factors.

RESULTS OF THE ANALYSIS AND MODELING OF THE IS DEVELOPMENT

The model [21-26] presented on the following table illustrates eight SO for achieving the GO: IS of reading of the energy meters consumption developed.

TABLE I: OOPP model of is reading of the energy meters consumption

Code	Activity
OG	IS of reading of the energy meters consumption developed
OS1	Management of the IS of reading of the energy meters consumption developed
R1-1	Improvement of the IS of reading of the energy meters consumption determined
R1-2	Assessment of the IS of reading of the energy meters consumption determined
R1-3	Control of the IS of reading of the energy meters consumption determined
R1-4	Maintenance of the IS of reading of the energy meters consumption determined

R1-5	Functioning of the IS of reading of the energy meters consumption determined
OS2	Security of the Information System of reading of the energy meters consumption developed
R2-1	Security of the information of reading of the energy meters consumption determined
R2-2	Confidentiality of the information of reading of the energy meters consumption determined
OS3	Circulation of the information of reading of the energy meters consumption developed
R3-1	Implementation of a secure information flow circuit of reading of the energy meters consumption determined
R3-2	Availability of timely information of reading of the energy meters consumption determined
OS4	Appropriate information media of reading of the energy meters consumption developed
R4-1	Operation of information media of reading of the energy meters consumption determined
R4-2	Conviviality of supports of reading of the energy meters consumption determined
R4-3	Availibility of supports of reading of the energy meters consumption determined
R4-4	Supports of the information of reading of the energy meters consumption determined
OS5	Analysis of effective information of reading of the energy meters consumption developed
R5-1	Actions of Improvement of reading of the energy meters consumption determined
R5-2	Causes of failure of reading of the energy meters consumption determined
R5-3	Failures of reading of the energy meters consumption determined
R5-4	Information traited of reading of the energy meters consumption determined
OS6	Efficient information processing of reading of the energy meters consumption developed
R6-1	Efficiency of the treatment system of reading of the energy meters consumption determined
R6-2	Information of reading of the energy meters consumption determined
R6-3	Information of reading of the energy meters consumption determined
OS7	Archive information of reading of the energy meters consumption developed
R7-1	Security of archived information of reading of the energy meters consumption determined
R7-2	Locations of archival information of reading of the energy meters consumption determined
R7-3	Supports of archival information of reading of the energy meters consumption determined
R7-4	Duration of archival information of reading of the energy meters consumption determined
R7-5	Archival information of reading of the energy meters consumption determined
OS8	Characterization (properties / elements) of the information of reading of the energy meters consumption developed
R8-1	Information need of reading of the energy meters consumption determined
R8-2	Information source of reading of the energy meters consumption determined
R8-3	Destinations for the information of reading of the energy meters consumption determined

READING OF THE ENERGY METERS CONSUMPTION

In this part, we propose a case study of the reading of the energy meters consumption. Then, the reading of the index of the electric energy meters, to identify and to manage the constructed data, we used a Datalogic Portable Terminal based on an operating system Windows CE.

In this applied operation, the Datalogic Potable Terminal perhaps exploited for the manual either the automatic reading of meters consumption. Then, the mobile terminal consists of an automatic description system that collects distinct integral tools. Opposed to the majority of the alternative tools of reading, these terminals are portable and mobile. Their limited size and the use of batteries enable more autonomous automatic identification.

A Datalogic is constituted of a screen with liquid crystals and an alphanumeric keyboard allowing to visualize the regrouped information and to catch a few variable data. The constructed data security was notably considered by the memory flash giving back impractical the damage of data; the existence of a rechargeable emergency battery; the automatic safeguard of the last tour.

In this applied operation, we exploited the model of the Datalogic Portable Terminal Kyman-NET™. It is one of the key elements of the terminal range portable mobile@works. It is quite robust and represents the solution of applications of the transport and the logistics.

In the next, we present the different function specifications by giving organization based on charts also architectures of the data and the interfacings.

The preliminary phase in the realization of the applied operation is the choice of the development environment (material and software) enabling to do the established specifications.

The applied operation presented has been developed by the operating system Microsoft Windows XP Sweet while using for the implementation of the information system, the database management system Microsoft Access. For the implementation of the interfacings and the data consultation, we exploited the development language Visual Basic 6.0.

This is why we achieved two applied operations: the first one is a Met-View applied operation and the second one is an applied operation of reading and writing of the data on the Datalogic Portable Terminal.

Figure 1 presents the flowchart of the Met-View applied operation.

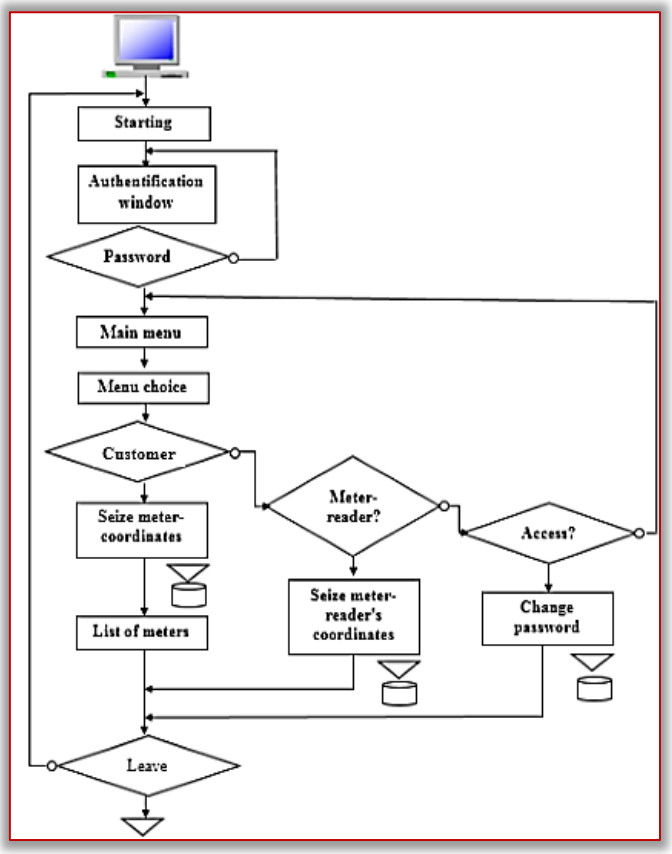

Figure 1. Flowchart of the Met-View applied operation

After starting the application Met-View, a window shows to the screen for some seconds next a window of password. Then, the user of this applied operation possesses a login and a password that he must seize to be able to reach the applied operation. The obligation of identification enables the access secure taking into account of the data importance that is going to be collected.

The window of the fundamental main menu of the Met-View applied operation introduces the main form of the operation that enables to reach many choices: access, meter-reader, customer, leave…

Figure 2 shows the flowchart of the Datalogic Portable Terminal applied operation that interest the reading and the writing of the data.

The customer window enables to manage subscribers' data. With a quiet click on the button that corresponds to the application. Then, the user will be able to: add a customer; suppress a customer; look for a customer; modify a customer's coordinates; annul an application.

The menu meter-reader enables the user to manage data of meter-readers. With a quite click on the button that corresponds to the application to do, the user will be able to: add a meter-reader; suppress a meter-reader; look for a meter-reader; modify a meter-reader's coordinates; annul an operation. This window enables the user to link for the meter-reader a Datalogic.

The window of access to the applied operation of reading and writing of data appears at the time of the call of the operation. It contains two fields; the first is reserved for the user's identification (meter-reader), the second for the password. In fact, every meter-reader possesses a login and a password that he must seize.

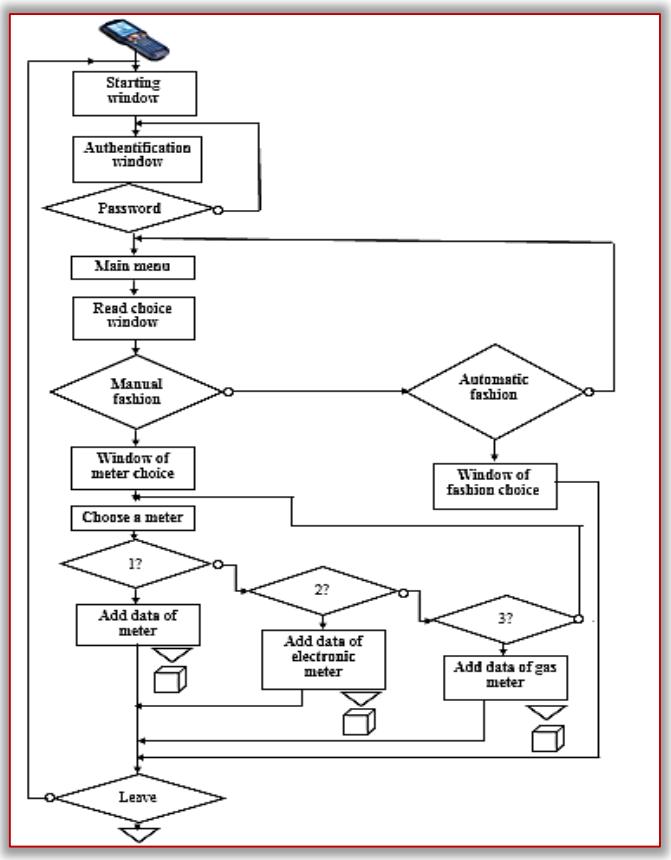

Figure 2. Flowchart of the Datalogic Portable Terminal applied operation

The window of the main menu of the second applied operation of the reading and the writing of the data on the Datalogic Portable Terminal enables to reach two fashions: manual and automatic.

The window of the manual fashion allows to want the type of the meter (electromechanical, electronic or gas).

The window of the electromechanical meters enables to want the zone, the tariff; it enables too the meter-reader to seize the index and the complication if it happens and record the data.

A second window for the electronic meters enables us to want the zone, the tariff. It enables us too the meter-reader to seize the index and the complication if it happens and registred data.

A third window of gas meters enables us to seize data (zone, n° of set, index and complication) regarding gas meters. All data regarding meters are registered in a file text of type block notes.

CONCLUSION

In this work, we have proposed an applied operation for the reading of the energy meters consumption and a contribution of Information System (IS) development of

reading of the energy meters consumption. Then, it is an essential attention for dispensers of energy around the world to have a few exact, exact data, instantaneously, on the energy consumption.

This applied operation allows us to associate a few central notions as the theoretical analysis of the operation and the realization.

Starting from this study of the proposal of a methodology of analysis and IS development of energy meters consumption presented in this work, we will enhance the analysis and modeling approach based of various techniques.

References

[1] G. Donngmei, "Study of the automatic reading of watt meter on the basis of ased on image processing technology", IEEE Conf. IEA: 2215-2218.
[2] S. Shuttao, B. Baosshu and D. Guyan, "Research on remote meter automatic reading based on computer vision transmission and distribution", IEEE/PES: 2006: 1-5.
[3] M. Eran and S. Deveney, "Power quality index meter Instrumenttation and Measurrement Technology", IEEE Conf. IMTC/2003, 3:1038-1043.
[4] E. Fitipaldi, L. Sambaio, and A. Alneida, "Selection of electrical energy supplier on the basis of multicrriteria decission aid", IEEE Int. Conf. SMC, 2002, 5:1919-1924
[5] www.industrysearch.com.au, website, [consulted mars 2021].
[6] H Werttani.and L. Najeh, "Overview of Smart Grids Architecture and Design", SmartNets2019, Hammamet Tunisia, 2019, October 16-18.
[7] B. Blake Levitt (11 October 2015). My Works - B. Blake Levit. blakelevitt.com.
[8] How to discover circuit errors in meter installations, 9th International Conf. on Mettering and Tariiffs for Energy Suply, 2011.
[9] A. Dus, "Wirelless communication system for energy meter reading", Int. Conf. on Advances in Recent Technologies in Comunication and Computing, 2009, 896-898.
[10] F. Delea and J. Casazza, "Distribution, a review of the technology and the marketplace understanding", Electrric Systems, 2004, pp. 85-95.
[11] A Dierks and U. Braun, "New means for testing energy meters", 8th International Conf. on Metering and Tariffs for Energy Supply, 1996, pp. 244- 248.
[12] B. Sachdeva and S. Chand, "ENC evaluation and analysis of electronic energy meter", Proceedings of the International Conf. on M.N. Electromagnetic Interfference and Comppatibility, 1999, pp. 190-192.
[13] L. Najeh, Methodology for designing supervisory systems: case study of a counting system of naturral gas, Journal of Electrical Engineering, 2009, vol. 8, N°2.
[14] L. Najeh, "Overview on Modeling and Design of Mechatronic Systems", Int. J. of Mechatronics and Automation, 2020, Vol.8, No.3.
[15] H. Werttani., J. Sallem and L Najeh., "Analysis and supervision of a SG system with a systemic tool", The Journal of Electricity, 2021, Vol.34, Issue 4.
[16] S. Pope, "Distributed control and measurement system for natural gas metering application", IEEE Int. Conf. on AQTR 2011, 4: 2-6.
[17] E. Martty, "La sécurité de l'approvisionnement électrique : une nécessaire complémentarité", 2008.
[18] www.optiscangroup.com, website, [consulted mars 2021].
[19] V. Kopitoff and C. Kym, "Google plans meter to detail home energy use", Chronicle, 2008.
[20] Department for Business, Energy & Industrial Strategy (15 October 2018), Smart meter roll-out: cost-benefit analysis 2018.
[21] Manuel pour l'application de la Planification des Interventions Par Objectifs (PIPO), 3ème Edition, Bruxelles 1992.
[22] LFA: Handbook for objectives-oriented planning, 1998.
[23] M.F. Karoui, J. Ben Sallem, L. Najeh, System Analysis and Information System Development of a Smart Grid, Independent Journal of Management and Production, Volume 14, Issue 4, 2021.
[24] J. El Khaldi, L. Bousslimi, A. Balti, L. Najeh, Study and analysis of the methods of the enterprise modelling, Design Engineering, 2022, Issue: 1, pp: 2945 – 2948.
[25] L. Najeh, J. Ben Salem, I. Jabri, T. Battikh, Using System Approach for Automation and Information System Development of a Printing System, JCSCS, 15 (1), 2022.
[26] L. Najeh, A. Balti, The Need for System Approach and Mechatronics for Agricultural Applications, JCSCS, 14 (1), 2021

ISSN: 2067-3809

[1.] Marian VINTILĂ, [2.] Cristian SORICĂ, [1.] Nicușor MANOLE, [1.] Mariana TOMA,
[1.] Ionel Lucian DUMITRESCU, [3.] Livia MAIOR, [2.] Laurențiu VLĂDUȚOIU

REDUCTION OF PESTICIDE RESIDUES FROM SURFACE OF FRESH TOMATOES USING OZONE (MICROBUBBLE) TREATMENT

[1.]Institute of Research - Development for the Processing and Marketing of Horticultural Products – "Horting", Bucharest, ROMANIA
[2.]National Institute of Research – Development for Machines and Installations Designed for Agriculture and Food Industry – INMA Bucharest, Bucharest, ROMÂNIA
[3.]Holland Farming Agro SRL, Bucharest, ROMÂNIA

Abstract: The research has looked at the effectiveness of washing tomatoes with ozonated water before processing. Washing was done by immersion in water with O_3 micro bubbling at 2.5 mg L^{-1} for 5 and 10 minutes, respectively at the temperature of 15°C. The removal of residues generated by treating tomatoes with Cyperguard 25 EC, Dithane M-45 and Topsin 70 WDG was examined. Mass spectrometry was used to determine the residues. At V1, the variant treated with Cypermethrin, the second and fourth peak have recorded the values of 0.6 mg/kg > 0.5 mg/kg, the value accepted as the maximum allowed limit. The analysis data confirmed that the solution used was significantly effective in removing pesticide residues, applied before the harvest.
Keywords: ozone; immersion; bubbling; pesticide residues

INTRODUCTION

The requirements regarding the existence of safe foods on the market, makes the food industry promote innovative technologies, in order to obtain high quality products with a high retention of nutrients and a sensory quality able to satisfy consumer demand.

In the case of vegetable origin food production, the problem of eliminating contaminants generated by the treatments carried out against pathogenic and harmful agents on the raw materials (vegetables and fruits) is a priority issue. Research has shown that they are persistent and their residues decrease very slowly (Nowacka A., 2009), so that the levels of benomyl, carbendazim, methyl thiophanate and thiabendazole residues were stable in apples stored at 0 - 2°C, and after 140–150 days the active ingredients were at 36– 60% of the initial level (Holland P. T. 1994).

The washing phase using various agents, a component of the technological flow of processing vegetables and fruits, achieves the reduction of impurities.

The efficiency of washing is influenced by several factors such as: the time elapsed since the last treatment and the location of the residue on the surface of the fruit, as well as the water solubility of a certain residue. The type of detergents as well as the temperature of the solution in which the washing is carried out, can considerably improve the efficiency of the process (Holland P. T. 1994).

The current trend to use "greener" food additives and the fact that regulatory authorities have approved and accepted that ozone can be used in green technologies, has led to the development of a number of ozone-based treatment solutions / systems.

Ozone (O3) acts against a wide spectrum of microorganisms, which makes it considered among the most powerful hygiene products. Ozone is found in the atmosphere and is the highly oxidizing allotropic form of oxygen (E0 = 2.07 V), so it can oxidize many organic compounds.

The way of generating ozone by passing air or gaseous oxygen through a high-voltage electric discharge, or by irradiating ultraviolet light, made it easy to use for sterilization, inactivation of viruses, deodorization, bleaching (discoloration), decomposition of organic matter, degradation of mycotoxins and others (Balawejder M. 2013). Due to the fact that ozone has the property of converting to oxygen through autolysis, it is recognized as safe for food contact applications.

Essentially, the reduction of chemical contaminants in food products with ozone is based on two different processes, i.e. washing with aqueous ozone solutions and gas phase ozone treatment. In current technologies fruits and vegetables, during the washing phase, can be sprayed/immersed in aqueous ozone solution.

MATERIALS AND METHODS

The research was carried out within the ADER 7.5.1 project, financed by the Ministry of Agriculture and Rural Development through the Sectoral Plan for research and development in the field of agriculture and rural

development - ADER 2022, where ICDIMP-Horting and INMA Bucharest were partners.

In order to ensure the effective washing of fruits and vegetables to remove residues from the active ingredients of pesticides used in the treatments carried out in horticultural crops, the following requirements must be met: the source of obtaining ozone must be atmospheric air; achieving an optimal concentration of O3 in the washing water; adapting the flow of ozonated solution to the working capacity of the washing installation.

Taking into account these requirements, the research team designed and built a demonstrative laboratory installation shown schematically in figure 1.

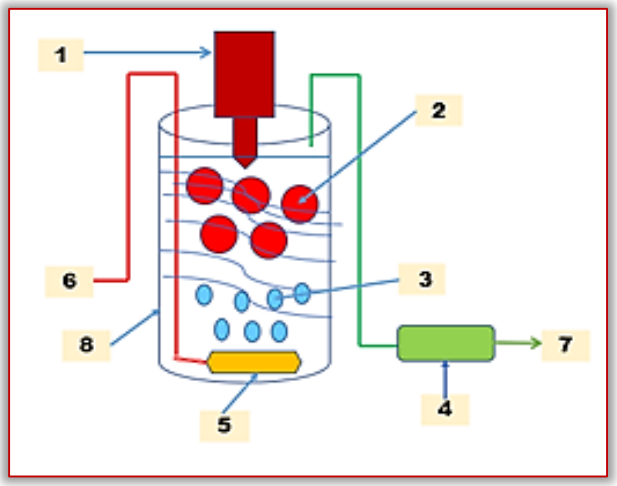

Figure 1 - Demonstrative installation for the use of ozone to remove pesticide residues
1 – O_3 concentration measuring device; 2 - Tomatoes treated with O_3 aqueous solution; 3 – Ozone; 4 - O_3 destruction unit; 5 – O_3 diffuser; 6 – Outlet from the ozone generator; 7 – Air outlet; 8 – Experimental vessel

The tomatoes were treated with the following substances:

- pyrethroid insecticide Cyperguard 25 EC, contains the active substance Cypermethrin 250g/l, is generally miscible with other fungicides, insecticides or foliar fertilizers and requires a pause time of 14 days;
- the systemic fungicide Topsin 70 WDG has Thiophanate methyl 70% as its active substance, and the pause time from the last treatment until harvesting is 3 days for vegetables and melons and 15 days for fruit trees and vines;
- contact fungicide, Dithane M-45 with active substance Mancozeb 80%, in which the pause time from the last treatment to harvesting is recommended to be 21 days for tomatoes treated to prevent brown spot and 14 days for the other diseases, 28 days when treating the trees (plum, apricot, peach), 28 days after treating the vine manna.

Starting from the scheme shown in figure 1, in order to carry out the laboratory determinations, the experimental installation shown in figure 2 was created.

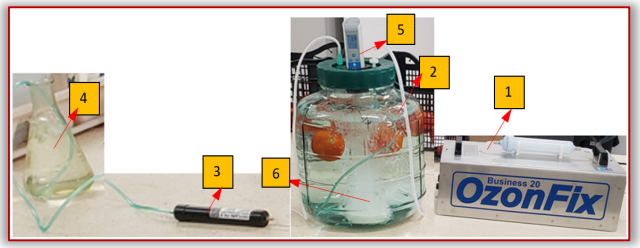

Figure 2 - Experimental installation
1- Ozone generator, 2- Wash vessel, 3- Residual ozone destruction unit, 4- Final residue collection vessel, 5- Apparatus for measuring the concentration of aqueous ozone solution, 6. Ozone diffuser (bubble stone)

The experiments were carried out on tomatoes, in order to establish the usefulness of ozone treatment for decontamination of the external surfaces of these fruits, before their use in processing technologies to obtain tomato juice or paste.

The variants and treatment parameters in the case of tomatoes are those presented in table 1.

Table 1. Variants and parameters of tomato treatment with ozonated water by bubbling

Treatment substances	Cyperguard 25 EC		Dithane M-45		Topsin 70 WDG	
Variants	V1	V2	V3	V5	V6	V7
No. fruits	8	8	8	8	8	8
Solution temperature (°C)	15.00	15.00	15.00	15.00	15.00	15.00
Treatment duration (min)	5	10	5	10	5	10
O3 concentration (mg/l)	2.50	2.50	2.50	2.50	2.50	2.50
Control variants	M1		M2		M3	

During the experiments, the variable was the treatment duration of 5 and 10 minutes respectively. Aspects regarding the treatment method (bubble washing) can be found in figure 3.

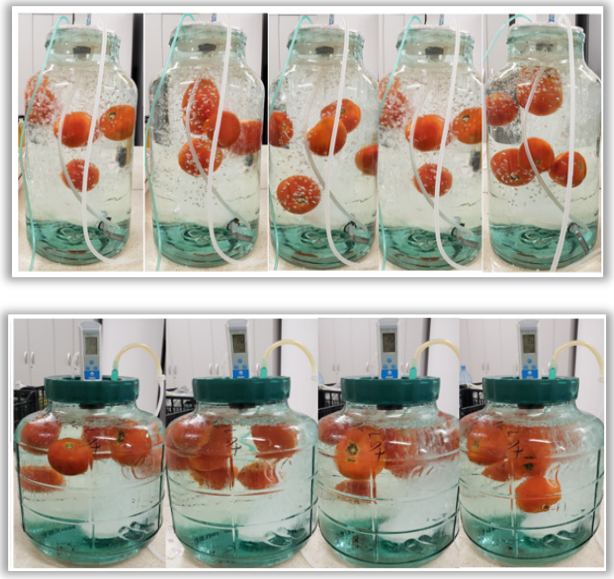

Figure 3 - Aspects of the washing process in O_3 solution

After performing these treatments, the samples were sent to the laboratory for residue determination using mass spectrometry.

The analyzes were carried out in the SC Holland Farming Agro SRL laboratory, on a GC-MSMS Thermo Scientific equipment, using the working procedure according to SR EN 15662:2018, for vegetable matter, with U% ≥ 80%.

RESULTS

In the tomato samples, pesticide residues were determined for the treatment with Cyperguard 25 EC pyrethroid insecticide (table 2).

Table 2. Pesticide residues after treatment with Cyperguard 25 EC

Pesticide residues	Concentration (mg/kg)	Maximum admissible limit (mg/kg)
M1 - control		
Cypermethrin 1	2.91	0.05
Cypermethrin 2	2.75	0.05
Cypermethrin 3	1.08	0.05
Cypermethrin 4	3.28	0.05
Treatment for 5 minutes – V1		
Cypermethrin 1	0.5	0.05
Cypermethrin 2	0.6	0.05
Cypermethrin 3	0.3	0.05
Cypermethrin 4	0.6	0.05
Treatment for 10 minutes V2		
Cypermethrin 1	0.2	0.05
Cypermethrin 2	0.2	0.05
Cypermethrin 3	0.1	0.05
Cypermethrin 4	0.2	0.05

In the treatments with Topsin 70 WDG and Dithane M-45 the concentration values determined for residues were < 0.01 (mg/kg) at a maximum allowed limit of 0.05 (mg/kg).

In the graph in figure 4, the values of the pesticide residues are represented comparatively, when the tomatoes were treated with Cyperguard 25 EC.

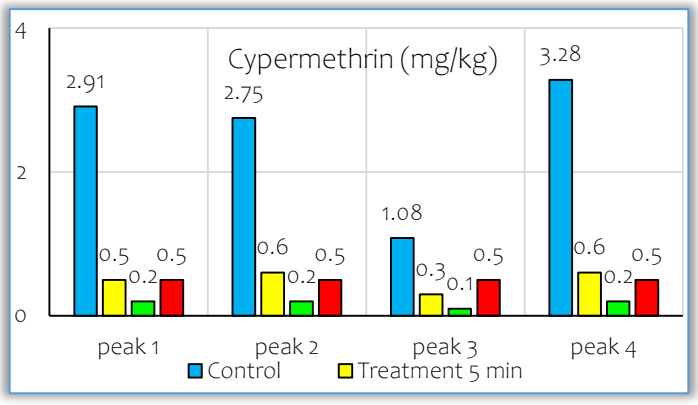

Figure 4 - Comparative values of the residues recorded when treated with Cyperguard 25 EC

Compared to the contamination values recorded in the control variant, when treated with ozonated water for 5 minutes, the determined values fluctuate around the allowed values (0.5 mg/kg), and the 10-minute treatment ensures that the determined values fall below the admissible limit.

CONCLUSIONS

The process of washing vegetables and fruits is mandatory before processing or consumption. This can be done by immersing in water or detergent solution, which removes a considerable part of the pesticides present in tomatoes. Washing tomatoes in water saturated with O3, with or without bubbling, is an efficient and environmentally friendly method of removing residues. In addition to the process of removing residues from the surface of tomatoes, there is also the possibility of their degradation. The treatment with a concentration solution of 2.50 mg/l ozone carried out for 10 minutes ensured the effective removal of pesticide residues generated by the treatment with Cyperguard 25 EC carried out 24 hours before. The use of ozone in the technological phases of processing and/or storage increases the shelf life of the products; however, it is important to consider the concentration applied because a high concentration of O3 can cause oxidation damage and changes in the color of the product.

Acknowledgments

This work was supported by a grant of the Ministry of Agriculture and Rural Development on the Sectoral Plan for Research and Development in the field of Agriculture and Rural Development – ADER 2022, contract no. ADER 7.5.1.

Note: This paper was presented at ISB–INMA TEH' 2022 – International Symposium on Technologies and Technical Systems in Agriculture, Food Industry and Environment, organized by University "POLITEHNICA" of Bucuresti, Faculty of Biotechnical Systems Engineering, National Institute for Research–Development of Machines and Installations designed for Agriculture and Food Industry (INMA Bucuresti), National Research & Development Institute for Food Bioresources (IBA Bucuresti), University of Agronomic Sciences and Veterinary Medicine of Bucuresti (UASVMB), Research–Development Institute for Plant Protection – (ICDPP Bucuresti), Research and Development Institute for Processing and Marketing of the Horticultural Products (HORTING), Hydraulics and Pneumatics Research Institute (INOE 2000 IHP) and Romanian Agricultural Mechanical Engineers Society (SIMAR), in Bucuresti, ROMANIA, in 6–7 October, 2022.

References

[1] Alexopoulos, A., Plessas, S., Ceciu, S., Lazar, V., Mantzourani, I., Voidarou, C., Stavropoulou, E., Bezirtzoglou, E. (2013). Evaluation of ozone efficacy on the reduction of microbial population of fresh cut lettuce (Lactuca sativa) and green bell pepper (Capsicum annuum). Food Control 2013, 30, 491–496

[2] Bermúdez-Aguirre, D., Barbosa-Cánovas, G.V. (2013). Disinfection of selected vegetables under nonthermal treatments: Chlorine, acid citric, ultraviolet light and ozone. Food Control 2013, 29, 82–90

[3] Chilosi G., Tagliavento V., Simonelli R. (2015). Application of Ozone Gas at Low Doses in the Cold Storage of Fruit and Vegetables. Proc. XIth Int. Controlled and Modified Atmosphere Research Conf. Eds.: M.L. Amodio and G. Colelli Acta Hort. 1071, ISHS 2015

[4] de Chiara M.L.V., Amodio M.L., Simonelli R., Colelli G.(2017). Testing of ozone generating equipment to reduce ethylene during postharvest storage of fresh produce. 11th International AIIA Conference: July 5-8, 2017 Bari – Italy "Biosystems Engineering addressing the human challenges of the 21st century"

[5] Feliziani, E., Romanazzia G., Smilanickb J. L. (2014). Application of low concentrations of ozone during the cold storage of table grapes. Postharvest Biology and Technology 93 (2014) 38–48
[6] Marino, M., Maifreni, M., Baggio, A., Innocente, N. (2018). Inactivation of Foodborne Bacteria Biofilms by Aqueous and Gaseous Ozone. Front. Microbiol. 2018, 9
[7] Rodriguesa, A. A. Z., de Queiroza M. E. L. R. and collaborators (2019). Use of ozone and detergent for removal of pesticides and improving storage quality of tomato. Food Research International 125 (2019) 108626
[8] Sarron, E. , Gadonna-Widehem, P., Aussena, T. (2021). Ozone Treatments for Preserving Fresh Vegetables Quality: A Critical Review. Foods 2021, 10, 605
[9] Tamaki, M., Ikeura, H. (2012). Removal of Residual Pesticides in Vegetables Using Ozone Microbubbles. 2012
[10] Trevor, V. (2004). Ozone Applications for Postharvest Disinfection of Edible Horticultural Crops. 2004 by the Regents of the University of California, Division of Agriculture and Natural Resources.
[11] Triandi Tjahjanto, R., Galuh, R., D., Wardhani, S. (2012). Ozone Determination: A Comparison of Quantitative Analysis Methods. J. Pure Appl. Chem. Res. 2012, 1, 18–25

ISSN: 2067-3809

ACTA TECHNICA CORVINIENSIS – BULLETIN OF ENGINEERING
TOME XVI [2023] | FASCICULE 4 [OCTOBER – DECEMBER]

[1.]T.S. ABDULKADIR, [1.]A.B. SULYMAN, [2.]A.A. MOHAMMED, [1,3.]A.S. AREMU, [1,2]A.W. SALAMI,
[1.]M. SURAJUDEEN, [1.]O.J. IJI, [1.]O.O. OLOFINTOYE, [4.]A.A. AFOLABI

A REVIEW OF SUSTAINABLE HYDROPOWER GENERATION IN NIGERIA

[1.]Department of Water Resources and Environmental Engineering, University of Ilorin, P.M.B. 1515, Ilorin, NIGERIA
[2.]National Centre for Hydropower Research and Development, University of Ilorin, KM 18, Ilorin–Ajase–Ipo Road, Opposite ARMTI, Ilorin, Kwara State, NIGERIA
[3.] Lower Niger River Basin Development Authority, Ilorin, Kwara State, NIGERIA
[4.] Department of Civil Engineering, University of Ilorin, P.M.B. 1515, Ilorin, NIGERIA

Abstract: Electricity is the core of every nation's socioeconomic development. Nigeria depends heavily on fossil fuel for electricity generation due to the vast deposits of crude oil and natural gas in the country. Nevertheless, the vast deposit of crude oil, Nigeria still generates less than 4000 MW of electricity with per capita consumption of about 0.03 kW. Hydropower, being one of the available sources of energy, can be transported instantaneously and pollution free to the consumers making it attractive as compared to other forms of energy. Hence, the authors reviewed the available literatures on hydropower generation to evaluate its sustainability in Nigeria context. The literature search was made as wide as possible to capture all relevant data required. The searches covered databases specific to scholarly articles on hydropower generation sustainability. From the studies, it is shown that the potentials of hydropower generation in Nigeria if fully exploited can significantly improve the energy mix of the country that would sustainably serve its population.

Keywords: Energy, Hydropower generation, Sustainability, Small hydropower

INTRODUCTION

Energy is one commodity on which the provision of goods and services depend. Its availability and optimal utilization are economic indices to measure countries' socioeconomic development. Recent researches have linked national standard of living to energy consumption showing that developed countries consume more energy than the developing countries. For the time immemorial, Nigeria is faced with acute shortage of power supply to its populace. The effect of epileptic power supply is conspicuous in the manufacturing sector where about 80% of factories are moribund. Statistically, the combined installed capacity of power stations in Nigeria is far below the country's electricity demand, resulting in epileptic supply of electricity. The situation is compounded by the failure of the existing power stations to operate at its installed capacity (Batalla *et al.*, 2004; Ajibola *et al.*, 2018; Akhator *et al.*, 2019). The sporadic supply of power in Nigeria affects every sphere of human endeavors. The catastrophic effects range from all forms of domestic discomfort to national humiliation. According to Ibe and Okedu (2015), maintaining a reliable electric power generation is therefore a very important issue in power system design and operation. Nigeria, being in the threshold of industrial development, has high energy demand. The country is endowed with rich reserves of conventional energy resources like: crude oil, natural gas, coal and hydro potential. However, coal, nuclear power, biomass and other renewable sources are presently not the major part of Nigeria's energy consumption mix. Meanwhile, most Nigeria electrical power stations currently are either thermal or hydropower. With the cost of oil being uncertain, alternative energy options need to be assessed and development plans expedited to enable a broad–based infrastructure. Electricity supply in the country has been through centralized generating station with high capacities. The supply was about 80% of the total electricity consumption in the country with about 6000 MW installed capacity from three large hydropower stations: Shiroro, Jebba and Kainji along with other five thermal power stations having maximum suppressed demand of about 3,500 MW.

The demand for electricity in Nigeria is shared between residential, industrial, commercial/street lighting in the proportions of 50:30:20 (Ismaila, 2017). It's estimated that 2 to 5% of the capacity of the national grid is contributed by private sector – Independent Power Producer (IPP). Private producers such as *Nigerian* Electricity Supply Corporation (*NESCO*), Shell, AES–Lagos, Bayelsa State gas turbine and Ajaokuta Steel Company sell power to Power Holding Company of Nigeria Plc (PHCN) for transmission and distribution to consumers. The other balance of power demand is being supplied by private generating sets.

The construction of the hydro plants often involves displacement of people and animals from their natural habitats and destruction of species of plants and animals. Therefore, its construction has substantial impact on its

immediate environment. The impact may be positive that are useful to the environment or negative that are hazardous to the environment. The effective management of these impacts to ensure a conducive, balance and sustainable environment is highly desirable. These impacts can be hydrological, ecological, social, economic, cultural, meteorological or human health impacts. Sule and Salami (2013) reported that, the environmental ramifications associated with electricity generation, transmission and distribution have become of great importance in power systems planning, design and operations. In every technologically advanced countries of the world, public electricity distribution and supply dominates the industrial scene in the scale of its capital investment requirements, huge tonnage of primary fuel it consumes and its rapid growing demands for large, complex and technically sophisticated plants and equipment.

Globally, the most widely used form of renewable energy that accounts for 16% of world electricity consumption and 3,427 terawatt–hours of electricity production is hydroelectric energy (Samadi–Boroujen, 2012; Olukanni *et al.*, 2016). Hydropower generating stations generally depend on inflow of water and available net head (Okoro and Chikuni, 2010; Abdulkadir *et al.*, 2012). It is a flexible source of electricity since plants can be ramped up and down very quickly to adapt to changing energy demands. The current trend in hydropower system operations focus on multiple uses of water in order to maximize human needs and demands connected to economic and social activities of the community. Hydropower generation was estimated to be about 35.6% of the Nigeria's electricity sources with gas estimated at 39.8% and oil at 24.8% (Obadote, 2009). However, a range of factors limit hydropower potential which includes river discharge and its variation, landscape topography and environmental considerations, technical capacity, turbine design, limitations of the electrical transmission system, technical flaws and functionality of the energy market (Worman, 2012). Studies have shown that climate change may affect water resources which lead to significant variation of the potential for hydropower (Fahmy *et al.*, 1994; Nogueria *et al.*, 2008; Bosona and Gebresenbet, 2010).

The African continent is endowed with enormous hydropower potential that needs to be harnessed. Despite this huge potential which is enough to meet all the electricity needs of the continent, only a small fraction has been exploited. This could be due to the major technical, financial and environmental challenges that need to be overcome (Sambo, 2010). Hydropower currently makes about 20% contribution to the global electricity supply, second to fossil fuel. Nigeria depends heavily on fossil fuel for electricity generation due to the vast deposits of crude oil and natural gas in the country. Notwithstanding, Nigeria generates less than 4000 MW of electricity with per capita consumption of 0.03 kW (Ezirim *et al.*, 2016). This is the present situation despite the fact that the installed total capacity to generate electricity as far back as 1999 was put at 11,756 MW (Oparaku, 2007). Ohunakin (2010) highlighted that hydropower was the only source of electrical power in Nigeria before the discovery of crude oil. The shift in attention to fossil fuels due to the vast deposit of fossil fuel in the country led to the decay in the hydropower sector development. There is a growing concern that countries should reduce their dependence on fossil fuels for electricity generation and look to other cleaner technologies. Three major factors that improve the attractiveness of renewable energy sources, including hydropower: a growing global demand for electricity, the likely increase in fossil fuel prices, and the need for clean energy sources. Hydropower production is thus expected to increase threefold over the next 100 years (Sambo, 2010). Therefore, the likely obstacles to the sustainable hydropower generation such as climate change, sediment impact, dam and design capacities, are needed to be reviewed holistically. The aim of this study is to review published studies on sustainable hydropower generation in Nigeria with a focus on major hydropower dams in Nigeria.

HYDROPOWER DEVELOPMENT IN NIGERIA

Construction activities on the first hydropower station in Nigeria commenced in 1964 at Kainji on River Niger. The dam was commissioned in 1968 with an installed capacity of 320 MW, and by 1978, the station had 8 plants with total capacity of 760 MW. Later on, the tail water from Kainji dam was utilized to generate 540 MW at Jebba dam, 97 km downstream of Kainji dam. The third Hydro–Electric Power (HEP) station, the Shiroro dam in Niger State was commissioned in 1990 with an installed capacity of 600 MW bringing the total installed capacity of HEP in Nigeria to 1900 MW. There are a number of small hydropower stations, such as 3 MW plant in Bagel, 8 MW plant in Kura and 8 MW in Lere, 2 MW Station at Kwall fall on N'Gell River (River Kaduna) and 8 MW station at Kurra fall. The cumulative capacity of hydropower stations (small and large) is about 2000 MW. This accounts for 32% of the combined installed capacity of hydro, thermal and gas power stations in Nigeria (Zarma, 2006). The development of 2500 MW Mambilla hydropower station is in progress and the country still has potential for about 6000 MW hydropower station. Nigeria has just developed 23% of her feasible hydropower. This is very low compared to other African countries such as Lesotho which has developed 50% of her hydropower potential; Burkina Faso developed 46%, while Kenya has developed 34% of her hydropower potential (Zarma, 2006; Jimoh, 2009).

Potential Hydropower Sites in Nigeria

The power generation in Nigeria has been overwhelmed with various problems impeding its successful implementation. Nigeria has considerable hydro potential sources exemplified by her large rivers, small rivers and streams. Nigerian rivers are distributed all over the country with potential sites for hydropower scheme which can serve the urban, rural and isolated communities. Nigeria hydropower currently accounts for about 32% of the total installed commercial electric power capacity. The overall large–scale potential (exploitable) is in excess of 11,000 MW. An estimation of rivers Kaduna, Benue and Cross River at Shiroro, Makurdi and Ikom indicates that a total capacity of about 4,650 MW is available, while the estimate for the river Mambillla Plateau is put at about 2,330 MW. A large number of untapped hydropower potential of about 11,895 MW (Table 1) has been identified in various locations across the country (Ismaila, 2017).

Table 1: Hydropower potential locations and their capacities in Nigeria

Location	River	State	Potential Capacity (MW)
Mambilla	Danga	Taraba	3960
Lokoja	Niger	Kogi	1950
Makurdi	Benue	Benue	1060
Onitsha	Niger	Anambra	1050
Ikom	Cross	Cross River	730
Zungeru I	Kaduna	Niger	500
Zungeru II	Kaduna	Niger	450
Yola	Benue	Adamawa	360
Gurara	Gurara	Niger	300
Katsina Ala	Katsina Ala	Benue	260
Beli SE	Taraba	Kano	240
Donka	Niger	Adamawa	225
Afikpo	Cross	Ebonyi	180
Garin Dali	Taraba	Taraba	135
Gembu	Dongo	Taraba	130
Sarkin–Danko	Suntai	Taraba	45
Kiri	Gongola	Adamawa	40
Oudi	Mada	Benue	40
Richa I	Mosari	Nassarawa	35
Gwaram	Jama'are	Adamawa	30
Ifon	Osse	Ondo	30
Kashimbila	KatsinaAla	Benue	30
Korubo	Gongola	Adamawa	25
Kura I	Sanga	Kano	15
Richa II	Dafo	Kano	25
Mistakuku	Kurra	Plateau	20
Kura II	Sanga	Kano	25
Kafanchan	Kongun	Kaduna	5
Total			**11895**

(Source: Ismaila 2017; Akorede *et al.,* 2017)

Small Hydropower Potential of Nigeria

Small hydropower is considered a viable solution to the power challenges in Nigeria. Ohunakin *et al.* (2010) opined that Small Hydropower Potential (SHP) has been in existence in Nigeria since 1923 i.e., 45 years before the commissioning of the country's first large hydropower in Kainji. However, SHP technology is still at its infancy in Nigeria with the scheme operated in only three States of the country (Ohunaki *et al.,* 2011). If well deployed, SHP can be most affordable and accessible option to provide off–grid electricity services especially in rural communities (Akorede *et al.,* 2017). The Nigerian Electricity Supply Company (NESCO) was able to supply electricity to the old Benue–Plateau area from the mid–forties to the eighties with hydropower from the Kurra falls. Small hydro power plants are defined and classified as micro, mini or small. The definition of SHP and classification of capacity are dynamic and determined by indigenous development and growth in economy.

Indigenous development and growth in different countries economy has been the litmus test for definition and classification of SHP capacity. Hence, most countries have different definitions and classifications for SHP (Essan, 2007). In Nigeria, SHP is defined as hydropower station capable of generating up to 10 MW capacity as shown in Table 2. Plants with capacity up to 1 MW are considered as mini–hydropower, while micro–hydropower has capacity of up to 500 kW (Aliyu *et al.,* 2015).

Osokoya *et al.* (2013) recommended for Nigeria several units of small hydropower stations because of its affordability, maintainability, reduction in power losses through long transmission lines and avoidance of bureaucracy in government since they would be managed by smaller government units, i.e., the local government. Development of small hydropower projects would significantly reduce poverty and enhance quality of life in the communities they serve. Muhammadu and Usman (2020) highlighted factors affecting developments in the small hydropower sector, and efforts made to ensure capacity building for renewable energy, stimulation of the private sector, developing the markets for small hydropower, obtaining the necessary finance for small hydropower projects and the assistance of multilateral institutions in advancing small hydropower in the North central Nigeria.

Table 2: Classification of SHP in selected country and Organization

Country/ Organization	Micro (kW)	Mini (kW)	Small (kW)
Canada	Nil	<1,000	1001–1,500
China	<100	101–500	501–25,000
ESHA	Nil	Nil	<15,000
France	<500	501–2,000	Nil
IN–SHIP	<100	101–500	501–10,000
India	<100	<2,000	Nil
Japan	Nil	Nil	<10,000
Philippines	Nil	51–500	<15,000
New Zealand	Nil	<10,000	<50,000
Nigeria	≤500	501–1,000	1001–10,000
Sweden	Nil	Nil	101–15,000
UNIDO	<100	101–2,000	2,001–10,000
United Kingdom	<1000	Nil	Nil
USA	<500	501–2,000	<15,000
Zimbabwe	5–500	501–5,000	Nil

According to Energy commission of Nigeria (ECN, 2005), there was a survey which were carried out in 1980 to assessed SHP potentials in 277 locations (Table 3). The result shows that there are total potentials of around 734.3 MW in the surveyed locations. So far, about eight SHP stations (Table 4) with aggregate capacity of 37.0 MW have been installed in Nigeria by private companies and the government.

Table 3: SHP Surveyed States in Nigeria

State (Pre 1980)	River Basin	Total sites	Total capacity (MW)
Sokoto	Sokoto–Rima	22	30.6
Katsina	Sokoto–Rima	11	8.0
Niger	Niger	30	117.6
Kaduna	Niger	19	59.2
Kwara	Niger	12	38.8
Kano	Hadeija–Jamaare	28	46.2
Borno	Chad	28	20.8
Bauchi	Upper Benue	20	42.6
Gongola	Upper Benue	38	162.7
Plateau	Lower Benue	32	110.4
Benue	Lower Benue	19	69.2
Rivers	Cross River	18	258.1
Total		**277**	**734.2**

(ECN, 2005)

Table 4: Existing Small Hydropower schemed in Nigeria

S/No	River	State	Installed Capacity (MW)
1	Bagel I	Plateau	1
2	Bagel II	Plateau	2
3	Kurra	Plateau	8
4	Lere I	Plateau	4
5	Lere II	Plateau	4
6	*Bakalor	Sokoto	3
7	*Tiger	Kano	6
8	*Oyan	Ogun	9

* Needs rehabilitation

Optimizing Hydropower Operation and Management

Special attention should be devoted to adaptation measures to cope with the varied climate environment. Two prime options are addressed on operation and management of hydropower generation to adapt climate change. The first option is to enhance the optimal operation of cascade hydropower stations or single hydropower station with reservoir. Scheduling optimization could reduce the water spill with available capacity and storage. Although the dry scenario examined in that study had 20% less runoff than the base historical hydrology, system–wide, revenues decrease by less than 14% through optimally re–operating storage and generation facilities within existing capacities. Scheduling optimization of hydropower station on a river or basin, is to make full use of water resource at all levels. It can also adjust and compensate for the effects on each single station due to inter annual climate variability during the year. In this case, the most important thing is to optimize the hydropower operation pattern to maximize the revenue with limited capacity and available ancillary facilities (Zhang *et al.*, 2012). The second option, and not mutually exclusive, is to conduct an in–depth risk analysis of climate change impacts on hydropower generation and prepare emergency plan for climate extremes. Changes in mean climate impact caused by global warming on hydropower are relatively limited and easier to be controlled, but the extreme weather events such as floods and drought will seriously affect the production, transmission and distribution of hydropower generation. The frequency and intensity of regional extreme weather caused by climate change is clearly evident. This places potentially severe stress and high risk on hydropower systems. Therefore, it is critically significant for hydropower planners and decision–makers to analyze the potential risk of climate extreme events during the operation. Based on hydrological model forecasts and predictions, emergency plans under different extreme conditions should be established. By optimizing power generation, operation and management, the more efficient hydropower stations could not only increase their generation revenue but also play a significant socio–economic role for society.

Cost Associated with Hydropower

The costs associated with developing hydropower are very site–specific. Meeting environmental issues and the need to design the power plant to maximize its output vary from area to area. However, compared to other depletable and non–depletable energy sources, hydropower is among the least expensive of all the energy resources. Although the initial costs to develop and construct these facilities are not small, they have lower maintenance and operation costs. Taken together, the cost of electricity from hydroelectric plants ranges between 0.03 and 0.06 cents per kWh. This makes these power plants attractive to meet the increasing need to supply electricity (Schwailer, 1996). Construction costs for new hydropower projects in most countries including Nigeria are usually less than US $2 million/MW for large scale schemes (> 300 MW), and US $2 to US $4 million/MW for small– and medium–scale schemes (<300 MW) (IEA, 2014). A typical classification of hydropower scheme is presented in Table 5. It is important to note that the initial investment needs for particular projects must be studied individually owing to the unique nature of each hydropower project.

Table 5: Classification of cost associated with hydropower schemes

Category	Output (MW)	Storage	Power use	Investment costs (US$ millions/MW)
Small	< 10	Run of river	Base load	2 to 4
Medium	10 to 100	Run of river	Base load	2 to 3
Medium	100 to 300	Dam and reservoir	Base load and peak	2 to 3
Large	> 300	Dam and reservoir	Base load and peak	< 2

(Source: IEA, 2014)

Social and Environmental Costs of SHP Plants

Ohunakin (2010a) emphasized that social and environmental costs of hydropower are more prevalent for large–dam projects. Small–scale hydro projects have the least social and environmental effects. Dudhani *et al.* (2006) expressed that SHP projects are generally considered to be more environmentally favorable than both large hydro and fossil fuel powered plants because they do not involve serious deforestation, rehabilitation and submergence. Meanwhile, some carbon dioxide is produced during manufacture and construction of the project. This is a tiny fraction of the operating emissions of equivalent fossil–fuel electricity generation. Small dams and micro hydro facilities create less risk, but can form continuing hazards even after they have been decommissioned. For example, the Small Kelly Barnes Dam failed in 1967, causing 39 deaths with the Toccoa Flood, ten years after its power plant was decommissioned in 1957.

Renewable Energy Policy on Hydropower

In order to benefit from the huge SHP potentials in Nigeria, a vibrant renewable energy portfolio standard has to be formulated along the following lines as contained in (Sambo, 2007). These policies include:

- nation shall fully harness the hydropower potential available in the country for electricity generation.
- nation shall pay particular attention to the development of the mini and micro hydropower schemes.
- exploitation of the hydro resources shall be done in environmentally sustainable manner.
- private sector and indigenous participation in hydropower development shall be actively and generously promoted.

DISCUSSION AND CONCLUSION

This paper presented a critical review of the status of sustainable hydropower generation in Nigeria, and the potential to utilize them in meeting the current energy crisis facing the country. The potentials of small hydropower plants in Nigeria have been explored and confirmed to be very huge considering the fact that experts had assessed many sites in the country to have favourable conditions for SHP development. It has been shown that the exploitation of SHP potentials in twelve states could raise the available megawatts by more than 20 percent and improve the energy mix in Nigeria. Further, recommendations of Osokoya *et al.* (2013) could be helpful in enhancing the small hydropower generation in Nigeria.

The costs associated with developing hydropower are very site–specific base on environmental situation and the need to design the power plant. Although, the initial costs to develop and construct these facilities are not small, however, they have lower maintenance and operation costs. The cost of electricity from hydroelectric plants ranges between 0.03 and 0.06 cents per kilowatt.hr. Construction costs for new hydropower projects in most countries including Nigeria are usually less than US $2 million/MW for large scale schemes (> 300 MW), and US $2 to US $4 million/MW for small– and medium–scale schemes (<300 MW).

Several factors such as sedimentation, climate changes and operation and maintenance of the hydropower can affect the sustainable generation of hydropower in Nigeria. Sedimentation affects hydropower generation due to a loss of reservoir storage or by damaging the mechanical components of the facilities. Sediment deposited in reservoirs may also present additional and compounding structural loads to a hydropower dam and may also become liquefied under dynamic loading from an earthquake. Methods of managing sediment at hydropower facilities fall under three general categories: those that divert sediment around or through the reservoir, those that remove deposited sediments, and those that minimize the amount of sediment reaching the facility. A variety of sediment management strategies have been employed at facilities in Nigeria, with many successful implementations documented. Appropriate sediment management at hydropower facilities can be achieved through consideration of sediment concerns during all phases of the project, design, construction and operation.

The operation and maintenance costs are relatively low for hydropower plants compared to other forms of power generation. However, many low to middle income countries such as Nigeria struggle to meet standard maintenance schedules through lack of resources which then leads to loss of performance. The required operation and maintenance varies widely, according to the scheme's location, capacity factor, generation strategy, whether the station is manned or unmanned, whether it is a storage or run of river scheme, the annual production, the number of starts and stops, as well as numerous other factors. Underfunded and neglected operation and maintenance reduces power output and shortens the life of the plants. In systems with adequate spare capacity outages of plant components can be planned, for their inspection and, if necessary, repair and replacement should be done to improve the performances of the hydropower.

It is very important to harness all the hydropower potential in Nigeria sustainably in order to boost the socio–economic development of the country. The selection, design, construction and operation of hydropower projects need to take into account it environmental and social impacts in a way that is sympathetic to the environment and society. The

government should be committed to promote renewable forms of energy, especially the hydropower projects where it is feasible and practicable. In the rural area in the country where the livelihoods of people are underpinned by the presence of the healthy and diverse ecosystems that provide them with sustenance, the issue of sustainability is of paramount important.

Also, there can be no sustainable development without the demonstration of sound and equitable distribution of economic benefits. For this reason, economic considerations are central in the decision–making processes associated with hydropower projects. The efficient use of economic resources requires that the best options are selected and that the alternatives have been carefully evaluated. Furthermore, there are no hidden and unforeseen costs that could emerge in the future. Demand growth has been rapid and the availability of funds and grants is not keeping pace with the increasing capital requirements of the sector.

Development of Nigeria energy space will result in industrialization and improved standard of living if energy demands for various sectors of the economic is met. Igweonu and Joshua, (2012) emphasized that SHP potentials in Nigeria is massive considering the numerous sites assessed and certified by experts. Extensive review of hydropower generation in Nigeria proves not only to be a renewable source but also sustainable. However, energy demand is yet to be met thereby creating a vacuum for development of sustainable energy in Nigeria. It can be concluded that SHP systems would alleviate the unavailability of power and it could be enhanced by optimizing their design, construction and operation techniques. It is recommended that efforts and policy are required to encourage and develop the technical skills needed for the investors to be active in SHP.

References

[1] Abdulkadir, T.S.; Sule, B.F. and Salami, A.W. Application of Artificial Neural Network Model to the Management of Hydropower Reservoirs along River Niger, Nigeria. Annals of Faculty Engineering Hunedoara–International Journal of Engineering, Romania. Tome X –FASCICULE 3; 419–424, 2012.

[2] Ajibola, O.O.E.; Ajala, O.S.; Akanmu, J.O. and Balogun, O.J. Improvement of hydroelectric power generation using pumped storage system, Nigerian Journal of Technology, 37(1), 191–199, 2018.

[3] Akhator, P.E.; Obanor, A.I. and Sadjere, E.G. Electricity situation and potential development in Nigeria using off–grid green energy solutions, Journal of Applied Sciences and Environmental Management 23(3), 527–537, 2019.

[4] Akorede, M.F.; Ibrahim, O.; Amuda, S.A.; Otuoze, A.O. and Olufeagba, B.J. Current status and outlook of renewable energy development in Nigeria. Nigerian Journal of Technology 36(1) () 196–212, 2017.

[5] Aliyu, A.S.; Dada, J.O. and Adam, I.K. Current status and future prospects of renewable energy in Nigeria. Renewable and sustainable energy reviews, 48, 336–346. 2015.

[6] Batalla, R.J.; Gomez, C.M. and Kondolf, G.M. Reservoir–induced hydrological changes in the Ebro River basin (NE Spain). Journal of Hydrology, 290 (1–2), 117–136, 2004.

[7] Bosona, T.G. and Gebresenbet, G. Modelling hydropower plant system to improve its reservoir operation. International Journal of Water Resources and Environmental Engineering 2(4), 87–94, 2010.

[8] Dudhani, S.; Inamdar, S. and Sinha, A.K. Assessment of small hydro power potentials using remote sensing data for sustainable development in India. Energy Policy 34, 3195–3205, 2006.

[9] Energy Commission of Nigeria ECN. Renewable Energy Master Plan. Nigeria, 2005.

[10] Essan, A.A. Sustainable energy development: The small hydro power option. The 1st Proceedings of the International Workshop on Renewable Energy Resources for Sustainable Development Africa, IWRESDA, 68–84, 2007.

[11] Ezirim, G.; Onyemaechi, E. and Freedom, O. The political economy of Nigeria's power sector reforms: Challenges and prospects, 2005–2015. Mediterranean Journal of Social Sciences, 7(4), 443, 2016.

[12] Fahmy, H.S.; King, J.P.; Wentzel, M.W. and Seton, J.A. Economic optimization of river management using genetic algorithms. American Society of Agricultural Engineers, St. Joseph, Mich. Paper no. 943034, ASCE 1994 International Summer Meeting, 1994.

[13] IEA, International Energy Agency. WEO–2014 Special Report: Africa Energy Outlook – Analysis (2014). Available online at: https://www.iea.org/reports/africa–energy–outlook–2014

[14] Igweonu, E.I. and Joshua, R.B. Small hydropower (SHP) development in Nigeria: issues, challenges and prospects. Global Journal of Pure and Applied Sciences, 18(1), 53–58, 2012.

[15] Ibe, A.O. and Okedu, K.E. Optimized electricity generation in Nigeria. Nigerian Journal of Engineering Management, 8(4), 7–16, 2015.

[16] Jimoh, O.D. Operation of hydropower systems in Nigeria. Opening ceremony of National Centre for Hydropower Research and Development (NACHRED), Energy Commission of Nigeria, 2009.

[17] Muhammadu, M.M. and Usman, J. Small hydropower development in North–Central of Nigeria: An assessment, Journal of Advanced Research in Applied Mechanics, 69(1) 7–16, 2020.

[18] Nogueria, M.; GReis–Oliveira, P.C. and Britto, Y.T. Zooplankton assemblages (Copepoda and Cladocera) in a cascade of reservoirs of a large tropical river (SE Brazil), Limmetica, 27, 151–170, 2008.

[19] Obadote, D.J. Energy crisis in Nigeria: Technical issues and solutions, Power Sector Conference, June 25– 27, 2009.

[20] Ohunakin, O.S. Energy utilization and renewable energy source in Nigeria, Journal of Engineering and Applied Science 5, 171–177. 2010a.

[21] Ohunakin, O.S. Small hydro power (SHP) development in Nigeria: An assessment and option for sustainable development. Nigerian Society of Engineers, Abuja, 1–16, 2010.

[22] Ohunakin, O.S.; Ojolo, S.J. and Ajayi, O.O. Small hydropower (SHP) development in Nigeria: An assessment. Renewable and Sustainable Energy Reviews, 15(4), 2006–2013, 2011.

[23] Okoro, O.I. and Chikuni, E. Power sector reforms in Nigeria: Opportunities and challenges. Journal of Energy in South Africa, 18(3), 52–57, 2010.

[24] Olukanni, D.O.; Adejumo, T.A. and Salami, A.W. Assessment of Jebba hydropower dam operation for improved energy production and flood management. ARPN Journal of Engineering and Applied Sciences 11(13), 8450–8467, 2016.

[25] Oparaku, O.U. Decentralized electric power generation in Nigeria: The role of renewable energy resources. The 1st Proceedings of the International Workshop on Renewable Energy Resources for Sustainable Development Africa, IWRESDA, 28–36, 2007.

[26] Osokoya, O.O.; Ojikutu, A.O.; Olayiwola, O.O. and Chinedum, C.W. Enhancing small hydropower generation in Nigeria, Journal of Sustainable Energy Eng., 1(2), 113–126, 2013.
[27] Samadi–Boroujen, H. Hydropower practice and application. Hydropower Practice and Application, Intech, Croatia, 2012.
[28] Sambo, A.S. Renewable energy development in Nigeria. A Paper Presented at the World Future Council Strategy Workshop on Renewable Energy, Accra, Ghana, 21–24, 2010.
[29] Sambo, A.S. Renewable energy development in Nigeria: A situation report. The 1st proceedings of the International workshop on renewable energy resources for sustainable development Africa, IWRESDA, 1–12, 2007.
[30] Schwailer, A.E. Energy technology: Sources of power, London, Thomson Learning, 1996.
[31] Sule, B.F. and Salami, A.W. Hydrological and environmental impact of hydropower dam operation in Nigeria. University of Ilorin Press, 2013.
[32] Worman, A. Hydrological statistics for regulating hydropower. Hydropower Practice and Application, Intech, Croatia, 41–60, 2012.
[33] Zarma, I.H. Hydropower resources in Nigeria. Being a Country Position Paper Presented at 2nd Hydro Power for Today Conference International Centre on Small Hydro Power (IC–SHP), Hangzhou, China, 2006.
[34] Zhang, L.B.; Jin, J.L.; Zhang, Z.Y.; Zhang, H. and Zhao, Y.G. Brief discussion of several issues on development of hydropower energy under climate change. Journal of Water Resources Research. 1, 501–504, 2012.

ISSN: 2067-3809

Fascicule 4
[October – December]
tome XVI
[2023]

ACTA Technica CORVINIENSIS
BULLETIN OF ENGINEERING

ISSN: 2067-3809

MANUSCRIPT PREPARATION – GENERAL GUIDELINES

Manuscripts submitted for consideration to **ACTA TECHNICA CORVINIENSIS – Bulletin of Engineering** must conform to the following requirements that will facilitate preparation of the article for publication. These instructions are written in a form that satisfies all of the formatting requirements for the author manuscript. Please use them as a template in preparing your manuscript. Authors must take special care to follow these instructions concerning margins.

INVITATION

We are looking forward to a fruitful collaboration and we welcome you to publish in our ACTA TECHNICA CORVINIENSIS – Bulletin of Engineering. You are invited to contribute review or research papers as well as opinion in the fields of science and technology including engineering. We accept contributions (full papers) in the fields of applied sciences and technology including all branches of engineering and management.

ACTA TECHNICA CORVINIENSIS – Bulletin of Engineering publishes invited review papers covering the full spectrum of engineering and management. The reviews, both experimental and theoretical, provide general background information as well as a critical assessment on topics in a state of flux. We are primarily interested in those contributions which bring new insights, and papers will be selected on the basis of the importance of the new knowledge they provide.

Submission of a paper implies that the work described has not been published previously (except in the form of an abstract or as part of a published lecture or academic thesis) that it is not under consideration for publication elsewhere. It is not accepted to submit materials which in any way violate copyrights of third persons or law rights. An author is fully responsible ethically and legally for breaking given conditions or misleading the Editor or the Publisher.

ACTA TECHNICA CORVINIENSIS – Bulletin of Engineering is an international and interdisciplinary journal which reports on scientific and technical contributions. Every year, in four online issues (fascicules 1–4), ACTA TECHNICA CORVINIENSIS – Bulletin of Engineering [e-ISSN: 2067-3809] publishes a series of reviews covering the most exciting and developing areas of engineering. Each issue contains papers reviewed by international researchers who are experts in their fields. The result is a journal that gives the scientists and engineers the opportunity to keep informed of all the current developments in their own, and related, areas of research, ensuring the new ideas across an increasingly the interdisciplinary field. Topical reviews in materials science and engineering, each including:

- surveys of work accomplished to date
- current trends in research and applications
- future prospects.

As an open-access journal ACTA TECHNICA CORVINIENSIS – Bulletin of Engineering will serve the whole engineering research community, offering a stimulating combination of the following:

- Research Papers – concise, high impact original research articles,
- Scientific Papers – concise, high impact original theoretical articles,
- Perspectives – commissioned commentaries highlighting the impact and wider implications of research appearing in the journal.

ACTA TECHNICA CORVINIENSIS – Bulletin of Engineering encourages the submission of comments on papers published particularly in our journal. The journal publishes articles focused on topics of current interest within the scope of the journal and coordinated by invited guest editors. Interested authors are invited to contact one of the Editors for further details.

BASIC MANUSCRIPT REQUIREMENTS

The basic instructions and manuscript requirements are simple:

- Manuscript shall be formatted for an A4 size page.
- The all margins of page (top, bottom, left, and right) shall be 20 mm.
- The text shall have both the left and right margins justified.
- Single-spaced text, tables, and references, written with 11 or 12-point Georgia or Times New Roman typeface.
- No Line numbering on any pages and no page numbers.
- Manuscript length must not exceed 15 pages (including text and references).
- Number of the figures and tables combined must not exceed 20.
- Manuscripts that exceed these guidelines will be subject to reductions in length.

The original of the technical paper will be sent through e-mail as attached document (*.doc, Windows 95 or higher). Manuscripts should be submitted to e-mail: redactie@fih.upt.ro, with mention "for ACTA TECHNICA CORVINIENSIS".

STRUCTURE

The manuscript should be organized in the following order: Title of the paper, Authors' names and affiliation, Abstract, Key Words, Introduction, Body of the paper (in sequential headings), Discussion & Results, Conclusion or Concluding

Remarks, Acknowledgements (where applicable), References, and Appendices (where applicable).

THE TITLE

The title is centered on the page and is CAPITALIZED AND SET IN BOLDFACE (font size 14 pt). It should adequately describe the content of the paper. An abbreviated title of less than 60 characters (including spaces) should also be suggested. Maximum length of title: 20 words.

AUTHOR'S NAME AND AFFILIATION

The author's name(s) follows the title and is also centered on the page (font size 11 pt). A blank line is required between the title and the author's name(s). Last names should be spelled out in full and succeeded by author's initials. The author's affiliation (in font size 11 pt) is provided below. Phone and fax numbers do not appear.

ABSTRACT

State the paper's purpose, methods or procedures presentation, new results, and conclusions are presented. A nonmathematical abstract, not exceeding 200 words, is required for all papers. It should be an abbreviated, accurate presentation of the contents of the paper. It should contain sufficient information to enable readers to decide whether they should obtain and read the entire paper. Do not cite references in the abstract.

KEY WORDS

The author should provide a list of three to five key words that clearly describe the subject matter of the paper.

TEXT LAYOUT

The manuscript must be typed single spacing. Use extra line spacing between equations, illustrations, figures and tables. The body of the text should be prepared using Georgia or Times New Roman. The font size used for preparation of the manuscript must be 11 or 12 points. The first paragraph following a heading should not be indented. The following paragraphs must be indented 10 mm. Note that there is no line spacing between paragraphs unless a subheading is used. Symbols for physical quantities in the text should be written in italics. Conclude the text with a summary or conclusion section. Spell out all initials, acronyms, or abbreviations (not units of measure) at first use. Put the initials or abbreviation in parentheses after the spelled-out version. The manuscript must be writing in the third person ("the author concludes... ").

FIGURES AND TABLES

Figures (diagrams and photographs) should be numbered consecutively using Arabic numbers. They should be placed in the text soon after the point where they are referenced. Figures should be centered in a column and should have a figure caption placed underneath. Captions should be centered in the column, in the format "Figure 1" and are in upper and lower case letters.

When referring to a figure in the body of the text, the abbreviation "Figure" is used illustrations must be submitted in digital format, with a good resolution. Table captions appear centered above the table in upper and lower case letters.

When referring to a table in the text, "Table" with the proper number is used. Captions should be centered in the column, in the format "Table 1" and are in upper and lower case letters. Tables are numbered consecutively and independently of any figures. All figures and tables must be incorporated into the text.

EQUATIONS & MATHEMATICAL EXPRESSIONS

Place equations on separate lines, centered, and numbered in parentheses at the right margin. Equation numbers should appear in parentheses and be numbered consecutively. All equation numbers must appear on the right-hand side of the equation and should be referred to within the text.

CONCLUSIONS

A conclusion section must be included and should indicate clearly the advantages, limitations and possible applications of the paper. Discuss about future work.

Acknowledgements

An acknowledgement section may be presented after the conclusion, if desired. Individuals or units other than authors who were of direct help in the work could be acknowledged by a brief statement following the text. The acknowledgment should give essential credits, but its length should be kept to a minimum; word count should be <100 words.

References

References should be listed together at the end of the paper in alphabetical order by author's surname. List of references indent 10 mm from the second line of each references. Personal communications and unpublished data are not acceptable references.

- *Journal Papers:* Surname 1, Initials; Surname 2, Initials and Surname 3, Initials: Title, Journal Name, volume (number), pages, year.
- *Books:* Surname 1, Initials and Surname 2, Initials: Title, Edition (if existent), Place of publication, Publisher, year.
- *Proceedings Papers:* Surname 1, Initials; Surname 2, Initials and Surname 3, Initials: Paper title, Proceedings title, pages, year.

ISSN: 2067-3809

INDEXES & DATABASES

We are very pleased to inform that our international scientific journal ACTA TECHNICA CORVINIENSIS – Bulletin of Engineering completed its 15 years of publication successfully [2008–2022, Tome I–XV].
In a very short period the ACTA TECHNICA CORVINIENSIS – Bulletin of Engineering has acquired global presence and scholars from all over the world have taken it with great enthusiasm.
We are extremely grateful and heartily acknowledge the kind of support and encouragement from all contributors and all collaborators!

ACTA TECHNICA CORVINIENSIS – Bulletin of Engineering is accredited and ranked in the "B+" CATEGORY Journal by CNCSIS – The National University Research Council's Classification of Romanian Journals, position no. 940 (http://cncsis.gov.ro/).
ACTA TECHNICA CORVINIENSIS – Bulletin of Engineering is a part of the ROAD, the Directory of Open Access scholarly Resources (http://road.issn.org/).

ACTA TECHNICA CORVINIENSIS – Bulletin of Engineering is also indexed in the digital libraries of the following world's universities and research centers:

WorldCat – the world's largest library catalog
https://www.worldcat.org/
National Lybrary of Australia
http://trove.nla.gov.au/
University Library of Regensburg – GIGA German Institute of Global and Area Studies
http://opac.giga-hamburg.de/ezb/
Simon Fraser University – Electronic Journals Library
http://cufts2.lib.sfu.ca/
University of Wisconsin – Madison Libraries
http://library.wisc.edu/
University of Toronto Libraries
http://search.library.utoronto.ca/
The University of Queensland
https://www.library.uq.edu.au/
The New York Public Library
http://nypl.bibliocommons.com/
State Library of New South Wales
http://library.sl.nsw.gov.au/
University of Alberta Libraries – University of Alberta
http://www.library.ualberta.ca/
The University of Hong Kong Libraries
http://sunzi.lib.hku.hk/
The University Library – The University of California
http://harvest.lib.ucdavis.edu/

ACTA TECHNICA CORVINIENSIS – Bulletin of Engineering is indexed, abstracted and covered in the world–known bibliographical databases and directories including:

INDEX COPERNICUS – JOURNAL MASTER LIST
http://journals.indexcopernicus.com/
GENAMICSJOURNALSEEK Database
http://journalseek.net/
DOAJ – Directory of Open Access Journals
http://www.doaj.org/
EVISA Database
http://www.speciation.net/
CHEMICAL ABSTRACTS SERVICE (CAS)
http://www.cas.org/
EBSCO Publishing
http://www.ebscohost.com/
GOOGLE SCHOLAR
http://scholar.google.com
SCIRUS – Elsevier
http://www.scirus.com/
ULRICHSweb – Global serials directory
http://ulrichsweb.serialssolutions.com
getCITED
http://www.getcited.org
BASE – Bielefeld Academic Search Engine
http://www.base-search.net
Electronic Journals Library
http://rzblx1.uni-regensburg.de
Open J–Gate
http://www.openj-gate.com
ProQUEST Research Library
http://www.proquest.com
Directory of Research Journals Indexing
http://www.drji.org/
Directory Indexing of International Research Journals
http://www.citefactor.org/

ISSN: 2067-3809